# UNIVERSITÀ DI SIENA 1240

Dipartimento di Scienze fisiche, della Terra e dell'ambiente

## Dottorato in Scienze e tecnologie ambientali, geologiche e polari

34° Ciclo

Coordinatore: Prof. Simone Bastianoni

# ECOTOXICITY AND SUB-LETHAL EFFECTS OF ACCIDENTALLY DISPERSED AND PURPOSELY PRODUCED NANOPARTICLES THROUGH A MULTI-TROPHIC APPROACH

Settore scientifico disciplinare: BIO/07

*Candidata*

Arianna Bellingeri

Università degli Studi di Siena

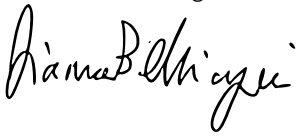

*Firma digitale della candidata*

Arianna Bellingeri

Signed 19/04/2022

*Tutore*

Ilaria Corsi

Università degli Studi di Siena

Anno accademico di conseguimento del titolo di Dottore di ricerca

2020/21

Università degli Studi di Siena
Dottorato in Scienze e tecnologie ambientali, geologiche e polari
34° Ciclo

*Data dell'esame finale*
29/04/2022

*Commissione giudicatrice*
Prof. Massimiliano Scalici, Dipartimento di Scienze, Università di Roma Tre

Prof.ssa Maria Maisano, Dipartimento di Scienze chimiche, biologiche, farmaceutiche e ambientali, Università degli Studi di Messina

*Esperto/i*
Prof.ssa Silvia Casini, Dipartimento di Scienze fisiche, della Terra e dell'ambiente, Università degli Studi di Siena

*Supplenti*
Prof. Giovanni Libralato, Dipartimento di Biologia, Università degli Studi di Napoli Federico II

# Table of Contents

## ABBREVIATIONS

3MPS: 3-mercapto-a-propanesulfonate

$AgNO_3$: Silver nitrate

AgNP3MPS: silver nanoparticles with 3-mercapto-a-propanesulfonate

AgNPcitLcys: silver nanoparticles with citrate and L-cysteine

AgNPs: Silver nanoparticles

CIT: Citrate

CNTs: Carbon nanotubes

CTRL: Control

DCF-DA: Dichlorofluorescein-diacetate

DCF: Dichlorofluorescein

DIC: Differential interference contrast microscopy

DLS: Dynamic light scattering

DO: Dissolved oxygen

DOC: Dissolved organic carbon

DOM: Dissolved organic matter

ENMs: Engineered nanomaterials

ENPs: Engineered nanoparticles

EPS: Extracellular polymeric substance

ESEM: Environmental scanning electron microscopy

F/2: ISO 10253 (2006) marine water algal medium

FPP: Fultoportula processes

FT-IR: Fourier transform infrared spectroscopy

ICP-MS: Inductively coupled plasma mass spectrometry

L-CYS: L- cysteine

LB: Luria-bertani broth

LSPR: Localized surface plasmon resonance

MHRW: Moderately hard reconstituted water

MQW: Milli-Q water

NEXAFS: Near red x-ray absorption fine structure

NMs: Nanomaterials

NOM: Natural organic matter

NPs: Nanoparticles

NSW: Natural seawater

PDI: Polydispersity index

PECs: Predicted environmental concentrations

POM: Particulate organic matter

PS NPs: Polystyrene nanoparticles

PS-COOH NPs: Carboxy-modified polystyrene nanoparticles

PS-$NH_2$ NPs: Amino-modified polystyrene nanoparticles

PS: Polystyrene

ROS: Reactive oxygen species

SDS: Sodium dodecyl sulfate

SR-XPS: Synchrotron radiation x-ray photoelectron spectroscopy

TEM: Transmission electron microscopy

TG201: OECD 201 (2011) freshwater algal medium

WTTP: Wastewater treatment plant

YCT: Yeast cereal leaves and trout chow

## THESIS STRUCTURE

The general introduction of this PhD thesis summarizes the main characteristics of engineered nanoparticles (ENPs) and how media characteristics and natural organic matter are able to influence their interaction with biota, with a focus on polystyrene nanoparticles (PS NPs) and silver nanoparticles (AgNPs).

The thesis is divided into four chapters. Each chapter is provided with a graphical and a written abstract summarizing the main points of the chapter. An introduction then sets out the main issue addressed in the chapter and summarizes the state of the art on the investigated matter. A methodological section follows, with detailed methods of NP characterization and conduction of ecotoxicity assays. The core of each chapter is expressed in the results and discussion session, in which the obtained data are presented and hypotheses on their interpretation are formulated. A concluding paragraph summarizes the main results. At the end of each chapter a list of references is present. Supplementary appendix with supplementary material is included.

Chapter 1 investigates lethal and sub-lethal effects on the marine diatom *Skeletonema marinoi* upon chronic exposure to PS NPs. A particular focus on the ecological implications linked to the observed effects is reported.

Chapter 2 provides the first evaluation of the ecological safety of the novel AgNPs bifunctionalized with citrate and L-cysteine (AgNPcitLcys), to be applied as sensors and remediation tools of Hg contaminated waters. The promising results allowed a much deeper investigation of AgNPcitLcys ecotoxicity in chapter 3 in which the concentration range is broadened as well as exposure period and tested organisms.

In chapter 4, AgNPcitLcys mode of action towards microalgae and bacteria was compared with that of a differently coated AgNP, with 3-mercapto-a-propanesulfonate (AgNP3MPS).

Part of the work presented in this PhD thesis has been published or is under review from peer-reviewed journals:

- **Bellingeri A**, Casabianca S, Capellacci S, Faleri C, Paccagnini E, Lupetti P, Koelmans AA, Penna A, Corsi I (2020): Impact of Polystyrene Nanoparticles on Marine Diatom *Skeletonema marinoi* Chain Assemblages and Consequences on their Ecological Role in Marine Ecosystems. *Environmental Pollution* 262, 114268

- Prosposito P, Burratti L, **Bellingeri A**, Protano G, Faleri C, Corsi I, Battocchio C, Iucci G, Tortora L, Secchi V (2019): Bifunctionalized Silver Nanoparticles as $Hg^{2+}$ Plasmonic Sensor in Water: Synthesis, Characterizations, and Ecosafety. *Nanomaterials* 9, 1353

- **Bellingeri A,** Scattoni M, Venditti I, Battocchio C, Faleri C, Protano G, Corsi I, (2021): Innocent Until Proven Guilty: Chronic Toxicity of AgNPcitLcys for Water Remediation Reveals the Need to Reconsider Ecosafety Testing. Under revision at *Environmental Science: Nano*.

## ABSTRACT

The use of nanotechnology in everyday life received a boost in the last twenty years thanks to improved performances and adjustable properties of engineered nanomaterials (ENMs) and nanoparticles (NPs) compared to traditional materials. ENMs and NPs are purposely produced for a wide variety of applications and, as recently discovered, are also accidentally formed during some industrial processes. Being so extensively employed they end up into the natural environment and their occurrence, especially in the aquatic environment, has been recently confirmed, although only for selected NPs.

In fact, due to technical limitations in the detection of NPs in natural matrices, the actual concentrations are mostly established based on predicted environmental concentrations (PECs), in the range of ng-mg $L^{-1}$. The consequences of environmental exposure for aquatic organisms, especially in the long-term, are not well-understood and, due to the large variety of features contributing to NP diversity, common guidelines for NP risk assessment are in their infancy. The aim of this thesis was to investigate the effects of two different type of NPs, polystyrene nanoparticles (PS NPs) as proxy for nanoplastics and silver nanoparticles (AgNPs), toward aquatic microorganisms at different levels of ecological organization. Selected organisms belonging to the bacterial, microalgal, and microcrustacean communities, from the freshwater and the marine environment, have been investigated. Both NPs were thoroughly characterized for their properties and their behaviour in exposure media by means of dynamic light scattering (DLS), transmission electron microscopy (TEM) and, in the case of AgNP, inductively coupled plasma mass spectrometry (ICP-MS) for the assessment of ion release. When possible, all the elements possibly interfering with the observed effects were determined and reported, in order to help in the correct assessment of NP mode of action in terms of ecotoxicity. AgNP synthesis process was reported in detail, while additives in PS NP suspension were listed and their final concentration in exposure media was calculated. Moreover, for a more correct interpretation of NP behaviour data, the composition of all exposure media and their physico-chemical parameters were reported and considered in data analysis. All biological models were tested for acute toxicity and, when allowed by the organism ecology, chronic toxicity was assessed as well. Particular attention was given

to sub-lethal effects occurring upon exposure to NPs and how these could be linked to more detrimental effects in the long-term and furthermore having implications at the ecological level. Results enriched the data pool on NP ecotoxicity at various levels of aquatic food chains, while also highlighting the importance of long-term exposure and sub-lethal effects. Marine diatom exposed to PS NPs showed no effect on growth but resulted in PS NP adhesion to the algal surface and reduced chain length of algal cells, with possible implications for algal buoyancy and bloom formation. The first evaluation of novel AgNPs designed for water remediation successfully resulted in low dissolution and no toxicity for two freshwater and marine microalgae. A more thorough investigation, however, showed effects in the long-term especially for marine microcrustaceans and suggested a toxicity linked to the AgNP nano-size rather than to dissolved Ag values. Effect comparison of two differently coated AgNP to bacteria and microalgae revealed a different mode of action based on coatings: one confirmed to be influenced by the nano-size while for the other a dissolution-based toxicity was observed. Overall results showed that the consequences of NP exposure more likely originate from the physical interaction with the organism membrane/cell wall or body surface in long-term exposure scenarios, and with, often, unexpected outcomes compared to traditional toxicity endpoints (*i.e.,* cell growth and mortality). New ecotoxicological outcomes should be considered in order to provide a more realistic assessment of the risk associated to NP use and discharge in the aquatic environment, while a more ecologically-based design for new generations of ENMs should be promoted.

# INTRODUCTION

## ENMS BEHAVIOUR IN AQUEOUS MEDIA AND INTERACTION WITH ORGANIC MATTER AND BIOTA

Traditionally, engineered nanomaterials (ENMs) are defined as those materials with one dimension under 100 nm, while nanoparticles (NPs) are materials with at least two dimensions between 1 and 100 nm (BSI, 2007; SCENIHR, 2007). This definition comes from the unique mechanical, optical and catalytic properties and electrical conductivity, owned by ENMs thanks to their nano-size. Natural NPs have always existed in the environment, even though with a wider size range (1 nm–10 µm), being named ultrafine particles and colloids, depending on the environmental compartment (*i.e.,* air, water, or soil) (Lead and Wilkinson, 2006). Carbonaceous nanomaterials were the first to be discovered (1985) and then produced (1991) as carbon nanotubes (CNTs), soon causing health concern for humans due to their similarity of behaviour with asbestos (Service, 1998). Since then, the enormous production and use of ENMs has brought to question whether they would have an impact also on natural ecosystems, and how this could be mitigated (Klaine et al., 2008).

The peculiar nature of NPs, in between bulk and molecular state of matter, posed the need to update traditional risk assessment protocols, originally conceived for contaminants having their predominant bioavailable form in the soluble one. The high surface reactivity of NPs precludes the possibility to predict the processes at the NP–cell interface relying only on the chemical composition and molecular structure of the material, as it is for water soluble compounds (Fubini, 1997). Thus, in recent years, the scientific community has been developing guidelines for the ecological risk assessment of ENMs, in order to assure the accuracy and reproducibility of nanoecotoxicology test results (Peijnenburg et al., 2015; Petersen et al., 2015; Scott-Fordsmand et al., 2017; OECD 317, 2021).

One of the main concerns of nanotoxicology is the correct quantification of NPs exposure during bioassays (Petersen et al., 2015). Due to their 'particulate' nature, NPs in the aquatic environment are subject to aggregation, precipitation and/or dissolution, that can drastically change which environmental compartments and organisms are affected. The behaviour in exposure media is related

both to NPs characteristics (*e.g.,* coating, size, shape, number of particles, …) and characteristics of the surrounding media (*e.g.,* ionic strength, divalent and trivalent ions, organic matter, temperature, light, …). To add further complexity, NPs were observed to develop a layer of tightly bound proteins on their surface when dispersed in biological fluids (bio-corona) or of high molecular weight biopolymers when in complex aquatic media such as seawater (eco-corona), deeply influencing their behaviour and toxicity (Monopoli et al., 2013; Grassi et al., 2020).

As pointed out by Scott-Fordsman et al. (2017), current regulatory risk assessments are lacking a sufficient description of the material characteristics, as well as that of NPs behaviour. Such knowledge gaps are limiting the correct design of fate and exposure models. The interaction with organisms is, in fact, a consequence of NPs behaviour in exposure media. At the cellular level, the uptake of NPs is first characterized by adhesion to cells, which is driven both by cell membrane/wall characteristics and by the physical chemical properties of NPs and their associated eco-/bio-coronas, which, in turn, depend on the surrounding environment and NPs interaction with natural and biological molecules. All these factors concur to define NPs identity to the biological systems and govern the recognition by membrane receptors, thus regulating their uptake and toxicity, as widely described in human cell models (Handy et al., 2008; Lesniak et al., 2012). All these bio-nano interactions contribute to the complex dynamics that are mandatory to be considered when performing bioassays in order to obtain a more realistic risk assessment of NPs exposure and effects in the natural environment (Corsi et al., 2020) (Figure 1).

Among the large variety of NPs applied in the industry and in consumer products, two were chosen for this study: polystyrene nanoparticles (PS NPs) and silver nanoparticles (AgNPs). Being profoundly different from each other, they perfectly fulfil the first purpose of this research, which is to investigate the interactions of ENPs with biota and how these play a role in defining the toxic mode of action of nanoparticles. Both have peculiar characteristics and are highly representative for, respectively, a category of emerging contaminants of concern such as nanoplastics, and the most abundantly produced ENM known as metallic NPs.

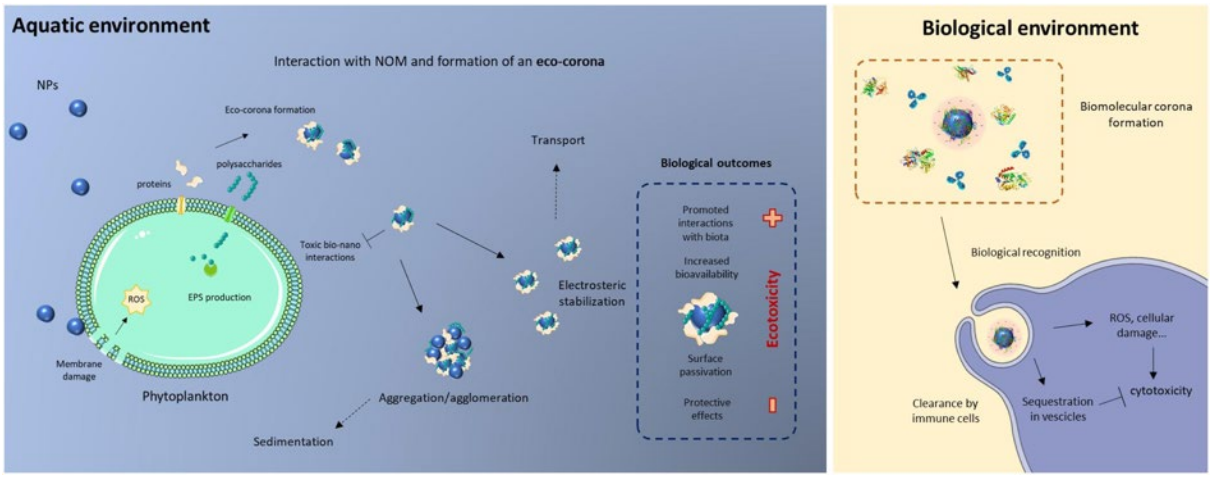


**Figure 1.** Schematic illustration of the bio-nano interactions taking place in the aquatic and biological environment. Left: possible interactions between nanoparticles (NPs) dispersed water and biomolecules making up the natural organic matter pool (NOM), such as microalgal/cyanobacterial extracellular polymeric substances (EPS). Right: the cellular processes following biomolecular corona formation in biological fluids of invertebrate organisms. From Corsi et al., (2020).

Nanoplastics are considered to be mainly a by-product of the fragmentation of plastic debris dispersed in the environment and of industrial processes, hence their characteristics are hardly manageable. In this case, research is needed for the understanding of the hazard, present and future, posed by a group of contaminants which are, for most parts, still unknown.

Ag NPs, instead, thanks to the possibility of tuning their properties at will, are produced and applied in many different fields, among which the environmental applications are growing. Their use in environmental remediation is promising, in terms of sensitivity e specificity, but their synthesis must be carefully designed in order to overcome any possible adverse outcome linked to AgNPs intrinsic toxicity.

## 1. Polystyrene Nanoparticles

Polymeric NPs are incorporated in consumer and manufacturing products, from biosensors to cosmetics and drug delivery devices (Velev and Kaler, 1999; Jiménez-Fernández et al., 2014; Hernandez et al., 2017). Their release in natural aquatic systems from wastewater treatment plants (WWTP) has been documented (Blair et al., 2017) as well as the *in situ* formation of nano-sized fragments from

breakdown processes (*e.g.,* fragmentation) of a wide variety of synthetic polymers under environmentally relevant conditions (*e.g.,* UV radiations, high temperatures, mechanical processes and biota) (Lambert and Wagner, 2016; Dawson et al., 2018). According to the latest definition, are considered nanoplastics all fragments of synthetic or heavily-modified natural polymers with sizes between 1 and 1000 nm (Hartmann et al., 2019).

In recent years, the occurrence of nanoplastics in natural waters has been demonstrated by Ter Halle et al. (2017) and Schirinzi et al. (2019) by detecting nano-sized (< 1 μm) polymeric fragments in estuarine and marine surface waters. Due to technological limitations, their quantification in the natural environment is still a challenge, thus a concentration range to which refer for environmentally realistic ecotoxicological studies is still under debate. Predicted environmental concentrations (PECs) are estimated to be in the range between 1 pg/L and 20 μg/L approximately (Lenz et al., 2016), which is above reported hazard/effect concentrations (from 0.1 mg/L to >100 mg/L) (Chae and An, 2017; Corsi et al., 2020; Corsi et al., 2021). However, given the extremely limited data, real environmental concentrations for nano-sized polymers could exceed PECs, especially in areas highly impacted by plastic pollution, thus approaching toxicity thresholds. Also, PECs are expected to increase based on growing production and application of nano-enabled products as well as fragmentations of larger plastic fragments already present in the aquatic environment (Andrady, 2017).

Polystyrene nanoparticles (PS NPs) have been widely used as a proxy for nanoplastic behaviour and toxicity to aquatic organisms. As extensively discussed through the literature (Wu et al., 2019; Corsi et al., 2020; Corsi et al., 2021), PS NPs behaviour in the aquatic environment is deeply influenced by media ionic strength and NP surface charge. For instance, in high ionic strength media such as seawater (35–40 ‰), PS NPs with negative surface charge (either plain or carboxy-modified) usually form aggregates in the μm-size range, while positively charged PS NPs (as for instance amino-modified -$NH_2$) generally maintain their nm-size (Bergami et al., 2016). In low ionic strength media such as freshwaters, PS NPs, of both positive and negative surface charge, usually avoid aggregating behaviours, keeping their nano-size (Bellingeri et al., 2019). On the other hand, in seawater, positively charged PS NPs exhibit an

aggregating behaviour in the presence of dissolved organic matter (DOM), while the aggregation of their negative counterparts is not influenced by DOM (Wu et al., 2019) or seems to be reduced (Grassi et al., 2020).

When DOM is involved, the resulting nanoplastic behaviour is not easy to predict as it is linked to the variability and the complex interactions with DOM functional groups and dissolved ions. The ionic strength of water media, again, adds further complexity. Natarajan and at al. (2020), reported a gradual increase of PS NPs hydrodynamic diameter (from ~250 to ~500 nm) in freshwater media due to the formation of an eco-corona upon their incubation with algal exudates for 12, 24 and 48 h. Conversely, Grassi et al. (2020) observed a reduction in the aggregating behaviour of PS NPs (from ~850 to ~650 nm) in seawater supplied with algal exudates, probably due to changes in NPs surface charge caused by exudates adsorption. Cai et al. (2018) report that PS NPs aggregation, also as a consequence of the interaction with DOM, is enhanced and coordinated by ions with higher valences, with elements such as calcium and iron having a higher aggregating potential compared to sodium.

The main source of DOM, which constitutes a large portion of the ocean bioavailable carbon pool and an important carbon source for filter- and deposit-feeders, are the extracellular polymeric substances (EPSs) excreted by phytoplankton and bacteria. Microalgae, as well as other organisms such as bacteria, cyanobacteria, fungi and yeasts can excrete exopolysaccharides (EPS), which are mainly constituted of long-chain polysaccharides, macromolecules belonging to the carbohydrate group, proteins and DNA. The production of EPS by microorganisms is responsible for important processes, such as organic aggregate formation, microbial colonization, and pollutant mobility (Decho, 1990; Decho and Gutierrez, 2017).

EPSs have been widely shown to interact with environmental pollutants, such as metals and organic molecules and, ultimately, also plastic and ENMs (Koukal et al., 2007; Miao et al., 2009; Quigg et al., 2013; Paquet et al., 2015; González-Fernández et al., 2019). The exposure of phytoplankton to PS NPs was observed to increase the protein-to-carbohydrate ratio (P/C) of excreted EPS, leading to the production of a matrix with increased stickiness (Shiu et al., 2020a). Depending on physico-chemical

conditions (pH, temperature, UV light, etc.) and DOM composition, DOM can organize in aggregates of >0.7 µm to form particulate organic matter (POM) (Decho and Gutierrez, 2017). Since DOM polymers are amphiphilic, their assemblage into microgels and consequent formation of POM is believed to be driven by both hydrophobic interactions and $Ca^{2+}$ bridging. The hydrophobic domains, mainly owned by proteins, are those involved in the interaction with the plastic surface. The assembly of microgels from EPS excreted by various phytoplankton species is induced and accelerated by PS NPs. This was shown to have a positive correlation to the protein content of EPS and brought to the formation of bigger aggregates compared to the absence of NPs (Chen et al., 2011; Shiu et al., 2020b). In this context, an alteration of the DOM-POM transition process could take place, together with the incorporation of nanoplastics inside biogenic aggregates. This might have implications for the vertical transport in the water column of both nanoplastics and organic aggregates (Long et al., 2015; Porter et al., 2018) (Figure 2).

Both micro- and nanoplastics entering marine ecosystems may incorporate into marine organic aggregates composed by biopolymers and phytoplankton, giving rise to the formation of hetero-aggregates (Michels et al., 2018; Cunha et al., 2019). The incorporation of nanoplastics and MPs within biogenic aggregates was demonstrated in laboratory generated marine snow and shown to mutually alter the behaviour of both plastics and marine snow. For instance, depending on the relative density of MPs, marine snow aggregates with incorporated MPs were observed to sank slower or faster than their counterparts with no MPs, while, for instance, promoting the transport to the benthic environment also of those polymers (*e.g.,* low-density MPs) that would otherwise float near the sea surface (Long et al., 2015; Porter et al., 2018). Some studies also demonstrated that this process greatly increased the ingestion of micro and nanoplastics by benthic filter feeders, causing the uptake of MPs up until 300 times more compared to the exposure to MPs in a marine snow-free medium (Ward and Kach, 2009; Porter et al., 2018) (Figure 2).

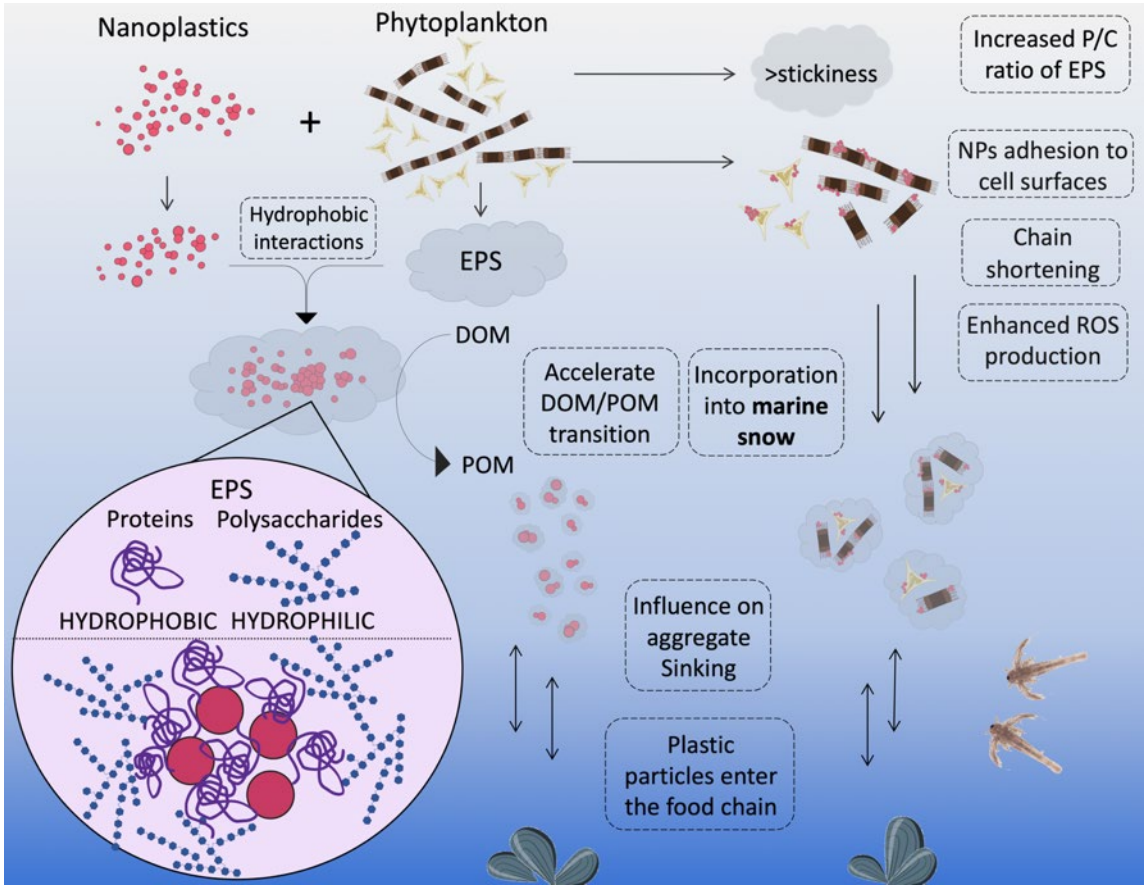


**Figure 2.** Schematic illustration of nanoplastic interactions with phytoplankton and EPS (exopolysaccharides) and resulting effects on their mutual fate.

Surface charge of PS NPs plays a role also in their bio-interaction and toxicity. Amino-modified positively charged PS NPs (PS-$NH_2$ NPs) result in higher toxicity compared to plain and carboxy-modified negatively charged PS NPs (PS-COOH NPs) (Figure 3). This is, in part, due to the different aggregating behaviour, which is directly linked to toxicity by influencing the overall size of the particles/aggregates: single particles and small aggregates are, in fact, able to cross cell membranes and reach internal compartments of cells and organs as opposed to bigger ones (Sendra et al., 2020).

PS NPs toxicity to phytoplankton species includes the inhibition of cell growth, physical adhesion and malformations, the impairment of membrane long-chain fatty acids, decrease of pigment content and photosynthetic yield as well as enhanced reactive oxygen species (ROS) production (Bergami et al., 2017; González-Fernández et al., 2019; Bellingeri et al., 2020; Gao et al., 2021). Although toxicity data are variable, negatively charged PS NPs exposure is usually associated to limited toxicity (Bergami et al.,

2017; Bellingeri et al., 2019; Sendra et al., 2019; Yi et al., 2019; Bellingeri et al., 2020) with no lethal outcomes up to very high concentrations (250-1000 mg/L) (Besseling et al., 2014; Sjollema et al., 2016); on the opposite, the more severe effects (*e.g.*, inhibition of algal growth and photosynthetic activity) are usually associated to positively charged PS NPs (*e.g.*, PS-$NH_2$) (Bergami et al., 2017).

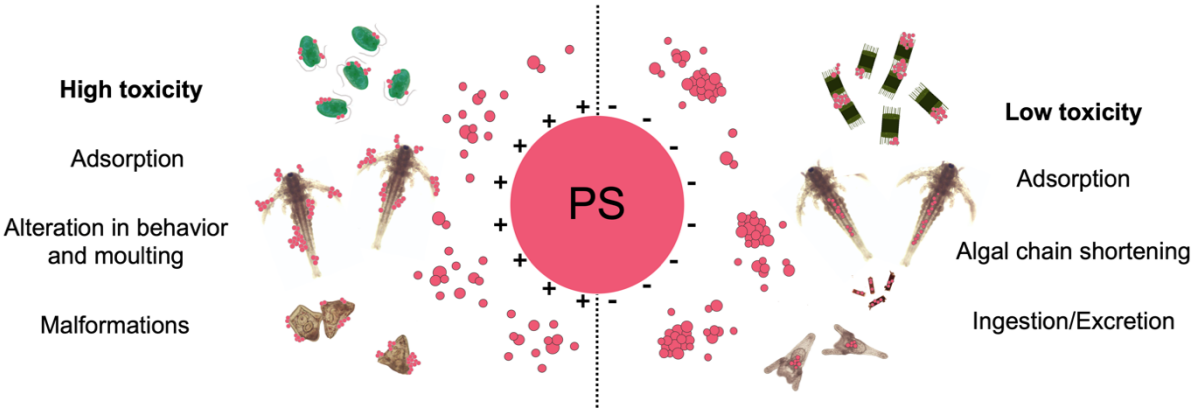


**Figure 3.** Behaviour and major known toxic effects of PS NPs having positive (left) and negative (right) surface charge to model marine plankton species (microalgae, brine shrimps and sea urchin larve). From Corsi et al., (2021).

The same trend is observed for zooplankton, to which the main outcome of negatively charged NPs exposure is the ingestion and accumulation inside the digestive tract, usually followed by egestion, with no significant reported mortality in acute exposures (Bergami et al., 2016; Gambardella et al., 2017; Manfra et al., 2017). PS-$NH_2$ instead, were reported to cause mortality, physiological alterations and neurotoxicity at lower concentrations ($EC_{50}$<5 mg/L) in zooplankton, mussels, oysters and sea urchin larvae and coelomocytes (Della Torre et al., 2014; Bergami et al., 2016; Balbi et al., 2017; Bergami et al., 2017; Tallec et al., 2018; Bergami et al., 2019; Varó et al., 2019).

The reported differences in toxicity among studies are in part due to different species sensitivity but also to the high variability existing among nanoplastics. Though most of the studies use PS NPs, the variability posed by different surface functional groups and consequent charge, sizes, and, especially,

chemicals associated to the NPs suspensions, play a fundamental role in determining the toxicity outcome.

The importance of considering the effects of chemicals present in NPs suspension or associated to the NPs themselves was recently highlighted. Many of the toxic effects recorded upon exposure to primary nanoplastics (*i.e.,* nanoplastics that were produced in their nano-size) were observed to be linked to the leaching or dispersions of chemicals included in NPs suspensions, such as surfactants, antimicrobials, monomers or non-covalently bound fluorescent chromophores. This could bring to an overestimation of the toxicity associated to the NPs (Pikuda et al., 2018).

## 2. Silver Nanoparticles

Silver nanoparticles (AgNPs) are recognized as being one the most widely used type of NPs in consumer products, especially for their efficient antimicrobial properties. Their fields of application are growing and thanks to their unique properties, AgNPs can be used for many different purposes, as in electronic devices, as anticancer agents, and for water pollution sensoring and remediation (Prosposito et al., 2016; Syafiuddin et al., 2017).

Consequently, they can end up in the aquatic environment, mainly from wastewater treatment plants (WWTPs) in which they have been estimated to reach concentrations in the range of ng–µg $L^{-1}$ (Cervantes-Avilés et al., 2019). However, according to the study of Nabi and at al. (2021) on five WWTPs in the United States, a high removal efficiency towards AgNPs (82-95%) was shown, with an effluent concentration range of 0.008–0.04 µg $L^{-1}$. Previously, Li et al. (2016) also reported a high removal efficiency for AgNPs in a WWTP in Germany (up to 96.4%), but the estimated annual release in the effluent was still high (~33 Kg of AgNPs). It appears that the smaller AgNPs are more likely to escape the treatment process, being consequently released in effluents, with an overall reduction in size from influent to effluent. Cervantes-Avilès and at al. (2019) report a reduced average size of AgNPs, from 100-200 nm to 50 nm, while Nabi and at al. (2021) report that more than 99% of AgNPs in effluents are smaller than 100 nm. A reduced size of NPs has often been associated with a higher risk of cellular

internalization and whole organism toxicity (Lankoff et al., 2012; Tsiola et al., 2017). For instance, in cellular exposure, the degree of agglomeration and thus the overall size of AgNPs was correlated to a different cellular localization, with smaller particles/aggregates being able to reach nuclear and mitochondrial compartments (Lankoff et al., 2012).

One of the main features influencing AgNP aquatic behaviour and toxicity is their ability to release Ag ions (Dong et al., 2017), known among the most toxic for aquatic species (Ratte, 1999). The dissolution of AgNPs firstly depends on intrinsic features of the particles, but also, and to a great extent, on extrinsic ones, such as physico-chemical properties of the receiving environment. AgNPs are one of the best examples of how experimental and environmental conditions are able to completely change the behavior and consequent toxicity of ENPs (Figure 3) (McLaughlin and Bonzongo, 2012; Lish et al., 2019). Using laboratory prepared synthetic media, Lish et al. (2019) observed that an increase in salinity corresponded to an increase in Ag ions release. However, this was not followed by an enhanced toxicity since Ag ions are bound by chloride species, thus reducing their bioavailability. $Cl^-$ is considered a weak Ag ligand, whose influence on AgNP dissolution, $Ag^+$ bioavailability and consequent toxicity, may vary according to Ag/Cl ratio, leading to non-linear biological responses with sometimes more severe effects at lower Ag concentrations (Levard et al., 2012; Li et al., 2020). The presence of oxidizing agents, such as dissolved oxygen and free Ag ligands, as well as other external factors such as low pH, can trigger the dissolution of AgNPs. Hydrogen peroxide ($H_2O_2$), which can also be produced by organisms together with other oxidizing molecules, was shown to greatly enhance the dissolution of AgNPs (Sigg and Lindauer, 2015). Organic matter rich in sulfur and nitrogen, such as humic and fulvic acids, plays a crucial role in natural waters against AgNP dissolution (Gunsolus et al., 2015), which results in a reduced toxicity (Kennedy et al., 2012). Similarly, a reduced dissolution and toxicity is associated to surface coatings composed of sulfur or sulfur containing molecules (Levard et al., 2013), such as cysteine (Prosposito et al., 2019), while, on the contrary, free cysteine was shown to induce AgNP dissolution (Gondikas et al., 2012). As summarized in figure 4, AgNP ecotoxicity is usually higher in freshwaters

compared to marine species, due to the aforementioned mitigating effect of chloride species, and is further lowered by the presence of organic matter.

A partial control of ion release can be obtained with surface functionalization. Literature reports tens of differently surface functionalized types of AgNPs, associated to a highly variable degree of particle dissolution (Gondikas et al., 2012; Schiavo et al., 2017; Wu et al., 2017; Lekamge et al., 2019). Surface coating reduces the particle contact with oxidizing agents, such as dissolved oxygen and reactive oxygen species (ROS), reducing the chances and the degree of dissolution. In addition, it also plays an indirect role, driving aggregation and surface charge which, in turn, influence the extent of the surface available for dissolution and the interaction with other molecules and organisms. Also, some types of coatings, such as those composed of molecules with reduced sulphur groups, are observed to be directly linked to a reduced toxicity (Levard et al., 2013; Pem et al., 2019).

Since there are many features able to influence AgNP toxicity (Figure 4), there is often no common field about which are the main driving forces of the observed negative effects to aquatic organisms. Dissolution rate and toxicity do not always go together as released ions often undergo chemical transformations depending on water chemistry, reducing their bioavailability, as demonstrated by Lish et al. (2019). In other circumstances, toxicity seems to be the result of more complex dynamics, being higher than what expected based on AgNP dissolution rate, leading to the hypothesis of a NP-specific toxicity (Malysheva et al., 2016; Kleiven et al., 2019). Some studies assign all the observed toxic effects to dissolved Ag while some others report an additional toxicity which they attribute to the nano-size. It is interestingly pointed out by Yang et al. (2012) how most studies reporting a dissolved Ag related toxicity are performed on multicellular organisms, while those claiming additional effects tested single cell organisms. Direct contact with single cells is often related to the production of exudates with oxidative potential, or even cellular internalization, leading to a possible additive toxicity.

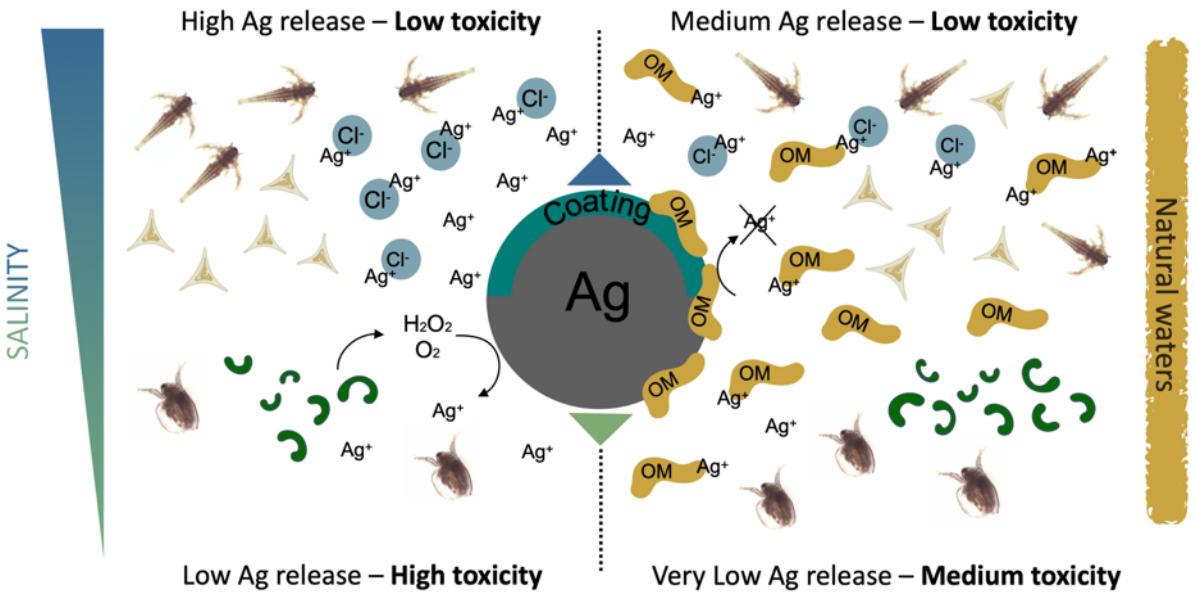


**Figure 4.** Release of Ag ions from AgNPs and toxicity to aquatic plankton organisms as influenced by environmental conditions and water chemistry. (OM: Organic Matter). (From Corsi et al., 2021).

All the previously described dynamics result in an extremely wide effect concentration range for AgNPs ($EC_{50}$ range from 1 µg $L^{-1}$ to >100 mg $L^{-1}$) (Angel et al., 2013; Becaro et al., 2015; Kos et al., 2016; Schiavo et al., 2017; Sendra et al., 2017; Tsiola et al., 2017; An et al., 2019; Lish et al., 2019; Dedman et al., 2020): this is due to their many different features and to the high variability of exposure conditions, both deeply influencing their behaviour and toxicity. But it is also caused by the big discrepancy between short-term and environmentally relevant chronic exposure scenarios (McLaughlin and Bonzongo, 2012; Dalzon et al., 2020) posing uncertainties for a realistic AgNP risk assessment (Lead et al., 2018). Although PECs (≤ µg $L^{-1}$) (Maurer-Jones et al., 2013; Lazareva and Keller, 2014) and reported effect concentrations rarely overlap, the increasing use and production of AgNPs as, for instance, sanitizing agents and antimicrobial textiles, also linked to the current sanitary emergency of COVID-19 worldwide pandemic (Hamouda et al., 2021; Valdez-Salas et al., 2021), could easily contribute in the near future to an increase of the PECs and associated risks (Syafiuddin et al., 2017).

## DISCLOSING ENMS EFFECTS TO AQUATIC ORGANISMS: THE IMPORTANCE OF SUB-LETHAL EFFECTS AND CHRONIC EXPOSURE

There is great debate in the scientific community about whether the environmental risk assessment of ENMs should focus on ecotoxicological studies using *in vitro* or *in vivo* tests and acute or chronic exposures, the latter being more environmentally realistic. Each method brings useful information, however, as said above, exposure conditions are of fundamental importance for assessing the potential risks associated to ENMs (*e.g.*, behaviour and bio-interaction). ENMs are expected to undergo numerous transformations when released into the natural environment, hence, their final form when reaching biota, either cells or whole organism, is unknown and can only be hypothesized. As reported by Grassi et al. (2020), the concept of the biomolecular corona acquires different connotations when applied to complex aquatic media as natural waters. Such so-called eco-corona, being usually composed of high molecular weight biopolymers, could be playing a more crucial role, compared to the biocorona, in defining the biological identity and behaviour of ENMs.

As allowed by technical limitations, ecotoxicological studies should mimic the characteristics of ENMs which are expected to be found in the natural aquatic environment. For instance, nanoplastics originating from fragmentation and weathering in the marine environment are expected to be negatively charged due to surface oxidation caused by UV-light and acquisition of functionalities such as carbonyl and carboxyl groups (Fotopoulou and Karapanagioti 2012; Gigault et al., 2016; Andrady, 2017; Lehner et al., 2019). The use of PS-COOH NPs should, hence, be considered more environmentally relevant as opposed to virgin PS NPs and $NH_2$-PS NPs which are less expected to be found in the natural environment.

Environmental interactions occurring in the aquatic media, including adsorption of existing pollutants or biological molecules (*i.e.,* EPS as mentioned above), can be able to significantly affect nanoplastics behaviour and biological effects. A recent study conducted using environmental nanoplastics obtained from weathered microplastics collected from the North Atlantic gyre showed more harmful effects to the marine diatom *Thalassiosira weissiflogii* compared to virgin ones (Baudrimont et al., 2020). The

heavy metals adsorbed on the surface of weathered nanoplastics were considered responsible for the observed higher toxicity rather than their nanoscale or polymeric properties.

More studies should focus on understanding such processes, starting from adhesion dynamics and temporal changes towards chemical and biological entities. Often, the exposure to ENMs, especially plastic NPs, results in side-effects which are usually not considered in standardized ecotoxicological protocols but could give us insights on possible ecological implications of the exposure. The physical impact of ENMs, as surface adhesion to organisms or gastric hindrance following ingestion, which are usually overlooked as toxicity endpoints, could be involved in determining chronic toxicity. The aforementioned affinity of EPS for the plastic surface is probably also involved in the documented adhesion of nanoplastics to phytoplankton cells. In fact, the adsorption of PS NPs on microalgae, as well as microcrustaceans, has been often documented (Bergami et al., 2016; Bergami et al., 2017; Nolte et al., 2017; Zhang et al., 2017; Bellingeri et al., 2019; Bellingeri et al., 2020) and, besides representing an entrance door to the food webs, gave insights on possible side-effects to be looking at when studying ENMs toxicity.

Although PS NPs have usually no or little effects on algal growth under standardized toxicity protocols (72 h), Hazeem and at al. (2020) observed a size-dependent inhibition of algal growth with associated increase in ROS production and photosynthesis impairment upon prolonged (38 days) exposure. The interaction at membrane level and adhesion of NPs to the cell surface caused morphological alteration and the shrinkage of cells, while the associated stress was probably the cause of a shift in EPS composition towards a higher protein content, as reported also by Shiu and at al. (2020a).

It is worth noting that most microcrustacean and microalgal toxicity studies are generally based on 48 or 72h exposures, and that the sub-lethal effects (*e.g.,* surface adhesion or ROS production) could result in dramatic outcomes in a more environmentally relevant scenario of prolonged exposure (Figure 5).

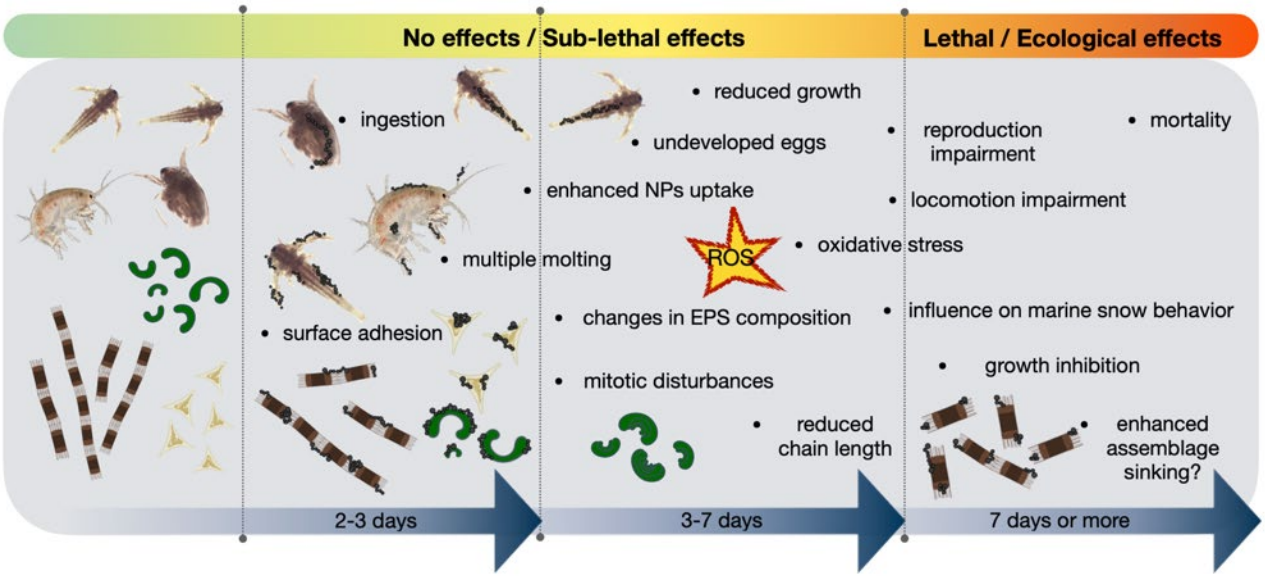


**Figure 5.** Examples of the subsequent toxic effects, from no or sub-lethal effects to lethal effects, to phyto and zooplankton upon NP exposure through time, from short (48–72h) to long (7+ days) term exposure. Not to scale.

As previously reported, the surface chemistry of ENMs often plays a more important role than the core constituents in establishing their acute toxicity. Mehennaoui and at al. (2018) observed the coating-dependent uptake of citrate (Cit) and polyethylene glycol (PEG) coated Ag and Au NPs by the amphipod *Gammarus fossarum*: the uptake was, in fact, higher for Cit-coated NPs compared to PEG-coated, regardless of their core constituents (*i.e.,* Ag and Au). The same trend was followed by the detection of NPs onto the cuticle of the amphipods, higher for Cit-coated NPs, leading to hypothesize that the enhanced uptake was driven by surface adhesion. Even if no acute (72 h) toxicity was recorded, in a subsequent study (Mehennaoui et al., 2021) a reduction in locomotion activity was recorded after a prolonged exposure (15 d) and hypothesized to be linked to a sensorial disruption due to the NPs adhesion to the appendages and body surface of *G. fossarum*.

Similarly, Lai and at al. (2021) compared the toxicity of differently coated Zinc NPs (ZnNPs) to the marine copepod *Tigriopus japonicus* and observed that a higher hydrophilicity of the coating caused a higher affinity of the ZnNPs for the copepod exoskeleton. These hydrophilic ZnNPs, despite the lower release of Zn ions compared to the hydrophobic ones, resulted in higher toxicity after chronic (21 d) but not

after acute (96 h) exposure, confirming the importance of chronic exposure as well that of the investigation of sub-lethal effects.

Another example is reported by two studies by Bergami et al. (2016; 2017) which observed the adhesion of positively charged PS-$NH_2$ NPs to the body surface of the brine shrimp *Artemia* and a consequent increase in the molting events in the 48 h, but no mortality. With a longer exposure period (14 d), however, a pronounced reduction in growth and increased mortality were observed, which were hypothesized to be linked to the higher energy demand caused by multiple molting in the attempt of getting rid of the physical adhesion of the PS NPs to the body surface.

These examples highlight the importance of focusing on sub-lethal effects as early warning signs in the evaluation of the ecotoxicological potential of ENMs, while a prolonged exposure should always be included in order to mimic real environmental scenarios. These strategies will help to obtain more environmentally relevant data and avoid the risk of underestimating the potential threat posed by certain pollutants, such as ENMs, to ecosystems.

## REFERENCES


An HJ, Sarkheil M, Park HS, Yu IJ, Johari SA (2019): Comparative toxicity of silver nanoparticles (AgNPs) and silver nanowires (AgNWs) on saltwater microcrustacean, *Artemia salina*. Comparative Biochemistry and Physiology Part C: Toxicology & Pharmacology 218, 62-69

Andrady AL (2017): The plastic in microplastics: a review. Marine Pollution Bulletin 119, 12-22

Angel BM, Batley GE, Jarolimek CV, Rogers NJ (2013): The impact of size on the fate and toxicity of nanoparticulate silver in aquatic systems. Chemosphere 93, 359-365

Balbi T, Camisassi G, Montagna M, Fabbri R, Franzellitti S, Carbone C, Dawson K, Canesi L (2017): Impact of cationic polystyrene nanoparticles (PS-NH2) on early embryo development of *Mytilus galloprovincialis*: Effects on shell formation. Chemosphere 186, 1-9

Baudrimont M, Arini A, Guégan C, Venel Z, Gigault J, Pedrono B, Prunier J, Maurice L, Ter Halle A, Feurtet-Mazel A (2020): Ecotoxicity of polyethylene nanoplastics from the North Atlantic oceanic gyre on freshwater and marine organisms (microalgae and filter-feeding bivalves). Environmental Science and Pollution Research 27, 3746-3755

Becaro AA, Jonsson CM, Puti FC, Siqueira MC, Mattoso LH, Correa DS, Ferreira MD (2015): Toxicity of PVA-stabilized silver nanoparticles to algae and microcrustaceans. Environmental Nanotechnology, Monitoring & Management 3, 22-29

Bellingeri A, Bergami E, Grassi G, Faleri C, Redondo-Hasselerharm P, Koelmans AA, Corsi I (2019): Combined effects of nanoplastics and copper on the freshwater alga Raphidocelis subcapitata. Aquatic Toxicology 210, 179-187

Bellingeri A, Casabianca S, Capellacci S, Faleri C, Paccagnini E, Lupetti P, Koelmans AA, Penna A, Corsi I (2020): Impact of polystyrene nanoparticles on marine diatom *Skeletonema marinoi* chain assemblages and consequences on their ecological role in marine ecosystems. Environmental Pollution 262, 114268

Bergami E, Bocci E, Vannuccini ML, Monopoli M, Salvati A, Dawson KA, Corsi I (2016): Nano-sized polystyrene affects feeding, behavior and physiology of brine shrimp *Artemia franciscana* larvae. Ecotoxicology and Environmental Safety 123, 18-25

Bergami E, Pugnalini S, Vannuccini M, Manfra L, Faleri C, Savorelli F, Dawson K, Corsi I (2017): Long-term toxicity of surface-charged polystyrene nanoplastics to marine planktonic species *Dunaliella tertiolecta* and *Artemia franciscana*. Aquatic Toxicology 189, 159-169

Bergami E, Emerenciano AK, González-Aravena M, Cárdenas C, Hernández P, Silva J, Corsi I (2019): Polystyrene nanoparticles affect the innate immune system of the Antarctic sea urchin *Sterechinus neumayeri*. Polar Biology 42, 743-757

Besseling E, Wang B, Lürling M, Koelmans AA (2014): Nanoplastic affects growth of *S. obliquus* and reproduction of *D. magna*. Environmental Science & Technology 48, 12336-12343

Blair RM, Waldron S, Phoenix V, Gauchotte-Lindsay C (2017): Micro-and nanoplastic pollution of freshwater and wastewater treatment systems. Springer Science Reviews 5, 19-30

BSI (2007): Terminology for Nanomaterials. In: Insitution BS (Hrsg.). PAS, London

Cai L, Hu L, Shi H, Ye J, Zhang Y, Kim H (2018): Effects of inorganic ions and natural organic matter on the aggregation of nanoplastics. Chemosphere 197, 142-151

Cervantes-Avilés P, Huang Y, Keller AA (2019): Multi-technique approach to study the stability of silver nanoparticles at predicted environmental concentrations in wastewater. Water Research 166, 115072

Chae Y, An Y-J (2017): Effects of micro-and nanoplastics on aquatic ecosystems: Current research trends and perspectives. Marine Pollution Bulletin 124, 624-632

Chen C-S, Anaya JM, Zhang S, Spurgin J, Chuang C-Y, Xu C, Miao A-J, Chen EY, Schwehr KA, Jiang Y (2011): Effects of engineered nanoparticles on the assembly of exopolymeric substances from phytoplankton. PLoS One 6, e21865

Corsi I, Bergami E, Grassi G (2020): Behavior and bio-interactions of anthropogenic particles in marine environment for a more realistic ecological risk assessment. Frontiers in Environmental Science 8, 60

Corsi I, Bellingeri A, Eliso MC, Grassi G, Liberatori G, Murano C, Sturba L, Vannuccini ML, Bergami E (2021): Eco-interactions of engineered nanomaterials in the marine environment: Towards an eco-design framework. Nanomaterials 11, 1903

Cunha C, Faria M, Nogueira N, Ferreira A, Cordeiro N (2019): Marine vs freshwater microalgae exopolymers as biosolutions to microplastics pollution. Environmental Pollution 249, 372-380

Dalzon B, Aude-Garcia C, Diemer H, Bons J, Marie-Desvergne C, Pérard J, Dubosson M, Collin-Faure V, Carapito C, Cianférani S (2020): The longer the worse: a combined proteomic and targeted study of the long-term versus short-term effects of silver nanoparticles on macrophages. Environmental Science: Nano 7, 2032-2046

Dawson AL, Kawaguchi S, King CK, Townsend KA, King R, Huston WM, Nash SMB (2018): Turning microplastics into nanoplastics through digestive fragmentation by antarctic krill. Nature Communications 9, 1001

Decho AW (1990): Microbial exopolymer secretions in ocean environments: their role (s) in food webs and marine processes. Oceanography and Marine Biology Annual Review 28, 73-153

Decho AW, Gutierrez T (2017): Microbial extracellular polymeric substances (EPSs) in ocean systems. Frontiers in Microbiology 8, 922

Dedman CJ, Newson GC, Davies G-L, Christie-Oleza JA (2020): Mechanisms of silver nanoparticle toxicity on the marine cyanobacterium *Prochlorococcus* under environmentally-relevant conditions. Science of The Total Environment 747, 141229

Della Torre C, Bergami E, Salvati A, Faleri C, Cirino P, Dawson K, Corsi I (2014): Accumulation and embryotoxicity of polystyrene nanoparticles at early stage of development of sea urchin embryos *Paracentrotus lividus.* Environmental Science & Technology 48, 12302-12311

Dong F, Mohd Zaidi NF, Valsami-Jones E, Kreft J-U (2017): Time-resolved toxicity study reveals the dynamic interactions between uncoated silver nanoparticles and bacteria. Nanotoxicology 11, 637-646

Fubini B (1997): Surface reactivity in the pathogenic response to particulates. Environmental Health Perspectives 105, 1013-1020

Gambardella C, Morgana S, Ferrando S, Bramini M, Piazza V, Costa E, Garaventa F, Faimali M (2017): Effects of polystyrene microbeads in marine planktonic crustaceans. Ecotoxicology and Environmental Safety 145, 250-257

Gao G, Zhao X, Jin P, Gao K, Beardall J (2021): Current understanding and challenges for aquatic primary producers in a world with rising micro-and nano-plastic levels. Journal of Hazardous Materials 406, 124685

Gondikas AP, Morris A, Reinsch BC, Marinakos SM, Lowry GV, Hsu-Kim H (2012): Cysteine-induced modifications of zero-valent silver nanomaterials: implications for particle

surface chemistry, aggregation, dissolution, and silver speciation. Environmental Science & Technology 46, 7037-7045

González-Fernández C, Toullec J, Lambert C, Le Goïc N, Seoane M, Moriceau B, Huvet A, Berchel M, Vincent D, Courcot L (2019): Do transparent exopolymeric particles (TEP) affect the toxicity of nanoplastics on *Chaetoceros neogracile*? Environmental Pollution 250, 873-882

Grassi G, Gabellieri E, Cioni P, Paccagnini E, Faleri C, Lupetti P, Corsi I, Morelli E (2020): Interplay between extracellular polymeric substances (EPS) from a marine diatom and model nanoplastic through eco-corona formation. Science of The Total Environment 725, 138457

Gunsolus IL, Mousavi MP, Hussein K, Bühlmann P, Haynes CL (2015): Effects of humic and fulvic acids on silver nanoparticle stability, dissolution, and toxicity. Environmental Science & Technology 49, 8078-8086

Hamouda T, Ibrahim HM, Kafafy H, Mashaly H, Mohamed NH, Aly NM (2021): Preparation of cellulose-based wipes treated with antimicrobial and antiviral silver nanoparticles as novel effective high-performance coronavirus fighter. International Journal of Biological Macromolecules 181, 990-1002

Handy RD, Owen R, Valsami-Jones E (2008): The ecotoxicology of nanoparticles and nanomaterials: current status, knowledge gaps, challenges, and future needs. Ecotoxicology 17, 315-325

Hartmann NB, Huffer T, Thompson RC, Hassellöv M, Verschoor A, Daugaard AE, Rist S, Karlsson T, Brennholt N, Cole M (2019): Are we speaking the same language? Recommendations for a definition and categorization framework for plastic debris. Environmental Science & Technology 53, 1039-1047

Hazeem LJ, Yesilay G, Bououdina M, Perna S, Cetin D, Suludere Z, Barras A, Boukherroub R (2020): Investigation of the toxic effects of different polystyrene micro-and nanoplastics on microalgae *Chlorella vulgaris* by analysis of cell viability, pigment content, oxidative stress and ultrastructural changes. Marine Pollution Bulletin 156, 111278

Hernandez LM, Yousefi N, Tufenkji N (2017): Are there nanoplastics in your personal care products? Environmental Science & Technology Letters 4, 280-285

Jiménez-Fernández E, Ruyra A, Roher N, Zuasti E, Infante C, Fernández-Díaz C (2014): Nanoparticles as a novel delivery system for vitamin C administration in aquaculture. Aquaculture 432, 426-433

Kennedy AJ, Chappell MA, Bednar AJ, Ryan AC, Laird JG, Stanley JK, Steevens JA (2012): Impact of organic carbon on the stability and toxicity of fresh and stored silver nanoparticles. Environmental Science & Technology 46, 10772-10780

Klaine SJ, Alvarez PJ, Batley GE, Fernandes TF, Handy RD, Lyon DY, Mahendra S, McLaughlin MJ, Lead JR (2008): Nanomaterials in the environment: behavior, fate, bioavailability, and effects. Environmental Toxicology and Chemistry: An International Journal 27, 1825-1851

Kleiven M, Macken A, Oughton DH (2019): Growth inhibition in Raphidocelis subcapita–Evidence of nanospecific toxicity of silver nanoparticles. Chemosphere 221, 785-792

Kos M, Kahru A, Drobne D, Singh S, Kalčíková G, Kühnel D, Rohit R, Gotvajn AŽ, Jemec A (2016): A case study to optimise and validate the brine shrimp *Artemia franciscana* immobilisation assay with silver nanoparticles: The role of harmonisation. Environmental Pollution 213, 173-183

Koukal B, Rosse P, Reinhardt A, Ferrari B, Wilkinson KJ, Loizeau J-L, Dominik J (2007): Effect of *Pseudokirchneriella subcapitata* (Chlorophyceae) exudates on metal toxicity and colloid aggregation. Water research 41, 63-70

Lai RWS, Kang H-M, Zhou G-J, Yung MMN, He YL, Ng AMC, Li X-y, Djurišić AB, Lee J-S, Leung KMY (2021): Hydrophobic Surface Coating Can Reduce Toxicity of Zinc Oxide Nanoparticles to the Marine Copepod *Tigriopus japonicus*. Environmental Science & Technology 55, 6917-6925

Lambert S, Wagner M (2016): Formation of microscopic particles during the degradation of different polymers. Chemosphere 161, 510-517

Lankoff A, Sandberg WJ, Wegierek-Ciuk A, Lisowska H, Refsnes M, Sartowska B, Schwarze PE, Meczynska-Wielgosz S, Wojewodzka M, Kruszewski M (2012): The effect of agglomeration state of silver and titanium dioxide nanoparticles on cellular response of HepG2, A549 and THP-1 cells. Toxicology Letters 208, 197-213

Lazareva A, Keller AA (2014): Estimating potential life cycle releases of engineered nanomaterials from wastewater treatment plants. Sustainable Chemistry & Engineering 2, 1656-1665

Lead JR, Wilkinson KJ (2006): Aquatic colloids and nanoparticles: current knowledge and future trends. Environmental Chemistry 3, 159-171

Lead JR, Batley GE, Alvarez PJ, Croteau MN, Handy RD, McLaughlin MJ, Judy JD, Schirmer K (2018): Nanomaterials in the environment: behavior, fate, bioavailability, and effects—an updated review. Environmental Toxicology and Chemistry 37, 2029-2063

Lekamge S, Miranda AF, Trestrail C, Pham B, Ball AS, Shukla R, Nugegoda D (2019): The Toxicity of non-aged and aged coated silver nanoparticles to freshwater alga *Raphidocelis subcapitata*. Environmental Toxicology and Chemistry 38, 2371-2382

Lenz R, Enders K, Nielsen TG (2016): Microplastic exposure studies should be environmentally realistic. Proceedings of the National Academy of Sciences 113, E4121-E4122

Lesniak A, Fenaroli F, Monopoli MP, Åberg C, Dawson KA, Salvati A (2012): Effects of the presence or absence of a protein corona on silica nanoparticle uptake and impact on cells. ACS Nano 6, 5845-5857

Levard C, Hotze EM, Lowry GV, Brown Jr GE (2012): Environmental transformations of silver nanoparticles: impact on stability and toxicity. Environmental Science & Technology 46, 6900-6914

Levard C, Hotze EM, Colman BP, Dale AL, Truong L, Yang X, Bone AJ, Brown Jr GE, Tanguay RL, Di Giulio RT (2013): Sulfidation of silver nanoparticles: natural antidote to their toxicity. Environmental Science & Technology 47, 13440-13448

Li L, Stoiber M, Wimmer A, Xu Z, Lindenblatt C, Helmreich B, Schuster M (2016): To what extent can full-scale wastewater treatment plant effluent influence the occurrence of silver-based nanoparticles in surface waters? Environmental Science & Technology 50, 6327-6333

Li P, Su M, Wang X, Zou X, Sun X, Shi J, Zhang H (2020): Environmental fate and behavior of silver nanoparticles in natural estuarine systems. Journal of Environmental Sciences 88, 248-259

Lish RAD, Johari SA, Sarkheil M, Yu IJ (2019): On how environmental and experimental conditions affect the results of aquatic nanotoxicology on brine shrimp (*Artemia salina*): A case of silver nanoparticles toxicity. Environmental Pollution 255, 113358

Long M, Moriceau B, Gallinari M, Lambert C, Huvet A, Raffray J, Soudant P (2015): Interactions between microplastics and phytoplankton aggregates: Impact on their respective fates. Marine Chemistry 175, 39-46

Malysheva A, Voelcker N, Holm PE, Lombi E (2016): Unraveling the complex behavior of AgNPs driving NP-cell interactions and toxicity to algal cells. Environmental Science & Technology 50, 12455-12463

Manfra L, Rotini A, Bergami E, Grassi G, Faleri C, Corsi I (2017): Comparative ecotoxicity of polystyrene nanoparticles in natural seawater and reconstituted seawater using the rotifer *Brachionus plicatilis*. Ecotoxicology and Environmental Safety 145, 557-563

Maurer-Jones MA, Gunsolus IL, Murphy CJ, Haynes CL (2013): Toxicity of engineered nanoparticles in the environment. Analytical chemistry 85, 3036-3049

McLaughlin J, Bonzongo JCJ (2012): Effects of natural water chemistry on nanosilver behavior and toxicity to *Ceriodaphnia dubia* and P*seudokirchneriella subcapitata*. Environmental Toxicology and Chemistry 31, 168-175

Mehennaoui K, Cambier S, Serchi T, Ziebel J, Lentzen E, Valle N, Guérold F, Thomann J-S, Giamberini L, Gutleb AC (2018): Do the pristine physico-chemical properties of silver and gold nanoparticles influence uptake and molecular effects on *Gammarus fossarum* (Crustacea Amphipoda)? Science of the Total Environment 643, 1200-1215

Mehennaoui K, Cambier S, Minguez L, Serchi T, Guerold F, Gutleb AC, Giamberini L (2021): Sub-chronic effects of AgNPs and AuNPs on *Gammarus fossarum* (Crustacea Amphipoda): From molecular to behavioural responses. Ecotoxicology and Environmental Safety 210, 111775

Miao A-J, Schwehr KA, Xu C, Zhang S-J, Luo Z, Quigg A, Santschi PH (2009): The algal toxicity of silver engineered nanoparticles and detoxification by exopolymeric substances. Environmental Pollution 157, 3034-3041

Michels J, Stippkugel A, Lenz M, Wirtz K, Engel A (2018): Rapid aggregation of biofilm-covered microplastics with marine biogenic particles. Proceedings of the Royal Society B 285, 20181203

Monopoli MP, Pitek AS, Lynch I, Dawson KA (2013): Formation and characterization of the nanoparticle–protein corona. In: Bergese P, Hamad-Schifferli K (eds) Nanomaterial Interfaces in Biology. Methods in Molecular Biology (Methods and Protocols) 1025, 137-155

Nabi MM, Wang J, Meyer M, Croteau M-N, Ismail N, Baalousha M (2021): Concentrations and size distribution of TiO2 and Ag engineered particles in five wastewater treatment plants in the United States. Science of The Total Environment 753, 142017

Natarajan L, Omer S, Jetly N, Jenifer MA, Chandrasekaran N, Suraishkumar G, Mukherjee A (2020): Eco-corona formation lessens the toxic effects of polystyrene nanoplastics towards marine microalgae *Chlorella sp.* Environmental Research 188, 109842

Nolte TM, Hartmann NB, Kleijn JM, Garnæs J, van de Meent D, Hendriks AJ, Baun A (2017): The toxicity of plastic nanoparticles to green algae as influenced by surface modification, medium hardness and cellular adsorption. Aquatic Toxicology 183, 11-20

OECD, 317 (2020): Guidance document on aquatic and sediment toxicological testing of nanomaterials. OECD Publishing

Paquet N, Lavoie M, Maloney F, Duval JF, Campbell PG, Fortin C (2015): Cadmium accumulation and toxicity in the unicellular alga *Pseudokirchneriella subcapitata*: Influence of metal-binding exudates and exposure time. Environmental Toxicology and Chemistry 34, 1524-1532

Peijnenburg WJ, Baalousha M, Chen J, Chaudry Q, Von der kammer F, Kuhlbusch TA, Lead J, Nickel C, Quik JT, Renker M (2015): A review of the properties and processes determining the fate of engineered nanomaterials in the aquatic environment. Critical Reviews in Environmental Science and Technology 45, 2084-2134

Pem B, Pongrac IM, Ulm L, Pavičić I, Vrček V, Jurašin DD, Ljubojević M, Krivohlavek A, Vrček IV (2019): Toxicity and safety study of silver and gold nanoparticles functionalized with cysteine and glutathione. Beilstein Journal of Nanotechnology 10, 1802-1817

Petersen EJ, Diamond SA, Kennedy AJ, Goss GG, Ho K, Lead J, Hanna SK, Hartmann NB, Hund-Rinke K, Mader B (2015): Adapting OECD aquatic toxicity tests for use with manufactured nanomaterials: key issues and consensus recommendations. Environmental Science & Technology 49, 9532-9547

Pikuda O, Xu EG, Berk D, Tufenkji N (2018): Toxicity assessments of micro-and nanoplastics can be confounded by preservatives in commercial formulations. Environmental Science & Technology Letters 6, 21-25

Porter A, Lyons BP, Galloway TS, Lewis C (2018): Role of marine snows in microplastic fate and bioavailability. Environmental Science & Technology 52, 7111-7119

Prosposito P, Mochi F, Ciotta E, Casalboni M, De Matteis F, Venditti I, Fontana L, Testa G, Fratoddi I (2016): Hydrophilic silver nanoparticles with tunable optical properties: Application for the detection of heavy metals in water. Beilstein Journal of Nanotechnology 7, 1654-1661

Prosposito P, Burratti L, Bellingeri A, Protano G, Faleri C, Corsi I, Battocchio C, Iucci G, Tortora L, Secchi V (2019): Bifunctionalized Silver Nanoparticles as Hg2+ Plasmonic Sensor in Water: Synthesis, Characterizations, and Ecosafety. Nanomaterials 9, 1353

Quigg A, Chin W-C, Chen C-S, Zhang S, Jiang Y, Miao A-J, Schwehr KA, Xu C, Santschi PH (2013): Direct and indirect toxic effects of engineered nanoparticles on algae: role of natural organic matter. ACS Sustainable Chemistry & Engineering 1, 686-702

Ratte HT (1999): Bioaccumulation and toxicity of silver compounds: a review. Environmental Toxicology and Chemistry: An International Journal 18, 89-108

SCENIHR (Scientific Committee on Emerging and Newly-Identified Health Risks) (2007): The appropriateness of the risk assessment methodology in accordance with the Technical Guidance Documents for new and existing substances for assessing the risks of nanomaterials, 21-22 June 2007

Schiavo S, Duroudier N, Bilbao E, Mikolaczyk M, Schäfer J, Cajaraville M, Manzo S (2017): Effects of PVP/PEI coated and uncoated silver NPs and PVP/PEI coating agent on three species of marine microalgae. Science of the Total Environment 577, 45-53

Schirinzi GF, Llorca M, Seró R, Moyano E, Barceló D, Abad E, Farré M (2019): Trace analysis of polystyrene microplastics in natural waters. Chemosphere 236, 124321

Scott-Fordsmand JJ, Peijnenburg WJ, Semenzin E, Nowack B, Hunt N, Hristozov D, Marcomini A, Irfan MA, Jiménez AS, Landsiedel R (2017): Environmental risk assessment strategy for nanomaterials. International Journal of Environmental Research and Public Health 14, 1251

Sendra M, Yeste M, Gatica J, Moreno-Garrido I, Blasco J (2017): Direct and indirect effects of silver nanoparticles on freshwater and marine microalgae (*Chlamydomonas reinhardtii* and *Phaeodactylum tricornutum*). Chemosphere 179, 279-289

Sendra M, Staffieri E, Yeste MP, Moreno-Garrido I, Gatica JM, Corsi I, Blasco J (2019): Are the primary characteristics of polystyrene nanoplastics responsible for toxicity and

ad/absorption in the marine diatom *Phaeodactylum tricornutum*? Environmental Pollution 249, 610-619

Sendra M, Saco A, Yeste MP, Romero A, Novoa B, Figueras A (2020): Nanoplastics: From tissue accumulation to cell translocation into *Mytilus galloprovincialis* hemocytes. resilience of immune cells exposed to nanoplastics and nanoplastics plus *Vibrio splendidus* combination. Journal of Hazardous Materials 388, 121788

Service RF (1998): Superstrong nanotubes show they are smart, too. Science 281, 940-942

Shiu RF, Vazquez CI, Chiang CY, Chiu MH, Chen CS, Ni CW, Gong GC, Quigg A, Santschi PH, Chin WC (2020a): Nano-and microplastics trigger secretion of protein-rich extracellular polymeric substances from phytoplankton. Science of the Total Environment 748, 141469

Shiu RF, Vazquez CI, Tsai YY, Torres GV, Chen CS, Santschi PH, Quigg A, Chin WC (2020b): Nano-plastics induce aquatic particulate organic matter (microgels) formation. Science of The Total Environment 706, 135681

Sigg L, Lindauer U (2015): Silver nanoparticle dissolution in the presence of ligands and of hydrogen peroxide. Environmental Pollution 206, 582-587

Sjollema SB, Redondo-Hasselerharm P, Leslie HA, Kraak MH, Vethaak AD (2016): Do plastic particles affect microalgal photosynthesis and growth? Aquatic Toxicology 170, 259-261

Syafiuddin A, Salim MR, Beng Hong Kueh A, Hadibarata T, Nur H (2017): A review of silver nanoparticles: research trends, global consumption, synthesis, properties, and future challenges. Journal of the Chinese Chemical Society 64, 732-756

Tallec K, Huvet A, Di Poi C, González-Fernández C, Lambert C, Petton B, Le Goïc N, Berchel M, Soudant P, Paul-Pont I (2018): Nanoplastics impaired oyster free living stages, gametes and embryos. Environmental Pollution 242, 1226-1235

Ter Halle A, Jeanneau L, Martignac M, Jardé E, Pedrono B, Brach L, Gigault J (2017): Nanoplastic in the North Atlantic Subtropical Gyre. Environmental Science & Technology 51, 13689-13697

Tsiola A, Pitta P, Callol AJ, Kagiorgi M, Kalantzi I, Mylona K, Santi I, Toncelli C, Pergantis S, Tsapakis M (2017): The impact of silver nanoparticles on marine plankton dynamics: dependence on coating, size and concentration. Science of the Total Environment 601, 1838-1848

Valdez-Salas B, Beltran-Partida E, Nelson Cheng JS-C, Valdez-Salas EA, Curiel-Alvarez M, Ibarra-Wiley R (2021): Promotion of surgical masks antimicrobial activity by disinfection and impregnation with disinfectant silver nanoparticles. International Journal of Nanomedicine 16, 2689

Varó I, Perini A, Torreblanca A, Garcia Y, Bergami E, Vannuccini ML, Corsi I (2019): Time-dependent effects of polystyrene nanoparticles in brine shrimp *Artemia franciscana* at physiological, biochemical and molecular levels. Science of The Total Environment 675, 570-580

Velev O, Kaler E (1999): In situ assembly of colloidal particles into miniaturized biosensors. Langmuir 15, 3693-3698

Ward JE, Kach DJ (2009): Marine aggregates facilitate ingestion of nanoparticles by suspension-feeding bivalves. Marine Environmental Research 68, 137-142

Wu F, Harper BJ, Harper SL (2017): Differential dissolution and toxicity of surface functionalized silver nanoparticles in small-scale microcosms: impacts of community complexity. Environmental Science: Nano 4, 359-372

Wu J, Jiang R, Lin W, Ouyang G (2019): Effect of salinity and humic acid on the aggregation and toxicity of polystyrene nanoplastics with different functional groups and charges. Environmental Pollution 245, 836-843

Yang X, Gondikas AP, Marinakos SM, Auffan M, Liu J, Hsu-Kim H, Meyer JN (2012): Mechanism of silver nanoparticle toxicity is dependent on dissolved silver and surface coating in *Caenorhabditis elegans*. Environmental Science & Technology 46, 1119-1127

Yi X, Wang J, Li Z, Zhang Z, Chi T, Guo M, Li W, Zhou H (2019): The effect of polystyrene plastics on the toxicity of triphenyltin to the marine diatom *Skeletonema costatum*—influence of plastic particle size. Environmental Science and Pollution Research 26, 25445-25451

Zhang C, Chen X, Wang J, Tan L (2017): Toxic effects of microplastic on marine microalgae *Skeletonema costatum*: interactions between microplastic and algae. Environmental Pollution 220, 1282-1288

CHAPTER 1

PS NP SUBLETHAL EFFECTS IN MICROALGAE: Impact of polystyrene nanoparticles on marine diatom *Skeletonema marinoi* chain assemblages and possible consequences on their ecological role in marine ecosystems

GRAPHICAL ABSTRACT

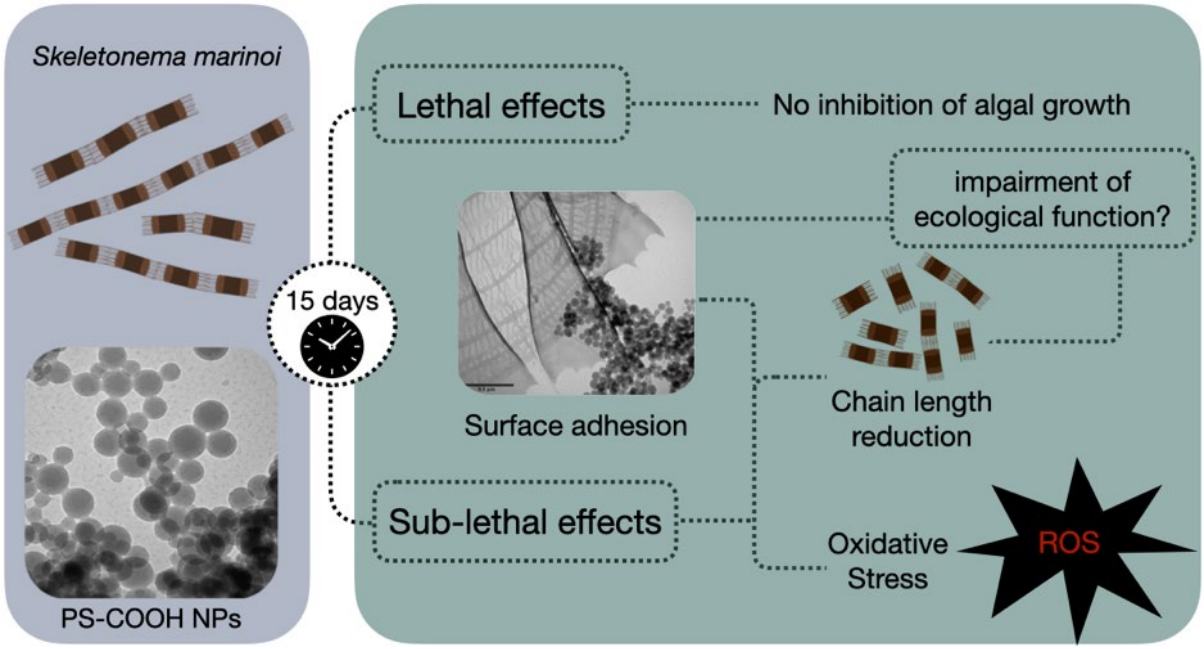

## ABSTRACT

Marine diatoms have been identified among the most abundant taxa of microorganisms associated with plastic waste collected at sea. However, the impact of nano-sized plastic fragments (nanoplastics) at single cell and population level is almost unknown. We exposed the marine diatom *Skeletonema marinoi* to model polystyrene nanoparticles with carboxylic acid groups (PS–COOH NPs, 90 nm) for 15 days (1, 10, 50 μg/mL). Growth, reactive oxygen species (ROS) production, and nano-bio-interactions were investigated. No effect on diatom growth was observed, however dynamic light scattering (DLS) demonstrated the formation of large PS–COOH NP aggregates which were localized at the diatoms' fultoportula process (FPP), as shown by TEM images. Increase production of ROS and reduction in chain length were also observed upon PS–COOH NP exposure ($p$<0.005). The observed PS-diatom interaction could have serious consequences on diatoms ecological role in the biogeochemical cycle of carbon, by interfering in the formation and sinking of aggregates responsible for atmospheric carbon fixation and sequestration in the ocean sea floor.

## 1. Introduction

Due to its conformation, highly populated coastlines and tourism, the Mediterranean sea is widely recognised to be severely impacted by plastic pollution (Suaria et al., 2016). Recent simulations estimate that the Mediterranean basin retains between 5% and 10% of the global plastic mass present at sea (Van Sebille et al., 2015). Being the most commonly used polymer for packaging and disposable items (PlasticsEurope, 2015), polystyrene (PS) is frequently found as waste in marine waters (Wan et al., 2018). The weathering of plastic caused by atmospheric agents (such as UV-light) and biota leads to fragmentation into ever smaller particles (Song et al., 2017; Wright and Kelly, 2017). Laboratory studies have demonstrated that PS fragmentation occurs down to submicron (100-1000 nm) and nanoscale particles (1-100 nm) in water media, and environmental weathering is considered the main driver (Gigault et al., 2016; Lambert and Wagner, 2016a; b; Ekvall et al., 2019). Recently, the occurrence of submicron plastic fragments was confirmed in the North Atlantic subtropical gyre (Ter Halle et al., 2017). Predicted environmental concentrations of nanoplastics are in the range of μg/L and are expected to increase in areas showing significant accumulation of plastic debris, such as for instance the Mediterranean Sea (Al-Sid-Cheikh et al., 2018).

Plastic fragments of various size floating on the sea surface can be colonized by bacteria and microalgae (Ye and Andrady, 1991; Lobelle and Cunliffe, 2011; Fazey and Ryan, 2016), which often differ among polymers and are generally referred to as the "plastisphere" (Carson et al., 2013; Zettler et al., 2013; Reisser et al., 2014; Oberbeckmann et al., 2015; Muthukrishnan et al., 2018). Diatoms are the most abundant taxa of microalgae found on plastic fragments collected at the sea surface (Masó et al., 2003; Carson et al., 2013; Zettler et al., 2013; Reisser et al., 2014; Masó et al., 2016; Muthukrishnan et al., 2018) which are thus able to spread both harmful species and toxins, as recently documented in a study on the Adriatic Sea (NE Mediterranean Sea) (Casabianca et al., 2019). Diatoms play fundamental ecological roles in marine ecology as primary producers, being also one of the basic constituents of marine food chains (Harris, 2012) and one of the main bloom-forming and exudate producing groups

of marine microalgae (Passow and Alldredge, 1994). Their exudates, known as exopolymeric substance (EPS), represent an important carbon source for the marine environment, playing a fundamental role in marine ecosystem ecology and functioning (Middelburg et al., 2000; Xiao and Zheng, 2016).

The formation of so called marine snow, made of macroscopic aggregates of detritus, living organisms and organic matter, mainly depends on the presence of phyto- and zooplankton and their exudates, with an important role played by algal blooms (Alldredge and Silver, 1988; Turner, 2002). The sinking of these organic aggregates contributes to carbon fluxes from the surface to the deep-sea (Harding, 1974).

The incorporation of plastic particles (both nano and micro) into natural marine aggregates has been studied in the laboratory and observed in the natural environment (Ward and Kach, 2009; Zhao et al., 2017; Summers et al., 2018). The interaction of microorganisms and their exudates with plastics is hypothesized to affect carbon fluxes, by modifying the sinking rates of marine snow and the bioavailability of small plastic particles for marine organisms (Ward and Kach, 2009; Long et al., 2015; Kooi et al., 2017).

A limited number of studies investigated the impact of nanoplastics on marine microalgae, and even less focused on their effects on diatoms. Available studies mainly consider acute effects at very high exposure concentration, which are probably not environmentally relevant (*e.g.*, ≥50-100 mg/L) (Besseling et al., 2014; Sjollema et al., 2016; Bergami et al., 2017; Nolte et al., 2017), and generally use short time exposure (72-96 h). Nanoplastic adhesion to microalgae has been documented, as well as the production of reactive oxygen species (ROS) and the reduction of photosynthetic yield (Bhattacharya et al., 2010; Bergami et al., 2017; Nolte et al., 2017; Chae et al., 2018; Bellingeri et al., 2019).

As nanoscale particles are very reactive and subject to transformations in aquatic media, their biological effects are often non-linear, and data interpretation becomes challenging (Peijnenburg et al., 2015; Rist and Hartmann, 2018). In an earlier study (Bellingeri et al., 2019), we suggested that standard ecotoxicological endpoints and time exposure may not be fully adequate to describe the effects of

nanoplastics to aquatic organisms, especially microalgae, and that risk assessment protocols should be updated to include the effects of NP exposure. Long-term studies should be coupled with short-term, and sub-lethal endpoints (*e.g.*, biochemical, physiological, morphological up to behavioural alterations), rather than only mortality, should be investigated (Bellingeri et al., 2019; Seoane et al., 2019) in order to better mimic environmentally relevant exposure scenarios.

Therefore, based on such scientific gaps, the present study investigated the impact of model polystyrene nanoparticles (PS NPs, 90 nm) functionalized with carboxylic groups (-COOH) on the marine diatom *S. marinoi,* among the most abundant on the Adriatic Sea (Penna et al., 2004; Totti et al., 2019), by chronic toxicity in term of algal growth and sub-lethal responses as reactive oxygen species (ROS) production and chain assemblages at 15 days .

## 2. Materials & Methods

### 2.1. Materials

Carboxylated polystyrene nanoparticles (PS-COOH NPs, subsequently referred to as PS NPs) were provided by the Physical Chemistry and Soft Matter Department in collaboration with the Food and Biobased Department of Wageningen University (The Netherlands) (Redondo-Hasselerharm et al., 2019; van Weert et al., 2019). The original stock solution was 41.91% w/w of PS NPs containing 0.4% w/w of covalently bound dye (rhodamine B methacrylate) and 1.2% w/w of sodium dodecyl sulfate (SDS). The distribution of SDS in the exposure medium was calculated in order to rule out that aqueous SDS concentrations could contribute to observed effects, if any (provided as Supporting Information). PS NPs leachates were not expected since the batch was synthetized without additives and therefore considered inert. Furthermore, stock was bubbled with clean air for 24 h to eliminate potential remaining styrene monomers and was diluted with MilliQ water (mQW) prior to the preparation of test solutions. Before use, each PS NP test solution was vortexed and bath sonicated for two minutes.

The SDS free aqueous concentration in our system was estimated to be between 0.16 and 0.95 mg/L at the highest PS NPs concentration tested. Literature data report that SDS has no effect on growth of the green alga *Scenedesmus obliquus*, up to 10 mg/L (Besseling et al., 2014), and is able to induce colony formation at concentrations higher than 5 mg/L (Lürling and Beekman, 2002). These threshold effect concentrations are one to two orders of magnitude higher than the predicted SDS concentration in our system, which thus suggests that SDS is not likely to interfere with effects of Nano-PS identified. However, we cannot completely exclude a possible interference of SDS in the observed effects as no literature data is available concerning the effect threshold for *S. marinoi*.

### 2.2. PS NP characterization

PS NP behaviour in diatom exposure medium (F/2) was characterized by Dynamic Light Scattering (DLS, Malvern instruments), combined with the Zetasizer Nano Series software (version 7.02, Particular

Sciences). Z-average (nm) and z-potential (mV) were determined at 50 μg/mL in mQW used for preparing PS NP stock solutions, and in F/2 used for algal exposure study.

### 2.3. Algal culture conditions and exposure study

*Skeletonema marinoi* CBA4 was maintained in F/2 medium (Guillard, 1975), at 16 ± 1 °C under a standard 12:12 h light-dark cycle; light was provided by cool-white fluorescent bulbs (photon flux of 100 $\mu Em^{-2} s^{-1}$). All exposure experiments were performed in 50 mL glass bottles containing *S. marinoi* at initial concentration of $1.0 \times 10^4$ cells/mL in artificial seawater (ASPM, Artificial Seawater Provasoli-McLachlan) (Guillard, 1975) enriched with F/2 medium components. Before exposure, PS NPs were briefly vortexed and bath sonicated (Bandelin, Germany) for 2 min at room temperature. Diatoms were exposed to PS NPs at the following concentrations: 0, 1, 10, 50 μg/mL, and exposure was carried out for 15 days (15 d). Each concentration was tested in triplicate and the experiment was repeated three times. *S. marinoi* growth was determined by cell density. Samples were harvested at intervals of 3–4 days and fixed with Lugol's iodine solution and stored at +4 °C. Cell density was determined using an inverted microscope (ZEISS Axiovert 40 CFL) at 400x magnification using a Sedgewick Rafter counting chamber. Both growth rate (μ) and inhibition of growth rate (Iμi) were determined. In particular, growth rate, defined as the instantaneous rate of increase, was calculated on the basis of the longest possible period of exponential growth using the equation: $\mu = \ln(Nt/N0)/\Delta t$, where N is the number of cells/mL, $\Delta t$ is the time interval (Wood et al., 2005). Inhibition of growth rate (Iμi) was then determined following a standard guideline (ISO, 2006) and considering the same growth rate time interval.

Diatom chain length was determined with the aid of imageJ software on pictures taken with an optical microscope (Olympus BX51 coupled with Olympus DP-software) of Lugol fixed samples. We counted the number of cells composing each chain over 100, randomly selected, chains for each replicate. The relative frequency of each group (chain composed by 1, 2, 3, 4, 5, 6, 7, 8, 9 and 10 cells) was then calculated.

## 2.4. Sub-lethal Effects

### *2.4.1. Skeletonema marinoi-PS NP interaction*

The physical interaction between algal cell and PS NPs at the end of the exposure period (15 d), was imaged through high resolution environmental scanning electron microscopy (ESEM, Quanta 400 (FEI)), and transmission electron microscopy (TEM, Tecnai G2 Spirit (FEI)). At the same time, light microscope Zeiss Axiophot equipped with interference contrast was used to record micrographs from algal samples using a AxioCam MRm fitted with AxioVision software. Different techniques were applied in an attempt to find the most suitable in describing PS NPs–diatom interaction and avoid the creation of artefacts due to sample preparation (Tiede et al., 2008; Mourdikoudis et al., 2018). To obtain ESEM images, unaltered samples of PS NPs exposed diatoms and controls were used. For TEM images, instead, diatoms were processed following two different procedures: a) diatoms were fixed in glutaraldehyde (1.5%) and then washed with mQW water and centrifuged (7,000 *g* for 15 min. at 20°C) twice, b) diatoms were kept fresh without fixation. For optical microscopy (both brightfield and differential interference contrast) diatoms were fixed with glutaraldehyde (1.5%) and washed using mQW before observation.

### *2.4.2.Quantification of ROS*

The production of reactive oxygen species (ROS) was measured by following the conversion of the non-fluorescent dihydrodichlorofluorescein diacetate ($H_2$DCF-DA) to the highly fluorescent compound 2', 7',-dichlorofluorescein (DCF) as described by Wang and Joseph (1999), recently adapted for algal cells by Morelli et al. (2018). Algae samples (2 mL) were spiked with 20 µL of a 1mM DCF-DA solution and kept under constant shaking at room temperature for 1h in the dark. Each replicate was tested in triplicate so nine measurements for each exposure concentration were obtained.

Fluorescence was determined in triplicate at 520 nm emission wavelength ($\lambda_{ex}$ = 485 nm) using a Victor 3 1420 multilabel Counter (PerkinElmer) and used for total ROS estimation. Tested blanks were F/2, F/2 + $H_2$DCF-DA and F/2 + $H_2$DCF-DA + 10 and 50 µg/mL PS NPs. No interference in fluorescence was

recorded in the presence of PS NPs. Background value (F/2 + $H_2$DCF-DA) was subtracted from the obtained fluorescence value of the samples. Fluorescent data were normalized to the cell density and expressed as fluorescence/cell density.

### 2.5. Statistical analysis

Statistical analyses were performed with non-parametric Mann-Whitney and Kruskal Wallis tests using PAST ver. 3.14 with a *p*-value <0.05 determining significance for growth inhibition, and with an unpaired t-test using R with a *p*-value <0.005 for ROS levels.

## 3. Results and Discussion

### 3.1. PS NP characterization in exposure media

DLS measurements showed a good dispersion of PS NPs in mQW, with a hydrodynamic diameter of 88.2 ± 2.9 nm and a Z-potential of -42 mV (Table 1). In F/2, a negative surface charge was still preserved (-22.8 mV) while the formation of large PS NP aggregates (hydrodynamic diameter 1793 ± 56.9 nm) was observed, in agreement with previous characterizations done in algal medium in artificial sea water (Bergami et al., 2016; Bergami et al., 2017).

**Table 1.** DLS measurements of hydrodynamic diameter (z-average), polydispersity index (PDI) and surface charge (z-potential) of PS NPs (50 µg/L) in mQW and F/2 medium at 25°C.

| | z-average (nm) | PDI | Z-potential (mV) |
|---|---|---|---|
| MilliQ | 92.9 ± 4.65 | 0.052 | -42 |
| F/2 | 1933 ± 525 | 0.697 | -22.2 |

### 3.2. Growth

No effects on diatom growth were observed upon exposure to PS NPs (1, 10 and 50 µg/mL) for 15 days (Hc = 0.63, p = 0.89). Growth rates were in the range of 0.61 - 0.66 per day, similarly in controls and exposed diatoms (Hc = 2.131, p = 0.5457) (Figure 1).

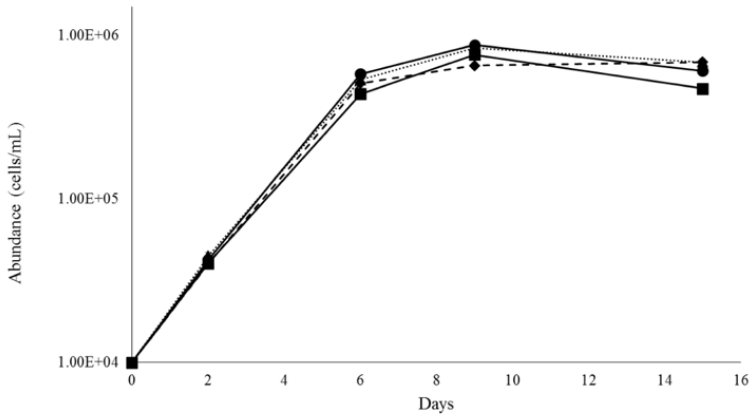


**Figure 1.** Maximum cell densities (cells/mL) of *S. marinoi* control (CTRL) (-▲-) and PS NPs exposed specimens: 1 µg PS/mL (-♦-), 10 µg PS/mL (-●-) and 50 µg PS/mL (-■-) exposure.

These findings are in agreement with previous studies in which PS NPs did not cause any effect on algal growth, both in fresh water and in sea water (Besseling et al., 2014; Sjollema et al., 2016; Bergami et al., 2017; Bellingeri et al., 2019). In a long-term (30-d) exposure study with *Chlorella pyrenoidosa* Mao et al. (2018) reported a growth phase-dependent inhibitory effect of PS NPs: a significant initial inhibition (38.5%) disappeared after 22 days, while at the end of exposure period (30-d) exposed algae showed an even higher cell density than control. On the contrary, *S. marinoi* exhibited a constant growth similar to controls during 15 days of exposure until the beginning of stationary phase (6-d) and at the end of exposure period (15-d). Regarding the SDS present in PS NP stock according to our calculation it results below probable effect threshold concentrations for phytoplankton.

### 3.3. Sub-lethal effects

TEM images clearly show PS aggregates interacting with the *S. marinoi* cell surface. Both in fixed and fresh (not fixed) diatom cells (Figure 2 b, d, f and Figure 3, respectively), the adhesion seems to be mainly localized in the terminal fultoportula processes (TFPP), the elongated structures responsible for chain formation and maintenance in this marine diatom (Figure 2 a, arrow).

Images obtained from fresh diatoms clearly show the adhesion of PS aggregates to the diatom cell surface (Figure 3), while in samples fixed with glutaraldehyde and further washed in mQW, such interaction is far less evident (Figure 2 b, d, f). Since TEM images are obtained when electrons are transmitted through the sample, in order to avoid any disturbance due to the presence of salts and organic matter, marine organisms are commonly washed in mQW before TEM analysis. However, based on our findings, fixation and washing significantly change the interaction of PS aggregates with diatom cell surface, producing an artefact which does not resemble the natural interaction occurring between *S. marinoi* and PS. Both sample-processing steps might alter the chemical composition of the medium and contribute to the removal of natural organic matter (*e.g.,* algal exudates).

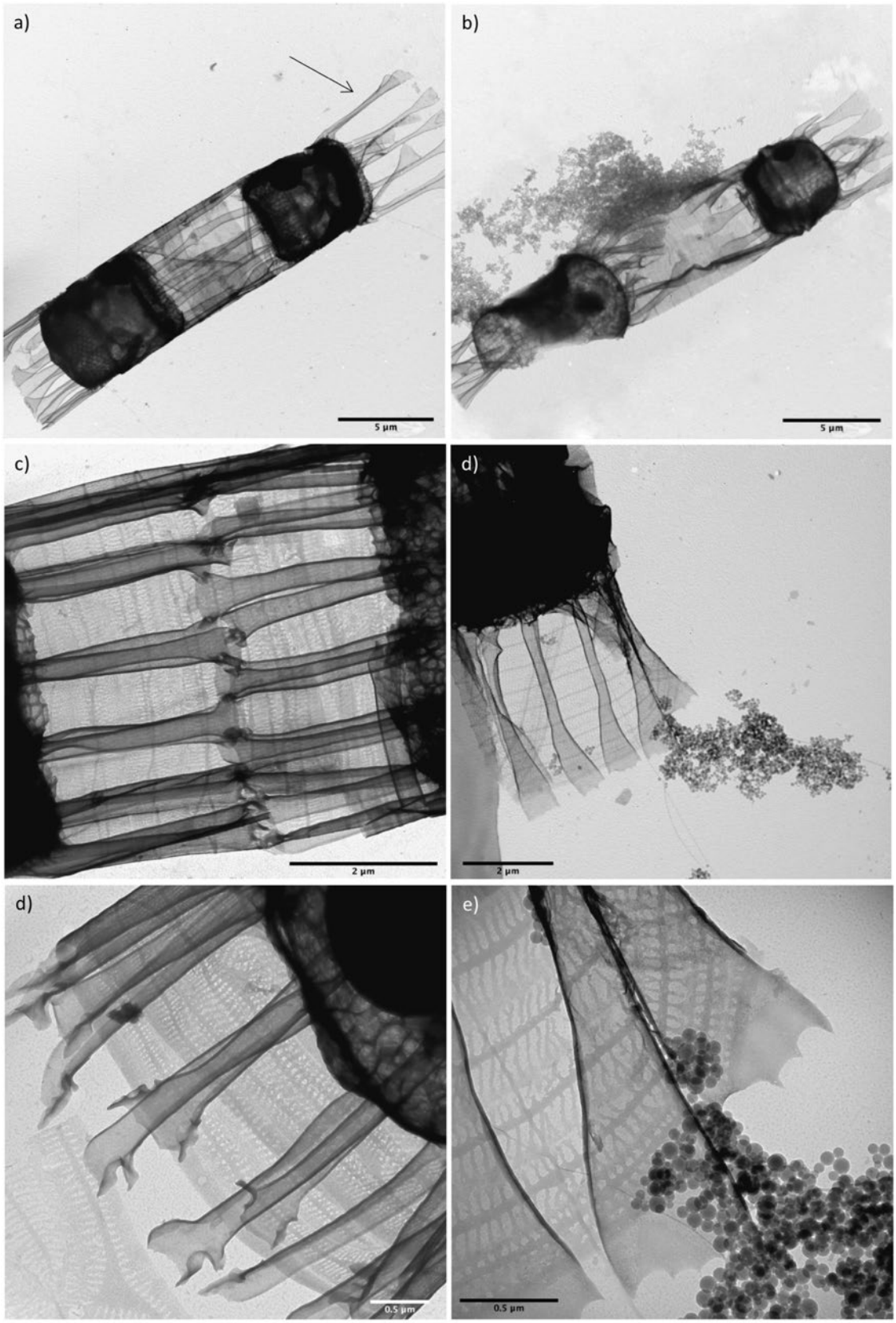


**Figure 2.** TEM images of *S. marinoi* samples fixed with glutharaldheyde (1.5%) and further washed with mQW; a, c, e) control cells, b, d, f) PS NPs exposed cells.

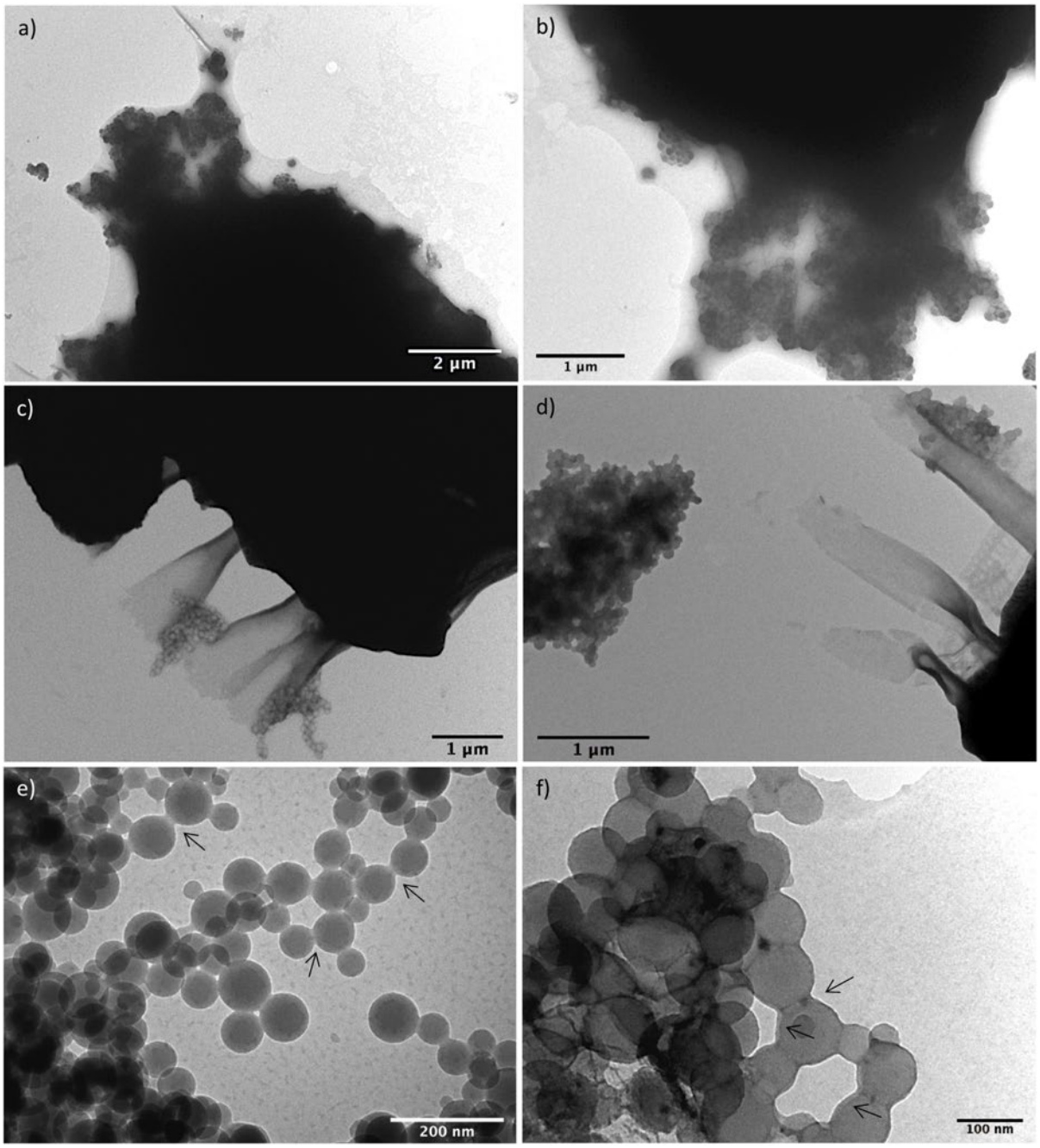


Figure 3. TEM images of *S. marinoi* fresh (not fixed) samples. a, b: PS aggregates entrapped with organic material; c, d: details of PS aggregates localized at FFP; e, f: higher magnification of PS aggregates embedded in organic materials presumably EPS and details of PS NPs rounded with organic material (see arrows).

Morphological alterations in diatom cells are also evident in both PS-exposed and controls, probably as a consequence of preparative methods, which is further confirmed by their absence in optical images (Figure 4). A further confirmation is obtained also by ESEM images where cells appeared to be altered both in control and exposed diatoms (Figure 5). Seoane et al. (2019) reported similar morphological

alterations in cells of the diatom *Chaetoceros gracile* processed for SEM analysis (fixed with glutaraldehyde and filtrated) both in controls and in those exposed to microplastics.

Sample preparation is a necessary step for TEM analysis, however, studies conducted with NPs, recognized some limitations due to a significant sample alteration (Tiede et al., 2008; Mourdikoudis et al., 2018). Moreover, working under vacuum conditions could also affect sample integrity and produce artefacts (Mavrocordatos et al., 2007). In the study of nano-bio-interactions, any preparative procedure which might affect the integrity of the sample should be avoided by using for instance ESEM, being recognized as a more conservative process, using fresh unprocessed samples (100% humidity). However, according to our findings, high levels of humidity might have reduced the contrast and made the smaller particles less detectable (Tiede et al., 2008). ESEM images (Figure 5), in fact, did not allow to detect algal cell-PS NPs interaction, probably because of the small size of the PS NPs and the presence of solution partially masking cell surface. PS NPs were not easy to identify but are probably represented by the brighter and grainy spots on the background of exposed cell images to PS NPs (Figure 5 c, d), which are not visible in control images (Figure 5 a, b).

Furthermore, TEM images highlighted an adhesion of diatom EPS to PS NPs as shown in figure 3 (e, f, see arrows). Chen et al. (2011) and Summers et al. (2018) already described the formation of plastic agglomerates held together by a biopolymer matrix, connecting and trapping the particles. Such process could be even more relevant for microalgae producing high amount of exudates as diatoms, with possible implications for their role on plastic behaviour and fate in the water column. The incorporation of plastics into algal and marine aggregates has been documented and shown to modify the buoyancy and sinking rates of aggregates, and to increase ingestion of plastic particles by suspension-feeding bivalves (Ward and Kach, 2009; Long et al., 2015; Porter et al., 2018).

EPS play many important roles in diatom ecology in terms of motility, adhesion and overall cell protection and colony formation (Hoagland et al., 1993), but more importantly, they play a key role in the formation of the siliceous frustule and also in protection against dissolution (Round et al., 1990;

Simpson and Volcano 2012). The observed adhesion of PS aggregates to the algal surface could be the result of EPS interaction with PS NPs and be linked to the observed effect on algal chain length.

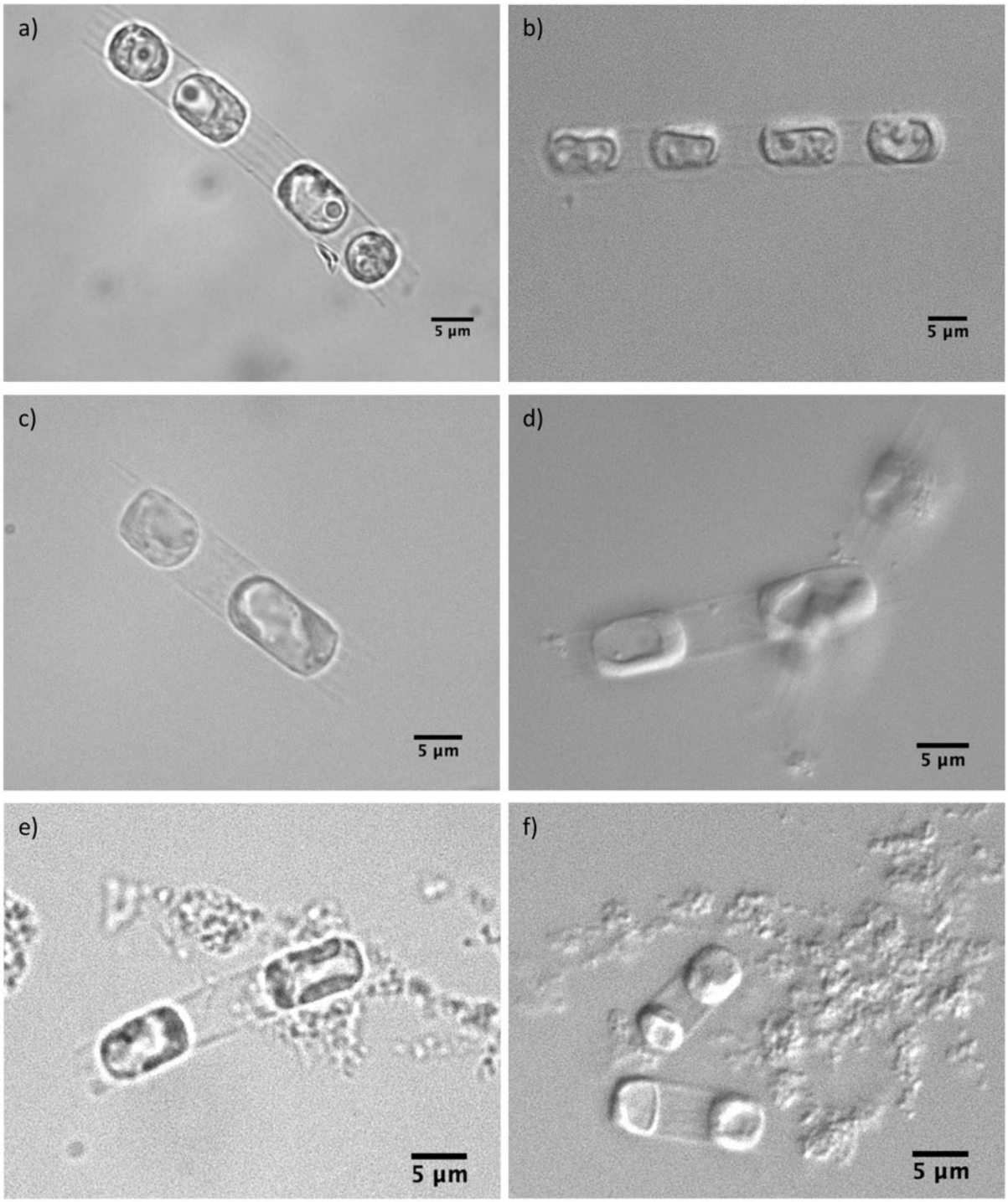


**Figure 4.** Optical (left) and differential interference contrast (DIC) microscopy (right) images of *S. marinoi* CTRL (a, b, magnification: 100x and 40x) and exposed to 10 µg PS/mL (c, d, magnification: 100x) and 50 µg PS/mL (e, f, magnification: 40x). Scale bar is 5 µm.

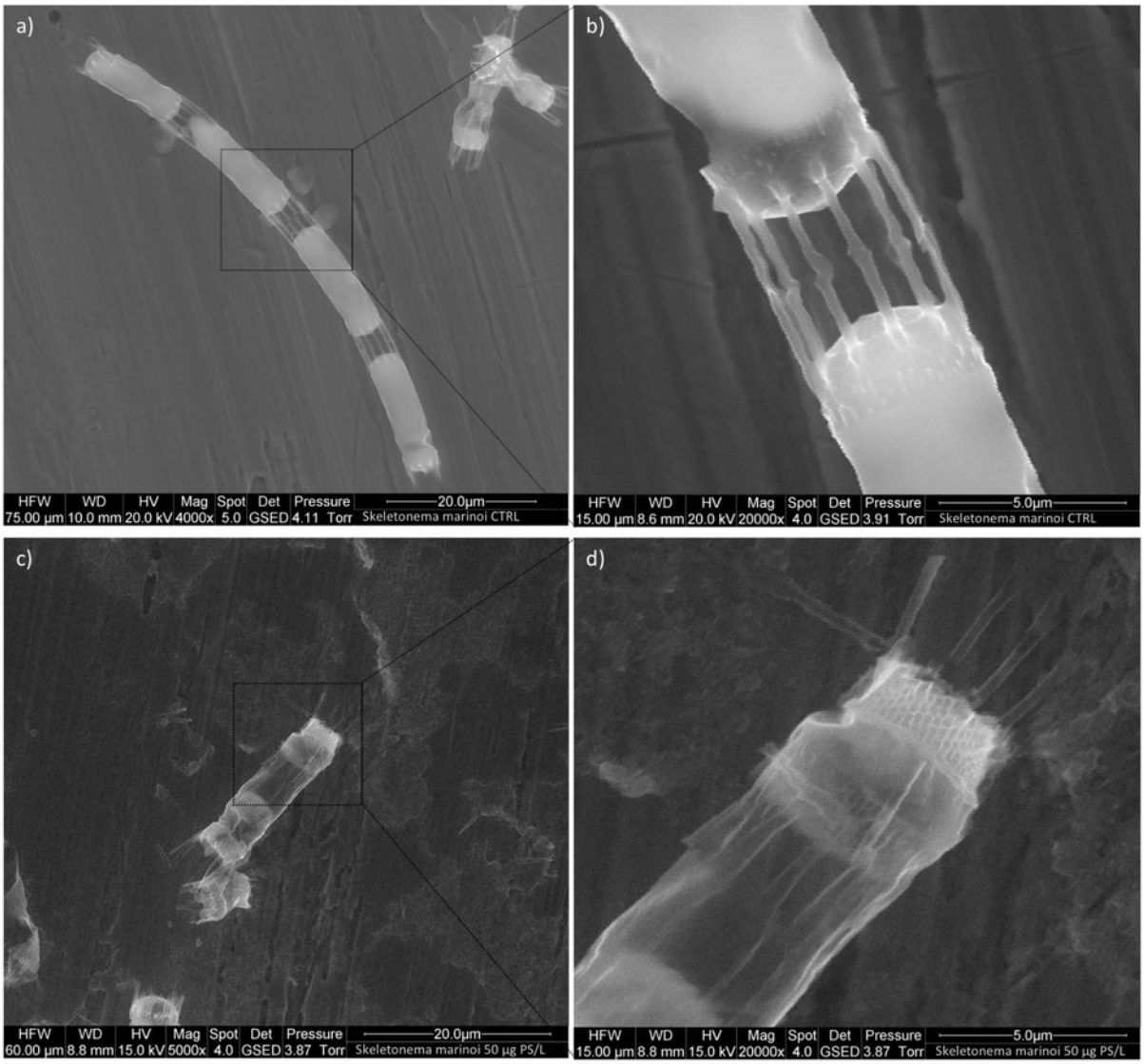


**Figure 5.** ESEM images of fresh (not fixed) samples of *S. marinoi:* (a, b) controls and (c, d) PS NP exposed cells.

The length of *S. marinoi* chains was significantly affected by PS NPs, at 10 and 50 µg/L exposure. Exposed algae showed a high percentage of single cells and 2-cell chains, altogether accounting for 95% and 84% of 10 and 50 µg/mL exposure, respectively. As opposed to control algae, in which single cells and 2-cells chains accounted for 36% of the observed chains, while 43% was represented by 4- and 8-cell chains (Figure 6, Tab. S1). At 1 µg/L exposure no difference in chain length was observed (data not reported). Shorter chain length could have serious consequences on diatoms ecology by impairing their buoyancy and enhancing their sinking rates with potential implications for the maintenance of phytoplankton productivity on the sea surface (Smayda and Boleyn, 1966). The assessment of the

floating capacity of algae was beyond the aim of our study, however our findings highlight the need for further investigations in order to better understand which consequences of nanoplastics exposure can be expected for the ecological role of diatoms.

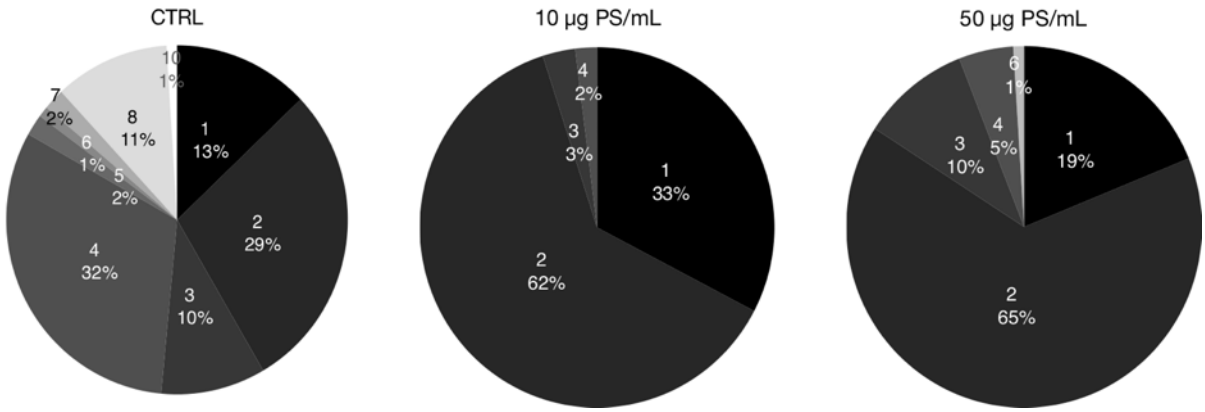


**Figure 6.** *S. marinoi* chains length expressed as percentage of different number of cells (1, 2, 3, 4, 5, 6, 7, 8, 9, 10) in control (CTRL) and PS NPs exposed (10 µg PS/mL and 50 µg PS/mL).

*S. marinoi* chains are composed of cells connected to one another by the fultoportula processes (FPP). The documented adhesion of PS aggregates to the FPP might be responsible for the shorter chains, since these structures play an important role by acting as a bridge between diatom cells, thus causing the assembly of the chain. Therefore, we hypothesize that the reduction in chain length is a consequence of PS NP adhesion to these structures. The adhesion may cause a localized stress and a weakening of the siliceous structures, causing shortening of the chains. Bhattacharya et al. (2010) suggested the occurrence of contact-induced stress following cell-PS NP interactions, resulting in enhanced ROS production. In fact, a concentration-dependent increase in ROS levels was observed in our study in diatom exposed to PS NPs (Figure 7). In particular, ROS significantly increased ($p < 0.005$) compared to the control for both 10 and 50 µg PS/mL.

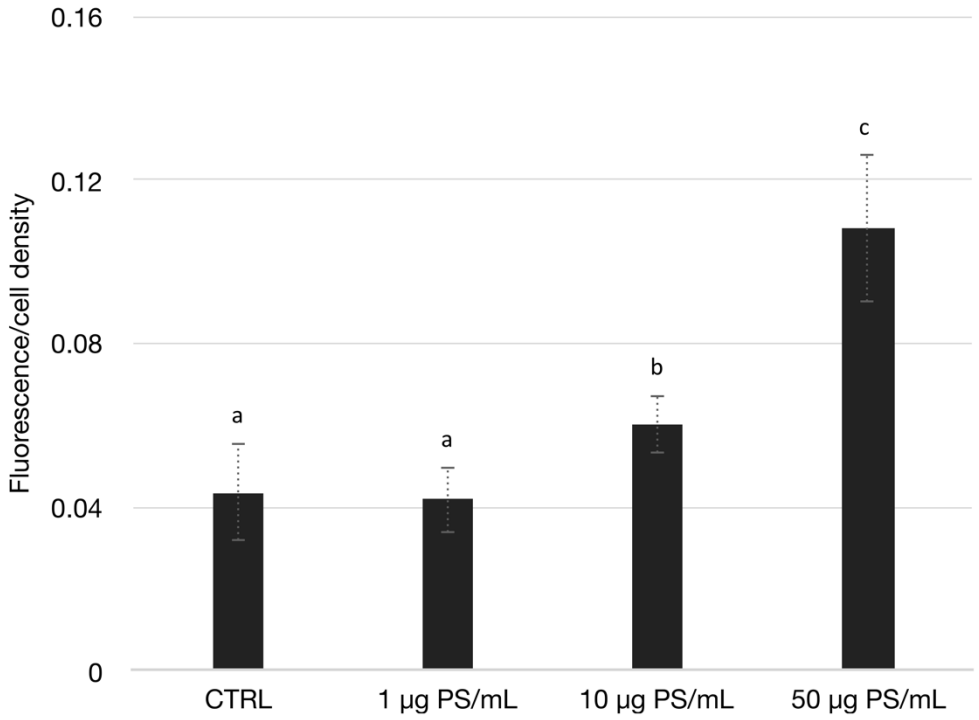


**Figure 7.** ROS levels in *S. marinoi* exposed to PS NPs (1,10, 50 µg PS/mL) and in controls. Data shown as fluorescence units/cell density (cells/mL) and presented as mean ± standard deviation. Data with different letters are statistically different with $p < 0.005$.

Such findings are in agreement with Liu et al. (2019) and Bhattacharya et al. (2010), who reported an increase in ROS production in microalgae exposed to uncharged and positively charged PS NPs, and with Morelli et al (2018) and Ševců et al. (2012) reporting similar results with metallic NPs, mainly metal oxides. Liu et al. (2019) also reported an increase in superoxide dismutase (SOD) activity at lower concentration (1 µg/L, 1 mg/L) of PS-COOH NPs probably as a sign of early oxidative stress response.

Concerning the observed chain length reduction, other hypotheses can be formulated. Takabashi et al. (2006) observed a positive correlation between nutrient availability and longer chains in *Skeletonema costatum*. The presence of PS NPs could cause a reduction in nutrient concentration through adsorption on their surface, thus influencing algal chain length. Alternatively, *S. marinoi* was demonstrated (Bergkvist et al., 2012; Bjærke et al., 2015) to be able to shorten its chains as a response to a size-

dependent grazing pressure, by copepod grazing selectively on longer chains. This resulted to be induced by chemical cues, produced either by the grazing copepods or by the algae being grazed. PS NPs could therefore activate the same molecular pathway involved in this predator escaping strategy and resulting in an algae self-induced reduction of chain length.

## 4. Conclusions

In this work we evaluated the impact of PS NPs on the marine diatom *S. marinoi* on a long exposure period (15 d). We measured growth inhibition and oxidative stress of *S. marinoi* as well as the physical interaction occurring between algal cells and PS NPs. Our findings highlighted no lethal effect of PS NPs to the marine diatom *S. marinoi*, while showing an increase in intracellular oxidative stress, the adhesion of PS NPs onto the algal surface and a reduction of diatom's chain length. The causal link between PN NPs adhesion and reduction of chain length was only hypothesized but, if confirmed, could result in changes in algal buoyancy as well as interference in the formation and sinking of aggregates, with potential repercussions on the carbon cycle. Further studies are needed in order to reveal potential ecological implications of this interaction, especially in a future scenario of increased global plastic pollution.

## 5. Acknowledgments

I thank Prof. Antonella Penna, Dr. Silvia Casabianca and Samuela Capellacci from the Biomolecular Science Departments of the University of Urbino Carlo Bo, for contributing to the experimental design and the carrying out of algal growth inhibition tests. I thank Prof. Albert A Koelmans from the Aquatic Ecology and Water Quality Management Group of the University of Wageningen who helped in the discussion of the data as well as in the modelling and calculations of residual SDS concentrations in exposure media. I thank Prof. Pietro Lupetti, Eugenio Paccagnini and Claudia Faleri from the Department of Life Sciences of the University of Siena for TEM and ESEM imaging. I thank Prof. Andrea M. Atrei from the Department of Biotechnology, Chemistry and Pharmaceutical of the University of Siena and Dr. Marianna Uva and Dr. Eugenio Macchia from CREA s.c.a.r.l. for DLS use. Also, I thank the following people of Wageningen University who kindly provided the PS-COOH nanoparticle batch functionalized with Rhodamine B dye: Dr. Paula Redondo Hasselerharm from the Aquatic Ecology and Water Quality Management Group, Joris Sprakel from the Physical Chemistry and Soft Matter Group and Remco Simonsz and Fresia Alvarado Chacón from Wageningen Food & Biobased Research.

SUPPORTING INFORMATION

Calculation of maximum SDS concentration in the systems

The nanostock had 1.2 wt% SDS in 56 wt% of water, this is 1200/0.056 = 21 429 mg/L.

This SDS concentration was present in the 0.004 mL of nano-PS stock added to the highest dose.

The total volume in the exposure system was 0.04 L, so 0.004 mL was diluted to approximately 40 mL, yielding a diluted total SDS concentration (CT) of 21 429 * 0.004/40 = 2.14 mg/L.

This total concentration CT (mg/L) sorbs partly to the algae, in which case we have:

$$CT = C_w + C_{algae} * [algae] \quad \text{(eq 1)}$$

In which $C_w$ is the free aqueous concentration (mg/L), $C_{algae}$ is the SDS concentration adsorbed to the algae (mg/kg) and [algae] is the concentration of algae in the system (kg/L).

Due to mixing and subsequent acclimatization, equilibrium can be assumed.

At equilibrium, $C_{algae}$ is related to $C_w$, via: $C_{algae}=K_d*C_w$, in which $K_d$ is the distribution coefficient (L/kg).

Combination yields $CT=C_w*(1+K_d*[algae])$ which now can be solved for $C_w$ if [algae] is known:

$$C_w=CT/(1+K_d*[algae]) \quad \text{(eq 2)}$$

The concentration of algae in the highest Nano-PS dose was on average 460 mg/L = [algae] = 460 E-6 kg/L

A literature value for the $K_d$ for marine water is 2700 L/kg (Hugh-Jones and Turner, 2005). This is for sediment. We can assume that for fresh algae, constituting 100% organic matter, the $K_d$ is an order of magnitude higher.

Therefore, $C_w$ = 2.14 / (1+ 27 000*460 E-6) = 0.16 mg/L

Without the assumption of higher $K_d$, this is 0.95 mg/L

Table S1. *S. marinoi* chains length expressed as relative frequency of different number of cells (1, 2, 3, 4, 5, 6, 7, 8, 9, 10) in control (CTRL) and PS NPs exposed (10 µg PS/mL and 50 µg PS/mL).

| N° of cell per chain | CTRL | 10 µg/mL | 50 µg/mL |
|---|---|---|---|
| 1 | 13 ± 2.2 | 33 ± 2.6 | 19 ± 3.8 |
| 2 | 29 ± 5.6 | 62 ± 4 | 65 ± 3.8 |
| 3 | 10 ± 2 | 3 ± 1.7 | 10 ± 2 |
| 4 | 32 ± 3.5 | 2 ± 1.2 | 5 ± 2.6 |
| 5 | 2 ± 1.2 | 0 | 0 |
| 6 | 1 ± 0.5 | 0 | 1 ± 0.6 |
| 7 | 2 ± 1.2 | 0 | 0 |
| 8 | 11 ± 1.5 | 0 | 0 |
| 9 | 0 | 0 | 0 |
| 10 | 1 ± 0.6 | 0 | 0 |

## REFERENCES


Al-Sid-Cheikh M, Rowland SJ, Stevenson K, Rouleau C, Henry TB, Thompson RC (2018): Uptake, Whole-body distribution, and depuration of nanoplastics by the scallop *Pecten maximus* at environmentally realistic concentrations. Environmental Science & Technology 52, 14480-14486

Alldredge AL, Silver MW (1988): Characteristics, dynamics and significance of marine snow. Progress in Oceanography 20, 41-82

Bellingeri A, Bergami E, Grassi G, Faleri C, Redondo-Hasselerharm P, Koelmans A, Corsi I (2019): Combined effects of nanoplastics and copper on the freshwater alga *Raphidocelis subcapitata*. Aquatic Toxicology 210, 179-187

Bergami E, Bocci E, Vannuccini ML, Monopoli M, Salvati A, Dawson KA, Corsi I (2016): Nano-sized polystyrene affects feeding, behavior and physiology of brine shrimp *Artemia franciscana* larvae. Ecotoxicology and Environmental Safety 123, 18-25

Bergami E, Pugnalini S, Vannuccini M, Manfra L, Faleri C, Savorelli F, Dawson K, Corsi I (2017): Long-term toxicity of surface-charged polystyrene nanoplastics to marine planktonic species *Dunaliella tertiolecta* and *Artemia franciscana*. Aquatic Toxicology 189, 159-169

Bergkvist J, Thor P, Jakobsen HH, Wängberg S-Å, Selander E (2012): Grazer-induced chain length plasticity reduces grazing risk in a marine diatom. Limnology and Oceanography 57, 318-324

Besseling E, Wang B, Lürling M, Koelmans AA (2014): Nanoplastic affects growth of *S. obliquus* and reproduction of *D. magna*. Environmental Science & Technology 48, 12336-12343

Bhattacharya P, Lin S, Turner JP, Ke PC (2010): Physical adsorption of charged plastic nanoparticles affects algal photosynthesis. The Journal of Physical Chemistry C 114, 16556-16561

Bjærke O, Jonsson PR, Alam A, Selander E (2015): Is chain length in phytoplankton regulated to evade predation? Journal of Plankton Research 37, 1110-1119

Carson HS, Nerheim MS, Carroll KA, Eriksen M (2013): The plastic-associated microorganisms of the North Pacific Gyre. Marine Pollution Bulletin 75, 126-132

Casabianca S, Cappellacci S, Giacobbe MG, Dell'Aversano C, Tartaglione L, Varriale F, Narizzano R, Risso F, Moretto P, Dagnino A, Bertolotto R, Barbone E, Ungaro N, Penna A (2019): Plastic-associated harmful microalgal assemblages in marine environment. Environmental Pollution 244, 617-626

Chae Y, Kim D, Kim SW, An Y-J (2018): Trophic transfer and individual impact of nano-sized polystyrene in a four-species freshwater food chain. Scientific Reports 8, 284

Chen C-S, Anaya JM, Zhang S, Spurgin J, Chuang C-Y, Xu C, Miao A-J, Chen EY, Schwehr KA, Jiang Y (2011): Effects of engineered nanoparticles on the assembly of exopolymeric substances from phytoplankton. PLoS One 6, e21865

Ekvall MT, Lundqvist M, Kelpsiene E, Šileikis E, Gunnarsson SB, Cedervall T (2019): Nanoplastics formed during the mechanical breakdown of daily-use polystyrene products. Nanoscale Advances 1, 1055-1061

Fazey FM, Ryan PG (2016): Biofouling on buoyant marine plastics: An experimental study into the effect of size on surface longevity. Environmental Pollution 210, 354-360

Gigault J, Pedrono B, Maxit B, Ter Halle A (2016): Marine plastic litter: the unanalyzed nano-fraction. Environmental Science: Nano 3, 346-350

Guillard RR (1975): Culture of phytoplankton for feeding marine invertebrates. In: Smith WL, Chanley MH (eds), Culture of Marine Invertebrate Animals. Springer, 29-60

Harding G (1974): The food of deep-sea copepods. Journal of the Marine Biological Association of the United Kingdom 54, 141-155

Hoagland KD, Rosowski JR, Gretz MR, Roemer SC (1993): Diatom extracellular polymeric substances: function, fine structure, chemistry, and physiology. Journal of Phycology 29, 537-566

Hugh-Jones T, Turner A (2005): Sorption of ionic surfactants to estuarine sediment and their influence on the sequestration of phenanthrene, *Environmental Science & Technol*ogy, 39, 1688-1697

ISO 10253 (2006): Water quality – Marine algal growth inhibition test with *Skeletonema costatum* and *Phaeodactylum tricornutum*, ISO/TC 147/SC 5 10253

Kooi M, Nes EHv, Scheffer M, Koelmans AA (2017): Ups and downs in the ocean: effects of biofouling on vertical transport of microplastics. Environmental Science & Technology 51, 7963-7971

Lambert S, Wagner M (2016a): Formation of microscopic particles during the degradation of different polymers. Chemosphere 161, 510-517

Lambert S, Wagner M (2016b): Characterisation of nanoplastics during the degradation of polystyrene. Chemosphere 145, 265-268

Liu Y, Wang Z, Wang S, Fang H, Ye N, Wang D (2019): Ecotoxicological effects on *Scenedesmus obliquus* and *Danio rerio* co-exposed to polystyrene nano-plastic particles and natural acidic organic polymer. Environmental Toxicology and Pharmacology 67, 21-28

Lobelle D, Cunliffe M (2011): Early microbial biofilm formation on marine plastic debris. Marine Pollution Bulletin 62, 197-200

Long M, Moriceau B, Gallinari M, Lambert C, Huvet A, Raffray J, Soudant P (2015): Interactions between microplastics and phytoplankton aggregates: Impact on their respective fates. Marine Chemistry 175, 39-46

Lürling M, Beekman W (2002): Extractable substances (anionic surfactants) from membrane filters induce morphological changes in the green alga *Scenedesmus obliquus* (Chlorophyceae). Environmental Toxicology and Chemistry 21, 1213-1218

Mao Y, Ai H, Chen Y, Zhang Z, Zeng P, Kang L, Li W, Gu W, He Q, Li H (2018): Phytoplankton response to polystyrene microplastics: Perspective from an entire growth period. Chemosphere 208, 59-68

Masó M, Garcés E, Pagès F, Camp J (2003): Drifting plastic debris as a potential vector for dispersing Harmful Algal Bloom (HAB) species. Scientia Marina 67, 107-111

Masó M, Fortuño JM, de Juan S, Demestre M (2016): Microfouling communities from pelagic and benthic marine plastic debris sampled across Mediterranean coastal waters. Scientia Marina 80, 117-127

Mavrocordatos D, Perret D, Leppard GG (2007): Strategies and advances in the characterisation of environmental colloids by electron microscopy. Iupac Series on Analytical and Physical Chemistry of Environmental Systems 10, 345

Middelburg JJ, Barranguet C, Boschker HT, Herman PM, Moens T, Heip CH (2000): The fate of intertidal microphytobenthos carbon: An in situ 13C-labeling study. Limnology and Oceanography 45, 1224-1234

Morelli E, Gabellieri E, Bonomini A, Tognotti D, Grassi G, Corsi I (2018): TiO2 nanoparticles in seawater: Aggregation and interactions with the green alga *Dunaliella tertiolecta*. Ecotoxicology and Environmental Safety 148, 184-193

Mourdikoudis S, Pallares RM, Thanh NT (2018): Characterization techniques for nanoparticles: Comparison and complementarity upon studying nanoparticle properties. Nanoscale 10, 12871-12934

Muthukrishnan T, Al Khaburi M, Abed RM (2018): Fouling microbial communities on plastics compared with wood and steel: Are they substrate- or location-specific? Microbial Ecology, 1-14

Nolte TM, Hartmann NB, Kleijn JM, Garnæs J, van de Meent D, Hendriks AJ, Baun A (2017): The toxicity of plastic nanoparticles to green algae as influenced by surface modification, medium hardness and cellular adsorption. Aquatic Toxicology 183, 11-20

Oberbeckmann S, Löder MG, Labrenz M (2015): Marine microplastic-associated biofilms–a review. Environmental Chemistry 12, 551-562

Passow U, Alldredge A (1994): Distribution, size and bacterial colonization of transparent exopolymer particles (TEP) in the ocean. Marine Ecology Progress Series, 185-198

Peijnenburg WJ, Baalousha M, Chen J, Chaudry Q, Von der kammer F, Kuhlbusch TA, Lead J, Nickel C, Quik JT, Renker M (2015): A review of the properties and processes determining the fate of engineered nanomaterials in the aquatic environment. Critical Reviews in Environmental Science and Technology 45, 2084-2134

Penna N, Capellacci S, Ricci F (2004): The influence of the Po River discharge on phytoplankton bloom dynamics along the coastline of Pesaro (Italy) in the Adriatic Sea. Marine Pollution Bulletin 48, 321-326

PlasticsEurope (2015): Plastic the facts 2015 - An analysis of European plastics production, demand and waste data. http://www.plasticseurope.org/Document/plastics---the-facts-2015.aspx?FolID=2

Porter A, Lyons BP, Galloway TS, Lewis C (2018): Role of marine snows in microplastic fate and bioavailability. Environmental Science & Technology 52, 7111-7119

Redondo-Hasselerharm PE, Gort G, Peeters, E.T.H.M., Koelmans AA (2020): Nano- and microplastics affect the composition of freshwater benthic communities in the long term. Science Advances 6, eaay4054

Reisser J, Shaw J, Hallegraeff G, Proietti M, Barnes DK, Thums M, Wilcox C, Hardesty BD, Pattiaratchi C (2014): Millimeter-sized marine plastics: a new pelagic habitat for microorganisms and invertebrates. PloS one 9, e100289

Rist S, Hartmann NB (2018): Aquatic ecotoxicity of microplastics and nanoplastics: lessons learned from engineered nanomaterials. In: Wagner M, Lambert S, (eds) Freshwater Microplastics. The Handbook of Environmental Chemistry, 25-49

Round FE, Crawford RM, Mann DG (1990): Diatoms: biology and morphology of the genera. Cambridge university press

Seoane M, González-Fernández C, Soudant P, Huvet A, Esperanza M, Cid Á, Paul-Pont I (2019): Polystyrene microbeads modulate the energy metabolism of the marine diatom *Chaetoceros neogracile*. Environmental Pollution 251, 363-371

Simpson TL, Volcani BE (2012): Silicon and siliceous structures in biological systems. Springer Science & Business Media

Sjollema SB, Redondo-Hasselerharm P, Leslie HA, Kraak MH, Vethaak AD (2016): Do plastic particles affect microalgal photosynthesis and growth? Aquatic Toxicology 170, 259-261

Smayda TJ, Boleyn BJ (1966): Experimental observations on the flotation of marine diatoms. II. *Skeletonema costatum* and *Rhizosolenia setigera*. Limnology and Oceanography 11, 18-34

Song YK, Hong SH, Jang M, Han GM, Jung SW, Shim WJ (2017): Combined effects of UV exposure duration and mechanical abrasion on microplastic fragmentation by polymer type. Environmental Science & Technology 51, 4368-4376

Suaria G, Avio CG, Mineo A, Lattin GL, Magaldi MG, Belmonte G, Moore CJ, Regoli F, Aliani S (2016): The Mediterranean plastic soup: synthetic polymers in Mediterranean surface waters. Scientific Reports 6, 37551

Summers S, Henry T, Gutierrez T (2018): Agglomeration of nano-and microplastic particles in seawater by autochthonous and de novo-produced sources of exopolymeric substances. Marine Pollution Bulletin 130, 258-267

Takabayashi M, Lew K, Johnson A, Marchi A, Dugdale R, Wilkerson FP (2006): The effect of nutrient availability and temperature on chain length of the diatom, *Skeletonema costatum*. Journal of Plankton Research 28, 831-840

Ter Halle A, Jeanneau L, Martignac M, Jardé E, Pedrono B, Brach L, Gigault J (2017): Nanoplastic in the North Atlantic Subtropical Gyre. Environmental Science & Technology 51, 13689-13697

Tiede K, Boxall AB, Tear SP, Lewis J, David H, Hassellöv M (2008): Detection and characterization of engineered nanoparticles in food and the environment. Food Additives and Contaminants 25, 795-821

Totti C, Romagnoli T, Accoroni S, Coluccelli A, Pellegrini M, Campanelli A, Grilli F, Marini M (2019): Phytoplankton communities in the northwestern Adriatic Sea: Interdecadal variability over a 30-years period (1988–2016) and relationships with meteoclimatic drivers. Journal of Marine Systems 193, 137-153

Turner JT (2002): Zooplankton fecal pellets, marine snow and sinking phytoplankton blooms. Aquatic Microbial Ecology 27, 57-102

Van Sebille E, Wilcox C, Lebreton L, Maximenko N, Hardesty BD, Van Franeker JA, Eriksen M, Siegel D, Galgani F, Law KL (2015): A global inventory of small floating plastic debris. Environmental Research Letters 10, 124006

van Weert S, Redondo-Hasselerharm PE, Diepens NJ, Koelmans AA (2019): Effects of nanoplastics and microplastics on the growth of sediment-rooted macrophytes. Science of the Total Environment 654, 1040-1047

Wan JK, Chu WL, Kok YY, Lee CS (2018): Distribution of Microplastics and Nanoplastics in Aquatic Ecosystems and Their Impacts on Aquatic Organisms, with Emphasis on Microalgae. Reviews of Environmental Contamination and Toxicology 246, 133-158

Ward JE, Kach DJ (2009): Marine aggregates facilitate ingestion of nanoparticles by suspension-feeding bivalves. Marine Environmental Research 68, 137-142

Wood AM, Everroad R, Wingard L (2005): Measuring growth rates in microalgal cultures. Algal Culturing Techniques 18, 269-288

Wright SL, Kelly FJ (2017): Plastic and human health: a micro issue? Environmental Science & Technology 51, 6634-6647

Xiao R, Zheng Y (2016): Overview of microalgal extracellular polymeric substances (EPS) and their applications. Biotechnology Advances 34, 1225-1244

Ye S, Andrady AL (1991): Fouling of floating plastic debris under Biscayne Bay exposure conditions. Marine Pollution Bulletin 22, 608-613

Zettler ER, Mincer TJ, Amaral-Zettler LA (2013): Life in the “plastisphere”: microbial communities on plastic marine debris. Environmental Science & Technology 47, 7137-7146

Zhao S, Danley M, Ward JE, Li D, Mincer TJ (2017): An approach for extraction, characterization and quantitation of microplastic in natural marine snow using Raman microscopy. Analytical Methods 9, 1470-1478

Ševců A, El-Temsah YS, Joner EJ, Černík M (2012): Oxidative stress induced in microorganisms by zero-valent iron nanoparticles. Microbes and Environments 27, 215

CHAPTER 2

# TOWARDS A SUSTAINABLE DESIGN OF NPs FOR ENVIRONMENTAL APPLICATION: Bifunctionalized silver nanoparticles as $Hg^{2+}$ plasmonic sensor in water: synthesis, characterizations and ecosafety

## GRAPHICAL ABSTRACT

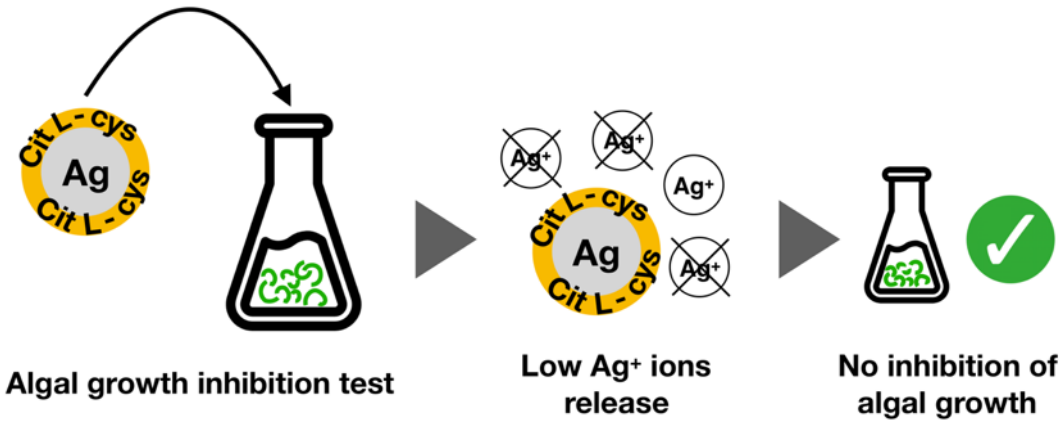

## ABSTRACT

In the present study hydrophilic silver nanoparticles (AgNPs), bifunctionalized with citrate (cit) and L-cysteine (Lcys), were synthetized. The AgNPcitLcys were thoroughly characterized by means of dynamic light scattering (DLS) and transmission electron microscopy (TEM), their molecular and electronic structure were investigated by fourier transform infrared spectroscopy (FT-IR), synchrotron radiation x-ray photoelectron spectroscopy (SR-XPS) and near red x-ray absorption fine structure (NEXAFS) techniques and the aqueous release of Ag ions in exposure media was assessed by inductively coupled plasma mass spectrometry (ICP-MS). Moreover, AgNPcitLcys were tested as plasmonic sensor in water with 16 different metal ions and, in view of their potential application as sensors in real water systems, the environmental safety (ecosafety) was assessed by using a standardized algal growth inhibition biassay (OECD 201 2011, ISO 10253 2006) with the freshwater microalga *Raphidocelis subcapitata* and the marine microalga *Phaeodactylum tricornutum*. The characterization confirmed the nanodimension of the AgNPcitLcys while the particles demonstrated to be sensitive to $Hg^{2+}$ in the range 1-10 ppm. The ecosafety assessment resulted in no toxicity for both microalgae at all AgNPcitLcys tested concentrations (1-500 μg/L), confirmed by the analysis of ion release which showed negligible release of Ag ions up to 500 μg/L of AgNPcitLcys. The great potential demonstrated by AgNPcitLcys in selective detection of environmental $Hg^{2+}$ may attract a great interest for several biological research fields, while the absence of toxicity for two model microalgal species belonging to different aquatic environments, is a first promising step for their application in water remediation strategies.

## 1. Introduction

Nanosized inorganic particles, of either simple or composite nature, display unique physical and chemical properties and represent an increasingly important material in the development of novel nanodevices which can be used in numerous fields, such as, catalysis, energy, optoelectronics, biomedicine, sensors. Several recent achievements offer the possibility of generating new types of nanostructured materials with designed surface and structural properties (Lin et al., 2010; Lohse and Murphy, 2012; Venditti, 2017; Zhang et al., 2018). Among other materials, silver nanoparticles (AgNPs) are deeply studied for their optical and antibacterial properties, easy functionalization and cheap preparations (Burdușel et al., 2018; Liu et al., 2018). Many studies employ AgNPs as optical sensor, using the localized surface plasmon resonance (LSPR) that is a specific feature of the colloidal silver nanoparticle solutions: the energy of the absorption maximum and the shape of the peak are strongly dependent on the size, shape and interparticle distance, but also on the surrounding environment, which can influence the degradation or aggregation of the particles (Bothra et al., 2013; Prosposito et al., 2016).

In particular, AgNPs have drawn attention for mercury sensor development, specially due to: i) their high sensitivity to $Hg^{2+}$ micro-level concentration change and due to the existence of redox chemistry of $Hg^{2+}$; ii) the surface (Ag°) resulting in Ag-Hg amalgam formation by means of etching of NPs; iii) soft-soft chemistry between heavy metals and sulfur containing stabilizing ligands on AgNP surfaces and thus causing a prominent change in the absorbance intensity and peak position (Zheng et al., 2012; Chen et al., 2016).

Surface functionalization plays a role both in stabilization and in reactivity of AgNPs. Therefore, the ligand surface chemistry is used to tune their sensing properties. For sensing application towards $Hg^{2+}$ ions, many ligands (such as N-cholyl-Lcysteine, citrate, 6-thioguanine) have been used for the surface modification of AgNPs, with high degree of selectivity and sensitivity (Duan et al., 2014; Annadhasan and Rajendiran, 2015; Jarujamrus et al., 2015; Zhan et al., 2017).

Nevertheless, the use of NPs for heavy metals removal known as nanoremediation is a matter of concern due to the potential risks associated with the scarcity of information regarding their behavior, fate and impact on environment and human health (Otto et al., 2008). In order to overcome such limitations, an ecosafe approach is developed with the aim to determine the ecotoxicity of AgNPs to organisms playing important ecological roles in aquatic ecosystems, such as for instance primary producers (Corsi et al., 2018). AgNPs are recognized to exert toxic effects to biota, both from fresh- and marine waters, from bacteria and microalgae to crustacean, mussels, fishes and mammalian cells (Navarro et al., 2008; Miao et al., 2009; Kittler et al., 2010; He et al., 2012; Gliga et al., 2014; Ivask et al., 2014; Becaro et al., 2015; Navarro et al., 2015; Sendra et al., 2017; Ale et al., 2019). Among these studies, those reporting $Ag^{+}$ release in exposure media (Navarro et al., 2008; Miao et al., 2009; Kittler et al., 2010; He et al., 2012; Ivask et al., 2014; Navarro et al., 2015; Sendra et al., 2017), report that AgNP toxicity often appears to be closely linked to the dissolution of the particles and consequent release of Ag ions during exposure. Based on such evidence of potential severe ecotoxicological outcomes, the ecosafety assessment of AgNPs is mandatory in order to avoid any potential toxicological risks associated with their application in environmental remediation.

In the present study AgNP functionalized with hydrophilic capping agents (*i.e.,* citric acid (cit) and L-Cysteine (L-cys)), AgNPcitLcys, were synthesized and characterized by means of UV-Vis, Fourier Transform Infrared (FT-IR), Synchrotron radiation-X-ray photoelectron (SR-XPS), Near Edge X-ray Absorption Fine Structure (NEXAFS) spectroscopies. Their nanodimensions were investigated by Dynamic Light Scattering (DLS) and Transmission Electron Microscope (TEM) analysis. AgNPs were tested as plasmonic sensor for heavy metal detection in water with 16 different metal ions. Moreover, in view of AgNP application in real water systems, their ecosafety was investigated through standardized ecotoxicological assessment using two different microalgal species, *R. subcapitata* and *P. tricornutum*, belonging to, respectively, the freshwater and the marine water environment.

## 2. Materials & Methods

A detailed description of AgNcitLcys synthesis and characterization methods carried out by Iole Venditti, Chiara Battocchio, Giovanna Iucci, Luca Tortora and Valeria Secchi from the Department of Sciences from Roma Tre University of Rome, Paolo Prosposito and Luca Buratti from the Department of Industrial Engineering from the Univerity of Rome Tor Vergata and Stefano Franchi from the Elettra-Sincrotrone of Trieste, can be found in the appendix following the end of the chapter.

### 2.1. AgNP characterization

Size distribution of AgNPcitLcys (50 mg/L) was investigated by means of DLS (Zetasizer Nano Series, Malvern instruments), combined with the Zetasizer Nano Series software (version 7.02, Particular Sciences) at T = 25.0 ± 0.2°C in milliQ water, as well as media used for toxicity assessment (freshwater, TG 201, and marine water, F/2). The particles were also investigated by TEM (Philips Morgagni 268 D electronics, at 80 KV and equipped with a MegaView II CCD camera) at 10 mg/L in MilliQ water. The obtained images were analysed with *ImageJ* for particles size measurement. A total of 180 particles were measured in two portions of two different images and the average size was calculated.

Ag release from the AgNPs has been assessed in both TG 201 and F/2 aqueous media, at the beginning (0 h) and at the end (72 h) of exposure period of ecotoxicological assays. Six solutions were prepared: TG 201, F/2, TG 201 + 500 µg AgNPs/L, F/2 + 500 µg AgNPs/L, TG 201 + 7 µg $AgNO_3$/L, F/2 + 7 µg $AgNO_3$/L. Solutions were kept in the same conditions as toxicity tests (21 ± 2 °C and 16/8 light-dark photoperiod) and mixed by shaking once a day. An aliquot of each solution was taken at both time points (0, 72 h) and centrifuged (5000 g, 40 min, 21 °C) by using a centrifugal filter device with a 3 kDa cut-off (Amicon Ultra-15 mL, Millipore, USA). The resulting filtrate was acidified with $HNO_3$ (10%) following the protocol by Sikder et al. (2018) and analysed by ICP-MS (Perkin Elmer NexION 350 spectrometer) for determining Ag concentration.

Further description of AgNPcitLcys characterization methods can be found in the appendix following the end of the chapter.

## 2.2. AgNP ecosafety tests

The intrinsic toxicity of AgNPs was investigated through standardized 72 h algal growth inhibition tests (OECD 201, 2011; ISO 10253, 2006) using two different algal species, belonging to the freshwater and to the marine water environment, *R. subcapitata* and *P. tricornutum*. Algae were cultured, respectively, in TG 201 medium and F/2 medium, in axenic and exponential growth conditions, at 18 ± 1 °C and 16/8 h light-dark cycle photoperiod. TG201 was prepared using milliQ water as dilution water, while F/2 was prepared using natural seawater (NSW, 40‰), previously filtered with a 0.22 µm membrane filter and kept at 4°C until use. Both media, once prepared, were and filtered with a 0.22 µm membrane filter to ensure sterility and kept at 4°C until use. Toxicity tests were performed using the same media used for algal culturing, modified only in their ethylenediaminetetraacetic acid (EDTA) concentrations (respectively, 0.05 mg/L for TG201 and 0.8 mg/L for F/2, previously checked to ensure acceptable algal growth) in order to reduce the introduction of chelating agents which are shown to interfere with heavy metals toxicity (Resgalla Jr et al., 2012; Leal et al., 2016). Algae were acclimated to test conditions in the modified media 72 h before the beginning of the test, under the following conditions: 21 ± 2 °C and 16/8 light-dark photoperiod.

PS single-use sterile multiwell were used for toxicity tests, with 2 mL volume capacity for each well. Initial algal concentration was $1x10^4$ cells/mL, and the tests were manually aerated every 24 h using a pipette with sterile tips. Exposure concentrations were 10, 25, 50, 100, 200, 500 µg AgNPs/L. $AgNO_3$ was used as positive control at the following exposure concentrations: 3.5, 7, 14, 21, 35 µg $AgNO_3$/L. In order to exclude any possible role of components of the coating to the toxicity of the AgNPs, citrate and L-Cysteine were tested separately, in the following concentrations: 0.5, 1, 2, 5, 10 mg/L.

## 3. Results and Discussion

TEM studies carried out on diluted samples (10 mg/L) in milliQ water show AgNPs with a variable size distribution and a tendency to aggregation (Figure 1a) but with an average single-particle diameter of 5 ± 2 nm, as measured manually by imageJ software in Figure 1b. DLS data (Table 1) report higher size values in milliQ water (133.7 ± 1.27 nm) compared to those obtained from TEM images. This discrepancy can be explained considering the relatively high (> 0.3) polydispersity index (PDI), showing a non-homogeneous dispersion of AgNPcitLcys in terms of size, with aggregates of variable sizes, as also visible in figure 1a, and to the fact that DLS estimated the hydrodynamic radius $<2R_H>$ of the particles in the aqueous environment. The variable size of the aggregates and the presence of smaller particles/aggregates (10-20 nm) is visible in the size distribution graph by volume (Figure 2), which gives a greater importance to smaller aggregates compared to the calculations by intensity. Therefore, the DLS data are not directly comparable with TEM data, as reported in the literature (D'Amato et al., 2003; De Angelis et al., 2014), but confirm, in both cases, the nanodimension of the AgNPs. In TG201, DLS data are in agreement with what reported for MilliQ water, while F/2 caused the AgNPcitLcys form aggregates with an average hydrodynamic diameter of 617 ± 47 nm. The completely different behaviour of AgNPcitLcys in F/2 compared to TG201 is related to the high ionic strength of the latter, which is known to enhance the aggregation of negatively charged NPs. Z- potential reflect this trend, confirming the relatively stable suspension in milliQ water and TG201 with values >I30I, which assure the electrical repulsion between the particles, and values close to 0 in F/2, due to the shielding effect of NSW cations on the negatively charged surface, which reduces the repulsion between the particles causing aggregation.

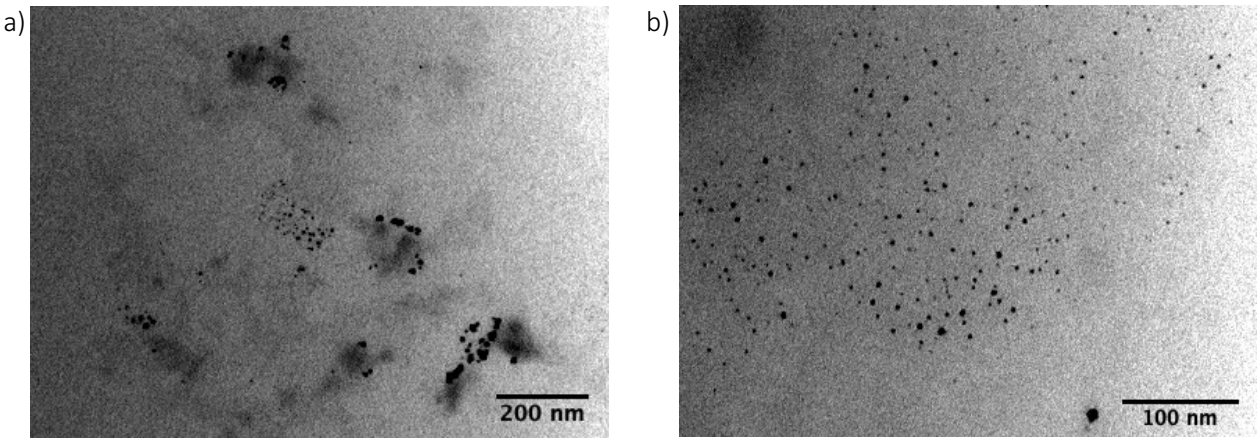


**Figure 1.** a), b) TEM images of AgNP in MilliQ water.

**Table 1.** Hydrodynamic diameter (z-average), PDI (PoliDispersity Index) and surface charge (z-potential) of AgNPs at 50 mg/L and 25°C, in MilliQ water, freshwater algal medium (TG201) and marine water algal medium (F/2).

| | MilliQ | TG201 | F/2 |
|---|---|---|---|
| Z-average (nm) | 133.7 ± 1.27 | 136.9 ± 4.9 | 617 ± 47 |
| PDI | 0.371 | 0.403 | 0.256 |
| Z-potential (mV) | -40.3 ± 1.37 | -33.4 ± 0.436 | -1.97 ± 1.66 |

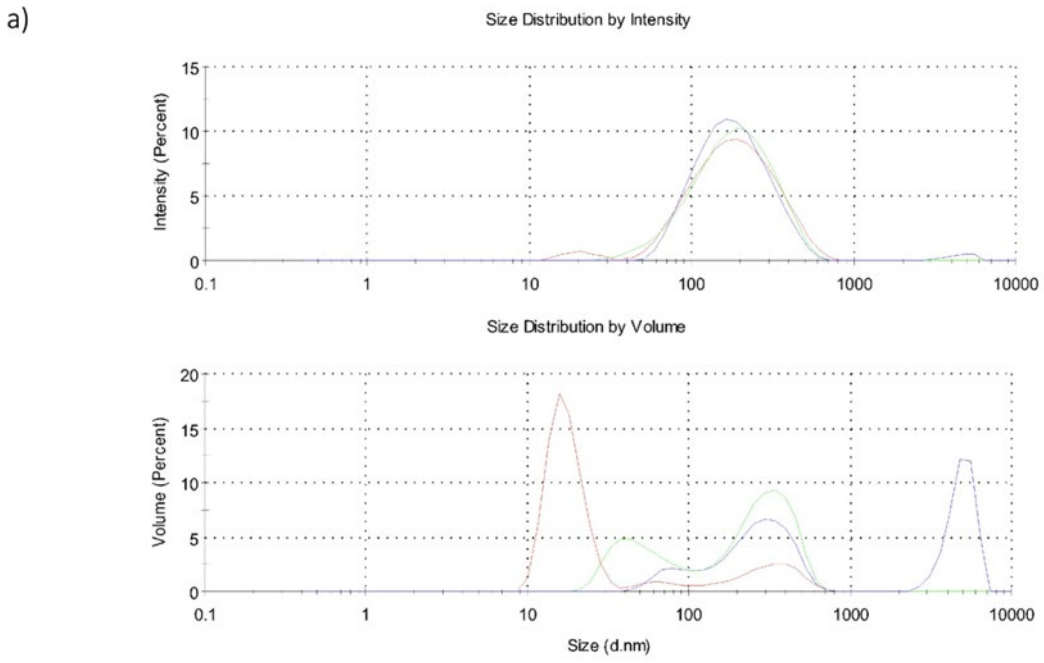

b)

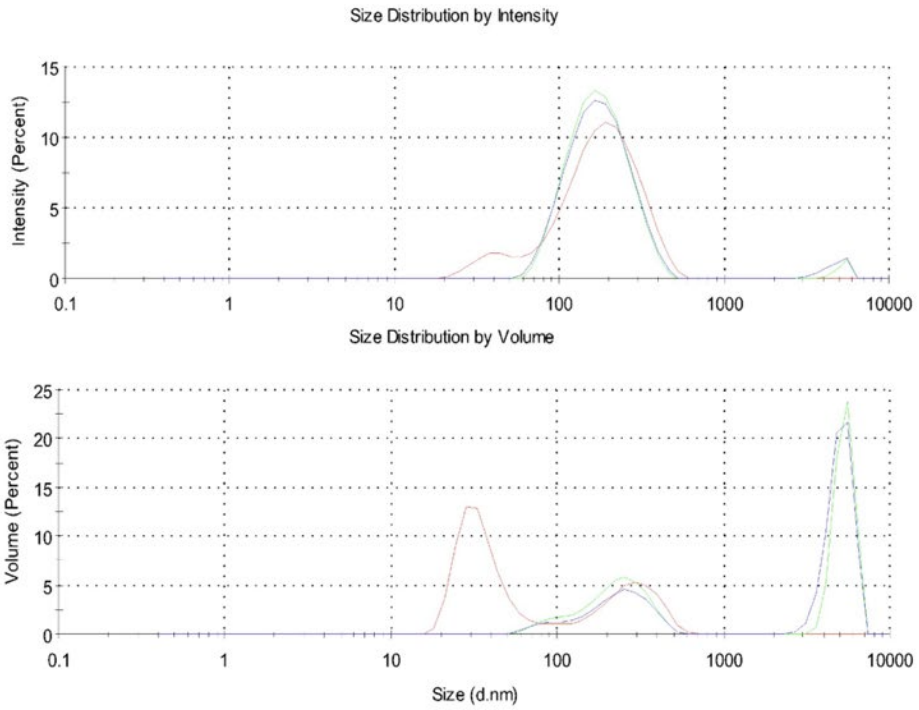


c)

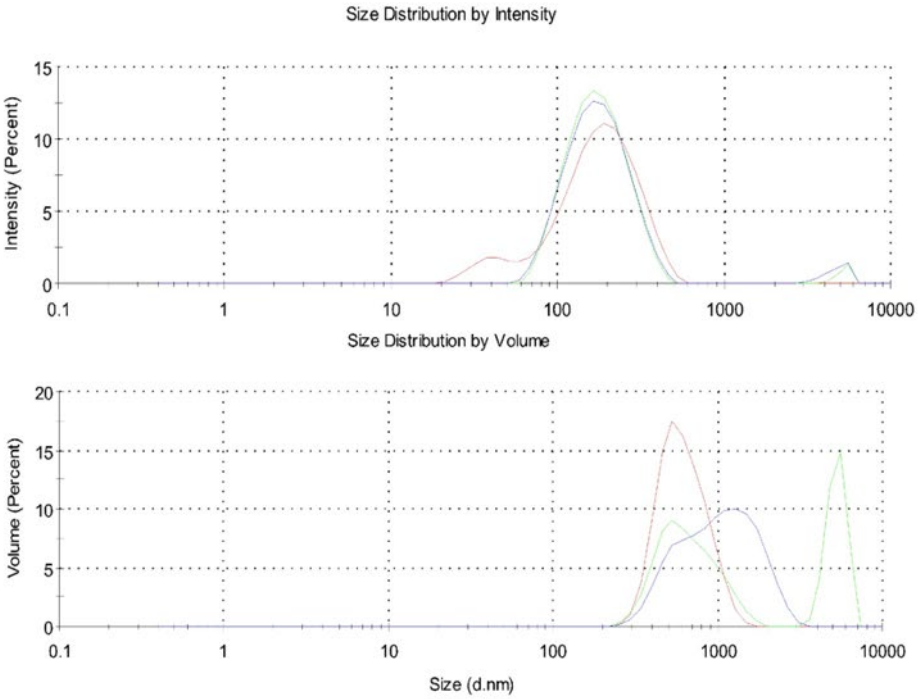


**Figure 2.** DLS size distribution graphs by intensity and by volume of AgNPcitLcys in a) milliQ water, b) TG201 and c) F/2.

Measurements of Ag concentration in fresh and marine aqueous media showed an almost absent Ag ions release from AgNPcitLcys (Table 2) as opposed to what observed in literature for other AgNPs with different types of coatings (Navarro et al., 2008; Miao et al., 2009; Kittler et al., 2010; He et al., 2012; Ivask et al., 2014; Navarro et al., 2015; Sendra et al., 2017). In fact, Ag concentrations in both TG201 medium (freshwater) and F/2 medium (marine water) with 500 µg AgNPs/L were low (up to 0.4 µg /L) and comparable with those measured in controls (up to 0.36 µg/L). However, it is to be noted that in the presence of AgNPs, Ag levels slightly increased after 72 h, from 0.19 to 0.4 µg/L in freshwater, and 0.15 to 0.37 µg/L in marine water. Since the dissolution of AgNPs is thought to be independent from particles aggregation state (Gunsolus et al., 2015), the reason for the lack of ion release is to be found in the particular coating of citrate and L-cysteine, which probably plays an important role in the almost absent dissolution of the AgNPcitLcys.

Table 2. Ag concentrations (expressed as µg/L) in freshwater and marine waters with algal medium solution (CTRL), as well as algal medium solutions with AgNPs (500 µg/L) and with $AgNO_3$ (7 µg /L).

| | TG 201 | | F/2 | |
|---|---|---|---|---|
| | 0 h | 72 h | 0 h | 72 h |
| CTRL | 0.36 ± 0.06 | 0.26 ± 0.08 | 0.27 ± 0.01 | 0.26 ± 0.02 |
| AgNPs | 0.19 ± 0.02 | 0.4 ± 0.06 | 0.15 ± 0.03 | 0.37 ± 0.03 |
| $AgNO_3$ | 4.42 ± 0.09 | 4.79 ± 0.18 | 4.37 ± 0.08 | 5.32 ± 0.22 |

Further AgNPcitLcys characterization results can be found in the appendix following the end of this chapter.

Algal toxicity tests with *R. subcapitata* and *P. tricornutum* exposed to AgNPs showed no inhibition of growth rate at all tested concentrations, as reported in Figure 3a. Moreover, exposed algae showed a slightly higher growth rate compared to the control (negative growth rate inhibition), at almost all tested concentrations. The observed enhanced increase, however, was not explained by positive control tests carried out with cit and L-cys, which had no effect on algal growth (Figure 4). Reference

toxicant ($AgNO_3$) showed a 60% inhibition of growth rate compared to the control of *R. subcapitata*, already at the lowest concentration tested (3.5 µg $AgNO_3$/L), confirming the toxicity of Ag for microalgae (Figure 3b). On the opposite, no effect on growth was observed for *P. tricornutum* exposed in the same conditions, confirming the drop in free Ag ions in solution due to complexation with $Cl^-$ ions in seawater as measured by Gunsolus et al. (2015)( Figure 3a, b).

a)

b)

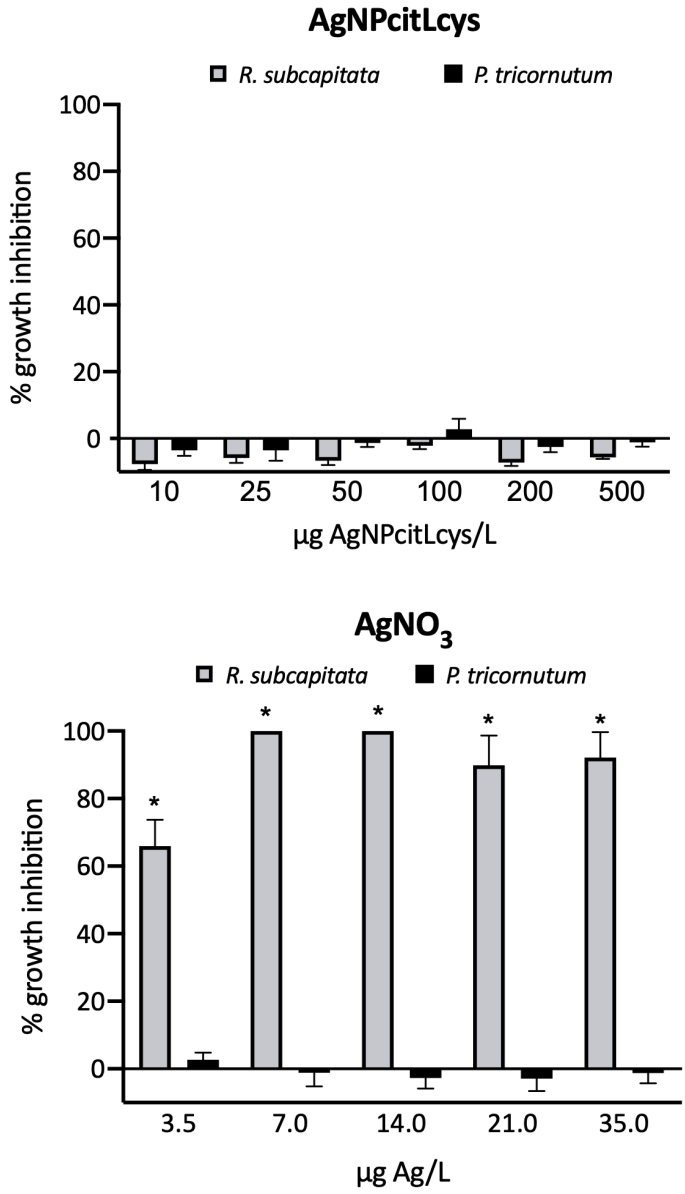


**Figure 3.** Percentage of growth rate inhibition compared to control of *R. subcapitata* and *P. tricornutum* exposed to a) AgNPcitLcys (10, 25, 50, 100, 200, 500 µg/L) and b) $AgNO_3$ (3.5, 7, 14, 21, 35 µg Ag/L) for 72h at 21 ± 2 °C and 16/8 light-dark photoperiod. Data shown as mean ± standard deviation. Column marked with * show statistically different values compared to control with $p<0.05$.

a)

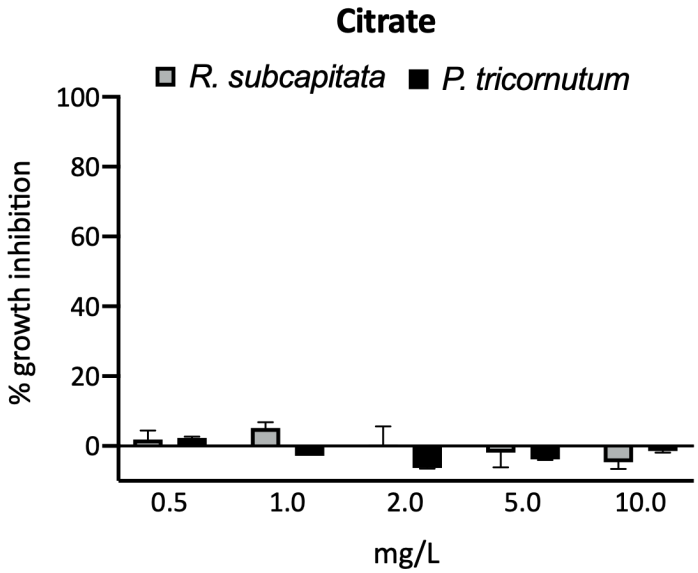


b)

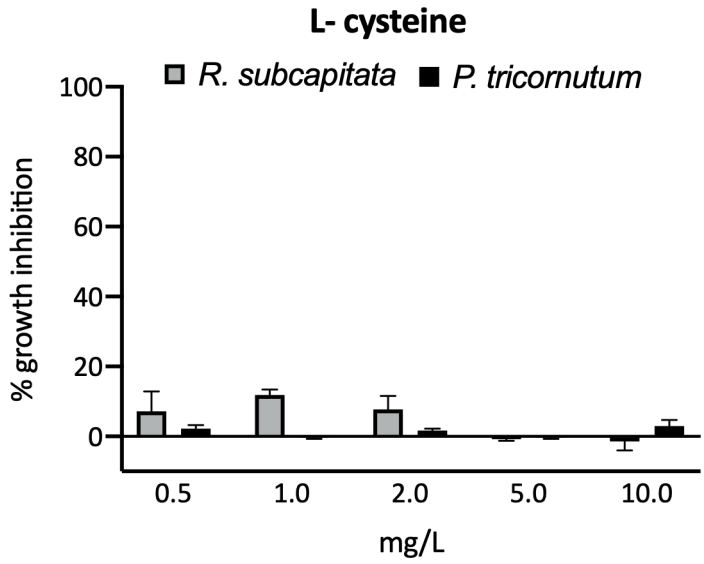


**Figure 4.** Percentage of growth rate inhibition compared to control of *R. subcapitata* and *P. tricornutum* exposed to a) citrate, b) L- cysteine at 0.5, 1, 2, 5, 10 mg/L, for 72h at 21 ± 2 °C and 16/8 light-dark photoperiod. Data shown as mean ± standard deviation.

The absence of toxicity for our AgNPcitLcys confirms chemical analysis results showing insufficient release of Ag ions to exert a toxic effect on both microalgae (Table 2). Such findings further validate the hypothesis by which AgNP toxicity is closely bound to the release of Ag ions (Miao et al., 2009; He et al., 2012; Ivask et al., 2014; Navarro et al., 2015). In fact, the dissolution of Ag from AgNPs, either pristine or coated (chitosan, lactate, polyvinylpyrrolidone, polyethelene glycol, gelatin, sodium

dodecylbenzenesulfonate, Cit, dexpanthenol, carbonate), has been reported by many studies (Navarro et al., 2008; Miao et al., 2009; Kittler et al., 2010; He et al., 2012; Ivask et al., 2014; Sharma et al., 2014; Navarro et al., 2015; Sendra et al., 2017; Sikder et al., 2018) and recognized to be linked to the observed toxicity to microalgae (Miao et al., 2009; He et al., 2012; Ivask et al., 2014; Navarro et al., 2015). Moreover, for particles smaller than 20 nm an additional dissolution-independent toxic effect seems to be playing a role (Gliga et al., 2014; Ivask et al., 2014), as some studies report what seems to be a nano-size dependent toxicity. However, despite being very small, AgNPcitLcys further confirm their integrity in terms of low Ag release.

The covalently-bound L-cysteine coating in addition to the citrate might be responsible for the observed low dissolution of Ag ions, since previous studies revealed that the citrate coating alone was not able to prevent such release in aqueous media (He et al., 2012; Ivask et al., 2014; Gunsolus et al., 2015; Navarro et al., 2015). Molecules with a high reduced sulfur content are known to bind metal ions; L-cysteine, thanks to the presence of a thiol group, is able to act as a strong Ag ligand (Luoma, 2008). Thiol groups could act either by binding Ag ions and blocking their release in the media, or by excluding oxidizing agents to come in contact with the particles surface, preventing its dissolution and consequent release of Ag ions in the medium (Liu et al., 2010). For instance, Gunsolus et al. (2015) reported a significant reduction of Ag ions release and of bactericidal activity of citrate-AgNPs upon incubation with natural organic matter rich in thiol groups. While some studies observed a reduction in the toxic effect of Ag-releasing AgNPs after addition of L-cysteine in solution, probably as a consequence of L-cysteine complexation of free Ag ions (Navarro et al., 2008; He et al., 2012; Navarro et al., 2015). However, information on L-cysteine effects on AgNP stability and dissolution are conflicting. The presence of free L-cysteine in solution has also been observed to enhance Ag ions release from AgNPs (Gondikas et al., 2012). In our study, however, the low Ag levels in exposure media confirmed that the combined Cit/L-cys coating was able to prevent prevents the release Ag ions from the particles and assure the absence of toxicity to microalgae. These results could be compared to what observed by Mu et al. (2015) for graphene oxide (GO) nanosheets which, when functionalized with covalently-bound L-

cysteine, showed to maintain all the physico-chemical properties of GO nanosheets, except for the toxic effects to zebrafish embryos. L-cysteine demonstrated, hence, and was confirmed by our study, to be a biocompatible molecule for nanomaterials and nanoparticles coating.

Since the main concern regarding the environmental application of AgNP is due to potential toxic effect to non-target aquatic species (Ivask et al., 2014), our findings clearly showed the ecosafety of AgNPs and promote their use in the aquatic environment.

## 4. Conclusions

In this work AgNPs functionalized with hydrophilic capping agents, (*i.e.,* citrate and L-cysteine), were synthesized and characterized by means of UV-Vis, FT-IR, SR-XPS and NEXAFS spectroscopies, confirming the surface functionalization. Their nanodimensions were confirmed by DLS and TEM analysis, while they showed high selectivity and sensitivity for $Hg^{2+}$ in water (concentration range: 1-10 ppm) respect to 16 different metal ions investigated. Measurements of Ag concentration in fresh and marine aqueous media showed low Ag ions release. AgNPcitLcys ecosafety was investigated through standardized algal toxicity tests with the microalgae *R. subcapitata* and *P. tricornutum*, belonging to the fresh and marine water environment, showing no inhibition of growth rate at all tested concentrations (10-500 mg/L). The lack of a toxic effect to microalgae is probably to be attributed to the cit/L-cys coating, also as a consequence of the observed low dissolution of Ag ions.

These results open new ways for AgNP sensing applications: in environmental tests on more complex biological systems, up to tests on real samples, both in fresh and saltwater.

## 5. Acknowledgments

For their contribution to this work, I thank Prof. Iole Venditti, Prof. Chiara Battocchio, Prof. Giovanna Iucci, Dr. Luca Tortora and Dr. Valeria Secchi from the Department of Sciences from Roma Tre University of Rome, Dr. Paolo Prosposito and Luca Buratti from the Department of Industrial Engineering from the Univerity of Rome Tor Vergata and Dr. Stefano Franchi from the Elettra-Sincrotrone of Trieste, for the synthesis and characterization of AgNPcitLcys. Also, I thank Claudia Faleri from the department of Life Sciences of the University of Siena for TEM imaging and Prof. Giuseppe Protano from the department of Physical, Earth and Environmental Sciences of the University of Siena for heavy metal analysis. I thank Prof. Andrea M. Atrei from the Department of Biotechnology, Chemistry and Pharmaceutical of the University of Siena and Dr.ssa Marianna Uva and Dr. Eugenio Macchia from CREA s.c.a.r.l. for DLS use.

## REFERENCES


Ale A, Liberatori G, Vannuccini ML, Bergami E, Ancora S, Mariotti G, Bianchi N, Galdopórpora JM, Desimone MF, Cazenave J (2019): Exposure to a nanosilver-enabled consumer product results in similar accumulation and toxicity of silver nanoparticles in the marine mussel *Mytilus galloprovincialis*. Aquatic Toxicology 211, 46-56

Annadhasan M, Rajendiran N (2015): Highly selective and sensitive colorimetric detection of Hg (II) ions using green synthesized silver nanoparticles. RSC Advances 5, 94513-94518

Becaro AA, Jonsson CM, Puti FC, Siqueira MC, Mattoso LH, Correa DS, Ferreira MD (2015): Toxicity of PVA-stabilized silver nanoparticles to algae and microcrustaceans. Environmental Nanotechnology, Monitoring & Management 3, 22-29

Bothra S, Solanki JN, Sahoo SK (2013): Functionalized silver nanoparticles as chemosensor for pH, Hg2+ and Fe3+ in aqueous medium. Sensors and Actuators B: Chemical 188, 937-943

Burdușel A-C, Gherasim O, Grumezescu AM, Mogoantă L, Ficai A, Andronescu E (2018): Biomedical applications of silver nanoparticles: An up-to-date overview. Nanomaterials 8, 681

Chen N, Zhang Y, Liu H, Wu X, Li Y, Miao L, Shen Z, Wu A (2016): High-performance colorimetric detection of Hg2+ based on triangular silver nanoprisms. ACS Sensors 1, 521-527

Corsi I, Winther-Nielsen M, Sethi R, Punta C, Della Torre C, Libralato G, Lofrano G, Sabatini L, Aiello M, Fiordi L (2018): Ecofriendly nanotechnologies and nanomaterials for environmental applications: Key issue and consensus recommendations for sustainable and ecosafe nanoremediation. Ecotoxicology and Environmental Safety 154, 237-244

D'Amato R, Medei L, Venditti I, Russo M, Falconieri M (2003): Chemical synthesis of polyphenylacetylene nanospheres with controlled dimensions for photonic crystals. Materials Science and Engineering: C 23, 861-865

De Angelis R, Venditti I, Fratoddi I, De Matteis F, Prosposito P, Cacciotti I, D'Amico L, Nanni F, Yadav A, Casalboni M (2014): From nanospheres to microribbons: Self-assembled Eosin Y doped PMMA nanoparticles as photonic crystals. Journal of Colloid and Interface Science 414, 24-32

Duan J, Yin H, Wei R, Wang W (2014): Facile colorimetric detection of Hg2+ based on anti-aggregation of silver nanoparticles. Biosensors and Bioelectronics 57, 139-142

Gliga AR, Skoglund S, Wallinder IO, Fadeel B, Karlsson HL (2014): Size-dependent cytotoxicity of silver nanoparticles in human lung cells: the role of cellular uptake, agglomeration and Ag release. Particle and Fibre Toxicology 11, 11

Gondikas AP, Morris A, Reinsch BC, Marinakos SM, Lowry GV, Hsu-Kim H (2012): Cysteine-induced modifications of zero-valent silver nanomaterials: implications for particle surface chemistry, aggregation, dissolution, and silver speciation. Environmental Science & Technology 46, 7037-7045

Gunsolus IL, Mousavi MP, Hussein K, Bühlmann P, Haynes CL (2015): Effects of humic and fulvic acids on silver nanoparticle stability, dissolution, and toxicity. Environmental Science & Technology 49, 8078-8086

He D, Dorantes-Aranda JJ, Waite TD (2012): Silver nanoparticle-algae interactions: Oxidative dissolution, reactive oxygen species generation and synergistic toxic effects. Environmental Science & Technology 46, 8731-8738

ISO 10253 (2006): Water quality – Marine algal growth inhibition test with *Skeletonema costatum* and *Phaeodactylum tricornutum*, ISO/TC 147/SC 5 10253

Ivask A, Kurvet I, Kasemets K, Blinova I, Aruoja V, Suppi S, Vija H, Käkinen A, Titma T, Heinlaan M (2014): Size-dependent toxicity of silver nanoparticles to bacteria, yeast, algae, crustaceans and mammalian cells in vitro. PloS one 9, e102108

Jarujamrus P, Amatatongchai M, Thima A, Khongrangdee T, Mongkontong C (2015): Selective colorimetric sensors based on the monitoring of an unmodified silver nanoparticles (AgNPs) reduction for a simple and rapid determination of mercury. Spectrochimica Acta Part A: Molecular and Biomolecular Spectroscopy 142, 86-93

Kittler S, Greulich C, Diendorf J, Koller M, Epple M (2010): Toxicity of silver nanoparticles increases during storage because of slow dissolution under release of silver ions. Chemistry of Materials 22, 4548-4554

Leal PP, Hurd CL, Sander SG, Armstrong E, Roleda MY (2016): Copper ecotoxicology of marine algae: a methodological appraisal. Chemistry and Ecology 32, 786-800

Lin C-Y, Yu C-J, Lin Y-H, Tseng W-L (2010): Colorimetric sensing of silver (I) and mercury (II) ions based on an assembly of tween 20-stabilized gold nanoparticles. Analytical Chemistry 82, 6830-6837

Liu G, Haiqi G, Li K, Xiang J, Lan T, Zhang Z (2018): Fabrication of silver nanoparticle sponge leather with durable antibacterial property. Journal of Colloid and Interface Science 514, 338-348

Liu J, Sonshine DA, Shervani S, Hurt RH (2010): Controlled release of biologically active silver from nanosilver surfaces. ACS Nano 4, 6903-6913

Lohse SE, Murphy CJ (2012): Applications of colloidal inorganic nanoparticles: from medicine to energy. Journal of the American Chemical Society 134, 15607-15620

Luoma SN (2008): Silver nanotechnologies and the environment. The Project on Emerging Nanotechnologies Report 15, 12-13

Miao A-J, Schwehr KA, Xu C, Zhang S-J, Luo Z, Quigg A, Santschi PH (2009): The algal toxicity of silver engineered nanoparticles and detoxification by exopolymeric substances. Environmental Pollution 157, 3034-3041

Mu L, Gao Y, Hu X (2015): L-Cysteine: A biocompatible, breathable and beneficial coating for graphene oxide. Biomaterials 52, 301-311

Navarro E, Piccapietra F, Wagner B, Marconi F, Kaegi R, Odzak N, Sigg L, Behra R (2008): Toxicity of silver nanoparticles to *Chlamydomonas reinhardtii*. Environmental Science & Technology 42, 8959-8964

Navarro E, Wagner B, Odzak N, Sigg L, Behra R (2015): Effects of differently coated silver nanoparticles on the photosynthesis of *Chlamydomonas reinhardtii.* Environmental Science & Technology 49, 8041-8047

OECD, 201 (2011) Test No. 201: Freshwater Alga and Cyanobacteria, Growth Inhibition Test , OECD Guidelines for the Testing of Chemicals, Section 2, OECD Publishing, Paris, https://doi.org/10.1787/9789264069923-en

Otto M, Floyd M, Bajpai S (2008): Nanotechnology for site remediation. Remediation Journal: The Journal of Environmental Cleanup Costs, Technologies & Techniques 19, 99-108

Prosposito P, Mochi F, Ciotta E, Casalboni M, De Matteis F, Venditti I, Fontana L, Testa G, Fratoddi I (2016): Hydrophilic silver nanoparticles with tunable optical properties: Application for the detection of heavy metals in water. Beilstein Journal of Nanotechnology 7, 1654-1661

Resgalla Jr C, Poleza F, Souza R, Máximo M, Radetski C (2012): Evaluation of effectiveness of EDTA and sodium thiosulfate in removing metal toxicity toward sea urchin embryo-larval applying the TIE. Chemosphere 89, 102-107

Sendra M, Yeste M, Gatica J, Moreno-Garrido I, Blasco J (2017): Direct and indirect effects of silver nanoparticles on freshwater and marine microalgae (*Chlamydomonas reinhardtii* and *Phaeodactylum tricornutum*). Chemosphere 179, 279-289

Sharma VK, Siskova KM, Zboril R, Gardea-Torresdey JL (2014): Organic-coated silver nanoparticles in biological and environmental conditions: fate, stability and toxicity. Advances in Colloid and Interface Science 204, 15-34

Sikder M, Lead JR, Chandler GT, Baalousha M (2018): A rapid approach for measuring silver nanoparticle concentration and dissolution in seawater by UV–Vis. Science of the Total Environment 618, 597-607

Venditti I (2017): Gold nanoparticles in photonic crystals applications: A review. Materials 10, 97

Zhan L, Yang T, Zhen SJ, Huang CZ (2017): Cytosine triphosphate-capped silver nanoparticles as a platform for visual and colorimetric determination of mercury (II) and chromium (III). Microchimica Acta 184, 3171-3178

Zhang Z, Shen W, Xue J, Liu Y, Liu Y, Yan P, Liu J, Tang J (2018): Recent advances in synthetic methods and applications of silver nanostructures. Nanoscale Research Letters 13, 1-18

Zheng W, Liang L, Gu B (2012): Mercury reduction and oxidation by reduced natural organic matter in anoxic environments. Environmental Science & Technology 46, 292-299

## APPENDIX

### 1. Materials and Methods_*AgNP synthesis and sensing tests*

Sodium citrate ($Na_3C_6H_5O_7$, cit), L-Cysteine ($C_3H_7NO_2S$, L-cys), silver nitrate ($AgNO_3$) and sodium borohydride ($NaBH_4$) have been used as received (Sigma Aldrich reagent grade). Heavy metal ions contamination was accomplished by using the following salts: $NaAsO_2$, $NaHAsO_4$ * $7H_2O$, $Ca(ClO_4)_2$, $Cd(NO_3)_2$, $CoCl_2$ * $6H_2O$, $CrCl_3$ * $6H_2O$, $Cu(NO_3)_2$, $FeCl_3$ * $6H_2O$, $Hg(NO_3)_2$ * $H_2O$, $KClO_4$, $Mg(ClO_4)_2$, $NaClO_4$, $NdCl_3$ * $6H_2O$, $NiCl_2$ * $6H_2O$, $Pb(NO_3)_2$, $Zn(NO_3)_2$ * $6H_2O$. For all the solutions, we used deionized water (electrical conductivity less than 1 μΩ/cm at room temperature) obtained from a water purification system (Millipore Milli-Q). All the reagents were purchased from Sigma Aldrich and were used without further purification.

UV-Vis spectra were run in $H_2O$ solution by using quartz cells with a Shimadzu 2401 PC UV-vis spectrophotometer and by using single-use UV-PMMA cuvettes with Perkin-Elmer Lambda 19 UV-Vis-NIR for sensing test characterization.

ATR-FTIR spectra have been recorded as films deposited by casting from water suspension with a FTIR spectrometer (Nicolet iS50, Thermo Fisher Scientific, Madison, WI, USA) equipped with a mid- and far-IR capable diamond ATR accessory. FT-IR spectra were recorded in the range between 350 and 4000 $cm^{-1}$ with a resolution of 4 $cm^{-1}$, a zero-filling factor of 2 and the co-addition of 64 scans. Data were acquired using OMNIC software (version 9.8.372), subtracting the air background spectrum obtained prior to each sample spectrum acquisition.

SR-XPS measurements were performed at the Elettra synchrotron radiation source (Trieste, Italy), using the Materials Science Beamline (MSB), that is positioned at the left end of the bending magnet 6.1. MSB is equipped with a plane grating monochromator providing SR light in the 21−1000 eV energy range. The UHV endstation, whose base pressure is of $2 \times 10^{-10}$ mbar, is equipped with a SPECS PHOIBOS 150 hemispherical electron analyser, low-energy electron diffraction optics, a dual-anode Mg/Al X-ray source, an ion gun, a sample manipulator with a K-type thermocouple attached to the rear side of the sample. For the here presented experiments we detected photoelectrons emitted by C1s, O1s, S2p, Ag3d, N 1s and Hg4f core levels, using a normal emission geometry. In order to maximize signals intensity, we selected a photon energy value of 630 eV (impinging at 60°) for all elements except S; in order to maximize the intensity of S2p signals, that was expected to be very low due to element dilution, the S2p core level was measured with photon energy = 350 eV. Charging correction of binding energies (BEs) was done using as a reference the aliphatic C 1s (BE 285.0 eV)(Chastain and King Jr, 1992). To fit core level spectra, we subtracted a Shirley background and then used Gaussian peak functions as signals components (Shirley, 1972).

NEXAFS experiments were carried out at the BEAR (Bending magnet for Emission Absorption and Reflectivity) beamline, installed at the left exit of the 8.1 bending magnet and located the ELETTRA third generation storage ring. The beamline optics can deliver photons having energy comprised between 5 eV and 1600 eV with selectable degree of ellipticity. The carbon K-edge spectra were recorded at normal (90°) and grazing (20°) incidence relative to the sample surface of the linearly polarized photon beam; however, no angular effects were detected. Calibration of the photon energy and resolution was carried out at the K absorption edges of Ar, $N_2$ and Ne. In order to normalize the spectra, a straight line fitting the part of the spectrum below the edge was subtracted and the value recorded at 330.00 eV was assessed to 1.

The AgNPs stabilized with citrate (cit) and L-Cysteine (L-cys) were prepared and characterized in analogy to literature reports (Majzik et al., 2010; Venditti et al., 2017). 1.47 g of sodium citrate were dissolved in 50 mL of distilled water (0.01 M), 0.006 g of L-cys in 25 mL of distilled water (0.002 M) and 0.21 g of $AgNO_3$ in 25 mL of distilled water (0.05 M). Then, 25 mL of L-cys solution, 10 mL of Cit solution and 2.5 mL of $AgNO_3$ solution were added sequentially in a 100 ml flask, provided with a magnetic stir. The mixture was degassed with Argon for 10 minutes, then 4 mL of $NaBH_4$ solution (0.016 g in 4 mL distilled water) were added. The mixture was allowed to react at room temperature for 2 hours and at the end the brown solution was recollected and purified by centrifugation (13000 rpm, 10 min, 2 times with deionized water). AgNPs main characterizations: UV-Vis ($\lambda_{max}$ nm, $H_2O$) = 400 nm; $<2R_H>$ (nm, $H_2O$) = 8 ± 1; TEM Ø = 5 ± 2 nm.

A fixed volume of AgNPs in water (typical concentration 1.6 mg/ml) was mixed with a fixed volume of water solution containing the heavy metal ions at specific concentration. After five minutes of interaction of the nanoparticles with the metal ions, the optical absorption spectra were collected in order to verify possible changes (shape, energy and intensity) of the typical localized surface plasmon resonance (LSPR). The response to several metal ions at different concentrations from 25 ppm down to 1 ppm was tested by UV-Vis spectroscopy.

## *2.* Results and Discussion

### 2.1. AgNP synthesis and sensing tests

The synthesis of AgNPs by wet chemical reduction is a useful method to obtain spherical nanoparticles with tuned sizes and opportune capping agent (Venditti et al., 2017). In this work, AgNPs have been prepared by the reduction in aqueous solution of silver nitrate with sodium borohydride as strong reducing agent. Two different capping agents have been chosen (Figure 4a): cit, crucial to induce a high hydrophilic behavior, and L-cys, to induce selective interaction with the environment.

In fact, it is well known that the amino group can easily interact with the chemical environment and in particular with $Hg^{2+}$ ions (Chai et al., 2009). In order to avoid the excessive presence of L-cys, leading to nanoparticles aggregation, the molar ratio Ag/Cit/L-cys = 1/4/2 was chosen. The obtained AgNPs scheme is shown in Figure 1a. After careful purification, AgNPs have been characterized by means of UV-Vis, FTIR and XPS spectroscopies. The UV-Vis spectrum (Figure 4b) showed the typical LSPR band, at $\lambda_{max}$ = 400 nm, confirming the nanodimensions. Moreover, FTIR investigations showed the presence of Cit and L-cys on the particles, as reported in Figure 4c.

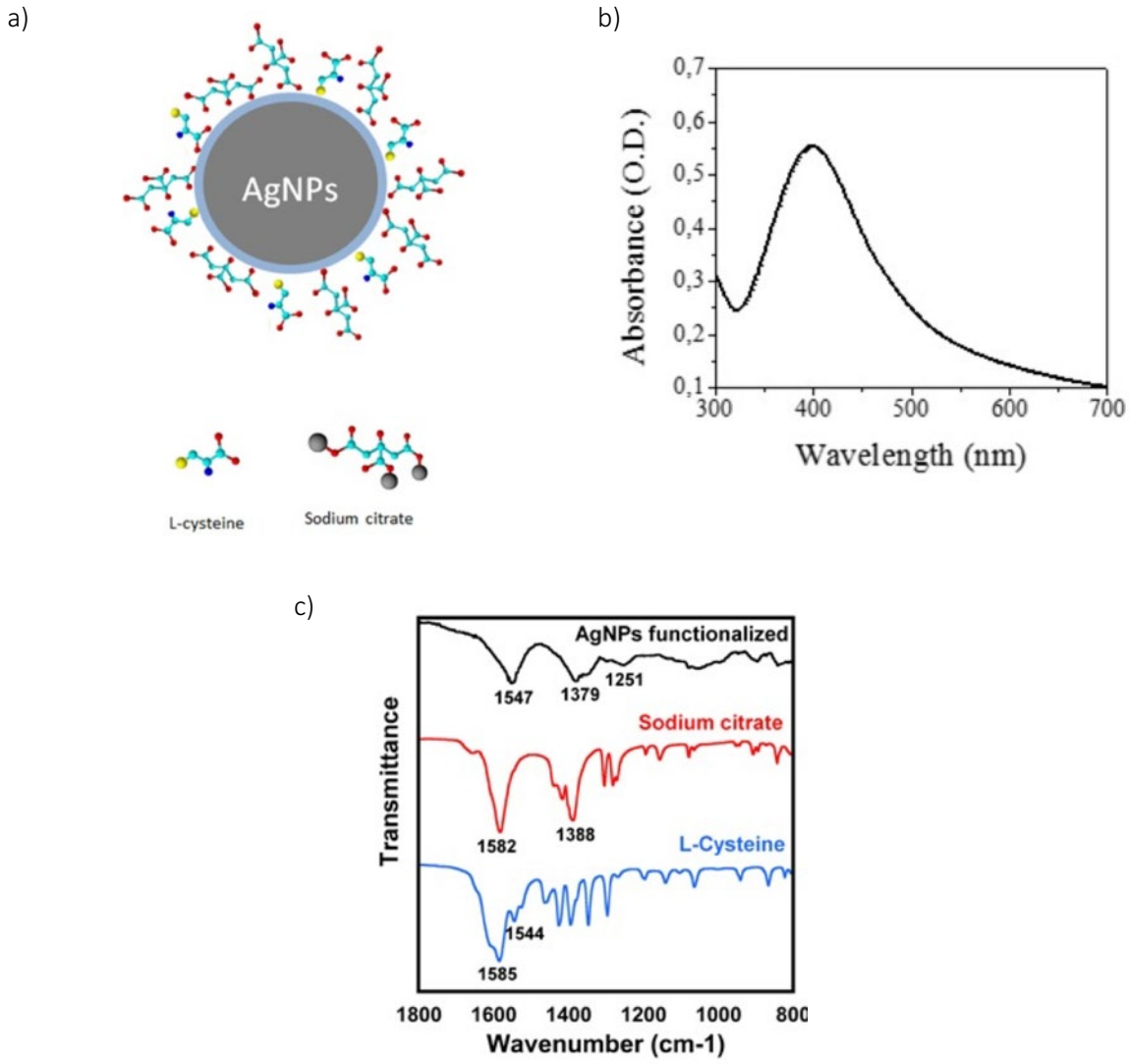


**Figure 4. a)** Scheme of bifuntionalized AgNPs; **b)** UV-Vis spectrum in water of AgNPs, with LSPR band centred at 400 nm; **c)** ATR-FTIR spectra of bifunctionalized AgNPs (Top) and the capping agents, cit (Center), and L-cys (Bottom).

When the ATR-FTIR spectrum of AgNP bifunctionalized with cit and L-cys was compared with reference spectra of these capping agents (Figure 4c), it is immediately evident the absence of the band at ~1582 $cm^{-1}$ ($\nu_{as}(COO^-)$) in AgNP spectrum. This could be interpreted as evidence that most carboxylate groups of the citrate and cysteine are attached to the surface of the AgNPs. In fact, a similar results was observed by Frost et al (2017), who studied the ATR-FTIR spectra of citrate-capped AgNPs and Au-NPs; only for AgNPs, they observed the disappearance of the $\nu_{as}(COO^-)$ peak and interpreted this result in terms of adsorption geometry of the citrate molecule, with all the three carboxylate groups interacting with the AgNP surface: the $\nu_{as}(COO^-)$ lying parallel to the AgNP surfaces results in an infrared-inactive transition. The main contributions to the symmetric and asymmetric stretching vibration of the carboxylate group are obviously mainly due to the citrate molecule, that is present in higher concentration on the AgNPs; however, it seems reasonable to hypothesize a similar reactivity for the different carboxylate groups. Moreover, in the AgNP spectrum is present a broad peak at ~1547 $cm^{-1}$ that could be due to the overlapping between the N-H bending of cysteine and the residual carboxylate groups not attached to the AgNP surface. The functionalization with cit and L-cys can be also supported by the presence in the AgNP spectrum of a broad peak centered at 1379 $cm^{-1}$ indicating the $COO^-$ symmetric stretching vibrations; the peak position is slightly shifted to lower wavenumber compared to the free carboxylate anion, as already evidenced by Frost et al (2017).

The main contribution to the carboxylate peak is the broad peak centered at 3300 $cm^{-1}$ which is attributed to the stretching vibrations of the hydroxyl group (ν (O-H)) (data not shown) probably coming from water adsorbed onto nanoparticles surface. We were not able to detect any S-H band around 2550 $cm^{-1}$, that would indicate the presence of free L-cys on the AgNP surface (Li et al., 2012; Shi et al., 2014). The intensity of this peak in the spectrum of L-cys is actually rather low; however, XPS results confirm the absence of S-H groups.

To support FTIR data, AgNPs were also investigated by NEXAFS spectroscopy. C k edge spectra of AgNPs were recorded at normal, magic and grazing incidence; however, no angle dependent effect was detected; therefore, the C k-edge spectrum of AgNPs is shown in Figure 5. The main feature in the spectrum is the 1s→π* consisting of two peaks located at 287.7 and 288.8 eV, with a shoulder at 285.5 eV. According to literature, the 1s→π* transition related to the C=O bond in the carboxylate of L-cys is expected at 288.6 eV; similar values are expected for carboxyl groups. Moreover, L-cys is expected to show a 1s→ σ* peak related to the C-S bond at about 287.3 eV (Zubavichus et al., 2009). Therefore, we can assign this complex band to overlap between π*C=O and σ*C-S transitions. The broad bands located at about 294 and 300 eV are related to 1s→ σ* transitions of C-H and C=O bonds respectively. The overall spectrum yields prove of successful capping of the AgNP surface by both cit and L-cys.

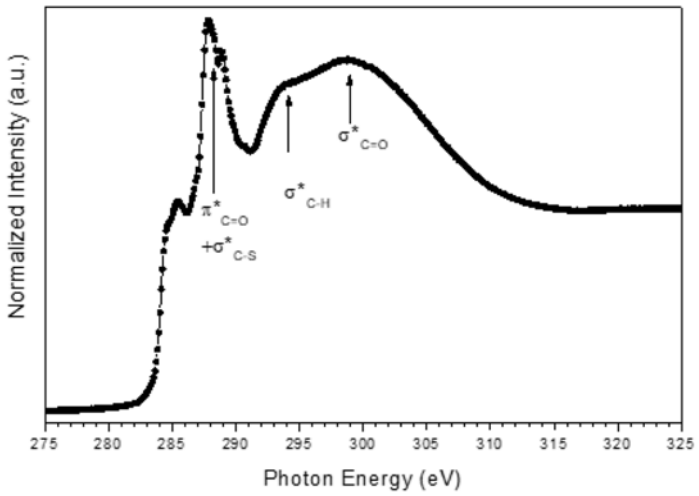


Figure 5. C k-edge NEXAFS spectrum of AgNPS recorded at 20° incidence angle.

Sensing tests were performed by checking the optical absorption spectra of the contaminated systems with respect to the reference AgNPcitLcys water solution. In Figure 6a the absorption spectra of AgNPs in water solutions without (reference solution) and with different concentrations of $Hg^{2+}$ ions in the range 1 to 10 ppm, are reported. An evident red shift of the band peak energy, together with an increase of the intensity and a broadening of the band with the increasing concentration of ions can be appreciated. The same type of measurement has been performed for all the 16 ions listed in the experimental part for concentration from 10 ppm down to the lowest concentration of 1 ppm. Figure 6c shows the red shift of the absorption band of all the metal ions tested at the concentration of 2.5 ppm. A significant change has been detected only for $Hg^{2+}$ ions while for all the other ions the absorption bands remain almost constant within the error bars.

The limit of detection (LOD) of the nanosensor for the analysis of $Hg^{2+}$ was determined from the calibration curves. The LOD was determined from three times the standard deviation of the blank signal, obtaining a value equal to 0.6 ppm. The obtained LOD was found to be comparable with other AgNP systems and the experimental results for the determination of $Hg^{2+}$ obtained by some other methods are listed in Table 3 for comparison (Chai et al., 2009; Lin et al., 2010; Forough and Farhadi, 2011; Farhadi et al., 2012; Alam et al., 2015; Ma et al., 2016b; Buduru et al., 2017).

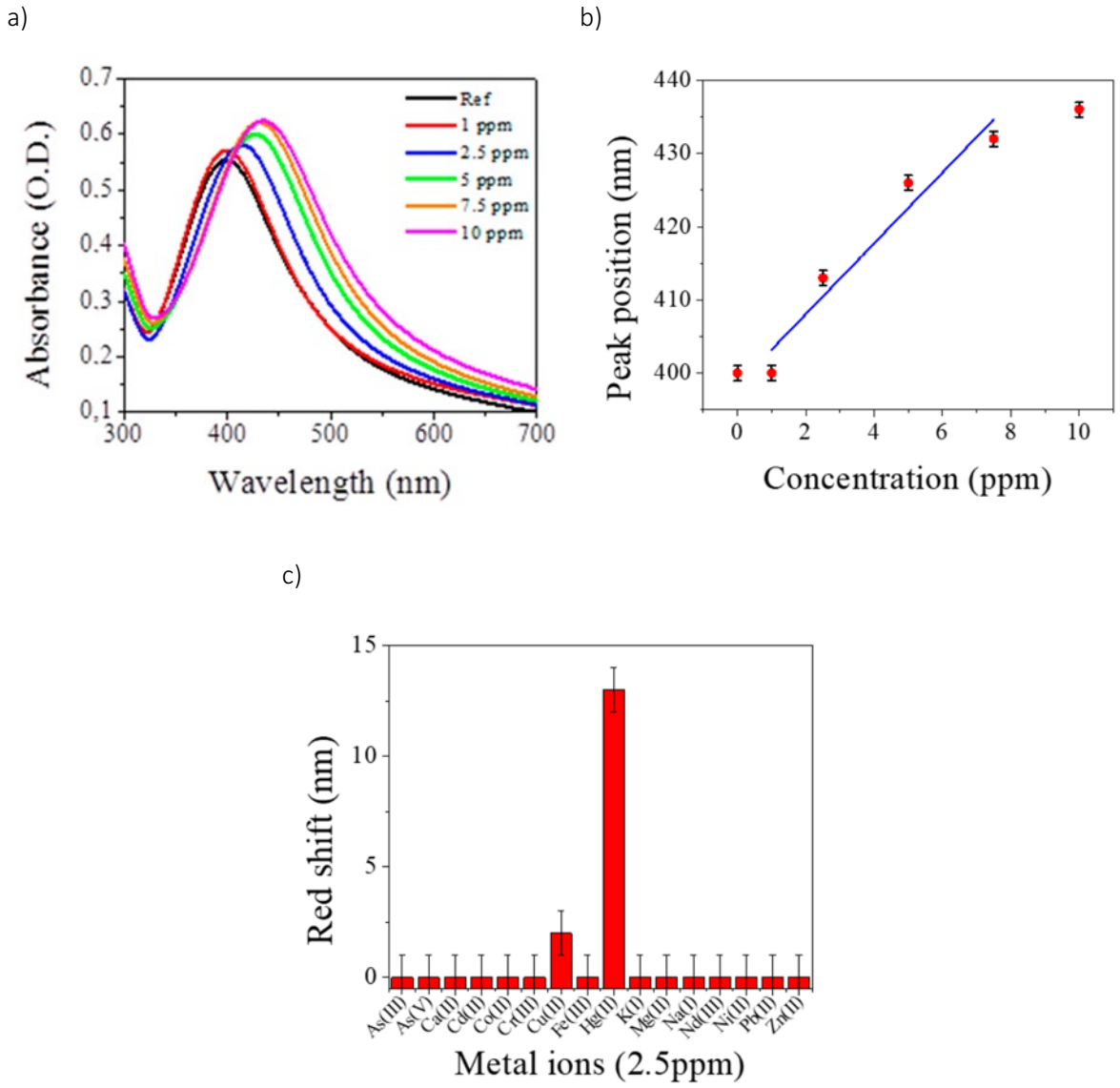


**Figure 6.** a) Absorption spectra of AgNP water solutions without and with different concentrations of $Hg^{2+}$ listed in the figure; b) calibration curve as a function of $Hg^{2+}$ concentration; c) redshift of the absorption band maximum in presence of all the metal ions tested at concentration of 2.5 ppm.

**Table 3.** Comparison between dimension and limit of detection (LOD) of some metal NPs used as a colorimetric sensor for the detection of $Hg^{2+}$.

| Metal NPs functionalization | NPs diameter (nm) | $Hg^{2+}$ detection limit (LOD) (M) | References |
|---|---|---|---|
| Citrate/Lcysteine-AgNPs | 5 ± 2 | $3.0 \times 10^{-6}$ (0.6 ppm) | This work |
| Tween 20-AuNPs | - | $1.0 \times 10^{-7}$ | (Lin et al., 2010) |
| L-cys-AuNPs | - | $1.0 \times 10^{-7}$ | (Chai et al., 2009) |
| *Acanthe phylum bracteatum* AgNPs | 29-68 | $2.2 \times 10^{-6}$ | (Forough and Farhadi, 2011) |
| L-cysteine AgNPs | 10 | $1.0 \times 10^{-8}$ | (Ma et al., 2016b) |
| Glutamine/Histidine AgNPs | 5.5 ± 1.0 | $9.0 \times 10^{-7}$ | (Buduru et al., 2017) |
| Glutathione AgNPs | 3.9 ± 0.6 | $> 1.0 \times 10^{-7}$ | (Alam et al., 2015) |

## 2.2. SR-XPS characterization of AgNPs and AgNPs-$Hg^{2+}$

Synchrotron radiation induced X-ray spectroscopy measurements allowed to probe the interaction between AgNPs and $Hg^{2+}$ ions. Spectra were collected at C1s, N1s, O1s, Ag3d, S2p and Hg4f core levels. All the individuated spectral components confirm AgNP stability, and cit and L-cys capping efficiency. C1s spectrum has three components at 285.00, 286.46 and 288.45 eV BE, respectively associated with aliphatic carbons (mainly impurities, that are always observed in samples prepared in air by liquid solutions); O1s spectra, reported in Figure 7c, also show three different kinds of oxygen atoms, respectively belonging to carbonyl (C=O) functional groups (532.00 eV BE), hydroxyl moieties (-OH, 533.00 eV BE) and physisorbed water (small contribution at about 534.5 eV BE). The atomic ratio between C=O and –OH is C=O/-OH = 1/1.4, very close to the C=O/-OH = 1/1.3 that is theoretically expected for a Cit/L-cys stoichiometry = 2/1, as in the synthetic procedure reported in Materials and Methods. N1s spectrum was also collected, showing a single component centred at 400.24 eV, as expected for amine-like nitrogens. Indeed, C1s, O1s and N1s data analysis confirm the molecular stability of the AgNPs, also after interaction with $Hg^{2+}$ ions.

Generally speaking, the most indicative signals for the surface-structure analysis of metal nanoparticles capped with thiols are M (Au4f, Ag3d) and S2p core levels; for this purpose, Ag3d and S2p spectra are reported in Figure 7 and will be here discussed in detail.

Ag3d spectra (Figure 7a) are asymmetric at high BE, a common feature in capped nanoparticles, indicating that at least two different kinds of silver atoms compose the nanoparticle: the spin-orbit pair at lower BE values (Ag3d5/2 = 368.08 eV) is associated with metallic silver at the NPs core; the signal at higher BE, of very small intensity (about 9% of the whole signal) is due to positively charged silver atoms at the NP surface, interacting with the capping molecule (Mochi et al., 2018; Rinaldi et al., 2019). S2p spectra are also composite, showing two spin orbit pairs of very similar intensity (atomic percent are 54.4% lower BE - 45.6 % higher BE); interestingly, the two signals are both indicative for sulphur atoms covalently bonded to silver, but with two different hybridizations: the spin-orbit pair at lower BE (S2p3/2 = 161.05 eV) is indicative for S-Ag bonds with sp hybridized sulphur; the signal at higher BE (S2p3/2 = 162.09 eV) suggests S-Ag bonds with sp3 S atoms (Carlini et al., 2017). It is noteworthy that no physisorbed thiol moieties appear (R-SH S2p3/2 signals are expected around 163 – 164 eV BE); this finding is in excellent agreement with the hypothesis made by A Majzik et al. (2010) based on $^{1}H$ NMR studies and suggesting that in metal nanoparticles stabilized by mixed Cit and L-cys capping agents the L-cys molecules preferentially tend to directly bond the metal surface, inducing the most part of Cit molecules to form a shell around the first L-cys layer, in a “layer-by-layer”-like arrangement. It is noteworthy that XPS data do not allow excluding that some Cit molecules could intercalate between L-

cys and directly interact with Ag atoms at the NP surface, as evidenced by IR spectroscopy results. The last signal reported in Figure 7d is the Hg4f spectrum. As evidenced in the figure, two spin-orbit pairs can be individuated; the first signal ($Hf4f_{7/2}$ BE = 100.10 eV) can be associated with metallic Hg atoms (Sun et al., 1980); the components at higher BE ($Hg4f_{7/2}$ = 100.85 eV) are consistent with literature data reported for $Hg^{2+}$ ions in oxides or coordination compounds. The occurrence of a signal indicative for metallic Hg is in excellent agreement with the findings reported in Frost et al. (2017), where for AgNP stabilized by cit molecules and interacting with Hg(II) ions, a direct interaction between Hg and Ag atoms at the nanoparticle surface was envisaged. To better understand the chemistry and geometry of Hg(II) – AgNPs interaction, XAS experiments at the Hg $L_{III}$-edge are in programme. Actually, X-ray absorption experiments will allow to directly probe the local coordination chemistry of the metal ion, providing information complementary to the SR-XPS data and allowing for a precise description of the Hg coordination site.

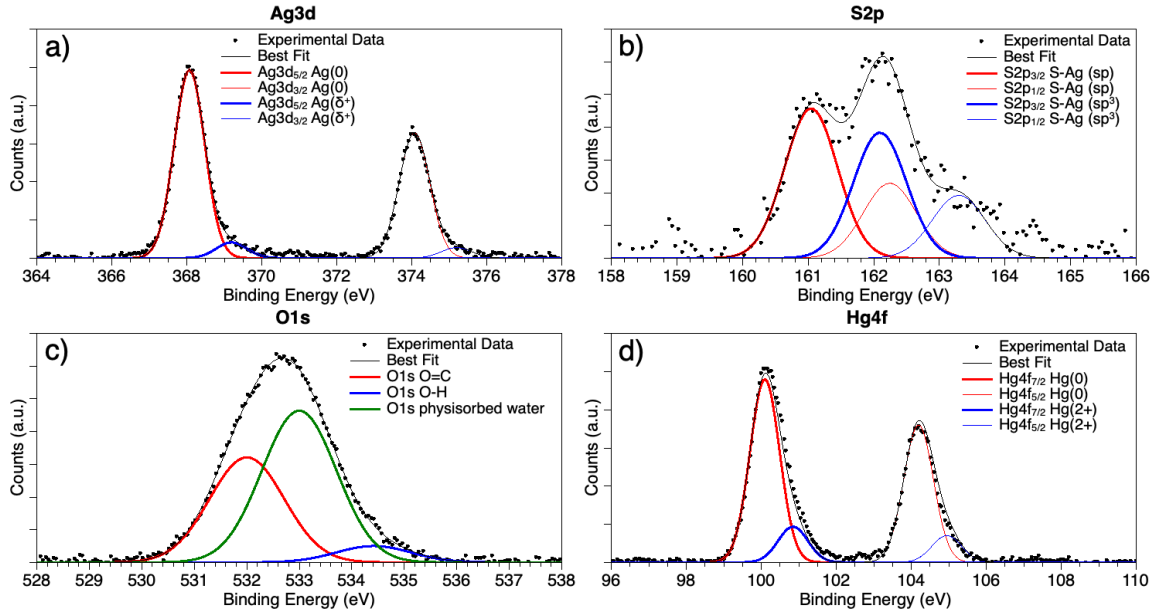


**Figure 7.** SR-XPS spectra collected on AgNPs-$Hg^{2+}$ aggregates at a) Ag3d, b) S2p, c) O1s and d) Hg4f core levels.

## APPENDIX References


Alam A, Ravindran A, Chandran P, Khan SS (2015): Highly selective colorimetric detection and estimation of Hg2+ at nano-molar concentration by silver nanoparticles in the presence of glutathione. Spectrochimica Acta Part A: Molecular and Biomolecular Spectroscopy 137, 503-508

Buduru P, Reddy BSR, Naidu N (2017): Functionalization of silver nanoparticles with glutamine and histidine for simple and selective detection of Hg2+ ion in water samples. Sensors and Actuators B: Chemical 244, 972-982

Carlini L, Fasolato C, Postorino P, Fratoddi I, Venditti I, Testa G, Battocchio C (2017): Comparison between silver and gold nanoparticles stabilized with negatively charged hydrophilic thiols: SR-XPS and SERS as probes for structural differences and similarities. Colloids and Surfaces A: Physicochemical and Engineering Aspects 532, 183-188

Chai F, Wang C, Wang T, Ma Z, Su Z (2009): L-cysteine functionalized gold nanoparticles for the colorimetric detection of Hg2+ induced by ultraviolet light. Nanotechnology 21, 025501

Chastain J, King Jr RC (1992): Handbook of X-ray photoelectron spectroscopy. Perkin-Elmer Corporation 40, 221

Farhadi K, Forough M, Molaei R, Hajizadeh S, Rafipour A (2012): Highly selective Hg2+ colorimetric sensor using green synthesized and unmodified silver nanoparticles. Sensors and Actuators B: Chemical 161, 880-885

Forough M, Farhadi K (2011): Biological and green synthesis of silver nanoparticles. Turkish Journal of Engineering and Environmental Sciences 34, 281-287

Frost MS, Dempsey MJ, Whitehead DE (2017): The response of citrate functionalised gold and silver nanoparticles to the addition of heavy metal ions. Colloids and Surfaces A: Physicochemical and Engineering Aspects 518, 15-24

Li S, Liu P, Wang Q (2012): Study on the effect of surface modifier on self-aggregation behavior of Ag nano-particle. Applied Surface Science 263, 613-618

Lin C-Y, Yu C-J, Lin Y-H, Tseng W-L (2010): Colorimetric sensing of silver (I) and mercury (II) ions based on an assembly of tween 20-stabilized gold nanoparticles. Analytical Chemistry 82, 6830-6837

Ma Y, Pang Y, Liu F, Xu H, Shen X (2016): Microwave-assisted ultrafast synthesis of silver nanoparticles for detection of Hg2+. Spectrochimica Acta Part A: Molecular and Biomolecular Spectroscopy 153, 206-211

Majzik A, Fülöp L, Csapó E, Bogár F, Martinek T, Penke B, Bíró G, Dékány I (2010): Functionalization of gold nanoparticles with amino acid, β-amyloid peptides and fragment. Colloids and Surfaces B: Biointerfaces 81, 235-241

Mochi F, Burratti L, Fratoddi I, Venditti I, Battocchio C, Carlini L, Iucci G, Casalboni M, De Matteis F, Casciardi S (2018): Interaction of colloidal silver nanoparticles with Co2+ and Ni2+ in water for sensing application. Nanomaterials 8, 488

Rinaldi F, Del Favero E, Moeller J, Hanieh PN, Passeri D, Rossi M, Angeloni L, Venditti I, Marianecci C, Carafa M (2019): Hydrophilic silver nanoparticles loaded into niosomes: Physical–chemical characterization in view of biological applications. Nanomaterials 9, 1177

Shi J, Sun X, Zou X, Zhang H (2014): Amino acid-dependent transformations of citrate-coated silver nanoparticles: impact on morphology, stability and toxicity. Toxicology Letters 229, 17-24

Shirley DA (1972): High-resolution X-ray photoemission spectrum of the valence bands of gold. Physical Review B 5, 4709

Sun T, Buchner S, Byer N (1980): Oxide and interface properties of anodic films on Hg1− x Cd x Te. Journal of Vacuum Science and Technology 17, 1067-1073

Venditti I, Testa G, Sciubba F, Carlini L, Porcaro F, Meneghini C, Mobilio S, Battocchio C, Fratoddi I (2017): Hydrophilic metal nanoparticles functionalized by 2-Diethylaminoethanethiol: a close look at the metal–ligand interaction and interface chemical structure. The Journal of Physical Chemistry C 121, 8002-8013

Zubavichus Y, Shaporenko A, Grunze M, Zharnikov M (2009): NEXAFS spectroscopy of biological molecules: From amino acids to functional proteins. Nuclear Instruments and Methods in Physics Research Section A: Accelerators, Spectrometers, Detectors and Associated Equipment 603, 111-114

CHAPTER 3

LONG TERM TOXICITY OF AgNP: **Innocent Until Proven Guilty: Chronic Toxicity of AgNPcitLcys for Water Remediation Reveals the Need to Reconsider Ecosafety Testing**

GRAPHICAL ABSTRACT

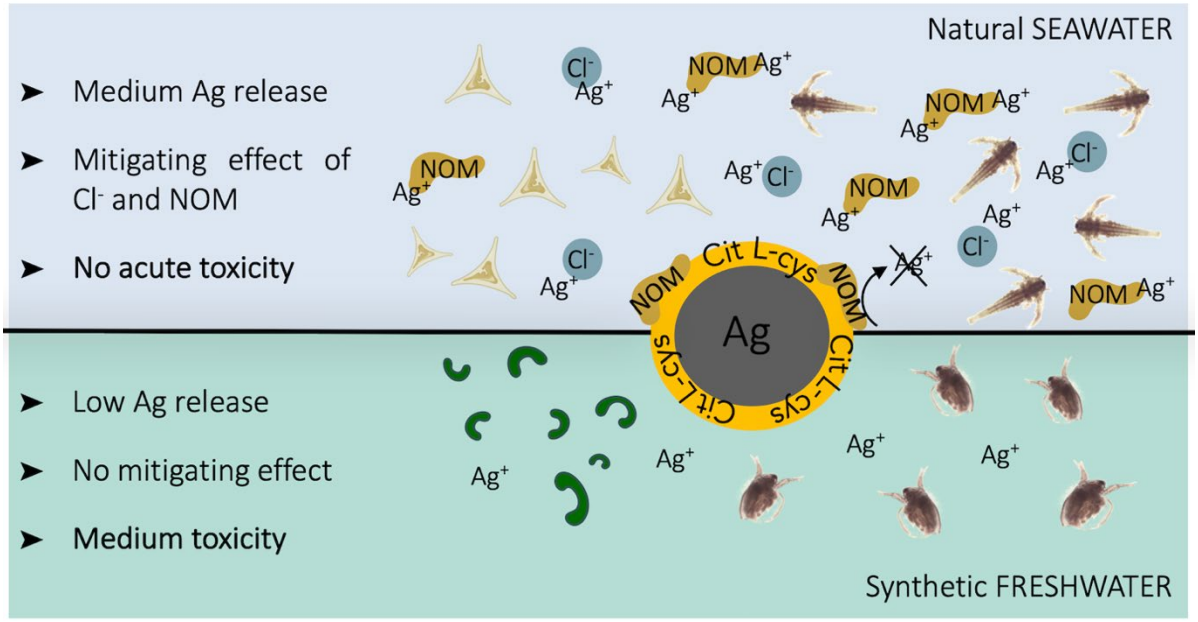

## ABSTRACT

Silver nanoparticles (AgNPs) are widely employed in everyday consumer products as biocides but can be also applied as sensors, adsorbents and photocatalysts for water pollution detection and remediation. However, their production and application should rely on safety assessment for possible human and environmental health implications. Here, we tested acute and chronic toxicity of novel AgNPs coated with citrate and L-cysteine (AgNPcitLcys) synthesized as sensor and adsorbent of $Hg^{2+}$ in polluted waters. AgNPcitLcys behavior and release of Ag ions were monitored in exposure media by dynamic light scattering (DLS) and inductively coupled plasma-mass spectrometry (ICP-MS). Freshwater and marine microalgae and microcrustaceans were exposed to a range of AgNPcitLcys concentrations (1 µg/L–100 mg/L) in order to resemble realistic exposure scenarios and establish an effect threshold. Acute toxicity to the microalgae *Raphidocelis subcapitata* and *Phaeodactylum tricornutum* (1-1000 µg/L) were assessed while both acute and chronic toxicity to the microcrustaceans *Ceriodaphnia dubia* (1-100 µg/L) and *Artemia franciscana* (0.1-100 mg/L) were investigated. AgNPcitLcys caused low or no acute toxicity to both microalgae ($EC_{50}$>1000 µg/L) and microcrustaceans, while chronic exposure (7-14 days) revealed severe effects in both *Ceriodaphnia dubia* and *Artemia franciscana* ($EC_{50}$, respectively, of 24 µg/L and 5.087 mg/L). Based on the measured low concentrations of dissolved Ag in exposure media, higher toxicity than expected was observed, in all investigated species, suggesting the occurrence of a nano-related effect. Our findings highlight the need to focus more on chronic rather than only acute toxicity, which can underestimate the risk posed by AgNPs, in order to promote their safety for environmental applications (ecosafety).

## 1. Introduction

Among engineered nanomaterials (ENMs) included in consumer products, silver nanoparticles (AgNPs) are one of the most widely employed, primarily because of their efficient antimicrobial properties (Tortella et al., 2020). AgNP main feature driving their biocidal potential is their ability to release Ag ions (Dong et al., 2017), known as being one of the most toxic in the aquatic environment (Ratte, 1999). However, AgNP fields of application are wide and include their employment as sensors, adsorbents and photocatalysts for water pollution, detection and remediation (Saravanan et al., 2017; Prosposito et al., 2019; Fiorati et al., 2020; Prosposito et al., 2020). AgNP release in wastewaters is high (estimated approx. 33 Kg AgNPs/year) despite up to 96.4% is retained by the water treatment process itself (Li et al., 2016). Therefore, organisms in the receiving water bodies are likely to be impacted by a chronic exposure to AgNPs, with consequences potentially more serious than a one-time acute exposure (Dalzon et al., 2020). Moreover, the impact to non-target species as for instance from commercial formulations containing nano-silver products are known to be often severe (Angel et al., 2013; McGillicuddy et al., 2017; Ale et al., 2019; Kalantzi et al., 2019; Ellis et al., 2020). Therefore, assessing the risk posed by AgNPs to aquatic organisms is a priority and caution should be taken from their design to their synthesis and production.

AgNPs undergo many reactions and transformations in the aquatic environment, depending on the surrounding physico-chemical conditions (*e.g.,* pH, oxidants, ionic strength, dissolved oxygen, organic matter, etc), and are shown to impact organisms at different levels of ecological organization, in both freshwater and marine ecosystems (Angel et al., 2013; Ivask et al., 2014; Becaro et al., 2015; Navarro et al., 2015; Ellis et al., 2020).

The severity of AgNP impact is highly variable, mainly because of the wide variety of combination of sizes, shapes and surface coatings driving their behaviour and bio-interactions (Angel et al., 2013; Ivask et al., 2014). Although dissolution and release of Ag ions is often recognised to be the first mechanism of toxicity of AgNPs (Kittler et al., 2010), controversy exists over this matter, with some studies blaming

Ag ions for the totality of the observed effects (He et al., 2012) and others blaming only, or mainly, the nano scale properties (Liu et al., 2019).

There is an open debate also around the role played by the coating type in determining AgNP toxicity. First because the coating determines surface charge, stability, aggregation and dissolution of AgNPs (Levard et al., 2013a; Lekamge et al., 2019; Marchioni et al., 2020), also in relation to the chemistry of the medium; properties of the surrounding environmental media (*e.g.,* salinity, organic matter, … ) are, in fact, able to completely change the toxicity outcomes of exposed biota by influencing AgNP dissolution, surface charge and aggregation (McLaughlin and Bonzongo, 2012; Lish et al., 2019). Ultimately, the coating type, together with its interaction within the receiving medium, is the discriminating factor driving the nano-bio-interactions of AgNPs with cells and organisms.

Hence, the toxicity of AgNPs is the result of a complex mixture of factors, as shown by the wide range of effect concentrations reported for aquatic organisms ($EC_{50}$ values for mortality range from <0.5 µg/L to >100 mg/L). Therefore, in order to unveil the mode of action and define the safety range for AgNP application, we tested newly developed AgNPs coated with citrate and L-cysteine (AgNPcitLcys), on organisms belonging to different trophic levels (primary producers and primary consumers), with different living strategies (autotroph and heterotroph) and belonging to different environments (fresh and marine waters), for acute and chronic toxicities (from 48h to 14d).

Selected species were the microalgae *R. subcapitata* and *P. tricornutum*, and the microcrustacean *C. dubia* and *A. franciscana,* respectively belonging to freshwater and marine environments. Exposure concentrations ranged from 1 µg/L to 100 mg/L, depending on organism's sensitivity, and included: values close to predicted environmental concentrations of low contaminated environments and water bodies receiving wastewater effluents (1-100 µg/L) (PEC: in the order of µg/L) (Lazareva and Keller, 2014; Cervantes-Avilés et al., 2019), and very high concentrations (0.1-100 mg/L) in order to establish an effect threshold.

Being synthetized as sensors and for the remediation of mercury contaminated waters, in our previous findings we confirmed no acute toxicity for AgNPcitLcys to both freshwater and marine microalgae

(Prosposito et al., 2019). Here we broadened the range of exposure concentration (1µg/L-100mg/L) added a new trophic level (microcrustaceans) and extend the exposure time by testing chronic toxicity in order to resemble a more realistic exposure scenario. Also, we intended on drawing attention to the importance of including the environmental safety (ecosafety) as a priority for limiting implications and improve nanomaterials applications based on an eco-safe by design strategy (eco-design) (Fiorati et al., 2020).

## 2. Materials & Methods

### 2.1. AgNP characterization

AgNPcitLcys (further called AgNPs) were synthesized by the Department of Sciences, University of Roma Tre according to the procedure described in Prosposito et al. (2019) and in chapter 2. Briefly: 25 mL of L-cysteine (L-cys) water solution (0.002 M), 10 mL of Citrate (cit) water solution (0.01 M) and 2.5 mL of $AgNO_3$ water solution (0.05 M) were mixed and degassed with Argon for 10 min; 4 mL of $NaBH_4$ solution (0.016 g in 4 mL distilled water) were added and the mixture was allowed to react for 2 h. Then the brown solution was collected and purified by centrifugation (13,000 rpm, 10 min, just 1 time for this work, with deionized water). AgNP molecular and electronic structure was investigated by Synchrotron Radiation-induced X-ray Photoelectron Spectroscopy (SR-XPS) and Near Edge X-ray Absorption Fine Structure (NEXAFS) Spectroscopy. UV-Vis spectra were collected by using quartz cells with a Shimadzu 2401 UV-vis spectrophotometer.

AgNP aqueous suspensions (50 mg/L) were further characterized by Dynamic Light Scattering (DLS) (Zetasizer Nano ZS90, Malvern, combined with the Zetasizer Nano Series software, version 7.02, Particular Sciences) and hydrodynamic diameter (Z-average, nm), polydispersity index (PDI) and surface charge (ζ-potential, mV) of 50 mg/L suspensions were measured in MilliQ water and in all media used for toxicity tests: TG201 and MHRW for freshwater species and F/2 and natural seawater (NSW) for marine ones. DLS measurements were performed at 25° C for MilliQ, at 21°C for TG201 and F/2 and at 25°C for MHRW and NSW, corresponding to the temperature used in toxicity tests.

AgNPs were also investigated by Dual-Beam (FIB/SEM) Helios Nanolab (FEI Company, Eindhoven, The Netherlands) and by TEM (Philips Morgagni 268 D electronics, at 80 KV and equipped with a MegaView II CCD camera) using a 10 mg/L suspension in MilliQ.

### 2.2. AgNP dissolution

The release of Ag ions from the AgNPs was assessed at the beginning (time 0) and at the end of the exposure times (72h for algae, 24h and 48h for microcrustaceans, being a semi-static chronic exposure

with medium renewal every 24 or 48h) in all media used for toxicity tests: TG201, MHRW, F/2 and NSW. Ag release was measured at the highest AgNP concentration tested for each test species: 1000 µg/L for microalgae, 100 µg/L for *C. dubia* and 100 mg/L for *A. franciscana*. Solutions were kept in the same conditions of temperature, light and photoperiod as used for toxicity tests (21°C, 4500 lux and continuous illumination for microalgae, 25°C, 400 lux and 16/8 h light/dark photoperiod for *C. dubia* and 25°C, in the dark for *A. franciscana*), and mixed by manual shaking once a day. An aliquot of each solution was taken at each measured time point (0 and 24, 48 or 72 h) and centrifuged (5000 g, 40 min) by using a centrifugal filter device with a 3 kDa cut-off (Amicon Ultra-15 mL, Millipore, USA). The resulting filtrate was acidified with $HNO_3$ (10%) and analysed for determining Ag concentration. As control, Ag concentrations were also measured in algal media (TG201 and F/2) and in algal media with added $AgNO_3$ (7 µg/L), as $AgNO_3$ was used as positive control for all toxicity tests.

The Ag concentrations were determined by inductively coupled plasma-mass spectrometry (ICP-MS) using the Perkin Elmer NexION 350 spectrometer (Waltham, MA, USA). The analytical accuracy was checked by comparing the certified and measured Ag concentration in the standard reference material SRM 1643e (Trace Elements in Water) of the National Institute of Standards and Technology (NIST). The analytical precision was evaluated by means of the percentage relative standard deviation (% RSD) of five replicate analyses of each water sample.

## 2.3. Acute toxicity

### *2.3.1. Microalgae*

Algal toxicity tests were performed with *R. subcapitata* and *P. tricornutum* as model microalgae for fresh and marine waters following the standardized protocols OECD 201 (2011) and ISO 10253 (2006). The algae were cultured in TG201 medium (*R. subcapitata*) and F/2 medium (*P. tricornutum*) and maintained in axenic exponential growth conditions at 18 ± 1 °C with a 16/8 h light-dark cycle photoperiod in a growth chamber.

Toxicity tests (72 h) were carried out in modified growth media in order to limit the amount of chelating agents (*i.e.*, EDTA), following recommendations for heavy metal toxicity testing (Resgalla Jr et al., 2012; Leal et al., 2016). EDTA final concentration in test media were 50 µg/L in TG201 and 0.8 mg/L in F/2, both previously proved to be able to ensure an optimal growth of both algae (data not shown).

Algae from a stock culture were inoculated 72 h prior to run the assay and maintained at 21 ± 1 °C and continuous illumination at 4500 lux. Tests were carried out in polystyrene single-use sterile multiwell with 2 mL capacity for each well. Initial algal concentration in toxicity tests was $1x10^4$ cells/mL and exposure concentrations of both AgNPs and $AgNO_3$ were as follows: 0, 1, 5, 10, 100, 500, 1000 µg/L. $AgNO_3$ was used as positive control. Three replicates for each exposure concentration were set. *R. subcapitata* multiwell plates were placed over an orbital shaker at 50 rpm to reduce algal settling and enabling gas exchanges. Every test was repeated three times. After 72 h, algae were fixed with a 1:1 lugol/ethanol solution and cell density was estimated by counting under optical microscope Olympus BX51 (40X), equipped with an improved Neubauer chamber for *P. tricornutum* and with an automated cell counter (LUNA II, Logos Biosystems) for *R. subcapitata*. The number of cells/mL, growth rate (µ) and inhibition of growth rate (Iµi) compared to control were determined.

#### *2.3.2. Ceriodaphnia dubia*

*C. dubia* ephippia were purchased from ECOTOX (LDS, Italy) and maintained in the dark at 4°C following instructions. The culture of specimens and conduction of toxicity tests were carried out following instructions from the 1002.0 EPA protocol guidelines (EPA, 2002). Cultures were started at least 3 weeks before the beginning of toxicity tests and kept at 25°C with a 16/8 h light/dark photoperiod and a light intensity of 400 lux at the water surface. The same conditions were used for toxicity tests. Specimens were cultured in moderately hard reconstituted water (MHRW) prepared following 1002.0 EPA protocol guidelines and fed daily with *R. subcapitata* and a combination of yeast, cereal leaves and trout chow (YCT). MHRW was aerated to ensure dissolved oxygen levels close to saturation and it was allowed to settle for at least 24 h before use. Adults were transferred in fresh culture medium twice a

week and, at the same time, pH, dissolved oxygen (DO), and conductivity were monitored to be always in the optimal range (7.7-8, 8.5-9 mg/L of DO and 0.2-0.3 ms/cm). After two weeks the adults were discarded, and new cultures were started with the produced neonates. All toxicity tests were conducted with neonates < 24h old belonging to the third brood of females kept in individual controlled cultures that had produced three broods and a minimum of 15 neonates in 7 days. *C. dubia* acute survival tests (48 h) were carried out with 10 neonates (< 24 h old) per replica and 3 replicates for every exposure concentration, respectively: 0, 1, 10, 100 µg/L for AgNPs and 0, 0.5, 1, 2 µg/L for $AgNO_3$. $AgNO_3$ was used as positive control. All tests were carried out in 25 mL glass beakers filled with 20 mL of MHRW and covered with a glass petri dish to prevent evaporation. After every medium renewal, glass beakers were cleaned with a 10% HCl solution prior to standard washing procedures in order to remove any trace of metal adsorbed to beaker walls. Specimens were not fed during exposure and the medium was not renewed. After 48 h the number of dead organisms was registered. The test was repeated twice.

### *2.3.3.Artemia franciscana*

Brine shrimp *A. franciscana* short-term acute toxicity test (48 h) was conducted according to the standardized protocol APAT IRSA CNR 8060 (CNR, 2003) and lately reported in ISO/TS 20787 (2017). Dehydrated cysts were purchased from ECOTOX (LDS) and kept in the dark at 4°C until use. Cyst were allowed to hatch in a Petri dish filled with filtered (0.22 µm) NSW for 24 h at 25 °C under continuous illumination of 5000 lux. NSW was aerated for 24 h before use and dissolved oxygen (DO) levels were always monitored and maintained at >80% of saturation level.

Newly hatched larvae < 24 h old (instar I nauplius stage) were placed in polystyrene single-use sterile multiwell with 2 mL capacity for each well (10 ± 2 animals x well) and exposed to AgNPs and $AgNO_3$ at the following concentrations: 0, 0.1, 1, 10, 100 mg/L. $AgNO_3$ was used as positive control. Three replicates for each exposure concentration were set. Multiwells were placed at 25°C in the dark for 48 h and animals were not fed during tests. After 48 h mortality was assessed by recording the number of nauplii not showing any movement for at least 10 seconds. Surviving specimens were rinsed with

deionized water and fixed in absolute ethanol and images were taken with the optical microscope Olympus BX51 coupled with Olympus DP-software. The test was considered acceptable if controls displayed an average mortality ≤ 20%. Every test was repeated three times.

### 2.4. Chronic toxicity

#### *2.4.1.Ceriodaphnia dubia*

*C. dubia* chronic reproduction tests (7 d) were carried out following the 1002.0 EPA protocol (EPA, 2002) with one neonate (< 24 h old) per replica and 10 replicates for every exposure concentration, respectively: 0, 1, 10, 100 µg/L for AgNPs and 0, 0.5, 1, 2 µg/L for $AgNO_3$, as positive control. Daily the organisms were transferred into fresh medium, fed with *R. subcapitata* and YCT and exposure was renewed. At medium renewal physico-chemical parameters (pH, DO, conductivity) were monitored in at least one beaker for every exposure concentration and eventual deaths were registered, while neonates, where presents, were counted and discarded. At medium renewal attention was also paid to molts, which were collected and observed for anomalies. Images of molts were taken with the optical microscope Olympus BX51 coupled with Olympus DP-software.

#### *2.4.2.Artemia franciscana*

*A. franciscana* long-term chronic toxicity test (14 d) was carried out following the protocol of Manfra et al. (2012). Newly hatched larvae < 24 h old (Instar I nauplius stage) were exposed in a final volume of 40 mL of filtered NSW in glass beakers (10 ± 2 animals each) at the following concentrations of AgNPs (0, 0.1, 1, 5, 10 mg/L) and $AgNO_3$ (0, 0.01, 0.1, 1 mg/L), as positive control. Three replicates for each exposure concentration were set. The glass beakers were covered with parafilm to avoid evaporation, leaving small gaps for air passage and placed at 25°C with a 14/10 h light/dark photoperiod and a light intensity of 900 lux at the water surface for 14 days. Exposure media were renewed every 2-3 days (day 2, 4, 7, 9, 11 and 14) and the animals were fed the green alga *Dunaliella tertiolecta* at the final concentration of $1x10^5$ cells/mL. At each medium renewal mortality assessed under a stereomicroscope

as previously described for acute toxicity test. After every medium renewal, glass beakers were cleaned with a 10% HCl solution prior to standard washing procedures in order to remove any trace of metal adsorbed to beaker walls. The test was repeated twice.

### 2.5. Statistical Analysis

$EC_{50}$ values were calculated with Graphpad Prism 8 using a non-linear regression analysis, while statistical significance between mean values were calculated with a nonparametric test (Kruskal-Wallis test).

## 3. Results

### 3.1. AgNP characterization

The DLS data in MilliQ show a substantial stability of AgNP size (range 150-200 nm) and polydispersity index (about 0.3) within 1 year from the synthesis (Table 1 and S1). Aggregation phenomena become important in exposure media with increasing salinity: the average diameter goes from $<2R_H> = 137 \pm 5$ nm in TG201 to $<2R_H> = 941 \pm 140$ nm in NSW and the polydispersity index from, respectively, 0.4 (fairly monodisperse sample) to 0.7 (polydisperse sample).

The Z potential data confirm the trend, showing colloidal particles very stable (<-30 mV) in MilliQ and in freshwater media (TG201, MHRW), while they become highly unstable (± 30 mV) with increased salinity of the media (F/2 and NSW).

SR-XPS data analysis confirmed AgNP stability, as well as to probe citrate and L-cysteine capping efficiency. More in detail, the spectral components individuated in S2p and Ag3d spectra indicated the formation of a covalent RS-Ag bond between L-cysteine molecules and silver atoms at the AgNP surface; the absence of a S2p feature due to free thiols (R-SH) suggested that L-cysteine molecules preferentially tend to directly bond the metal surface, as also reported in the literature (Majzik et al., 2010). In addition, the features individuated in the NEXAFS C k-edge spectrum confirmed the successful capping of the AgNP surface by both citrate and L-cysteine. Uv-vis spectra confirmed the AgNP plasmonic peak at 400 nm (Figure S1). A more in-depth investigation of AgNP stock, freshly synthetized and after 1 year from synthesis (see supporting material, Figure S1).

AgNP dissolution data show an overall low Ag ion release in all exposure media (Table 2). The lowest Ag ion dissolution was recorded in freshwater media (TG201 and MHRW) (under 1% of nominal AgNP concentrations), while in high ionic strength media (F/2 and NSW) reached 4.41 % after 72 h of incubation. The high Ag concentration measured in NSW, taking into account the high AgNPs concentration (100 mg/L), must be considered negligible as the release stays under 0.2% (0.172-0.111 %) of the nominal AgNPs. Negative and positive control analysis (Table S2) show a low occurrence of Ag

in dilution waters and confirm the efficacy of the method used for filtration which does not retain Ag ions. For more detailed information on media composition see supplementary material.

**Table 1.** Hydrodynamic diameter (Z-average), poly dispersity index (PDI) and surface charge (Z- potential) of AgNPs (50 mg/L) in MilliQ and exposure media used for toxicity testing (TG201, MHRW, F/2, NSW). Data shown as mean ± standard deviation.

| | MilliQ | TG201<br>*R. subcapitata* | MHRW<br>*C. dubia* | F/2<br>*P. tricornutum* | NSW<br>*A. franciscana* |
|---|---|---|---|---|---|
| Z-average (nm) | 143 ± 2 | 137 ± 5 | 156 ± 2 | 560 ± 7 | 941 ± 140 |
| PDI | 0.263 ± 0.017 | 0.4 ± 0.02 | 0.313 ± 0.066 | 0.741 ± 0.03 | 0.716 ± 0.13 |
| Z-potential (mV) | -51 ± 2 | -33 ± 0.43 | -37 ± 1 | -8 ± 3 | -9.9 ± 3 |

**Table 2.** Ag concentrations (expressed as µg/L) measured in exposure media incubated with AgNPs at different time points according to toxicity testing (0 and 24, 48 or 72 h). Data shown as mean ± standard deviation.

| parameters | medium | 0 h | 24 h | 48 h | 72 h |
|---|---|---|---|---|---|
| pH = 7.7-8<br>Salinity = 0 ‰<br>DO = 8.5-9 mg/L<br>Conductivity = 0.2-0.3 ms/cm | TG201 + 1000 µg AgNP/L | 1.06 ± 0.09 (0.106%) | --- | --- | 1.32 ± 0.07 (0.132%) |
| | MHRW + 100 µg AgNP/L | 0.79 ± 0.06 (0.79%) | 0.56 ± 0.05 (0.56%) | 0.6 ± 0.05 (0.6%) | --- |
| pH = 7.7-8<br>Salinity = 40 ‰<br>DO = 7.8-8 mg/L<br>Conductivity = 55-60 ms/cm | F/2 + 1000 µg AgNP/L | 13.75 ± 0.41 (1.37%) | --- | --- | 44.14 ± 0.56 (4.41%) |
| | NSW + 100 mg AgNP/L | 172.92 ± 8.32 (0.172%) | --- | 111.40 ± 5.79 (0.111%) | --- |

3.2. Acute toxicity tests

*3.2.1. Freshwater and marine algae*

AgNPs caused a significant but low inhibition of growth in a concentration dependent manner in the freshwater alga *R. subcapitata* at 100, 500 and 1000 µg/L of exposure ($p$<0.05) with a maximum inhibition value of 21.23 ± 8.47 % at the highest concentration tested (1000 µg/L) (Figure 1a). No $EC_{50}$ was calculated since it resulted to be over the maximum tested concentration. On the contrary, $AgNO_3$ caused a significant inhibition of growth already at 5 µg/L with a calculated $EC_{50}$ of 5.039 µg Ag/L (Figure S2a). Interestingly, both AgNPs and $AgNO_3$ caused a mild increase of algal growth at the lowest concentration tested (1 µg/L), even if not statistically significant.

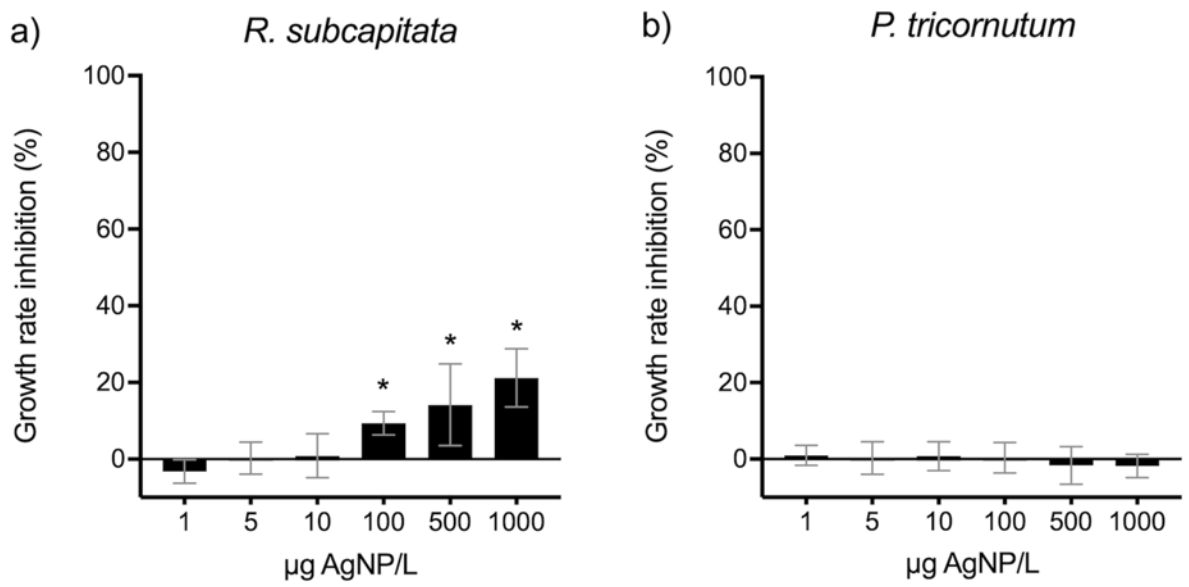


**Figure 1.** Growth rate inhibition compared to control of a) *R. subcapitata* and b) *P. tricornutum* exposed to AgNPs. Data shown as mean ± standard deviation. Column marked with * are significantly different from controls ($p$<0.05).

No inhibition of growth was recorded for the marine alga *P. tricornutum* exposed to AgNPs at all tested concentrations (1-1000 µg/L) (Figure 1b) despite the higher dissolved Ag value (Table 2), compared to TG201. The concentration of dissolved Ag at the highest AgNP concentration (1000 µg/L) after 72 h incubation is 44.14 ± 0.56 µg Ag/L. The lack of observed inhibitory effect agrees with what observed in

the $AgNO_3$ exposure, which resulted in a significant inhibition only at the highest concentrations tested (500 and 1000 µg/L) ($p$<0.05), with a calculated $EC_{50}$ value of 510.4 µg/L (Figure S2b).

### *3.2.2. Ceriodaphnia dubia*

Immobilization rates for acute exposure (48 h) of *C. dubia* to AgNPs are shown in Figure 2a. Data obtained for AgNP exposure show high variability of responses, with a significant immobilization rate already at the lowest concentration tested (1 µg/L) ($p$<0.005). Immobilization rate values ranged from 13.3 ± 11 % to 43.3 ± 11 % and showed a v-shaped trend with the lowest value observed for the intermediate exposure concentration (10 µg/L) and a calculated $EC_{50}$ value of 95.88 µg/L.

Results obtained for the exposure to $AgNO_3$ showed a significant immobilization rate compared to control only at the highest exposure concentration (2 µg Ag/L), with a calculated $EC_{50}$ value of 1.69 µg Ag/L (Fig. S2e).

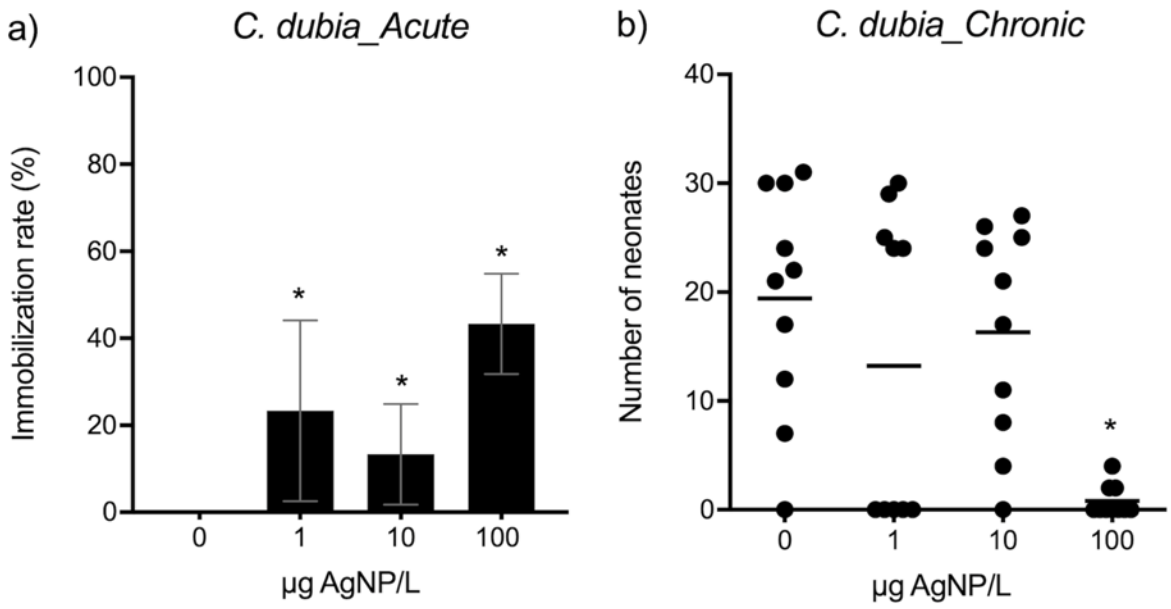


Figure 2. Immobilization rate and number of neonates of *C. dubia* exposed to AgNPs in acute (48 h) (a) and chronic (7 d) (b) toxicity test. For a) data are shown as mean ± standard deviation, while in b) every dot represents the total number of neonates produced in 7 days by each exposed female (10 for each treatment), while lines represent the mean number of neonates produced for every treatment. Data marked with * show significant differences ($p$<0.005) compared to control.

*3.2.3.Artemia franciscana*

Acute exposure (48 h) to AgNPs resulted in no lethal effect for *A. franciscana* nauplii up to the highest exposure concentration tested (100 mg/L) (Figure 3a).

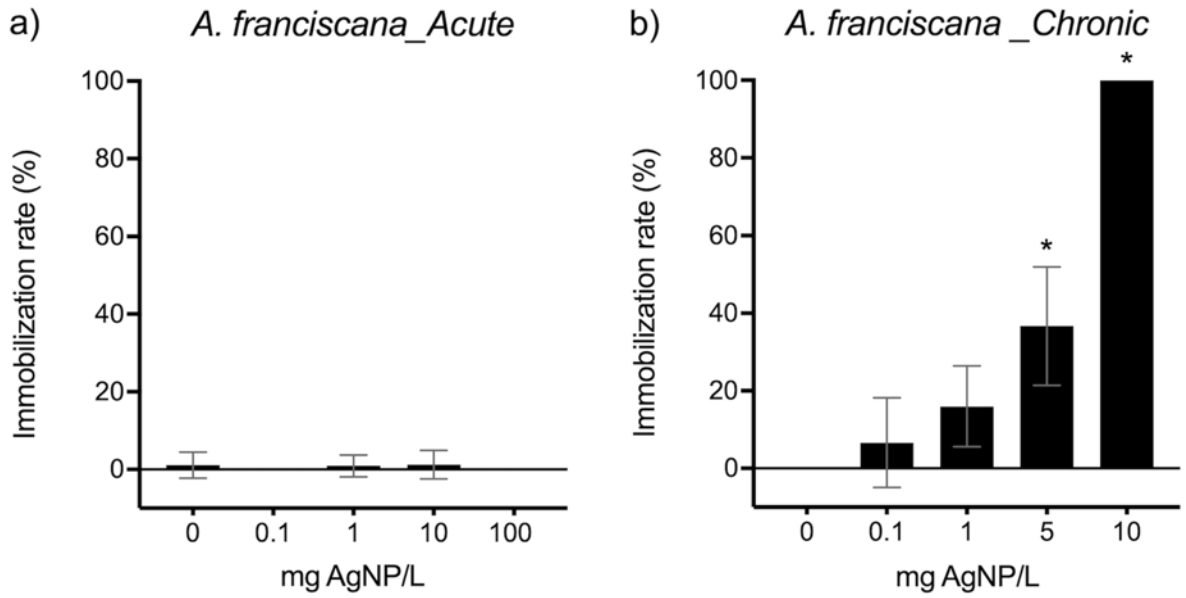


Figure 3. Immobilization rate of microcrustacean *A. franciscana* exposed to AgNPs in acute (48 h) (a) and chronic (14 d) (b) exposure. Data shown as mean ± standard deviation. Columns marked with * show significant differences ($p$<0.005) compared to control.

However, many sub-lethal outcomes were observed. A concentration dependent increase of AgNPs aggregates in the digestive tracts of brine shrimp were observed (Figure 4 b-e). At the highest exposure concentrations (10, 100 mg/L) some animals showed a low level of swimming activity, sometimes intermittent. Egestion was also taking place, as some images captured AgNP aggregates in the terminal part of the digestive tracts (Figure 5d), while live footage of the animals under the optical microscope (data not shown) showed AgNP aggregates being transported along the intestinal tract through peristaltic movement. No evidence of external adhesion of AgNPs on *A. franciscana* appendices or body were found, while some animals presented a black-spotted pattern through their body which would appear to be localized on the inside of the body, but outside the intestinal tract (Figure 5 a-c).

On the contrary, acute exposure to $AgNO_3$ resulted in a maximum immobilization rate of 41.1 ± 8.38 %, but only for 10 mg Ag/L exposure, with no significant effect at the other tested concentrations (Figure S2c). As observed for AgNPs, specimens exposed to the higher $AgNO_3$ concentrations (10, 100 mg Ag/L) showed the presence of black matter inside the intestinal tract, even if to a lower extent compared to AgNP exposure (Figure S3).

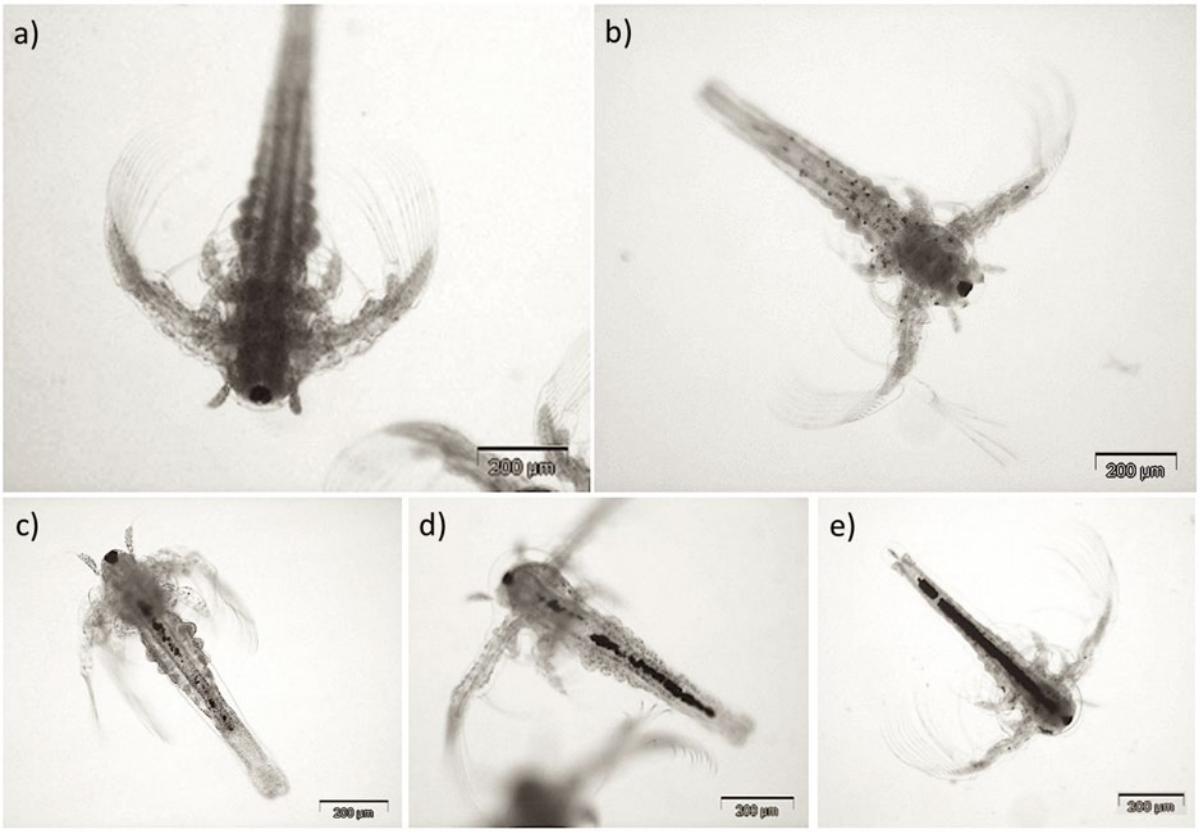


**Figure 4.** *A. franciscana* after 48 h exposure to different AgNP concentrations: 0 (a), 0.1 (b), 1 (c), 10 (d), 100 (e) mg/L. Images show the dose-dependent increase of AgNPs inside the animal gut.

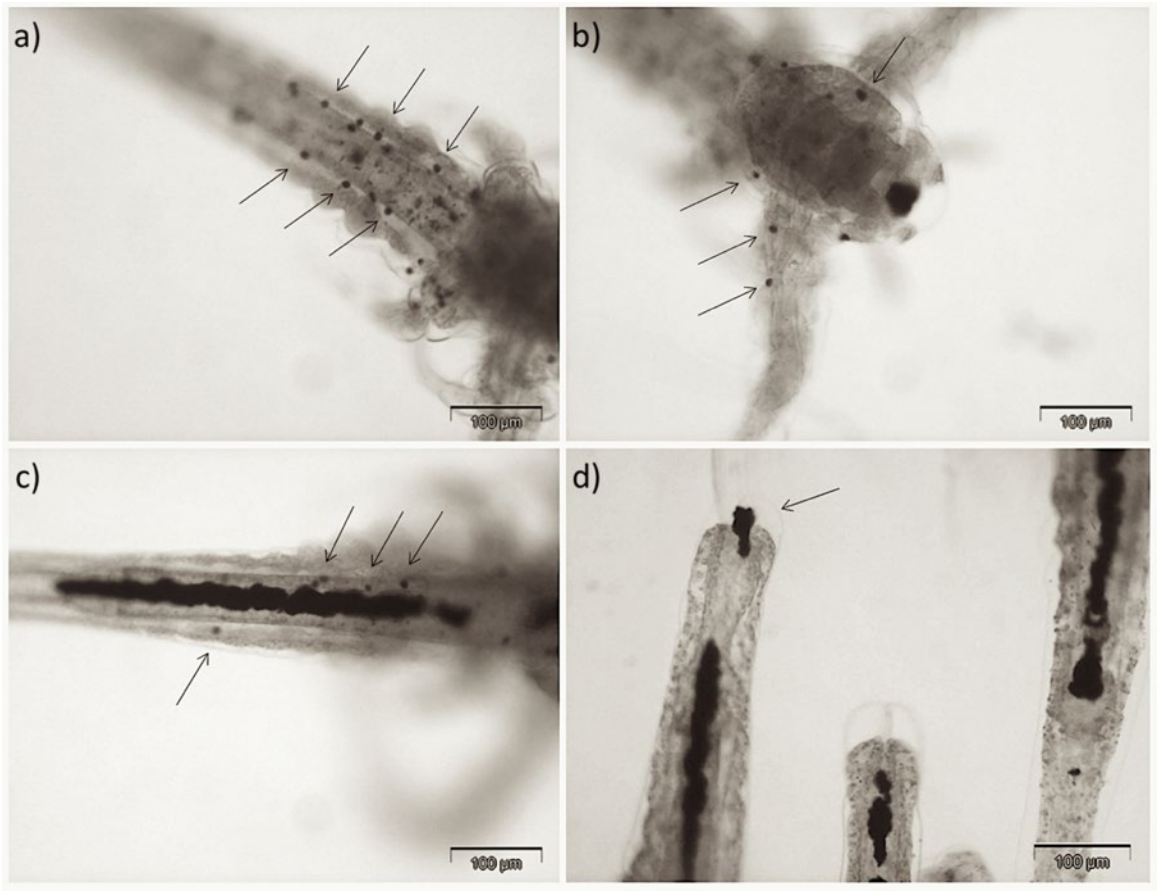


**Figure 5.** Details of *A. franciscana* after 48 h exposure to AgNPs: a) and b) show animals from the 0.1 mg/L exposure, the arrows indicate dark spots inside the animal body; c) and d) show animals from the 100 mg/L exposure: in c) the arrows indicate the same dark spot of previous images and in d) the egestion of ingested AgNP aggregates.

### 3.3. Chronic toxicity tests

#### *3.3.1. Ceriodaphnia dubia*

Chronic toxicity tests with *C. dubia* were in line with tests acceptability criteria defined by EPA protocol, with at least 80% survival of control organisms and a minimum of 60% of surviving control females producing three broods with at least 15 neonates.

Reproduction data obtained from the chronic assay showed again a trend comparable to what was observed for survival, which was, however, greatly influenced by the high mortality showed by organisms exposed to the lowest concentration (1 µg/L) (Figure S4a). In fact, for AgNP exposure, the

strongest effects on reproduction are observed for lowest and highest exposure concentrations, but with only those exposed to the highest concentration showing a significant impairment of the reproductive capacity compared to the control (Figure 2b) and a calculated $EC_{50}$ of 24.96 µg AgNP/L. The low average number of neonates in the group exposed to 1 µg/L is in line with the observed high mortality in the first 48 h of exposure (50%), in agreement with what observed in the acute test; on the contrary the average number of neonates for surviving female was comparable to controls. In fact, calculating the average number of neonates for females that survived to the first 48 h of exposure, the outcome is different with the 1 µg/L exposure showing the highest value (26.4), followed by control (21.5), 10 µg/L (18.1) and 100 µg/L (0.88) exposure.

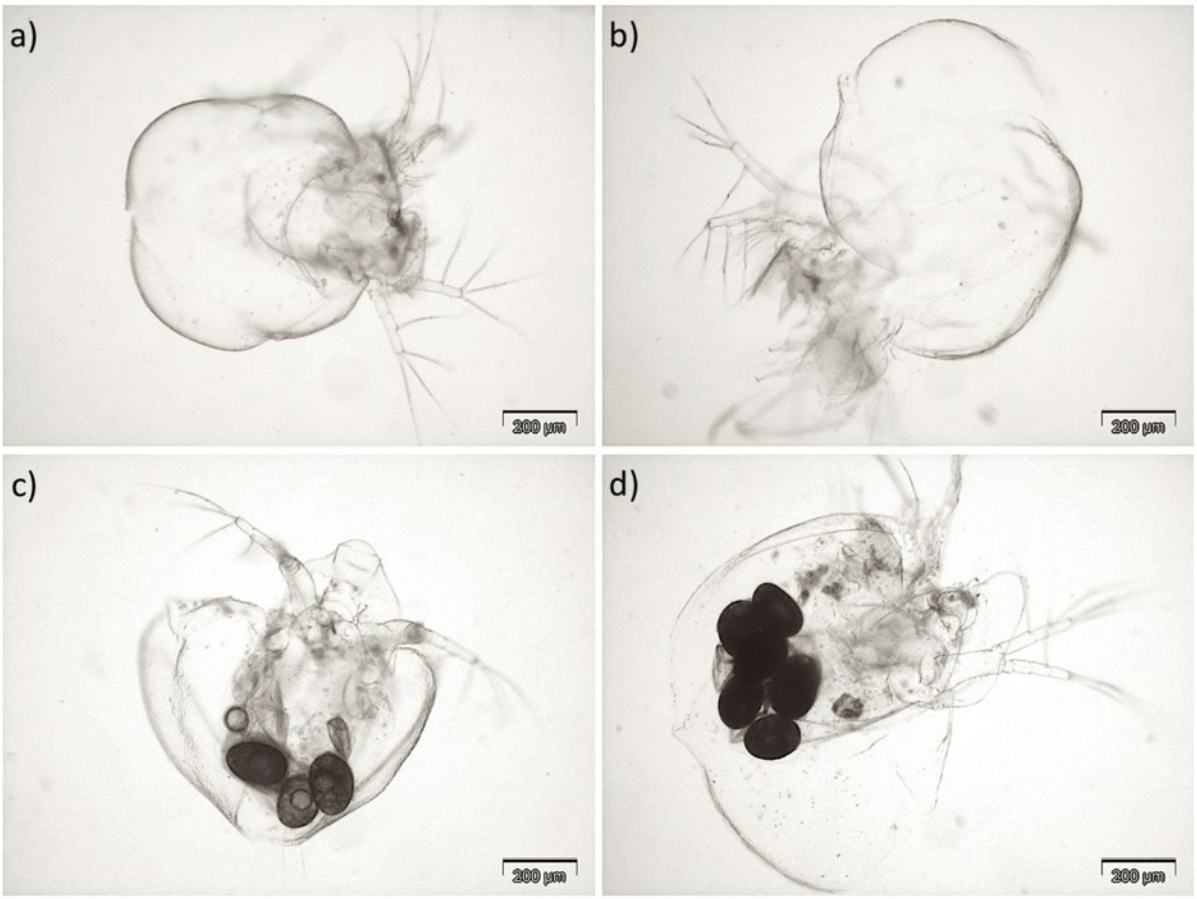


Figure 6. *C. dubia* molts from chronic toxicity test with AgNPs (a, c) and $AgNO_3$ (b, d). a) and b) images show molts of control organisms without any undeveloped eggs on their inside while c) is from 100 µg AgNP/L exposed organisms and d) is from 1 µg $AgNO_3$/L exposed organisms, both showing molts with undeveloped eggs on their inside.

Exposure to $AgNO_3$ caused a much more linear decrease in the reproductive capacity of *C. dubia* (Fig. S2f), already starting from the lowest exposure concentration but showing a significant difference compared to control only at 2 µg/L, in agreement with what observed in the acute exposure ($EC_{50}$ = 0.8 µg Ag/L).

All specimens exposed to either AgNPs or $AgNO_3$ were unable to reproduce and showed the same outcome: during daily check, exposure groups that had not produced a brood, showed a discarded molt full of unhatched eggs at the bottom of the beaker (Figure 6 c, d). This was observed for 100 µg/L AgNP exposure and 1 and 2 µg/L $AgNO_3$, while molts collected from controls resulted empty (Figure 6 a, b).

### *3.3.2.Artemia franciscana*

Chronic exposure allowed to establish an effect threshold for AgNPs, with a calculated $EC_{50}$ values of 5.087 mg/L for *A. franciscana* (Figure 3b). Exposure to AgNPs resulted in no or low (<20%) toxicity up to 1 mg/L, while ending in the death of 100% of tested organisms at day 14 at the highest exposure concentration (10 mg/L). The same was observed for specimens exposed to $AgNO_3$ at 1 mg/L (Figure S2d), which resulted in a 10% survival rate at the end of the exposure period ($EC_{50}$ 0.402 mg/L) even if with a different trend. In fact, $AgNO_3$ exposed organisms showed an increased mortality already after 4 days of exposure while for AgNP exposed organisms, mortality was observed only after 9 days of exposure (Figure S5).

## 4. Discussion

DLS results show a substantial stability of AgNP size and polydispersity in MilliQ and freshwater media, also up to 1 year from their synthesis, while the formation of aggregates increased with salinity (Venditti et al., 2007; Bhattacharjee, 2016). The Z potential data confirm such trend (Bhattacharjee, 2016), showing colloidal particles highly stable in MilliQ and freshwater media (TG201, MHRW), while they become highly unstable in seawater media.

In agreement with the current knowledge, the dissolution of AgNPs increased with the increasing salinity (Lish et al., 2019) and decreased with increasing AgNP concentration (Sikder et al., 2018). In fact, given a similar salinity of the exposure media, the dissolution was higher for lower AgNP concentrations: from 0.6–0.79% of 100 μg/L in MHRW to 0.106–0.132% of 1000 μg/L in TG201 (freshwater), and from 1.37–4.41% of 1000 μg/L in F/2 to 0.111–0.172% of 100 mg/L in NSW (marine water).

Chloride ions ($Cl^-$) are mostly responsible for the observed higher dissolution of AgNPs with increased salinity of the aqueous media but could also be playing an opposite role in freshwater media, by lowering dissolution in TG201 medium compared to MHRW. The interaction of $Cl^-$ with AgNPs and its consequences on dissolution follows a complex dynamic as it depends on Cl/Ag ratio which, in turn, drives the formation of soluble or insoluble Ag-Cl complexes (Levard et al., 2013b). In conditions of low Cl/Ag ratio, as it is in the case of TG201 medium, AgNPs experience an enhanced stability due to the formation of an insoluble AgCl layer onto the NP surface, which inhibits dissolution. This does not happen in MHRW medium in which no chloride species are present (see formulations in supporting material). The contribution of $Cl^-$ could explain the lower dissolution in TG201 compared to MHRW, also helped by the higher AgNP concentration (Sikder et al., 2018). On the contrary, at higher Cl/Ag ratio, as in marine media, the formation of soluble AgCl complexes ($(AgCl_x)^{(x-1)-}$) promotes the dissolution of AgNP, leading to a higher amount of ions in solution (Ho et al., 2010; Li et al., 2010).

Such interaction with $Cl^-$ needs to be preceded by the oxidation of AgNP surface by an oxidizing agent, such as $O_2$, and it can be prevented, together with AgNP dissolution, by the presence of reduced sulphur

groups. The sulfidation of AgNPs, in fact, strongly decreases further oxidation, reducing ion release (Levard et al., 2011). This mechanism is already implemented by L-cysteine molecules of AgNP coating, which probably acts by shielding the particle surface from excessive oxidation, leading to reduced dissolution. Such dissolution rate of AgNPs (0.07–4.38%) resulted low when compared to reported values for other AgNP stocks (range 0.6–29.66%) (Ivask et al., 2014; Malysheva et al., 2016; Schiavo et al., 2017; Wu et al., 2017; Lish et al., 2019). However, dissolution data are not always easy to compare since a wide range of coatings, concentrations, media and exposure time have been used, all parameters known to have an influence on AgNP dissolution. Available data on citrate-coated AgNP (cit-AgNPs), as the most frequently used in (eco)toxicity studies and similar to the ones used in this work, usually report higher dissolution values (Angel et al., 2013; Ivask et al., 2014; Lish et al., 2019). Such findings highlight the importance of the combined coating of citrate and L-cysteine of the AgNPs used in this study in reducing Ag ion dissolution in aqueous suspensions. Also in freshwater media, the dissolution range found for our AgNPs (0.106–0.79%) results lower than what is reported in the literature for cit-AgNPs (1.4–7.3%) (Angel et al., 2013; Ivask et al., 2014; Lish et al., 2019). In marine water we've seen a maximum of 4.41% dissolution while literature data are variable: the very high dissolution rate (21.8%) reported by Lish et al. (2019) for cit-AgNPs in artificial seawater (ASW) is in contrast with that reported by Angel et al. (2013) (3.7%) in NSW. This is probably due to the use of NSW, whose natural organic matter (NOM) is abundant in reduced sulphur groups, providing protection against oxidation and partially counteracting the enhanced dissolution caused by the high Cl/Ag ratio of NSW. This most likely happened also in our study, in which NSW was used and the shielding effect of L-cysteine was further improved by the presence of NOM. However, the value obtained by Angel et al.(2013) of 3.7% dissolution, comes from a 40 mg/L concentration of cit-AgNPs, as opposed to 1 mg/L used in our study, and could, proportionally, represent a higher dissolution of AgNPs since dissolution is inversely related to concentration (Sikder et al., 2018). It is also worth mentioning that data on freshwater dissolution obtained in this study, which are not influenced by the presence of NOM, are lower than literature reported data for cit-AgNPs, for a wide range of concentrations (1–40 mg/L).

Ecotoxicity results followed what anticipated by dissolution values, showing an overall low acute toxicity for both freshwater and marine species.

In fact, obtained $EC_{50}$ for AgNPs of *R. subcapitata* is higher compared to the available literature data for cit-AgNPs (Angel et al., 2013; Ivask et al., 2014; Malysheva et al., 2016) and other differently coated AgNPs (Ribeiro et al., 2014; Kleiven et al., 2019) (Table 3), while values for $AgNO_3$ are in the same order of magnitude. However, the observed inhibition of growth caused by AgNP exposure, cannot be fully explained by dissolved Ag, whose maximum value for the highest tested concentration (1000 µg AgNP/L) after 72 h is 1.32 ± 0.07 µg Ag/L. Some studies report that the ion-driven toxicity is often not explaining the observed impact of AgNPs to microalgae (Malysheva et al., 2016) and a nanospecific effect could be inferred (Kleiven et al., 2019). Malysheva et al. (2016) concluded that the main predicting feature of AgNP toxicity is not the amount of dissolved Ag but rather the amount of internalized Ag, which depends on cell-AgNP physical interaction, mainly driven by the surface functionalization of the AgNPs. This partly agrees with what reported by Zhang et al. (2020) who observed different toxicity pathways being activated in response to the exposure of the green alga *Chlorella vulgaris* to negatively or positively charged AgNPs. These authors indicated that among the differentially expressed proteins upon AgNP exposure, many of them were specifically regulated by NPs surface charges, being hence triggered only by the coating type, regardless of the effect of Ag exposure. In particular, the exposure to cit-AgNPs (negatively charged) is reported to cause a disruption in the energy metabolism of cells, interfering with the mitochondrial respiratory chain and interrupting the synthesis of ATP (Zhang et al. (2020). As DLS data show, aggregation is lower in freshwater media, meaning that there is a higher number of single particles and/or small aggregates able to directly interact with cell membranes, increasing the chances of being phagocytized or diffuse in the bilayer. A study by Lankoff et al. (2012) on human cell lines exposed to AgNPs, demonstrated that the degree of agglomeration is able to influence cellular localization and toxicity, with larger aggregates being found only in cytoplasm and smaller aggregates or single particles being able to cross nuclear and mitochondrial membranes. Despite the fact that toxicity is a combination of different factors and also

depends on cell types, Lankoff et al. (2012) conclude that cell stress and death was more pronounced when cells were exposed to smaller aggregates, compared to bigger ones. Therefore, the different degree of aggregation could have influenced the ability of AgNP to cross cell membranes in our tested freshwater species, enhancing their presence in cytoplasm and intracellular compartments, leading to a higher toxicity. This could explain the observed reduced growth of *R. subcapitata* in our study despite the very low release of Ag in the exposure medium. Another explanation could be found in the fact that the analysis of dissolved Ag was conducted in the exposure media without the test species; therefore the observed toxicity could be the result of oxidative effects linked to algal interaction with AgNPs (Navarro et al., 2015; Wu et al., 2017) might play a role in the observed toxicity.

The sensitivity of the marine microalga *P. tricornutum* to Ag was confirmed by comparison of the $EC_{50}$ value obtained for $AgNO_3$ with those reported by other studies, while literature $EC_{50}$ values for AgNPs were found to be highly variable. Since in our study no effect threshold was identified for *P. tricornutum*, from the comparison made with studies using a similar range of exposure concentrations (1-1000 µg/L), a lower toxicity is observed for our AgNPs (Schiavo et al., 2017; Sendra et al., 2017). However, the studies using higher exposure concentrations indicated $EC_{50}$ values of up to 4.7 mg/L (Angel et al., 2013; Schiavo et al., 2017), confirming how exposure conditions and NP surface coatings can significantly affect AgNP toxicity. In particular, the use of NSW *vs* ASW plays an important role: both cited studies reporting a higher toxicity compared to our work (Schiavo et al., 2017; Sendra et al., 2017) were, in fact, conducted using ASW, and could not benefit from the mitigating effect of NOM, while Angel and co-authors(Angel et al., 2013) used NSW and report an $EC_{50}$ of 2.38 mg/L for cit-AgNP to *P. tricornutum*. As also previously discussed, the presence of NOM is able to influence the dissolution of AgNPs but also to reduce the bioavailability and toxicity of free metallic ions in solution. This probably explains why, even if AgNPs showed a higher dissolution value in F/2 compared to TG201, *P. tricornutum* didn't suffer any negative effect up to 1 mg/L exposure.

Results on acute exposure in microcrustacean confirmed what was already observed for microalgae: low toxicity limited to freshwater species and no effects for marine ones.

Calculated $EC_{50}$ (95.88 µg/L) for acute exposure of *C. dubia* are higher compared to those reported in the literature (0.482–27 µg/L) in similar exposure conditions (*e.g.,* using synthetic exposure media) (McLaughlin and Bonzongo, 2012; Harmon et al., 2017). However, a much wider $EC_{50}$ range (0.433–221 µg/L) was reported by McLaughlin & Bonzongo (2012) for exposure in natural waters with low and high dissolved organic carbon (DOC) content, respectively. DOC, as well as NOM, is able to lower the toxicity of metal-based NP. Interestingly, our $EC_{50}$ value (95.88 µg/L), obtained using synthetic freshwater media, results to be closer to the $EC_{50}$ obtained by McLaughlin and Bonzongo in the medium with high DOC content (221 µg/L) compared to that obtained in the low DOC content (0.433 µg/L). Such findings support the hypothesis that the double molecules coating of citrate and L-cysteine, similarly to DOC, contributes to the shielding effect of AgNPs against oxidation, reducing dissolution and toxicity.

Available data on acute toxicity of AgNPs to brine shrimp *Artemia sp.* mostly refer to *A. salina* and $EC_{50}$ values range from <0.1 to 77.5 mg/L with few studies reporting values >100 mg/L (Becaro et al., 2015; Gambardella et al., 2015; Kos et al., 2016; An et al., 2019; Lish et al., 2019). To the best of our knowledge, this is the first study reporting a total lack of acute effects for *Artemia sp.* nauplii up to 100 mg/L AgNPs.

However, the observed sub-lethal effects such as the concentration-dependent ingestion of AgNPs and the reduction in swimming speed, were already reported (Gambardella et al., 2015; Kachenton et al., 2018; An et al., 2019) and should be considered as warning signal for what we observed in the chronic exposure. Kachenton et al. (2018) correlated the ingestion of AgNPs to histopathological lesions of the intestinal tract, while Gambardella et al. (2015) showed that the swimming speed alteration endpoint was more sensitive than mortality in predicting AgNP toxicity. Since swimming performance in brine shrimp is strictly associated to feeding, a prolonged, even if mild, impairment could affect organism growth and survival. In fact, the observed mild reduction of swimming speed in the acute test upon 10 mg/L exposure could have caused the reduction of growth in the chronic test after 7 days (data not shown) and the incidence of mortality at day 14.

Chronic exposure defines a different outcome compared to acute exposure, in particular for *A. franciscana*. The chronic exposure of *C. dubia* has halved the $EC_{50}$ for $AgNO_3$ compared to acute exposure, while causing almost a 4-fold reduction of the $EC_{50}$ for AgNPs. Data of AgNP exposure, however, didn't show a clear trend. The lowest tested concentration (1 µg/L) caused a higher mortality at early-developmental stages of *C. dubia*, compared to 10 µg/L, in both acute and chronic exposure. For both $AgNO_3$ and AgNPs, the reduced reproductive capacity was associated with a similar outcome of discarded molts with unhatched eggs. *C. dubia* females carry their eggs in a brood chamber below the carapace and release the new-borns shortly before molting (Smirnov, 2017). The presence of aborted eggs has been already documented for other cladoceran species upon exposure to lead (Araujo et al., 2019) and to the fungicide carbendazim (Ribeiro et al., 2011; Silva et al., 2017). Although the production of aborted or sterile (non-developing) eggs is considered to be rather common among cladocerans, it is known to be aggravated by unfavourable conditions or exposure to toxic substances (Smirnov, 2017).

While the outcome of *C. dubia* chronic exposure was anticipated by the short-term assay, the same cannot be said for *A. franciscana*, which reported a 100% mortality for concentrations lower than those not causing any effect in the short-time exposure (10 mg/L). Moreover, even if both AgNPs and $AgNO_3$ needed the whole exposure period (14 d) to reach 100% mortality, the time-trend appeared to be different: specimens exposed to $AgNO_3$ showed an increase in mortality already after 2 days of exposure, while those exposed to AgNPs only after 7 days (Figure S5). The different timing in the observed mortality is in agreement with what was already observed by Li et al. (2017) for ROS induction in human TK6 cells, which took only 30 minutes for $Ag^+$ exposure while needed 24 h for AgNP exposure. The same study concluded that, even if both AgNPs and $Ag^+$ were able to induce cytotoxicity and genotoxicity through ROS generation, different mechanisms were probably involved in its induction. In fact, while for $Ag^+$ exposure ROS generation was most likely caused by Ag ions, the same was not true for AgNPs for which levels of dissolved Ag were too low to exert an effect and a NP-related toxicity seemed to take place (Li et al., 2017). It is possible that the prolonged ingestion and detention of AgNPs

inside *Artemia*'s gut, or the continuous intake of AgNPs, even if with a low release of Ag ions, could have led to an increased dissolution and absorption of Ag through the intestinal layer, which accumulated over time in the animal's body. This could have combined with histopathological lesions in the intestinal tract as observed by Kachenton et al. (2018) upon AgNP ingestion. These processes are indeed slower than the direct exposure to Ag ions from the medium and could explain the toxicity observed in chronic, and not in acute, exposure. The timing difference in the occurrence of exposure symptoms between this study and the literature, reporting effects upon acute exposure, could be due to the aforementioned protective role played by the coating, which delayed the dissolution and consequently the occurrence of toxic effects, or to a different toxicity mechanism. For instance, the delay in the appearance of exposure symptoms could be related to the different toxic pathways activated by a different physical interaction related to different coatings, thus confirming the importance of assessing the impact of long-term exposure scenarios to investigate potential negative nano-related effects. This was demonstrated, for instance, by two studies by Bergami et al. (2016; 2017) in which the acute (48h) exposure of the brine shrimp *A. franciscana* to amino-modified polystyrene nanoparticles (PS-$NH_2$ NPs) had no lethal effect but resulted in the adhesion of PS-$NH_2$ NPs on the body surface of the specimens, which increased the molting events. Upon chronic exposure the authors demonstrated how PSNP adhesion and disruption of molting caused a reduction of growth and increased mortality with $LC_{50}$ going from >100 μg/mL to 0.83 μg/mL. A longer exposure, in the case of AgNPs, could have resulted in higher levels of intracellular dissolved Ag, hence leading to a higher toxicity. However, while Malysheva et al. (2016) report that the best predictor of toxicity for AgNP exposure is, in fact, intracellular Ag, Dalzon et al. (2020) observed more severe effects in low-dose chronically exposed cells with low intracellular Ag, compared to high-dose acute exposed cells which had higher intracellular Ag; therefore underlying a clearly different outcome upon chronic exposure. Data obtained in this study show that not only chronic exposure aggravated the AgNP effects to *A. franciscana*, but rather revealed a toxicity that was not observed in the acute exposure, thus allowing to unveil the potential impact of AgNPs.

As already seen for *R. subcapitata*, even for *C. dubia* and *A. franciscana* the effects observed upon AgNP exposure cannot be fully explained by the amount of dissolved Ag. For instance, at the highest AgNP concentration for *C. dubia* (100 µg/L), dissolved Ag was 0.79 µg/L or lower, which is comparable to the concentration exerting no or negligible toxic effects upon $AgNO_3$ exposure (0.5 µg Ag/L), (Figure S2e, f). Hence, the observed toxicity upon exposure to 100 µg/L of AgNPs was higher than that expected based only on Ag dissolution data and a nano-related toxic effect could be hypothesized. Recent studies suggest that AgNPs are able to act at molecular level differently compared to Ag ions and that mechanisms of toxicity are triggered by NP size and surface coating (Hou et al., 2017; Zhang et al., 2020). This further validates the importance of investigating the physical interaction of NPs with cells and the whole body of exposed organisms, as a key to unravel mechanisms of action and predict long-term outcomes (Bellingeri et al., 2019; Bellingeri et al., 2020). Yue et al. (2015) demonstrated that while both $AgNO_3$ and AgNPs were able to destabilize lysosomal membrane in rainbow trout gill cell line, the effect was fully attenuated by the addition of a Ag ligand only for $AgNO_3$ exposure, suggesting a different mechanism of toxicity. In particular, the study hypothesizes that AgNPs are internalized through endocytosis and accumulate in the lysosomes, leading to lysosomal destabilization and dysfunction.

In addition, AgNPs resulted more toxic for freshwater species than for marine ones, despite one or two orders of magnitude lower Ag release. A combination of factors probably contributed to this difference: first the high aggregation of AgNPs, which alters their interaction with organisms, influencing the extent of ingestion and cellular internalization; then, the mitigating effect of chloride species and, most notably, of NOM. All these factors are related to the different chemistry of exposure media, which is able to influence not only AgNP behaviour and dissolution, but also Ag ion speciation and their bioavailability (Gunsolus et al., 2015). For starters, chloride ions, besides influencing AgNP dissolution by formation of soluble or insoluble Ag-Cl complexes, are also known to reduce the bioavailability and consequent toxicity of free $Ag^+$ (Lish et al., 2019; Li et al., 2020). Moreover, the use of synthetic or natural media, as previously discussed, can deeply influence the outcome of AgNP exposure, due to the presence of NOM. NOM can form a layer of high molecular weight biopolymers, known as eco-corona,

on AgNP surface, which modify their biological identity and behaviour in the aquatic environment and towards biota, influencing toxicity (Grassi et al., 2020). Depending on both NOM and media composition, NOM interaction with NPs can alter stability by neutralizing NP surface charge leading to aggregation or, instead, increasing electrostatic repulsion, leading to a reduced aggregation (Quigg et al., 2013). In the case of metallic NPs, such as AgNPs, NOM usually lowers their impact to aquatic organisms by lowering dissolution and binding free metal ions, reducing their bioavailability and toxicity (McLaughlin and Bonzongo, 2012; Sikder et al., 2018). In our study, we can hypothesize that the higher salinity is responsible for the higher dissolution in seawater compared to freshwater media, while the presence of NOM in NSW, together with chloride species, explains why the higher concentration of free Ag ions doesn't result in enhanced toxicity.

This further confirms the role of water chemistry on NP ecotoxicity and bio-interaction. From our data, there seems to be a higher correspondence between ecotoxicity and AgNP aggregation, compared to dissolution. Freshwater species, more clearly than seawater species, suffered from higher ecotoxicities than expected based on dissolution data. Lower aggregation and size of aggregates were observed in freshwater media, as also confirmed by data on surface charge, which are kept above the |30| mV limit, defining a stability threshold for NP suspensions. As previously discussed, the lower aggregation could have caused a higher interaction of the particle with the cell membrane, leading to a higher degree of internalization. This could explain the nano-related toxicity which was hypothesised upon the reduced AgNP dissolution. This brings up an issue also in terms of a realistic exposure scenario, since the freshwater environment is likely to be more heavily affected by AgNP pollution as a consequence of direct wastewater effluent discharge (Li et al., 2016). However, the observed higher toxicity of AgNPs for freshwater species compared to marine ones is still low if compared to literature, where various types of AgNPs were tested in similar exposure scenarios (Table 3). Many studies recognized in thiol groups of proteins potential target of AgNP interaction, which may, for instance, disrupt cellular antioxidant responses (Piao et al., 2011; Veronesi et al., 2015; Dalzon et al., 2020). By combining citrate with L-cysteine as in the coating of our AgNPs, not only the release of Ag ions is significantly reduced

but also a low interaction of AgNPs with biologically active molecules inside cells can be hypothesized, as shown by their low toxicity.

**Table 3.** $EC_{50}$ values for microalgae growth inhibition and microcrustacean immobilization rate and reproduction reported in literature and the one calculated in the present study. Literature data were selected based on similar exposure conditions as the one used in our study (*e.g.,* synthetic media/natural waters). N.C. = not calculated.

| | $EC_{50}$ | Literature $EC_{50}$ range | References |
|---|---|---|---|
| *R. subcapitata* | > 1 mg/L | 0.003 – 0.74 mg/L | Angel et al. 2013; Ribeiro et al. 2014; Sohn et al. 2015; Kleiven et al. 2019 |
| *P. tricornutum* | > 1 mg/L | 0.06 – 4.72 mg/L | Angel et al. 2013; Schiavo et al. 2017; Sendra et al. 2017 |
| *C. dubia*_Acute | 0.095 mg/L ($AgNO_3$=1.6 µg Ag/L) | 0.000482 – 0.027 mg/L | McLaughlin et al. 2012; Harmon et al. 2017 |
| *C. dubia* _Chronic | 0.024 mg/L ($AgNO_3$=0.8 µg Ag/L) | --- | --- |
| *A. franciscana*_Acute | > 100 mg/L ($AgNO_3$= N.C.) | <0.1 – >100 mg/L | Becaro et al. 2015; Kos et al. 2016; An et al. 2019; Lish et al. 2019 |
| *A. franciscana*_Chronic | 5.087 mg/L ($AgNO_3$=0.4 mg Ag/L) | --- | --- |

## 5. Conclusions

In this study we tested the environmental safety of novel bifunctionalized AgNPs coated with citrate and L-cysteine, suitable as water sensors (*i.e.,* mercury) and remediation, with the aim to promote an ecosafety approach. The role of surface coating in determining AgNP ecotoxicity under various aquatic scenarios (freshwater and marine) was highlighted, while chronic exposure demonstrated to be a more reliable way to assess environmental safety. Our ecotoxicity data confirmed how capping agents as citrate and L-cysteine reduced AgNP dissolution and Ag ion release. Low or no acute ecotoxicity was, in fact, observed while chronic exposure revealed severe effects on reproduction and survival of microcrustaceans, which, at least in the marine species, were not anticipated by acute exposure. Our findings support the hypothesis of an additional nano-related toxicity linked to AgNP exposure and confirm that longer exposure times are indeed necessary to unravel ecotoxic effects. The contribution of the nano-size and related surface interaction involved in AgNP toxicity should be further investigated, also in relation to the role they play in the occurrence of chronic-related toxic effects. The double coating of citrate and L-cysteine proved its efficiency in reducing AgNP toxicity while in the meantime, being able to serve as efficient material for environmental remediation. Our data highlight the importance of combining design and toxicity of NPs, an approach that should always be considered, and not only for NPs synthetized for environmental application.

## 6. Acknowledgments

For their contribution of this work, I thank Prof. Iole Venditti and Prof. Chiara Battocchio from the Department of Sciences from Roma Tre University of Rome for the synthesis and characterization of AgNPcitLcys. Also, I thank Claudia Faleri from the department of Life Sciences of the University of Siena for TEM imaging and Prof. Giuseppe Protano from the department of Physical, Earth and Environmental Sciences of the University of Siena for heavy metal analysis. I thank Prof. Andrea M. Atrei from the Department of Biotechnology, Chemistry and Pharmaceutical of the University of Siena and Dr. Marianna Uva and Dr. Eugenio Macchia from CREA s.c.a.r.l. for DLS use. I also thank Dr. Elisa Bergami, former lab-partner at the University of Siena, for giving me insights on *Artemia* culturing and biology, and Dr. Silvia Marchini from the national health institute (ISS) for valuable tips on *Ceriodaphnia* culturing.

SUPPORTING INFORMATION

**Table S1.** Main DLS data in Intensity and Volume for freshly synthetized AgNPs (time = 0) and for the same AgNPs after 1 year from synthesis (50mg/L in milli Q).

| | Time = 0 | Time = 1 years |
|---|---|---|
| $<2R_H>$ nm (PDL) in **Intensity** | 143 ± 25 (0,25) | 211 ± 30 (0,30) |
| $<2R_H>$ nm (PDL) in **Volume** | 178 ± 25 (0,25) | 209 ± 40 (0,4) |

**Table S2.** Ag concentrations (expressed as µg/L) in TG201 and F/2, and TG201 and F/2 with $AgNO_3$ (7 µg /L).

| parameters | medium | 0 h | 24 h | 48 h | 72 h |
|---|---|---|---|---|---|
| pH = 7.7-8<br>Salinity = 0 ‰<br>DO = 8.5-9 mg/L<br>Cond. = 0.2-0.3 ms/cm | TG201 | 0.36 ± 0.06 | --- | --- | 0.26 ± 0.08 |
| | TG201 + 7 µg $AgNO_3$/L | 4.42 ± 0.09 | --- | --- | 4.79 ± 0.18 |
| pH = 7.7-8<br>Salinity = 40 ‰<br>DO = 7.8-8 mg/L<br>Cond. = 55-60 ms/cm | F/2 | 0.27 ± 0.01 | --- | --- | 0.26 ± 0.02 |
| | F/2 + 7 µg $AgNO_3$/L | 4.37 ± 0.08 | --- | --- | 5.32 ± 0.22 |

Media composition:

- OECD TG201 medium (from OECD201 protocol, modified in $Na_2EDTA\ 2H_2O$ content: final concentration = 0.05 mg/L instead of 0.1 mg/L):

  Prepared by addition of the following salts to milliQ water:

| Component | Final concentration (mg/L) |
|---|---|
| $NaHCO_3$ | 50 |
| $NH_4Cl$ | 15 |
| $MgCl_2\ 6(H_2O)$ | 12 |
| $CaCl_2\ 2(H2O)$ | 18 |

| | |
|---|---|
| $MgSO_4$ 7($H_2O$) | 15 |
| $KH_2PO_4$ | 1.6 |
| $FeCl_3$ 6($H_2O$) | 0.064 |
| $Na_2EDTA$ 2($H_2O$) | 0.05 |
| $H_3BO_3$ | 0.185 |
| $MnCl_2$ 4($H_2O$) | 0.415 |
| $ZnCl_2$ | 0.003 |
| $CoCl_2$ 6($H_2O$) | 0.0015 |
| $Na_2MoO_4$ 2($H_2O$) | 0.007 |
| $CuCl_2$ 2($H_2O$) | 0.00001 |

PH= 7.7-8
Dissolved oxygen= 8.5-9 mg/L
Conductivity= 0.2-0.3 ms/cm

- MHRW (synthetic, moderately hard, reconstituted water from EPA 1002.0 protocol):
  Prepared by addition of the following salts to milliQ water:

| Component | Final concentration (mg/L) |
|---|---|
| $NaHCO_3$ | 96 |
| $CaSO_4$ 2$H_2O$ | 60 |
| $MgSO_4$ | 60 |
| KCl | 4 |

PH= 7.7-8
Dissolved oxygen= 8.5-9 mg/L
Conductivity = 0.2-0.3 ms/cm

- NSW (natural seawater collected from the Mediterranean Sea and kept at 4°C upon 0.22 µm filtration):

PH = 7.7-8
Salinity = 40 ‰
Dissolved oxygen = 7.8-8mg/L
Conductivity = 55-60 ms/cm

- F/2 medium (from ISO 10253 (2006) protocol):

Prepared by addition of the following salts to NSW:

| Component | Final concentration (mg/L) |
|---|---|
| $NaNO_3$ | 75 |
| $NaH_2PO_4$ $H_2O$ | 5 |
| $Na_2SiO_3 9H_2O$ | 30 |
| $FeCl_3$ $6H_2O$ | 0.630 |
| $Na_2EDTA$ $2H_2O$ | 0.8 |
| $CuSO_4$ $5H_2O$ | 0.00196 |
| $Na_2MoO_4$ $2H_2O$ | 0.00126 |
| $ZnSO_4$ $7H_2O$ | 0.0044 |
| $CoCl_2$ $6H_2O$ | 0.002 |
| $MnCl_2$ $4H_2O$ | 0.036 |
| Thiamine HCl (Vit. B1) | 0.100 |
| Biotin (vit. H) | 0.0005 |
| Cyanocobalamin (vit. B12) | 0.0005 |

PH = 7.7-8
Salinity = 40 ‰
Dissolved oxygen = 7.8-8mg/L
Conductivity = 55-60 ms/cm

a)

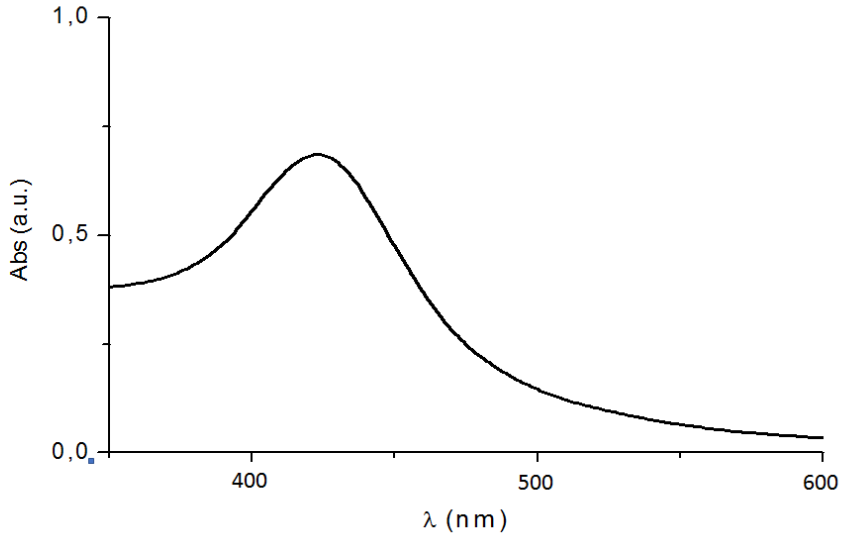

b)

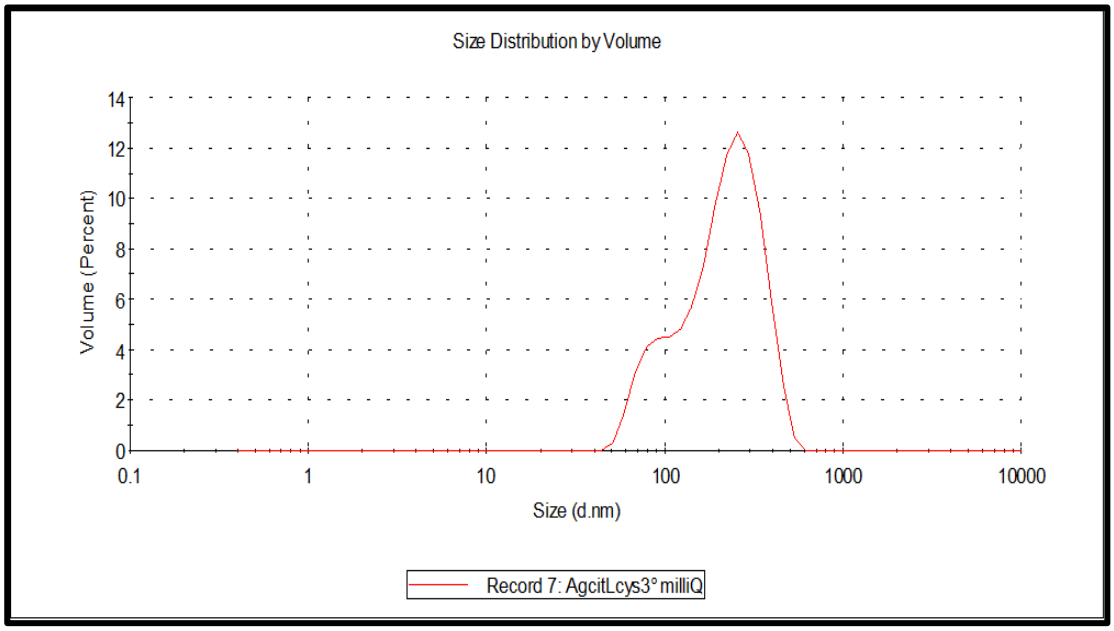
Size Distribution by Volume
Volume (Percent)
14
12
10
8
6
4
2
0
0.1
1
10
100
1000
10000
Size (d.nm)
Record 7: AgcitLcys3° milliQ

c)

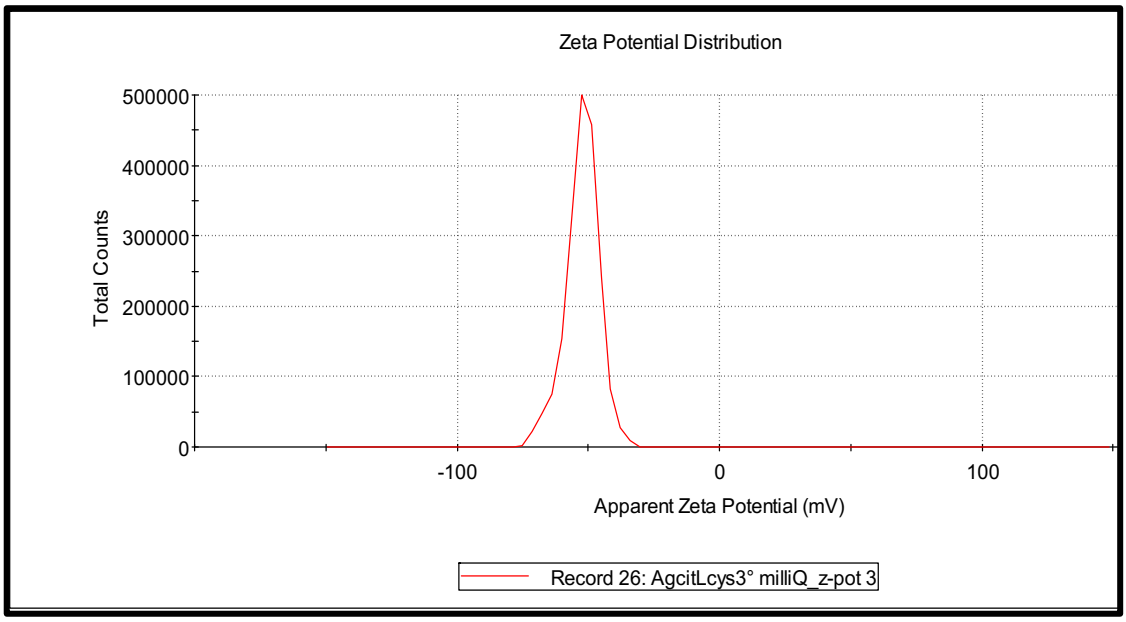
Zeta Potential Distribution
Total Counts
500000
400000
300000
200000
100000
0
-100
0
100
Apparent Zeta Potential (mV)
Record 26: AgcitLcys3° milliQ_z-pot 3

d)

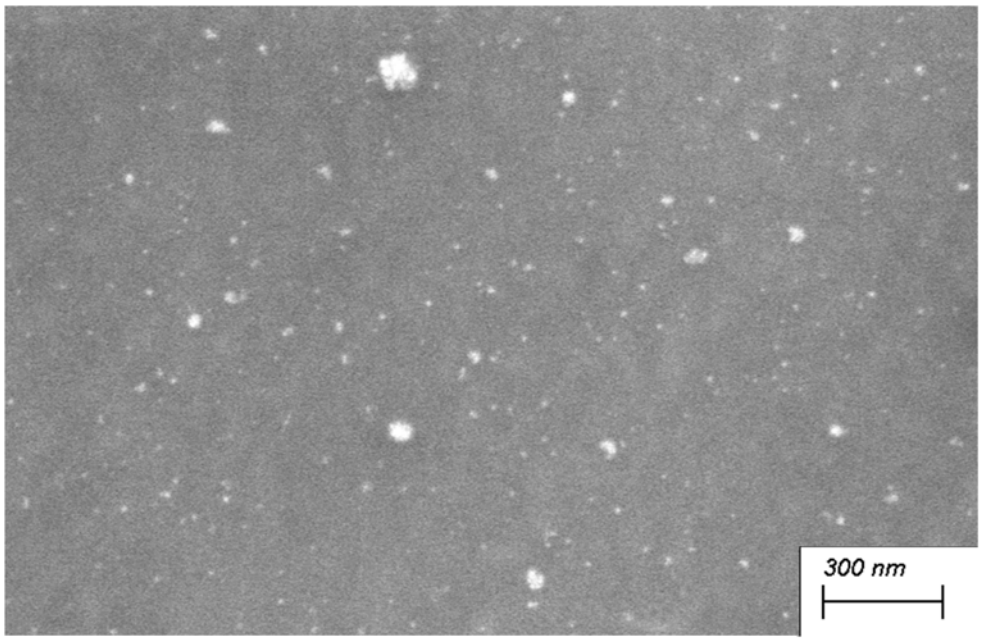


e)

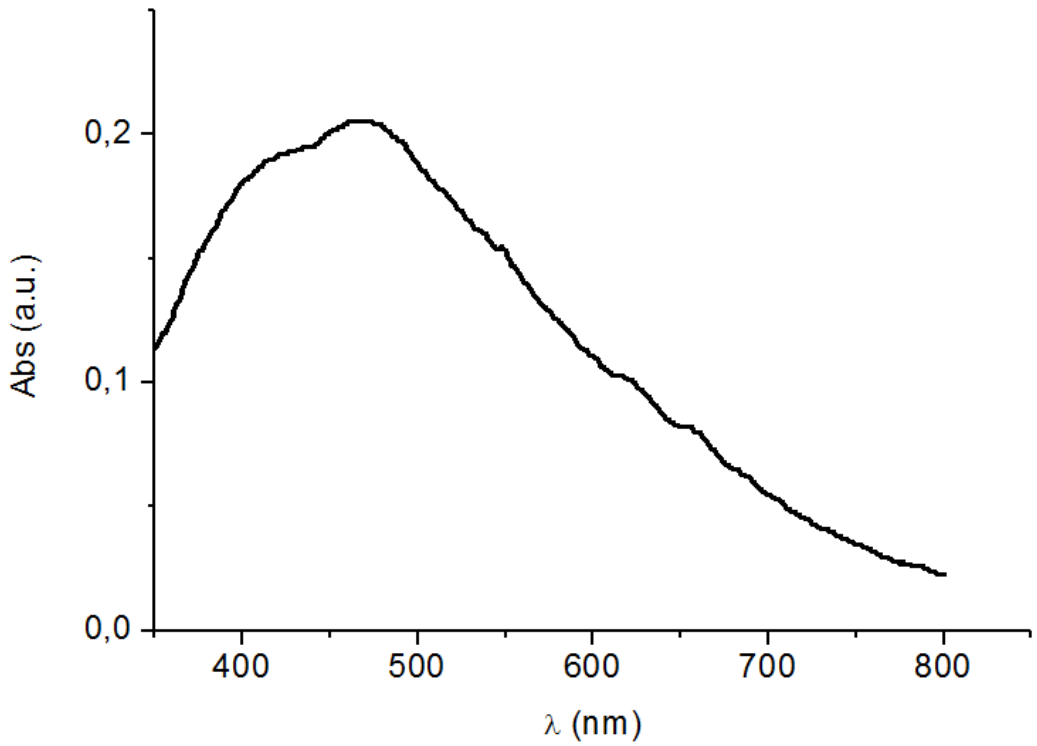

f)

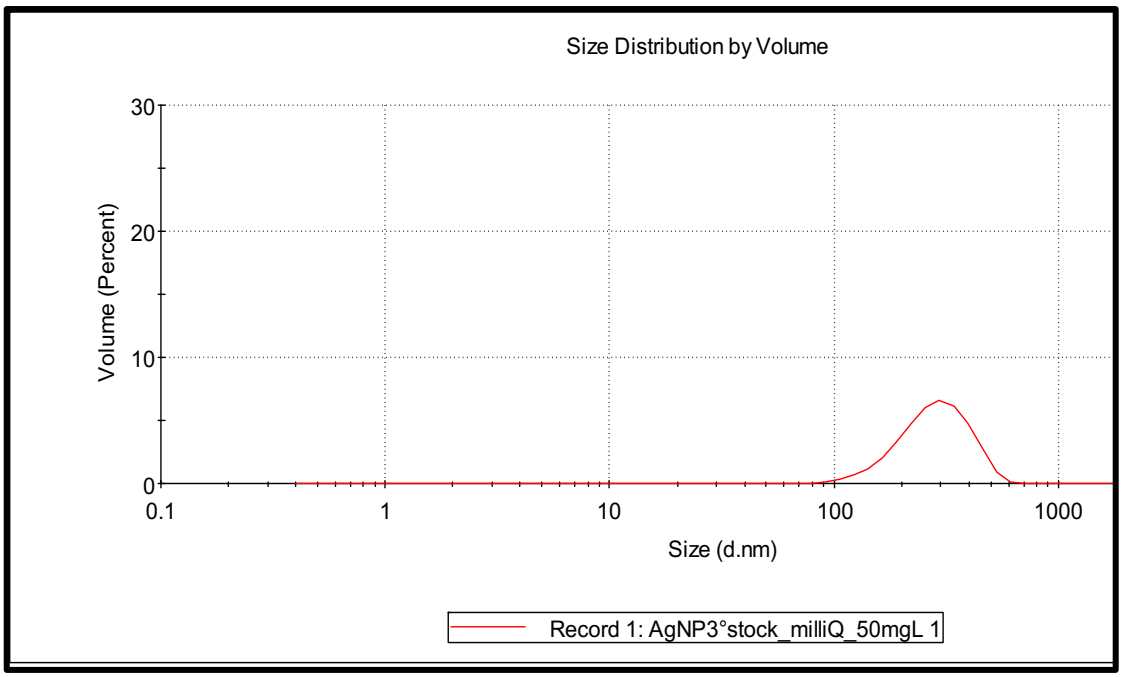
Size Distribution by Volume
Volume (Percent)
30
20
10
0
0.1
1
10
100
1000
Size (d.nm)
Record 1: AgNP3°stock_milliQ_50mgL 1

g)

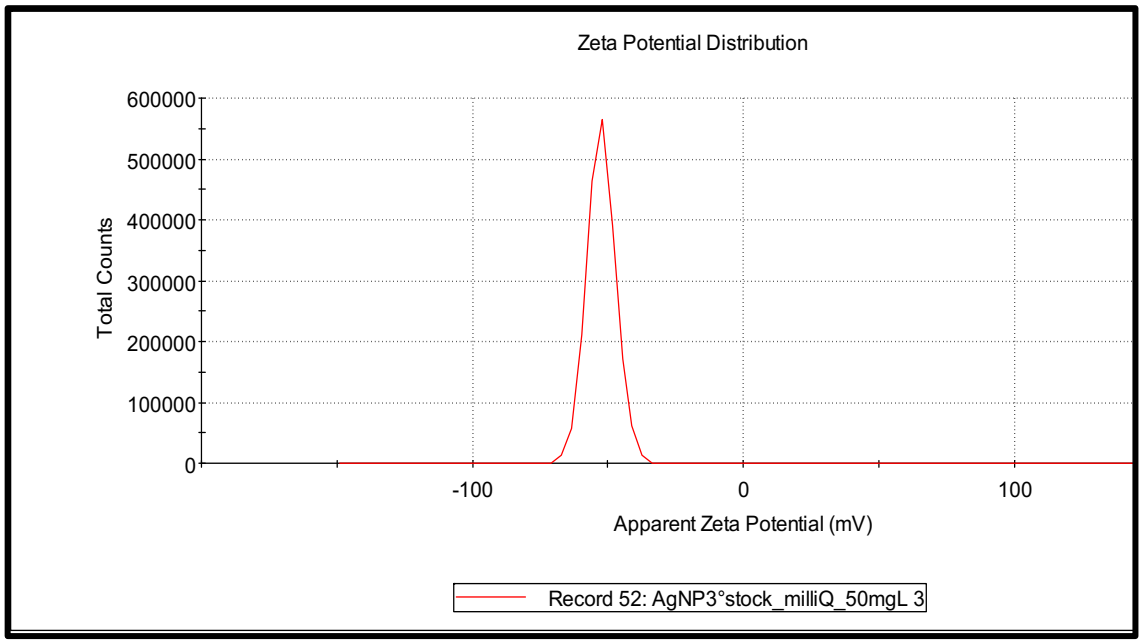
Zeta Potential Distribution
Total Counts
600000
500000
400000
300000
200000
100000
0
-100
0
100
Apparent Zeta Potential (mV)
Record 52: AgNP3°stock_milliQ_50mgL 3

h)

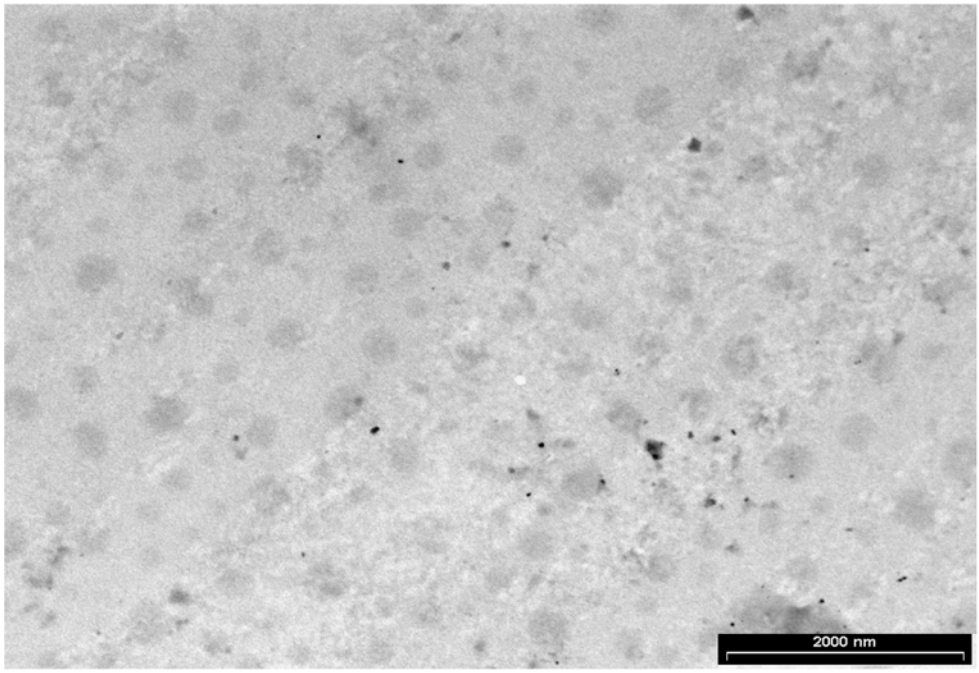


Figure S1. Main characterizations of AgNPs:

Freshly synthetized AgNPs:

a) Uv-vis spectrum in water, with SPR at 430 nm; b) $<R_H>$ = 178 ± 25 nm measurements and c) Zeta potential = -51 ± 2 mV (50mg/L in milli Q); d) SEM image of nanoparticles, with diameter around 15 nm

Same AgNPs after 1 year from synthesis:

e) Uv-vis spectrum, with SRP at 490 nm, f) $<R_H>$ = 209± 40 nm measurement, g) in milli Q and Zeta potential = -52 ± 1 mV (50mg/L in milli Q), h) TEM image nanoparticles with diameter around 25 nm.

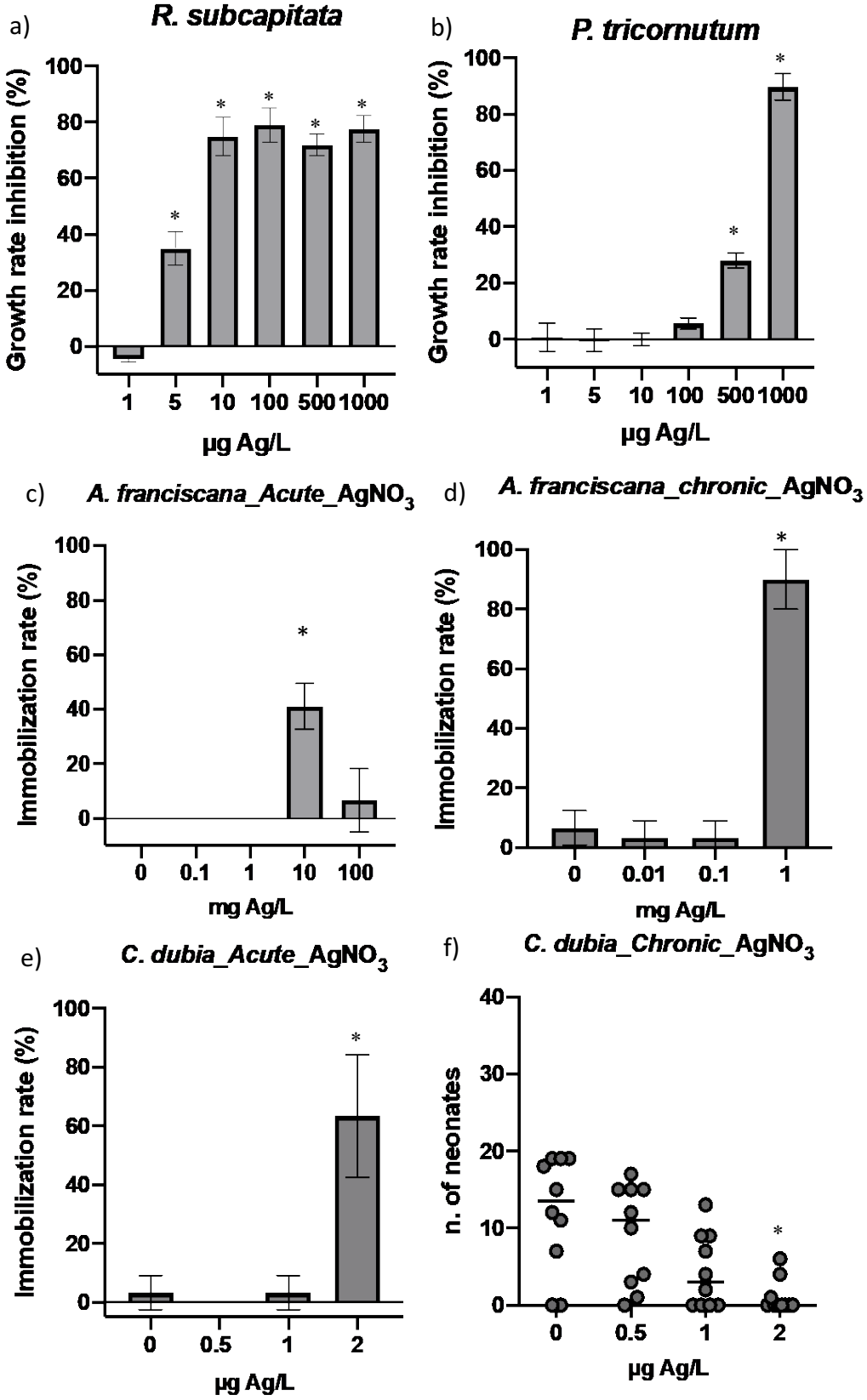


Figure S2. Toxic response to $AgNO_3$ exposure: growth rate inhibition compared to control of *R. subcapitata* and *P. tricornutum* (a, b); immobilization rate of *A. franciscana* acute and chronic exposure (c, d); immobilization rate of *C. dubia* in acute exposure (e) and number of neonates

in chronic exposure (f). Data shown as mean ± standard deviation except for f) in which every dot represents the total number of neonates produced in 7 days by each exposed female (10 for each treatment), while lines represent the mean number of neonates produced for every treatment. Column marked with * are significantly different from control ($p$<0.05).

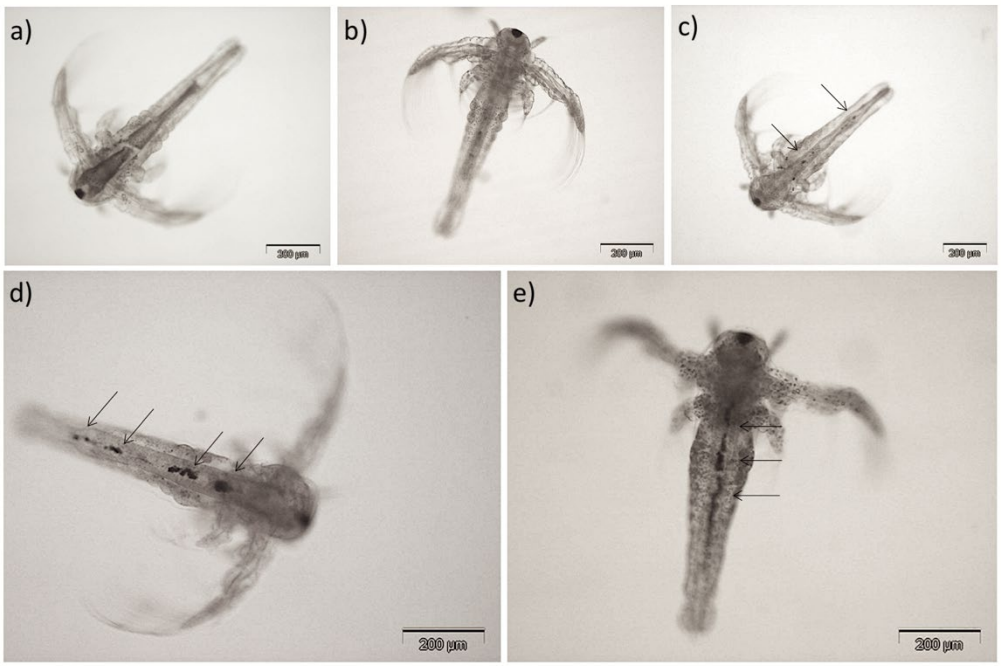


**Figure S3.** *A. franciscana* after 48 h exposure to different $AgNO_3$ concentrations: 0 (a), 0.1 (b), 1 (c), 10 (d), 100 (e) mg/L. Images show the dose-dependent increase of black matter inside the animal gut.

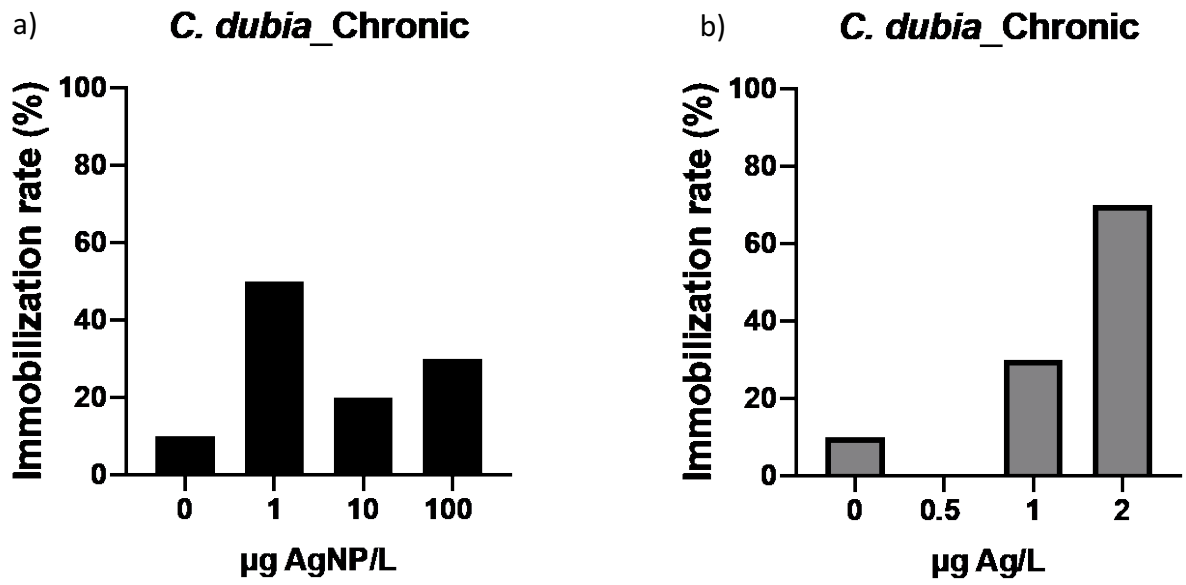


Figure S4. Immobilization rate of *C. dubia* exposed for 7d to AgNPs (a) and $AgNO_3$ (b).

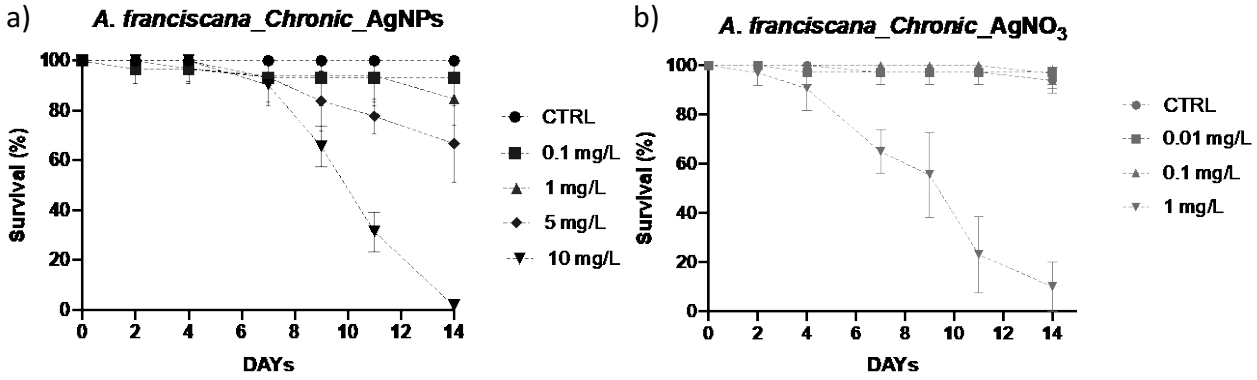


Figure S5. Survival of *A. franciscana* exposed for 14 d to AgNPs (a) and $AgNO_3$ (b) expressed as survival calculated on the whole exposure period.

## REFERENCES


Ale A, Liberatori G, Vannuccini ML, Bergami E, Ancora S, Mariotti G, Bianchi N, Galdopórpora JM, Desimone MF, Cazenave J (2019): Exposure to a nanosilver-enabled consumer product results in similar accumulation and toxicity of silver nanoparticles in the marine mussel *Mytilus galloprovincialis*. Aquatic Toxicology 211, 46-56

An HJ, Sarkheil M, Park HS, Yu IJ, Johari SA (2019): Comparative toxicity of silver nanoparticles (AgNPs) and silver nanowires (AgNWs) on saltwater microcrustacean, *Artemia salina*. Comparative Biochemistry and Physiology Part C: Toxicology & Pharmacology 218, 62-69

Angel BM, Batley GE, Jarolimek CV, Rogers NJ (2013): The impact of size on the fate and toxicity of nanoparticulate silver in aquatic systems. Chemosphere 93, 359-365

Araujo G, Pavlaki M, Soares A, Abessa D, Loureiro S (2019): Bioaccumulation and morphological traits in a multi-generation test with two Daphnia species exposed to lead. Chemosphere 219, 636-644

Becaro AA, Jonsson CM, Puti FC, Siqueira MC, Mattoso LH, Correa DS, Ferreira MD (2015): Toxicity of PVA-stabilized silver nanoparticles to algae and microcrustaceans. Environmental Nanotechnology, Monitoring & Management 3, 22-29

Bellingeri A, Bergami E, Grassi G, Faleri C, Redondo-Hasselerharm P, Koelmans A, Corsi I (2019): Combined effects of nanoplastics and copper on the freshwater alga Raphidocelis subcapitata. Aquatic Toxicology 210, 179-187

Bellingeri A, Casabianca S, Capellacci S, Faleri C, Paccagnini E, Lupetti P, Koelmans AA, Penna A, Corsi I (2020): Impact of polystyrene nanoparticles on marine diatom *Skeletonema marinoi* chain assemblages and consequences on their ecological role in marine ecosystems. Environmental Pollution 262, 114268

Bergami E, Bocci E, Vannuccini ML, Monopoli M, Salvati A, Dawson KA, Corsi I (2016): Nano-sized polystyrene affects feeding, behavior and physiology of brine shrimp *Artemia franciscana* larvae. Ecotoxicology and Environmental Safety 123, 18-25

Bergami E, Pugnalini S, Vannuccini M, Manfra L, Faleri C, Savorelli F, Dawson K, Corsi I (2017): Long-term toxicity of surface-charged polystyrene nanoplastics to marine planktonic species *Dunaliella tertiolecta* and *Artemia franciscana*. Aquatic Toxicology 189, 159-169

Bhattacharjee S (2016): DLS and zeta potential–what they are and what they are not? Journal of Controlled Release 235, 337-351

Cervantes-Avilés P, Huang Y, Keller AA (2019): Multi-technique approach to study the stability of silver nanoparticles at predicted environmental concentrations in wastewater. Water Research 166, 115072

CNR (2003): Metodo 8060 di valutazione della tossicità acuta con *Artemia sp*. Manuali e Linee Guida-Metodi analitici per le acque APAT IRSA CNR, 1043-1049

Dalzon B, Aude-Garcia C, Diemer H, Bons J, Marie-Desvergne C, Pérard J, Dubosson M, Collin-Faure V, Carapito C, Cianférani S (2020): The longer the worse: a combined proteomic and targeted study of the long-term versus short-term effects of silver nanoparticles on macrophages. Environmental Science: Nano

Dong F, Mohd Zaidi NF, Valsami-Jones E, Kreft J-U (2017): Time-resolved toxicity study reveals the dynamic interactions between uncoated silver nanoparticles and bacteria. Nanotoxicology 11, 637-646

Ellis LJA, Kissane S, Hoffman E, Brown JB, Valsami-Jones E, Colbourne J, Lynch I (2020): Multigenerational exposures of *Daphnia magna* to pristine and aged silver

nanoparticles: epigenetic changes and phenotypical ageing related effects. Small 16, 2000301

EPA (2002): 1002.0 Daphnid, C*eriodaphnia dubia,* Survival and Reproduction Test; Chronic Toxicity

Fiorati A, Bellingeri A, Punta C, Corsi I, Venditti I (2020): Silver nanoparticles for water pollution monitoring and treatments: ecosafety challenge and cellulose-based hybrids solution. Polymers 12, 1635

Gambardella C, Costa E, Piazza V, Fabbrocini A, Magi E, Faimali M, Garaventa F (2015): Effect of silver nanoparticles on marine organisms belonging to different trophic levels. Marine Environmental Research 111, 41-49

Grassi G, Gabellieri E, Cioni P, Paccagnini E, Faleri C, Lupetti P, Corsi I, Morelli E (2020): Interplay between extracellular polymeric substances (EPS) from a marine diatom and model nanoplastic through eco-corona formation. Science of The Total Environment 725, 138457

Gunsolus IL, Mousavi MP, Hussein K, Bühlmann P, Haynes CL (2015): Effects of humic and fulvic acids on silver nanoparticle stability, dissolution, and toxicity. Environmental Science & Technology 49, 8078-8086

Harmon AR, Kennedy AJ, Laird JG, Bednar AJ, Steevens JA (2017): Comparison of acute to chronic ratios between silver and gold nanoparticles, using *Ceriodaphnia dubia*. Nanotoxicology 11, 1127-1139

He D, Dorantes-Aranda JJ, Waite TD (2012): Silver nanoparticle-algae interactions: Oxidative dissolution, reactive oxygen species generation and synergistic toxic effects. Environmental Science & Technology 46, 8731-8738

Ho CM, Yau SKW, Lok CN, So MH, Che CM (2010): Oxidative dissolution of silver nanoparticles by biologically relevant oxidants: a kinetic and mechanistic study. Chemistry–An Asian Journal 5, 285-293

Hou J, Zhou Y, Wang C, Li S, Wang X (2017): Toxic effects and molecular mechanism of different types of silver nanoparticles to the aquatic crustacean *Daphnia magna*. Environmental Science & Technology 51, 12868-12878

ISO/10253 (2006): Water quality — Marine algal growth inhibition test with *Skeletonema costatum* and *Phaeodactylum tricornutum* https://www.iso.org/standard/34811.html

ISO/TS20787 (2017): Nanotechnologies—Aquatic toxicity assessment of manufactured nanomaterials in saltwater lakes using A*rtemia sp.* nauplii, https://www.iso.org/standard/69087.html

Ivask A, Kurvet I, Kasemets K, Blinova I, Aruoja V, Suppi S, Vija H, Käkinen A, Titma T, Heinlaan M (2014): Size-dependent toxicity of silver nanoparticles to bacteria, yeast, algae, crustaceans and mammalian cells in vitro. PloS one 9, e102108

Kachenton S, Whangpurikul V, Kangwanrangsan N, Tansatit T, Jiraungkoorskul W (2018): Siver nanoparticles toxicity in brine shrimp and its histopathological analysis. International Journal of Nanoscience 17, 1850007

Kalantzi I, Mylona K, Toncelli C, Bucheli TD, Knauer K, Pergantis SA, Pitta P, Tsiola A, Tsapakis M (2019): Ecotoxicity of silver nanoparticles on plankton organisms: a review. Journal of Nanoparticle Research 21, 65

Kittler S, Greulich C, Diendorf J, Koller M, Epple M (2010): Toxicity of silver nanoparticles increases during storage because of slow dissolution under release of silver ions. Chemistry of Materials 22, 4548-4554

Kleiven M, Macken A, Oughton DH (2019): Growth inhibition in *Raphidocelis subcapita*– Evidence of nanospecific toxicity of silver nanoparticles. Chemosphere 221, 785-792

Kos M, Kahru A, Drobne D, Singh S, Kalčíková G, Kühnel D, Rohit R, Gotvajn AŽ, Jemec A (2016): A case study to optimise and validate the brine shrimp *Artemia franciscana* immobilisation assay with silver nanoparticles: The role of harmonisation. Environmental Pollution 213, 173-183

Lankoff A, Sandberg WJ, Wegierek-Ciuk A, Lisowska H, Refsnes M, Sartowska B, Schwarze PE, Meczynska-Wielgosz S, Wojewodzka M, Kruszewski M (2012): The effect of agglomeration state of silver and titanium dioxide nanoparticles on cellular response of HepG2, A549 and THP-1 cells. Toxicology Letters 208, 197-213

Lazareva A, Keller AA (2014): Estimating potential life cycle releases of engineered nanomaterials from wastewater treatment plants. ACS Sustainable Chemistry & Engineering 2, 1656-1665

Leal PP, Hurd CL, Sander SG, Armstrong E, Roleda MY (2016): Copper ecotoxicology of marine algae: a methodological appraisal. Chemistry and Ecology 32, 786-800

Lekamge S, Miranda AF, Trestrail C, Pham B, Ball AS, Shukla R, Nugegoda D (2019): The Toxicity of non-aged and aged coated silver nanoparticles to freshwater alga *Raphidocelis subcapitata*. Environmental Toxicology and Chemistry 38, 2371-2382

Levard C, Reinsch BC, Michel FM, Oumahi C, Lowry GV, Brown Jr GE (2011): Sulfidation processes of PVP-coated silver nanoparticles in aqueous solution: impact on dissolution rate. Environmental Science & Technology 45, 5260-5266

Levard C, Hotze EM, Colman BP, Dale AL, Truong L, Yang X, Bone AJ, Brown Jr GE, Tanguay RL, Di Giulio RT (2013a): Sulfidation of silver nanoparticles: natural antidote to their toxicity. Environmental Science & Technology 47, 13440-13448

Levard Cm, Mitra S, Yang T, Jew AD, Badireddy AR, Lowry GV, Brown Jr GE (2013b): Effect of chloride on the dissolution rate of silver nanoparticles and toxicity to *E. coli*. Environmental Science & Technology 47, 5738-5745

Li L, Stoiber M, Wimmer A, Xu Z, Lindenblatt C, Helmreich B, Schuster M (2016): To what extent can full-scale wastewater treatment plant effluent influence the occurrence of silver-based nanoparticles in surface waters? Environmental Science & Technology 50, 6327-6333

Li P, Su M, Wang X, Zou X, Sun X, Shi J, Zhang H (2020): Environmental fate and behavior of silver nanoparticles in natural estuarine systems. Journal of Environmental Sciences 88, 248-259

Li X, Lenhart JJ, Walker HW (2010): Dissolution-accompanied aggregation kinetics of silver nanoparticles. Langmuir 26, 16690-16698

Li Y, Qin T, Ingle T, Yan J, He W, Yin J-J, Chen T (2017): Differential genotoxicity mechanisms of silver nanoparticles and silver ions. Archives of Toxicology 91, 509-519

Lish RAD, Johari SA, Sarkheil M, Yu IJ (2019): On how environmental and experimental conditions affect the results of aquatic nanotoxicology on brine shrimp (*Artemia salina*): A case of silver nanoparticles toxicity. Environmental Pollution 255, 113358

Liu X, Dumitrescu E, Kumar A, Austin D, Goia D, Wallace KN, Andreescu S (2019): Differential lethal and sublethal effects in embryonic zebrafish exposed to different sizes of silver nanoparticles. Environmental Pollution 248, 627-634

Majzik A, Fülöp L, Csapó E, Bogár F, Martinek T, Penke B, Bíró G, Dékány I (2010): Functionalization of gold nanoparticles with amino acid, β-amyloid peptides and fragment. Colloids and Surfaces B: Biointerfaces 81, 235-241

Malysheva A, Voelcker N, Holm PE, Lombi E (2016): Unraveling the complex behavior of AgNPs driving NP-cell interactions and toxicity to algal cells. Environmental Science & Technology 50, 12455-12463

Manfra L, Savorelli F, Pisapia M, Magaletti E, Cicero AM (2012): Long-term lethal toxicity test with the crustacean *Artemia franciscana*. JoVE (Journal of Visualized Experiments), e3790

Marchioni M, Veronesi G, Worms I, Ling WL, Gallon T, Leonard D, Gateau C, Chevallet M, Jouneau P-H, Carlini L (2020): Safer-by-design biocides made of tri-thiol bridged silver nanoparticle assemblies. Nanoscale Horizons 5, 507-513

McGillicuddy E, Murray I, Kavanagh S, Morrison L, Fogarty A, Cormican M, Dockery P, Prendergast M, Rowan N, Morris D (2017): Silver nanoparticles in the environment: Sources, detection and ecotoxicology. Science of the Total Environment 575, 231-246

McLaughlin J, Bonzongo JCJ (2012): Effects of natural water chemistry on nanosilver behavior and toxicity to *Ceriodaphnia dubia* and *Pseudokirchneriella subcapitata*. Environmental Toxicology and Chemistry 31, 168-175

Navarro E, Wagner B, Odzak N, Sigg L, Behra R (2015): Effects of differently coated silver nanoparticles on the photosynthesis of *Chlamydomonas reinhardtii*. Environmental Science & Technology 49, 8041-8047

OECD, 201 (2011) Test No. 201: Freshwater Alga and Cyanobacteria, Growth Inhibition Test , OECD Guidelines for the Testing of Chemicals, Section 2, OECD Publishing, Paris, https://doi.org/10.1787/9789264069923-en

Piao MJ, Kang KA, Lee IK, Kim HS, Kim S, Choi JY, Choi J, Hyun JW (2011): Silver nanoparticles induce oxidative cell damage in human liver cells through inhibition of reduced glutathione and induction of mitochondria-involved apoptosis. Toxicology Letters 201, 92-100

Prosposito P, Burratti L, Bellingeri A, Protano G, Faleri C, Corsi I, Battocchio C, Iucci G, Tortora L, Secchi V (2019): Bifunctionalized silver nanoparticles as Hg2+ plasmonic sensor in water: synthesis, characterizations, and ecosafety. Nanomaterials 9, 1353

Prosposito P, Burratti L, Venditti I (2020): Silver nanoparticles as colorimetric sensors for water pollutants. Chemosensors 8, 26

Quigg A, Chin W-C, Chen C-S, Zhang S, Jiang Y, Miao A-J, Schwehr KA, Xu C, Santschi PH (2013): Direct and indirect toxic effects of engineered nanoparticles on algae: role of natural organic matter. ACS Sustainable Chemistry & Engineering 1, 686-702

Ratte HT (1999): Bioaccumulation and toxicity of silver compounds: a review. Environmental Toxicology and Chemistry: An International Journal 18, 89-108

Resgalla Jr C, Poleza F, Souza R, Máximo M, Radetski C (2012): Evaluation of effectiveness of EDTA and sodium thiosulfate in removing metal toxicity toward sea urchin embryo-larval applying the TIE. Chemosphere 89, 102-107

Ribeiro F, Ferreira NC, Ferreira A, Soares AM, Loureiro S (2011): Is ultraviolet radiation a synergistic stressor in combined exposures? The case study of *Daphnia magna* exposure to UV and carbendazim. Aquatic Toxicology 102, 114-122

Ribeiro F, Gallego-Urrea JA, Jurkschat K, Crossley A, Hassellöv M, Taylor C, Soares AM, Loureiro S (2014): Silver nanoparticles and silver nitrate induce high toxicity to *Pseudokirchneriella subcapitata*, *Daphnia magna* and *Danio rerio*. Science of the Total Environment 466, 232-241

Saravanan C, Rajesh R, Kaviarasan T, Muthukumar K, Kavitake D, Shetty PH (2017): Synthesis of silver nanoparticles using bacterial exopolysaccharide and its application for degradation of azo-dyes. Biotechnology Reports 15, 33-40

Schiavo S, Duroudier N, Bilbao E, Mikolaczyk M, Schäfer J, Cajaraville M, Manzo S (2017): Effects of PVP/PEI coated and uncoated silver NPs and PVP/PEI coating agent on three species of marine microalgae. Science of the Total Environment 577, 45-53

Sendra M, Yeste M, Gatica J, Moreno-Garrido I, Blasco J (2017): Direct and indirect effects of silver nanoparticles on freshwater and marine microalgae (*Chlamydomonas reinhardtii* and *Phaeodactylum tricornutum*). Chemosphere 179, 279-289

Sikder M, Lead JR, Chandler GT, Baalousha M (2018): A rapid approach for measuring silver nanoparticle concentration and dissolution in seawater by UV–Vis. Science of the Total Environment 618, 597-607

Silva ARR, Cardoso DN, Cruz A, Pestana JL, Mendo S, Soares AM, Loureiro S (2017): Multigenerational effects of carbendazim in *Daphnia magna*. Environmental Toxicology and Chemistry 36, 383-394

Smirnov NN (2017): Physiology of the Cladocera. Academic Press

Tortella G, Rubilar O, Durán N, Diez M, Martínez M, Parada J, Seabra A (2020): Silver nanoparticles: Toxicity in model organisms as an overview of its hazard for human health and the environment. Journal of Hazardous Materials 390, 121974

Venditti I, D'Amato R, Russo MV, Falconieri M (2007): Synthesis of conjugated polymeric nanobeads for photonic bandgap materials. Sensors and Actuators B: Chemical 126, 35-40

Veronesi G, Aude-Garcia C, Kieffer I, Gallon T, Delangle P, Herlin-Boime N, Rabilloud T, Carrière M (2015): Exposure-dependent Ag+ release from silver nanoparticles and its complexation in AgS 2 sites in primary murine macrophages. Nanoscale 7, 7323-7330

Wu F, Harper BJ, Harper SL (2017): Differential dissolution and toxicity of surface functionalized silver nanoparticles in small-scale microcosms: impacts of community complexity. Environmental Science: Nano 4, 359-372

Yue Y, Behra R, Sigg L, Fernandez Freire P, Pillai S, Schirmer K (2015): Toxicity of silver nanoparticles to a fish gill cell line: Role of medium composition. Nanotoxicology 9, 54-63

Zhang J, Shen L, Xiang Q, Ling J, Zhou C, Hu J, Chen L (2020): Proteomics reveals surface electrical property-dependent toxic mechanisms of silver nanoparticles in *Chlorella vulgaris*. Environmental Pollution, 114743

CHAPTER 4

# Ag NPs TOXICITY TO BACTERIA AND MICROALGAE: Comparison of AgNPcitLcys and AgNP3MPS toxicity and mode of action

## GRAPHICAL ABSTRACT

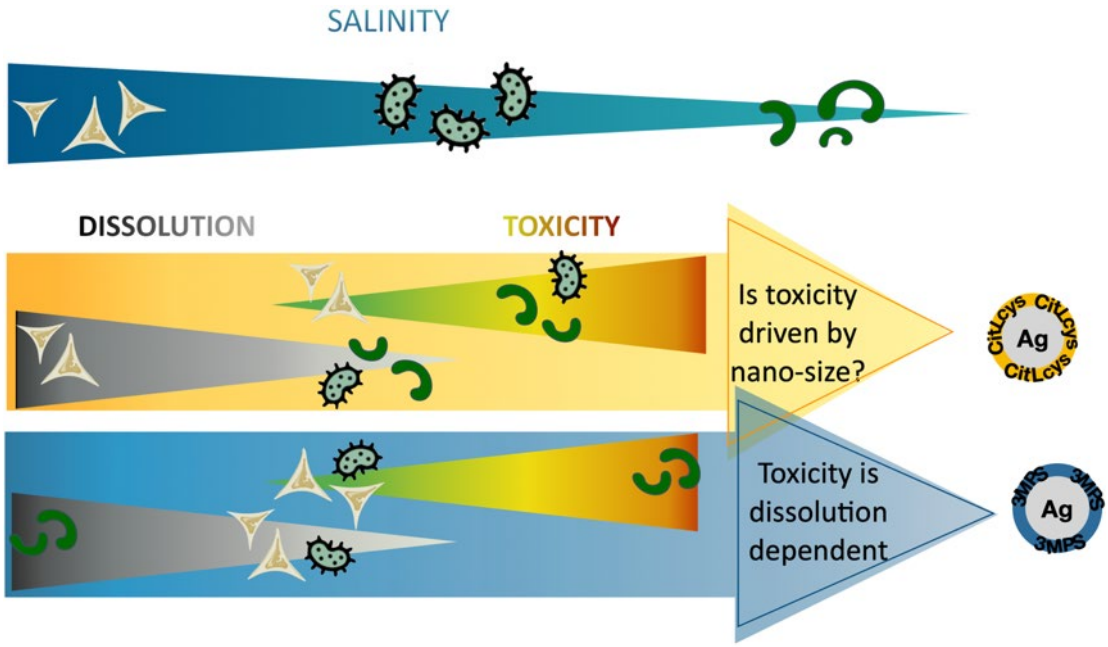

## ABSTRACT

AgNPs are thoroughly studied for their antimicrobial potential, but their mode of action towards bacteria, as well as to non-target organisms, is still not fully understood. The vast production and use of AgNPs inevitably increase their release into the aquatic environment, where fundamental constituents of the aquatic food chain can be affected. Our study aimed at comparing the toxicity of two coated AgNPs, with citrate and L-cysteine (AgNPcitLcys) and with 3-mercapto-a-propanesulfonate (AgNP3MPS), to unicellular organisms, as bacteria and microalgae. Both AgNP behaviour in bacteria and microalgae media was characterized by DLS and TEM while dissolution of Ag ions was measured by ICP-MS. Effects of AgNPs on microalgae growth inhibition and reactive oxygen species production (ROS) were evaluated on the freshwater *Raphidocelis subcapitata* and the marine *Phaeodactylum tricornutum*, and the antimicrobial potential was assessed in the gram-negative bacteria *Escherichia coli*. Particle characterization confirmed a nominal nano-size for both AgNPcitLcys and AgNP3MPS regardless of their different coatings, while they showed an increasing aggregation in exposure media, which increased as it did salinity. Dissolution was low and was differently influenced by media chemistry; in algal media it followed the trend of aggregation for both AgNPs, increasing with increased salinity and time of incubation, a very low dissolution for both AgNPs, which decreased with incubation time, was observed in bacterial medium probably due to its complex composition. In general, both AgNPcitLcys and AgNP3MPS showed low toxicity for bacteria and microalgae with a maximum 40% inhibition of growth for up to, respectively, 256 mg/L and 60 mg/L. The marine microalgae *Phaeodactylum tricornutum* resulted not affected by either AgNPcitLcys or AgNP3MPS exposure, while both *E. coli* and the freshwater *Raphidocelis subcapitata* showed higher toxicity than what expected based on the observed low dissolution values, but only for AgNPcitLcys exposure. A different mode of action towards organisms was hence hypothesized for the differently coated AgNPs, with a dissolution-related toxicity for AgNP3MPS and the occurrence of an additive toxicity for AgNPcitLcys, probably driven by organism-NP surface interaction, and related to the nano-size.

## 1. Introduction

Silver and silver NPs are known as highly effective antimicrobial agents against a wide range of bacteria, fungi and viruses. Their production and massive use have caused their release in in sewage waters and, consequently, in the resulting sludge and treated waters (Li et al., 2016). Predicted environmental concentrations (PECs) for surface waters in the range of ng-µg $L^{-1}$ (Lazareva and Keller, 2014; Cervantes-Avilés et al., 2019).

Microorganisms are basic constituents of aquatic food webs and, as such, play a central role in ecosystem regulation and balance. Shifts in microbial communities upon exposure to AgNPs have been recently documented with potential consequences on nutrient cycle processes, for example by inhibiting nitrification (Beddow et al., 2017). The emergence of Ag-resistant populations and the occurrence of antibiotic resistant genes have been also reported in AgNP environmentally exposed bacterial communities, as in polluted rivers and wastewater treatment plants (WWTP) (Ma et al., 2016; Siddiqui et al., 2019).

Many strains of microalgae have been also shown to be affected by AgNP exposure (Malysheva et al., 2016; Schiavo et al., 2017; Kalantzi et al., 2019; Kleiven et al., 2019; Zhang et al., 2020), with effect concentrations in a wide range, from µg/L to mg/L. Although several impairments in microalgae functions have been documented, the majority of studies conducted until now are often lacking information about AgNP behaviour and dissolution in the exposure media, both key elements in the understanding of mode of action (MoA) and ultimate toxicity. Up to now, the dissolution process has been recognized as main driver of AgNP toxicity, however, a nano-specific effect has been more recently hypothesized (Faiz et al., 2018; Kleiven et al., 2019; Theofilou et al., 2021). However, no scientific consensus has yet been reached on this matter. Some studies report that the direct physical interaction of AgNP with the organism surface/membrane is the trigger for the onset of toxicity (Sondi and Salopek-Sondi, 2004; Theofilou et al., 2021). This will surely be influenced by the binding strength, the time of interaction, the type of target, etc. Similarly, specific properties of the AgNP itself such as coating, surface charge and size, and by the transformations occurring when dispersed in a water

media, will also play a role (Kędziora et al., 2018; Sukhanova et al., 2018). Such high number of variables gives rise to current uncertainties behind AgNP MoA, as resulting from a complex interplay of factors.

The aim of the present work was to unravel the effect of two differently coated AgNPs, with L-cysteine (citLcys) and 3-mercapto-a-propanesulfonate (3MPS), in terms of the mode of action towards one strain of bacteria, *E. coli* JM109, and two strains of microalgae, the freshwater *R. subcapitata* and the marine *P. tricornutum*. Both bacteria and microalgae are unicellular organisms that can be directly and, potentially, heavily affected by AgNPs while belonging to two distinct domains of life, prokaryotic and eucaryotic. Belonging to different environments, AgNP behaviour and toxicity will be differently influenced by the peculiar characteristics of each media, providing valuable information on how AgNP MoA can be affected. Moreover, both taxa are basic constituents of aquatic and terrestrial food webs playing an essential ecological role, hence the understanding of AgNP mechanism of toxicity is of fundamental importance for risk assessment.

## 2. Materials and Methods

### 2.1. AgNP synthesis and characterization

AgNPs were synthetized and functionalized with two capping agents, namely citrate and L-cysteine (citLcys) and 3-mercapto-a-propanesulfonate (3MPS). AgNPs coated with the citLcys were synthesized by the Department of Sciences, University of Roma Tre according to the procedure described in chapter 2 and 3 and in (Prosposito et al., 2019). Briefly, for AgNPcitcys synthesis 1.47 g of sodium citrate were dissolved in 50 mL of distilled water (0.01 M), 0.006 g of L-cysteine were dissolved in 25 mL of distilled water (0.002 M) and 0.21 g of silver nitrate ($AgNO_3$) were dissolved in 25 mL of distilled water (0.05 M). Then, 25 mL of L-cysteine solution, 10 mL of Citrate solution and 2.5 mL of $AgNO_3$ solution were added sequentially in a 100 mL flask, provided with a magnetic stirrer. The mixture was degassed with Argon for 10 min, then 4 mL of sodium borohydride ($NaBH_4$) solution (0.016 g in 4 mL of distilled water) were added. The mixture was allowed to react at room temperature for 2 h and, at the end, the brown solution was collected.

AgNP3MPS were prepared using the procedure reported in Prosposito et al. (2016), as follows: a solution with $NaBH_4$ (0.233 g in 10 mL of distilled water) was mixed with a solution of $AgNO_3$ (0.1 g in 10 mL of distilled water) with concentration ratio $NaBH_4/AgNO_3$ 2:1. The $NaBH_4$ solution was cooled to 3 °C under vigorous stirring, then the $AgNO_3$ solution was added dropwise at approximately one drop per second. The volume ratio of the two solutions was $NaBH_4/AgNO_3$ 15:1. Finally 3MPS was added to reach the final ratio of $AgNO_3$/3MPS 1:0.1. Both batches of AgNPcitLcys and AgNP3MPS were stored at 4 °C until use.

Dynamic Light Scattering (DLS) (Zetasizer Nano ZS90, Malvern, combined with the Zetasizer Nano Series software, version 7.02, Particular Sciences) was used to investigate the hydrodynamic diameter (Z-average, nm), polydispersity index (PDI) and surface charge (ζ-potential, mV) of both batches in MilliQ water and in all media used for toxicity tests: TG201 and F/2 for microalgae and LB medium for bacteria (see media composition in table S1). DLS measurements were performed at 25°C and 100 mg/L

AgNPcitLcys and AgNP3MPS, to assure an optimal quality of the obtained data according to the instrument.

AgNPcitLcys and AgNP3MPS were also investigated by TEM (Philips Morgagni 268 D electronics, at 80 KV and equipped with a MegaView II CCD camera) in MilliQ water and in all media used for toxicity tests (TG201, F/2 and LB medium) using a 10 mg/L suspension of AgNPcitLcys and a 50 mg suspension for AgNP3MPS.

The release of Ag ions from both AgNPcitLcys and AgNP3MPS has been assessed at the beginning (1 h) and at the end of the exposure times (72 h for microalga and 24 h for bacteria) in all media used for toxicity tests: TG201, F/2 and LB medium. Ag release was measured at the highest AgNP concentration tested for each test species: 60 mg/L for microalgae and 256 mg/L for bacteria. Solutions were kept in the same conditions of temperature, light and photoperiod as used for toxicity tests (21°C, 4500 lux and continuous illumination for microalgae, 37°C in the dark for bacteria), and mixed by manual shaking once a day. An aliquot of each solution was taken at each measured time point (1 and 24 or 72 h) and centrifuged (5000 g, 40 min) by using a centrifugal filter device with a 3 kDa cut-off (Amicon Ultra-15 mL, Millipore, USA). The resulting filtrate was acidified with $HNO_3$ (10%) and analysed for determining Ag concentration. As control, Ag concentrations were also measured in tested media (TG201, F/2 and LB medium) and in tested media with added $AgNO_3$ (7 µg/L), as $AgNO_3$ was used as positive control for all toxicity tests. The Ag concentrations were determined by inductively coupled plasma-mass spectrometry (ICP-MS) using the Perkin Elmer NexION 350 spectrometer (Waltham, MA, USA). The analytical accuracy was checked by comparing the certified and measured Ag concentration in the standard reference material SRM 1643e (Trace Elements in Water) of the National Institute of Standards and Technology (NIST). The analytical precision was evaluated by means of the percentage relative standard deviation (% RSD) of five replicate analyses of each water sample.

## 2.2. Toxicity

### *2.2.1. Microalgae*

#### *2.2.1.1. Growth inhibition*

Algal toxicity tests were performed with the freshwater microalgae *R. subcapitata* and the marine *P. tricornutum* following standardized protocols (OECD 201, 2011; ISO 10253, 2006). The algae were cultured in TG201 medium (*R. subcapitata*), prepared using milliQ water as dilution water, and F/2 medium (*P. tricornutum*), prepared by using filtrated (0.45 µm) natural seawater (NSW) as dilution water, and maintained in axenic exponential growth conditions at 18 ± 1 °C with a 16/8 h light-dark cycle photoperiod in a growth chamber.

Toxicity tests (72 h) were carried out in modified growth media in order to limit the amount of chelating agents (*i.e.,* EDTA), following recommendations for heavy metal toxicity testing (Resgalla Jr et al., 2012; Leal et al., 2016). EDTA final concentration in test media were 50 µg/L in TG201 and 0.8 mg/L in F/2, both previously proved to be able to ensure an optimal growth of both algae (data not shown).

Algae from a stock culture were inoculated 72 h prior to run the assay and maintained at 21 ± 1 °C and continuous illumination at 4500 lux. Tests were carried out in polystyrene single-use sterile multi-well with 2 mL capacity for each well. Initial algal concentration in toxicity tests was $1x10^4$ cells/mL and exposure concentrations of AgNPcitLcys and AgNP3MPS were as follows: 0, 1, 5, 10, 15, 30, 60 mg/L, while for $AgNO_3$ different concentration range were chosen based on different specie sensitivity: 0, 1, 3, 5, 7, 10, 100 µg/L for *R. subcapitata* and 0, 1, 5, 10, 50, 100, 500, 1000 µg/L for *P. tricornutum*. $AgNO_3$ was used as positive control. Three replicates for each exposure concentrations were set. *R. subcapitata* multi-well plates were placed over an orbital shaker at 50 rpm to reduce algal settling and enabling gas exchanges. Every test was repeated three times. After 72 h, algae were fixed with a 1:1 lugol/ethanol solution and cell density was estimated both by counting under optical microscope Olympus BX51 (40X), equipped with an improved Neubauer chamber and by means of an automated cell counter (LUNA II, Logos Biosystems) for *R. subcapitata*. The number of cells/mL, growth rate (µ) and inhibition of growth rate (Iµi) compared to control were determined.

*R. subcapitata* and *P. tricornutum* were also exposed to the single components of the coatings (citrate, L-cysteine and 3MPS) at the following concentrations: 0.5, 1, 2, 5, 10 mg/L for citrate and L-cysteine and 100, 200, 400, 800 2000 µg/L for 3MPS, and checked for growth inhibition.

#### *2.2.1.2. Oxidative stress*

The production of reactive oxygen species (ROS) was measured by following the conversion of the non-fluorescent dihydrodichlorofluorescein diacetate ($H_2$DCF-DA) to the highly fluorescent compound 2', 7',-dichlorofluorescein (DCF) as described by (Wang and Joseph, 1999), recently adapted for algal cells by Morelli et al. (2018). For each exposure concentration, 650 µL of each of the three replicates were pooled together, spiked with 20 µL of a 1mM DCF-DA solution and kept under constant shaking at room temperature for 1h in the dark. Fluorescence was determined at 520 nm emission wavelength ($\lambda_{ex}$ = 485 nm) using a Victor 3 1420 multilabel Counter (PerkinElmer) and used for total ROS estimation. Nine measurements for each exposure concentration were obtained. Tested blanks were F/2 and TG201, F/2 + $H_2$DCF-DA and TG201 + $H_2$DCF-DA. Background value (either F/2 + $H_2$DCF-DA or TG201 + $H_2$DCF-DA) was subtracted from the obtained fluorescence value of the samples. Fluorescent data were normalized to the cell density and expressed as fluorescence/cell density.

### *2.2.2. Bacteria*

*Escherichia coli* JM109 (*E. coli*, Gram negative bacteria, biological safety level 1, Leibniz Institute DSMZ, German Collection of Microorganisms and Cell Cultures, Germany) were pre-cultured overnight at 37 °C in 5 mL of Luria-Bertani broth (LB) under shaking at 130 rpm, until reaching an optical density ($OD_{600nm}$) of ≈ 1, corresponding to ≈ $10^9$ bacteria/mL. The bacterial suspension was next diluted to a concentration of ≈ $10^6$ bacteria/mL. Afterwards, the bacterial suspension (50 µL) was inoculated with 50 µL of AgNPcitLcys and AgNP3MPS suspensions at various concentrations into separate wells of a 96-well plate (n = 3 wells/concentration/compound), then incubated at 37 °C for 24 hours. AgNPcitLcys and AgNP3MPS suspensions at final concentrations ranging from 250 to 0.06 µg/mL (2-fold serial

dilution) were used to assess the antibacterial activity. Bacteria inoculated in 50 µL of LB were used as controls of bacterial growth ($^{+}$CTRL, n = 3).

The antibacterial efficacy was evaluated by means of the turbidity method (*i.e.*, $OD_{600nm}$ measurements) (Campbell, 2010; Rossetti et al., 2019). Briefly, after 24 h incubation, bacterial growth inhibition was assessed by optical density ($OD_{600nm}$) measurements using a GENios Plus spectrophotometer (Tecan, Milan, Italy). For each AgNP concentration, the antibacterial efficiency was calculated according to the following equation: antibacterial activity (%) = $(1 - (OD_{600nm,\ eluate}/OD600nm,\ CTRL)) \times 100$.

### 2.3. Statistical Analysis

$EC_{50}$ values were calculated with Graphpad Prism 8 using a non-linear regression analysis, while statistical significance between mean values were calculated with a nonparametric test (Kruskal-Wallis test).

## 3. Results and Discussion

### 3.1. AgNPcitLcys and AgNP3MPS behaviour and Ag ion dissolution

DLS data obtained in milliQ water suspensions coupled with TEM images, show a marked difference in terms of size between AgNPcitLcys and AgNP3MPS (Table 1, Figure 1a, e). Z-average values calculated by intensity showed a similar hydrodynamic diameter (HD) for AgNPcitLcys (159 ± 9 nm, PDI 0.3) and AgNP3MPS (159 ± 69 nm, PDI 0.4); however, those calculated in volume, obtained selecting the most representative peaks from the distribution graphs (Figure S1), showed smaller nominal size for AgNP3MPS (2 ± 1 nm) compared to AgNPcitLcys (12.5 ± 1 nm). Such difference in size was also confirmed by TEM images (Figure 1a, e) which also revealed a slight difference in shapes, with AgNP3MPS appearing as dots while AgNPcitLcys more irregularly rounded. Z-potential values obtained for both suspensions in milliQ water are negative, confirming the chemistry of surface coatings and previous measurements carried out on similar batches of AgNPs (Table 1) (Prosposito et al., 2016; Prosposito et al., 2019).

In bacteria and microalgae exposure media, AgNP behaviour is affected by osmolarity, with an increasing formation of aggregates as salinity goes from 0‰ (TG201) to 20‰ (LB medium) and up to 40‰ (F/2). AgNP3MPS show a faster increasing trend in z-average values compared to AgNPcitLcys already in the microalgae freshwater medium TG201 (231 ± 123 nm) and further higher in bacteria LB medium (697 ± 272 nm) reaching similar values of AgNPcitLcys (656 ± 82 nm). An opposite trend is observed for marine microalgae medium F/2 in which AgNPcitLcys form the biggest aggregates (857 ± 61 nm) and z-potential value close to a net zero charge while AgNP3MPS aggregation seems to decrease. This trend, even if counter intuitive, can be understood by looking at the size distribution graphs of both intensity and volume for AgNP3MPS in F/2 (Figure S1). Since z-average values are calculated by the instruments itself by means of different algorithms, they always represent an approximation, especially in a complex medium such as NSW. As seen from the numerous peaks in the graphs, which were also changing over time together with the high PDI value (0.4-0.6), a settling behaviour of the AgNPs can be hypothesized. TEM also confirmed such behaviour with aggregates of

various size (Figure 1, h). DLS measurements are probably showing the smallest aggregates, while precipitation probably occurred for the bigger ones, which resulted undetected by the instrument. On the contrary, z-average values obtained for AgNPcitLcys seems to better fit with size distribution data showed in graphs where, at least for intensity values, a single peak centred around the mean size value reported by the algorithm is shown.

**Table 1.** Hydrodynamic diameter (Z- average), Polidispersity Index (PDI) and surface charge (Z- potential) of 100 mg/L AgNPcitLcys and AgNP3MPS at 25°C in different media: milliQ water, freshwater algal medium (TG201), bacterial medium (LB) and marine water algal medium (F/2). Z- average values are reported both as intensity and volume. Data are shown as mean ± standard deviation.

| | AgNPcitLcys | | | | AgNP3MPS | | | |
|---|---|---|---|---|---|---|---|---|
| | MilliQ | TG201 | LB | F/2 | MilliQ | TG201 | LB | F/2 |
| Z average intensity | 159 ± 9 | 144 ± 10 | 656 ± 82 | 857 ± 61 | 159 ± 69 | 231 ± 123 | 697 ± 272 | 239 ± 93 |
| Z average volume | 12.5 ± 1 | 116 ± 37 | 671 ± 4 | 2229 ± 1247 | 2 ± 1 | 5 ± 2 | 7 ± 9 | 1925 ± 2485 |
| PDI | 0.3 | 0.3 | 0.1 | 0.3 | 0.4 | 0.6 | 0.4 | 0.6 |
| Z potential (mV) | -42 ± 2 | -25 ± 0.3 | -13 ± 0.3 | -0.4 ± 2 | -33 ± 2.8 | -37 ± 3 | -7.6 ± 0.5 | -6 ± 3 |

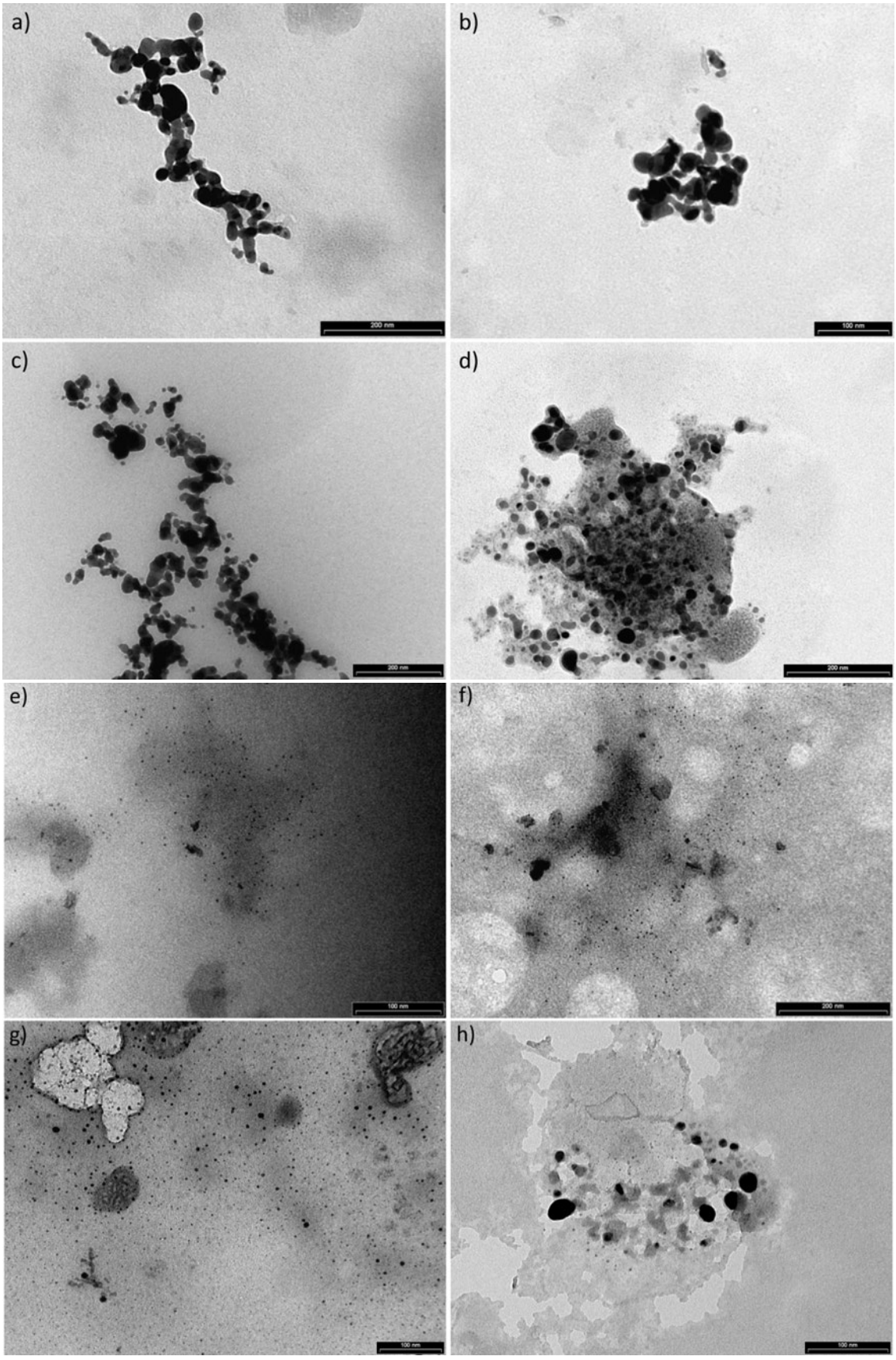


**Figure 1.** TEM images of 10 mg/L AgNPcitLcys (a-d) and 50 mg/L AgNP3MPS (e-h) in milliQ water (a, e), TG201 (b, f), LB medium (c, g) and F/2 (d, h). Scale bar is 100 nm for b, e, g, h and is 200 nm for a, c, d, f.

In agreement with recent findings (Lish et al., 2019), Ag release in algal media after 1 h of incubation showed that higher salinity corresponds to a higher dissolution, as shown in F/2 (40 ‰) compared to TG201 (0 ‰). In F/2 the dissolution was higher for the citLcys coated AgNPs (max 0.83% of nominal AgNP concentration), while in TG201 AgNP3MPS showed the highest dissolution (max 0.03%).

In LB medium, after 1 h of incubation a limited but measurable amount of dissolved Ag is release by both AgNPs, higher for AgNPcitLcys (0.027% of nominal AgNP concentration) than for AgNP3MPS (0.0025% of nominal AgNP concentration). AgNPcitLcys dissolution was confirmed to be highly influenced by salinity, with a dissolved Ag value in LB medium that stands, as salinity (20 ‰), in between the ones measured in TG201 (salinity 0 ‰) and F/2 (salinity 40 ‰). On the contrary, as far as AgNP3MPS, a clear trend with salinity of the medium cannot be seen, with a dissolved Ag value in F/2 lower than in TG201. However, besides media composition and salinity, probably also the difference in concentrations between algal and bacterial media plays a role in the observed differences in AgNPcitLcys and AgNP3MPS dissolution rates.

In algal media, a temporal trend for dissolution is observed, with Ag concentration increasing with incubation time (from 1 to 72 h), except for AgNPcitLcys in TG201 in which dissolution is very low and not changing with time. On the contrary, after 24 h of incubation in LB medium the measured concentrations showed a drastic decrease, reaching values close to zero for both AgNPs. As opposed to algal media, LB medium contains a protein fraction (Table S1), represented by tryptone, a mix of peptides generated by the enzymatic digestion of casein, and yeast extract. As reported by Ramamoorthy & Kushner (1975), some constituents of bacterial growth media can bind metal ions, reducing their potential negative effects on microorganisms.

Such behaviour has not yet being fully addressed since studies investigating AgNP toxicity to bacteria still use protein-rich media for bacterial growth without considering the occurrence of an interference with heavy metal exposure (Sondi and Salopek-Sondi, 2004; Theofilou et al., 2021). In our study filtration was performed prior to Ag analysis (cut-off is 3kDa), therefore part of the proteins and carbohydrates could have been retained in the filter, together with the bonded Ag ions. Moreover, the

formation of an eco-corona around the AgNPs cannot be ruled out since well documented in the literature also for other type of NPs (Lesniak et al., 2012; Hayashi et al., 2013; Monopoli et al., 2013; Grassi et al., 2020).

**Table 2.** Total Ag (µg/L) measured after incubation and filtration of AgNPcitLcys and AgNP3MPS at different time points (1, 24 and 72 h) in different exposure media: LB medium, TG201 and F/2.

| | Medium | 1h | 24h | 72h |
|---|---|---|---|---|
| AgNPcitLcys | TG201 (60 mg/L) | 2.08 ± 0.06 (0.0034%) | -- | 1.33 ± 0.1 (0.0022%) |
| | LB (256 mg/L) | 70.59 ± 1.57 (0.027%) | 1.64 ± 0.05 (0.00064%) | -- |
| | F/2 (60 mg/L) | 239.01 ± 1.83 (0.4%) | -- | 500.75 ± 14.5 (0.83%) |
| AgNP3MPS | TG201 (60 mg/L) | 11.01 ± 0.12 (0.018%) | -- | 18.42 ± 0.62 (0.03%) |
| | LB (256 mg/L) | 6.49 ± 0.14 (0.0025%) | 0.61 ± 0.07 (0.00024%) | -- |
| | F/2 (60 mg/L) | 59.15 ± 0.98 (0.1%) | -- | 95.16 ± 2.87 (0.16%) |
| $AgNO_3$ | TG201 (7 µg/L) | 4.42 ± 0.09 | -- | 4.79 ± 0.18 |
| | LB (7 µg/L) | 0.11 ± 0.01 | 0.07 ± 0.02 | -- |
| | F/2 (7 µg/L) | 4.37 ± 0.08 | -- | 5.32 ± 0.22 |

Therefore, either the binding of dissolved Ag ions, with consequent sequestration and reduction in bioavailability, as well as the corona formation around the AgNPs could be occurring. The partial bonding of the dissolved Ag ions to the peptides and carbohydrates of LB medium, which are then retained in the filter during filtration, could be hypothesized, together with the formation of a corona, which reduces dissolution. The investigation of the role played by medium components seems mandatory to fully understand the importance of dissolution in AgNP toxicity towards bacteria.

3.2. Toxicity

The inhibition of growth upon AgNP exposure strongly differed between freshwater and marine microalgae (Figure 2, a-b). The freshwater *R. subcapitata* shows higher sensitivity to both AgNPcitLcys and AgNP3MPS, starting from lower exposure concentrations (1-5 mg/L), which are still high compared to PECs for surface waters (1-100 µg/L) (Lazareva and Keller, 2014; Cervantes-Avilés et al., 2019). In particular, 3MPS coated AgNPs resulted more toxic than AgNPcitLcys to *R. subcapitata*, with a linear increase in growth rate inhibition up to more than 80% at 60 mg/L, while AgNPcitLcys reached a maximum inhibition value of 38.6%. On the contrary, both AgNPs did not cause any sign of toxicity towards *P. tricornutum* up to the highest concentration tested (60 mg/L).

The different sensitivity to Ag of *P. tricornutum* compared to *R. subcapitata* is also showed towards $AgNO_3$ exposure (Figure 2, c-d). Besides species-specific sensitivity to Ag, such difference could be due to the of chemistry of exposure media on metal speciation and bioavailability. In fact, both the high salinity (40‰) of F/2 and the presence of natural organic matter (NOM) are able to reduce the amount of bioavailable metal ions, for instance by formation of Cl-Ag complexes or Ag bonding by reduced sulphur groups of NOM macromolecules (Lish et al., 2019; Li et al., 2020).

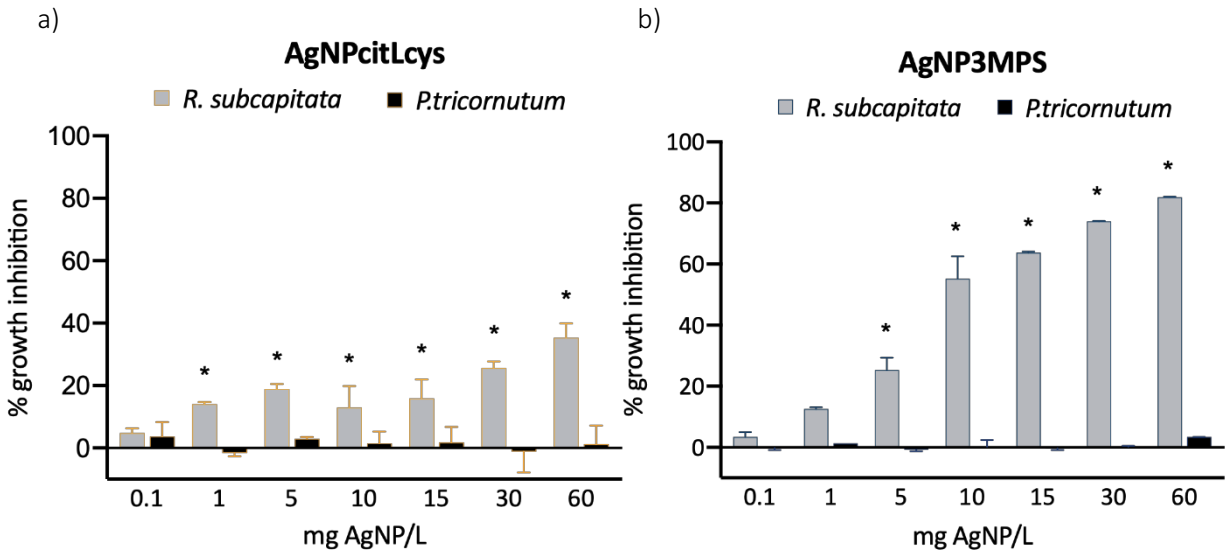

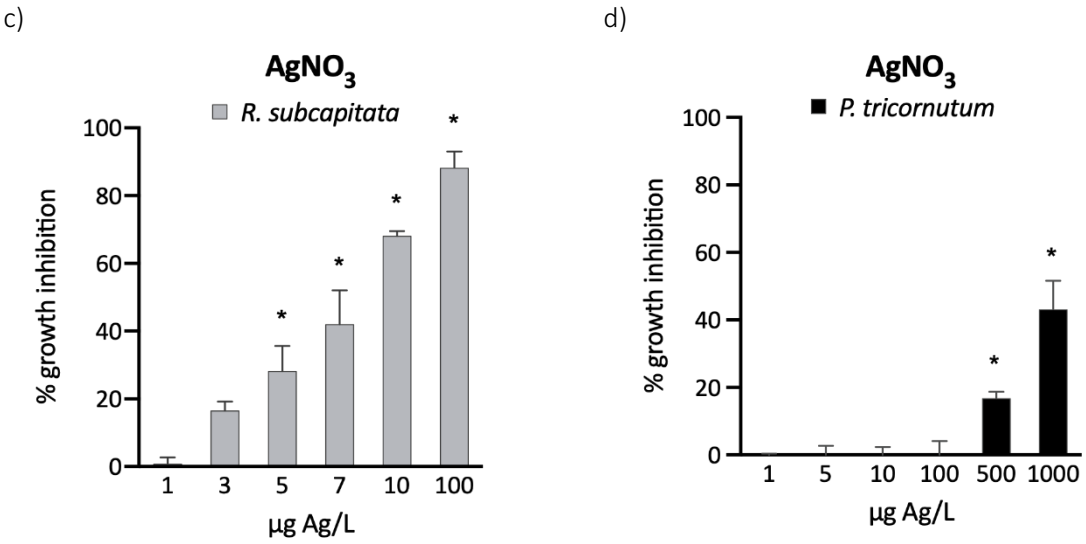


Figure 2. Inhibition of growth rate compared to control of R. *subcapitata* (grey) and *P. tricornutum* (black) exposed to AgNPcitLcys (a), AgNP3MPS (b) and $AgNO_3$ (c, d) for 72h. Data are shown as mean ± standard deviation. Columns marked with * are statistically different from control with $p<0.05$.

However, by comparing AgNP growth inhibition percentages with dissolved Ag values, the effect of AgNP3MPS exposure is predictable based on Ag values: 18.42 µg Ag/L caused an 80% growth inhibition in *R. subcapitata* while no effect is observed in *P. tricornutum* for a 95.16 µg/L of dissolved Ag, as expected based on $AgNO_3$ exposure. AgNPcitLcys instead, caused a 38.6% inhibition of growth at a dissolved Ag value of 1.33 µg/L, while no effect is observed for *P. tricornutum* at a dissolved Ag value of 500 µg/L. Based on $AgNO_3$ exposure, such exposure is enough to inhibit *P. tricornutum* growth. Hence, the effect of AgNPcitLcys exposure is higher than expected based on dissolution values for the freshwater microalga, but lower for the marine microalga.

Such difference suggests a different MoA towards cells, with AgNP3MPS toxicity being more closely linked to the amount of dissolved Ag ions compared to AgNPcitLcys, whose effects seem less predictable and more influenced by other factors. For instance, size distribution graphs for AgNPcitLcys in TG201 and F/2 show that the high salinity of F/2 generates aggregates with an average HD close to 1 µm, while in TG201 the HD is close the nano-size range (1-100 nm). The interaction of cells with smaller aggregates could influence intracellular localization and be more likely linked to cell death compared to exposure to bigger aggregates (Lankoff et al., 2012). Hence, the MoA of AgNPcitLcys

seems more closely related to the nano-size, confirming what already hypothesized and described in chapter 3. This could explain the higher toxicity to *R. subcapitata* than *P. tricornutum* compared to dissolution values.

The observed ROS content (Figure 3) in *R. subcapitata* confirmed what observed for growth, with a gradual increase with increasing AgNP concentrations, except for the highest concentration of AgNP3MPS in which a six-fold increase of ROS content is observed, similarly to $AgNO_3$ exposure. No increasing trend is, instead, observed in *P. tricornutum* upon exposure to either AgNPs or $AgNO_3$.

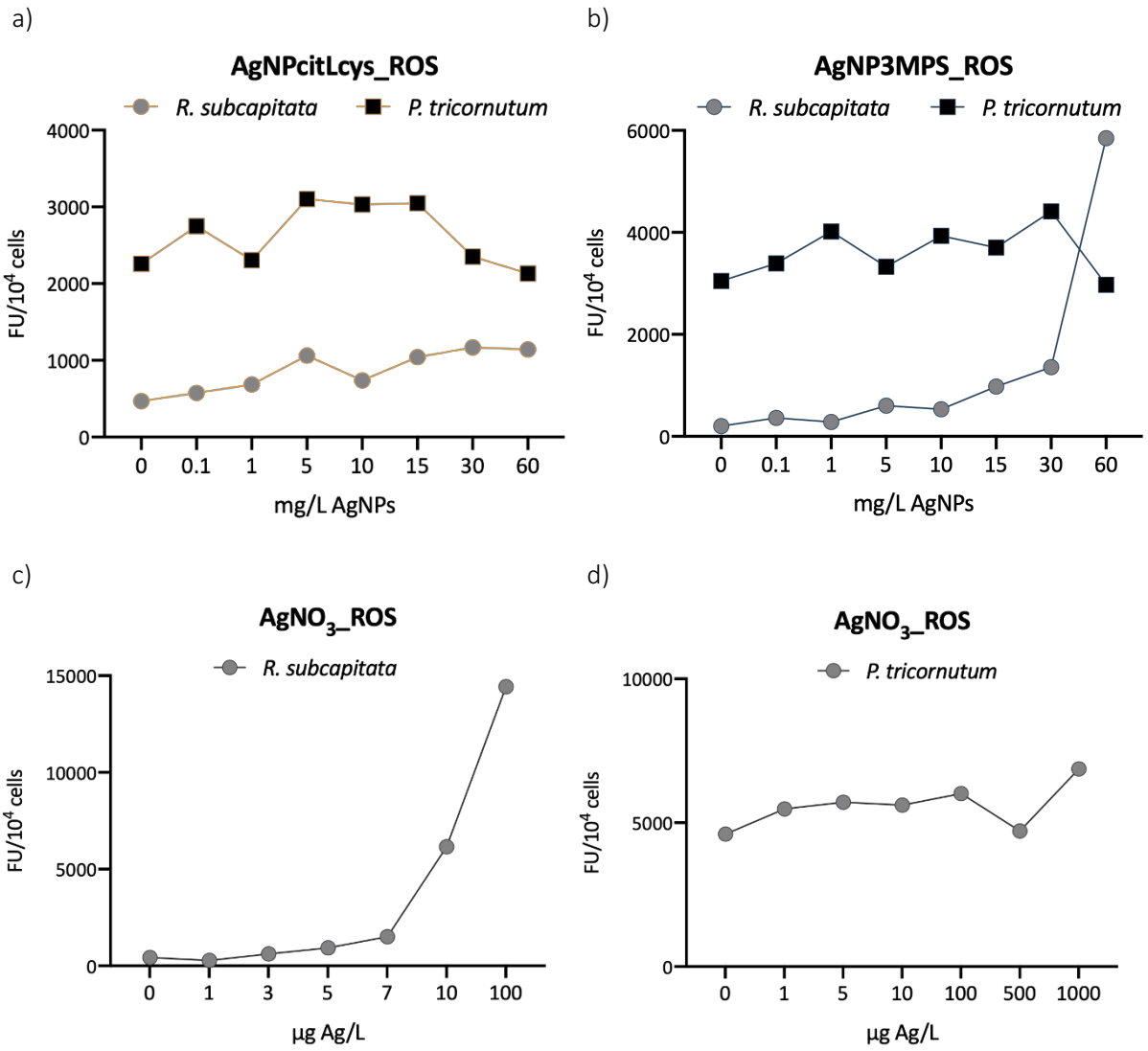


**Figure 3.** Reactive oxygen species (ROS) normalized to cell density and expressed as fluorescence units (FU) every $10^4$ cells, measured in *R. subcapitata* (grey) and *P. tricornutum* (black) exposed to AgNPcitLcys

(a), AgNP3MPS (b) and $AgNO_3$ (c, d) for 72h. Data marked with * show values significantly different from control with $p<0.05$.

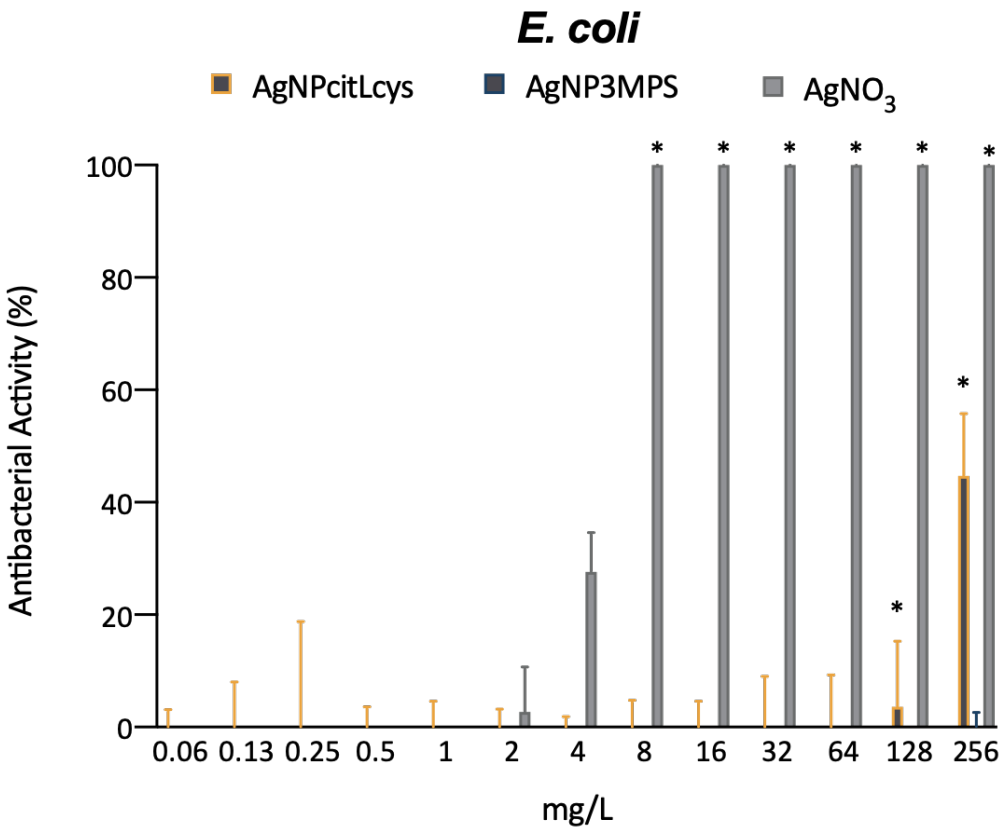


**Figure 4.** Antibacterial activity percentage of *E. coli* exposed to AgNPcitLcys (yellow bordered), AgNP3MPS (blue bordered) and $AgNO_3$ (grey bordered). Data are shown as mean ± standard deviation. Columns marked with * are statistically different from control with $p < 0.05$.

Again, the effect observed upon AgNPcitLcys exposure is higher than expected based on dissolved Ag value (1.64 µg/L), while the lack of effect observed for AgNP3MPS seems to be in line with the amount of measured Ag. As for other aquatic unicellular species, it has not yet been fully understood if Ag ions and AgNPs share the same MoA towards bacteria (Sondi and Salopek-Sondi, 2004; Morones et al., 2005; Li et al., 2017) or differ in the way they exert their antimicrobial activity (Theofilou et al., 2021). According to Theofilou et al. (2021), the high antimicrobial potential of AgNP compared to $AgNO_3$ towards *E. coli* stands in their direct physical interaction with the bacterial outer membrane (OM), which causes disturbances in charge distribution and leads to a loss of integrity of the OM. This is reported even in the case of negatively charged AgNPs which, according to Theofilou et al. (2021), could

be due to the partial oxidation of superficial Ag and the formation of a partial positive charge ($\partial^+$) onto AgNP surface. This direct physical interaction ultimately results in the formation of holes in the bacterial OM (Sondi and Salopek-Sondi, 2004; Theofilou et al., 2021), causing the entrance of AgNP with consequent oxidation and dissolution inside the cytoplasm. It is possible that, at this point, the MoA is the same as that of $AgNO_3$, however, the increased permeability of bacterial membrane caused by AgNPs could enhance their toxicity, even in the case of low Ag dissolution.

By comparing the $EC_{50}$ for $AgNO_3$ between *R. subcapitata*, *P. tricornutum* and *E. coli* (Table 3), *E. coli* results to be the least sensitive to Ag ($EC_{50}$ = 4.43 mg/L), while *R. subcapitata* is the most sensitive ($EC_{50}$ = 6.74 µg/L). The binding of free Ag ions by LB medium constituents could have lowered the amount of bioavailable Ag for *E. coli*, causing $AgNO_3$ to begin exerting an effect only from 2-4 mg/L. Even though dissolved Ag in LB medium for AgNPcitLcys is probably higher than the measured value due to the filtration of protein-bonded Ag, by assuming a dissolution in line with that of saline algal media (<1%), Ag value would still be too low to exert an effect on *E. coli*. Moreover, taking into consideration the role played by chloride ions and LB medium constituents on Ag ions bioavailability, an additional nano-toxicity for AgNPcitLcys exposure can be hypothesized also for *E. coli*.

As already observed for microalgae, also *E. coli* experiences a different toxicity between AgNPcitLCys and AgNP3MPS exposure. The toxicity of AgNPs toward cells is the complex result of multiple mechanisms and, by involving a physical interaction with the cell surface, it can be influenced by size, shape, surface charge and coating of AgNPs (Sukhanova et al., 2018). Among those, AgNPcitLcys and AgNP3MPS mainly differ in coating, therefore the coating themselves, citrate, L-cysteine and 3MPS, were tested for algal toxicity and showed no or negligible effects on *R. subcapitata* and *P. tricornutum* growth (Figures S3). Although, no toxicity test with coating constituents was carried out in *E. coli*, literature studies report that citrate can be used as an alternative source of carbon by *E. coli* and can, thus, be considered harmless (Vaughn et al., 1950). On the other hand, L-cysteine although being an essential amino acid for both prokaryotes and eukaryotes, when free in solution at high concentrations is known to be toxic for many organisms, including bacteria (Shimada et al., 2016). The toxicity of

bonded-L-cysteine to bacteria is not clear, however, since one of the proposed mechanisms of toxicity for free L-cysteine is by interference with membrane enzymes, it is possible that the coating of AgNPcitLcys is playing a role in the observed inhibition of bacterial growth (Kari et al., 1971).

As also confirmed by the literature, often the NP coatings drives the majority of the observed differences in toxicity between AgNPs (Hou et al., 2017), and, similarly, the properties of cell walls and/or membranes (Sukhanova et al., 2018). For instance, Gram-negative bacteria are more susceptible to AgNP toxicity compared to Gram-positive ones (Sutterlin et al. 2012; Godoy-Gallardo et al., 2021). Hence, the peculiar surface properties of each cell type, together with the characteristic of the testing media, could be involved in the different degree of toxicity observed.

The lack of toxic effect of AgNP3MPS in saline media (LB and F/2) could be linked to lower stability of the NP and higher tendency to aggregation, which can reduce the direct contact of single NPs with cells. AgNP3MPS toxicity is, in fact, visible only in the freshwater algal species *R. subcapitata* in which the AgNPs are present as single particles (Figure S1) and are able to interact with cell membrane, as opposed to when dispersed in LB and F/2 media. A higher toxicity is usually associated to smaller NPs (< 5 nm), which are able to enter cells non-specifically and can also penetrate the nucleus membrane (Lankoff et al., 2012; Zhang et al., 2015). However, the microalga *R. subcapitata* is the only one tested in absence of chloride ions, proteins and organic matter, having no defence against free Ag ions. In fact, the effect observed upon AgNP3MPS exposure is also in line with what expected based on dissolution values, for all organisms, which could be the main MoA of AgNP3MPS toxicity.

**Table 3.** $EC_{50}$ values calculated for *R. subcapitata*, *P. tricornutum* and *E. coli* exposed to AgNPcitLcys, AgNP3MPS and $AgNO_3$.

| $EC_{50}$ | *R. subcapitata* | *P. tricornutum* | *E. coli* |
|---|---|---|---|
| AgNPcitLcys | > 60 mg/L | > 60 mg/L | > 256 mg/L |
| AgNP3MPS | 7.57 mg/L (CI 95% 6.5-8.61) | > 60 mg/L | > 256 mg/L |
| $AgNO_3$ | 6.74 µg/L (CI 95% 6.18-7.36) | > 1 mg/L | 4.43 mg/L |

On the contrary, it is possible that both *R. subcapitata* and *E. coli* share the same mechanism of toxicity of AgNPcitLcys, as both seem to experience an additive toxicity besides the one coming from ion dissolution. Faiz and at al. (2018) underline that the particulate Ag remaining after AgNP dissolution is not inert and is able to induce lethal intracellular levels of ROS in bacteria, as opposed to $AgNO_3$ which only caused sub-lethal cytotoxicity. Surface interaction is one of the most credited ways to explain the addictive toxicity of AgNPs towards bacteria (Sondi and Salopek-Sondi, 2004; Theofilou et al., 2021), and was also often hypothesized to constitute the basis of NPs toxicity towards numerous other organisms (Bergami et al., 2016; Bergami et al., 2017; Bellingeri et al., 2020). Gram-negative bacteria like *E. coli* have a complex cell wall composed of two concentric membranes, inner (IM) and outer membrane (OM), with a layer of peptidoglycans in between. The OM, which interacts with the external environment, is composed of glycolipids, mainly lipopolysaccharides, with various types of proteins associated (Silhavy et al., 2010). Microalgal cell wall, on the contrary, is composed of cellulose and glycoproteins in the case of the green algae (*Chlorophyceae*) as *R. subcapitata* (Domozych et al., 2012) and of silica and polysaccharides in the case of the diatom *P. tricornutum* (Le Costaouëc et al. 2017). However, if the precise composition of bacterial cell wall is well-known and studied, it is not the same for microalgae, especially in *R. subcapitata*, for which no information on its composition is available. Among the three, the more diverse seems to be the silicified one of *P. tricornutum* which could act as a protective shell, hindering the surface interaction of *P. tricornutum* cells with AgNPcitLcys. This could explain, together with the higher AgNP aggregation, the lower toxicity recorded for *P. tricornutum* upon AgNPcitLcys exposure compared to dissolution value. Lacking a silicified cell-wall, *E. coli* and *R. subcapitata* could, instead, be sharing a similar mode of interaction with AgNPcitLcys, which could explain the occurrence of a nano-related additive effect on the observed toxicity of AgNPcitLcys towards them.

## 4. Conclusions

Our study aimed at comparing the toxicity of two differently coated types of AgNPs to unicellular organisms, as bacteria and freshwater and marine microalgae as target and non-target organisms of AgNPs. AgNPcitLcys and AgNP3MPS toxicity was low to both microalgae and bacteria. However, the different coating appeared to influence AgNP MoA: AgNP3MPS toxicity seemed to be driven by dissolution, being always predictable based on dissolved Ag values, while AgNPcitLcys showed a higher toxicity than expected based on dissolution values for *R. subcapitata* and *E. coli*, and a lower toxicity for *P. tricornutum*. A nano-related toxicity was, hence, hypothesized for AgNPcitLcys, attributed to the interaction of organisms with less (*R. subcapitata* and *E. coli*) or more (*P. tricornutum*) aggregated AgNPs, in turn influenced by the salinity of the media and by surface characteristics of both organisms and AgNPs.

## 5. Acknowledgments

For their contribution to this work, I thank Prof. Gabriele Candiani and Dr. Nina Bono from the Department of Chemistry, Materials and Chemical Engineering “Giulio Natta” of the Politecnico di Milano which contributed to the experimental design and conducted toxicity tests with *E. coli*. I thank Prof. Andrea M. Atrei from the Department of Biotechnology, Chemistry and Pharmaceutical of the University of Siena and Dr. Marianna Uva and Dr. Eugenio Macchia from CREA s.c.a.r.l. for DLS use. I should also thank Prof. Giuseppe Protano from the Department of Physics, Earth and Environmental Sciences of the University of Siena for heavy metal analysis and Claudia Faleri from the Department of Life Sciences of the University of Siena for TEM imaging.

SUPPORTING INFORMATION

**Table S1.** Final composition of exposure media: TG201, F/2 and LB medium. OECD TG201 medium is prepared by addition of salts to milliQ water following OECD201 protocol, modified in $Na_2EDTA\ 2H_2O$ content: final concentration is 0.05 mg/L instead of 0.1 mg/L. TG201 is prepared. F/2 medium is prepared by addition of salts to natural seawater following ISO 10253 (2006) protocol and modified in $Na_2EDTA\ 2H_2O$ content: final concentration is 0.8 mg/L instead of 4 mg/L.

| TG201 | LB medium | F/2 |
|---|---|---|
| 50 mg/L $NaHCO_3$ | 10 g/L Tryptone | 75 mg/L $NaNO_3$ |
| 15 mg/L $NH_4Cl$ | 10 g/L NaCl | 5 mg/L $NaH_2PO_4\ H_2O$ |
| 12 mg/L $MgCl_2\ 6(H_2O)$ | 5 g/L Yeast extract | 30 mg/L $Na_2SiO_3 9H_2O$ |
| 18 mg/L $CaCl_2\ 2(H_2O)$ | pH = 7.15 | 0.63 mg/L $FeCl_3\ 6H_2O$ |
| 15 mg/L $MgSO_4\ 7(H_2O)$ | Salinity = 20 ‰ | 0.8 mg/L $Na_2EDTA\ 2H_2O$ |
| 1.6 mg/L $KH_2PO_4$ | | 0.00196 mg/L $CuSO_4\ 5H_2O$ |
| 0.064 mg/L $FeCl_3\ 6(H_2O)$ | | 0.00126 mg/L $Na_2MoO_4\ 2H_2O$ |
| 0.05 mg/L $Na_2EDTA\ 2(H_2O)$ | | 0.0044 mg/L $ZnSO_4\ 7H_2O$ |
| 0.185 mg/L $H_3BO_3$ | | 0.002 mg/L $CoCl_2\ 6H_2O$ |
| 0.415 mg/L $MnCl_2\ 4(H_2O)$ | | 0.036 mg/L $MnCl_2\ 4H_2O$ |
| 0.003 mg/L $ZnCl_2$ | | 0.1 mg/L Thiamine HCl (Vit. B1) |
| 0.0015 mg/L $CoCl_2\ 6(H_2O)$ | | 0.0005 mg/L Biotin (vit. H) |
| 0.007 mg/L $Na_2MoO_4\ 2(H_2O)$ | | 0.0005 mg/L Cyanocobalamin (vit. B12) |
| 0.00001 mg/L $CuCl_2\ 2(H_2O)$ | | PH = 7.7-8 |
| PH= 7.7-8 | | Salinity = 40 ‰ |
| Salinity = 0 ‰ | | Dissolved oxygen = 7.8-8mg/L |
| Dissolved oxygen= 8.5-9 mg/L | | Conductivity = 55-60 ms/cm |
| Conductivity= 0.2-0.3 ms/cm | | |

**Table S2.** Ag concentrations expressed as µg/L measured in TG201, F/2 and LB medium, with and without 7 µg/L of $AgNO_3$.

| parameters | medium | 0 h | 24 h | 48 h | 72 h |
|---|---|---|---|---|---|
| pH = 7.7-8<br>Salinity = 0 ‰ | TG201 | 0.36 ± 0.06 | -- | -- | 0.26 ± 0.08 |
| | TG201 + $AgNO_3$ | 4.42 ± 0.09 | -- | -- | 4.79 ± 0.18 |
| pH = 7.7-8<br>Salinity = 40 ‰ | F/2 | 0.27 ± 0.01 | -- | -- | 0.26 ± 0.02 |
| | F/2 + $AgNO_3$ | 4.37 ± 0.08 | -- | -- | 5.32 ± 0.22 |
| pH = 7.15<br>Salinity = 20 ‰ | LB | 0.16 ± 0.02 | -- | -- | -- |
| | LB + $AgNO_3$ | 0.11 ± 0.01 | 0.07 ± 0.02 | -- | -- |

**Figure S1.** Comparison of DLS size distribution graphs of AgNPcitLcys and AgNP3MPS by intensity and by volume in milliQ water, TG201 and F/2.

- **AgNPcitLCys in milliQ water:**

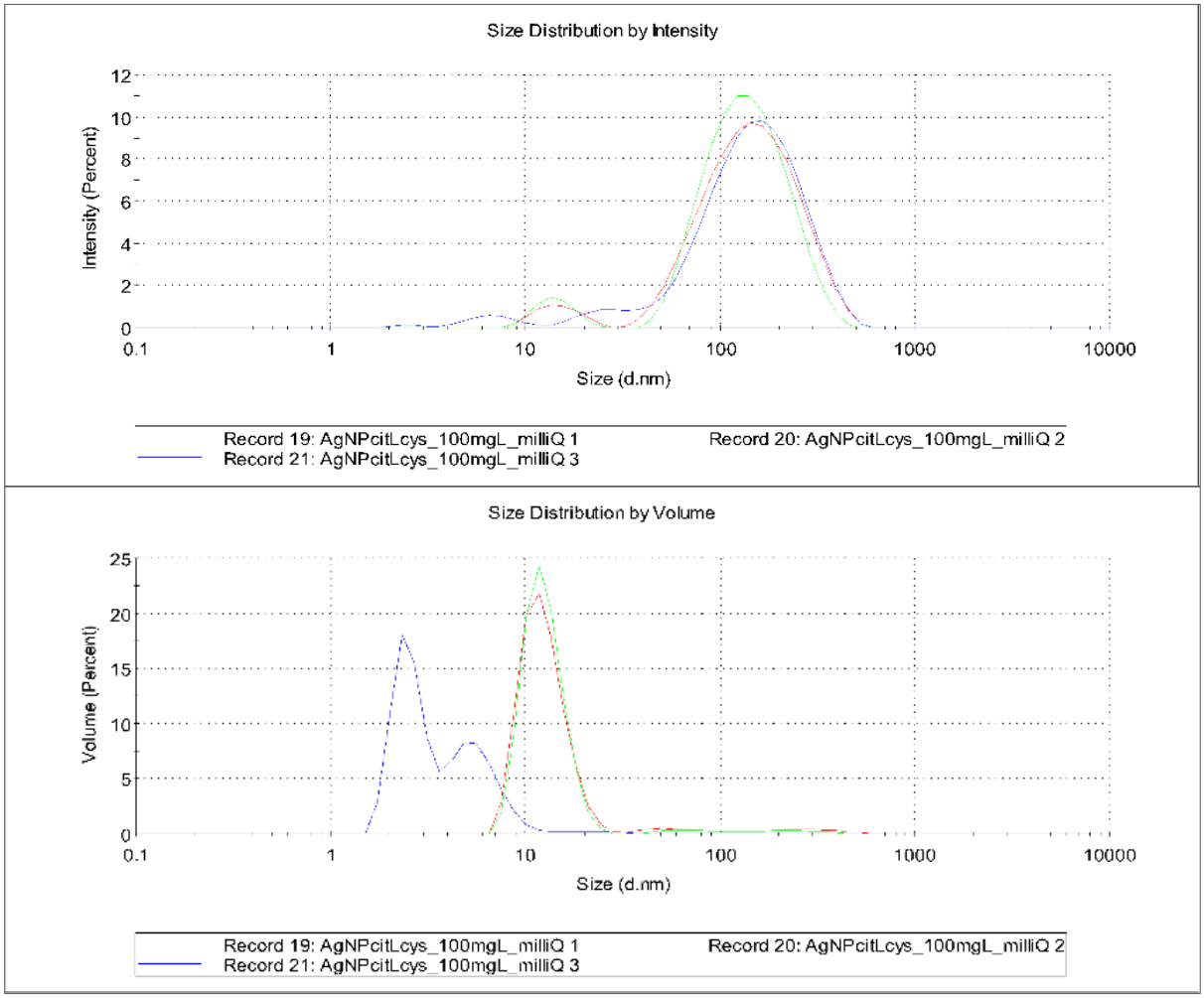

- AgNPcitLcys in TG201 medium:

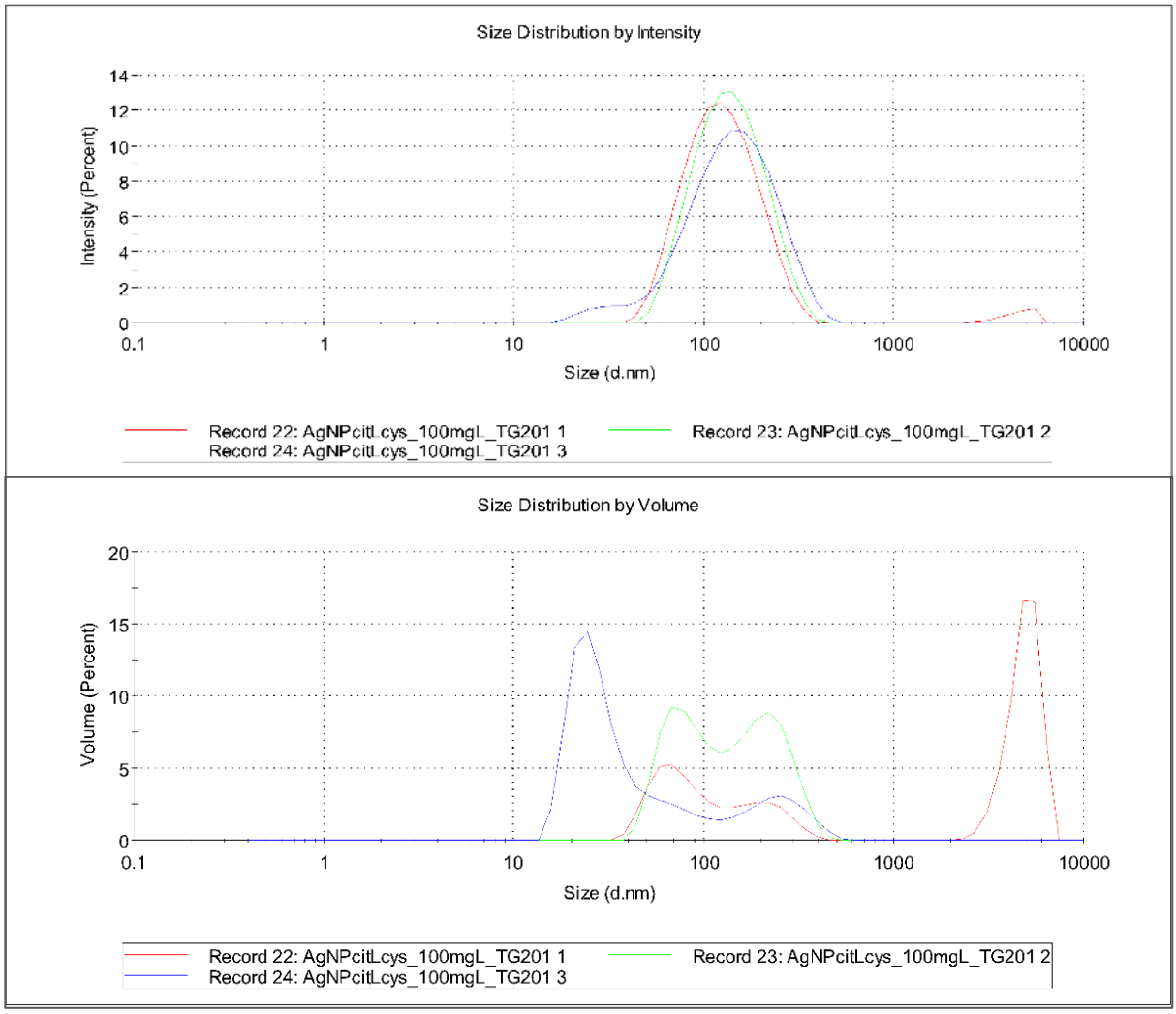


- AgNPcitLcys in LB medium:

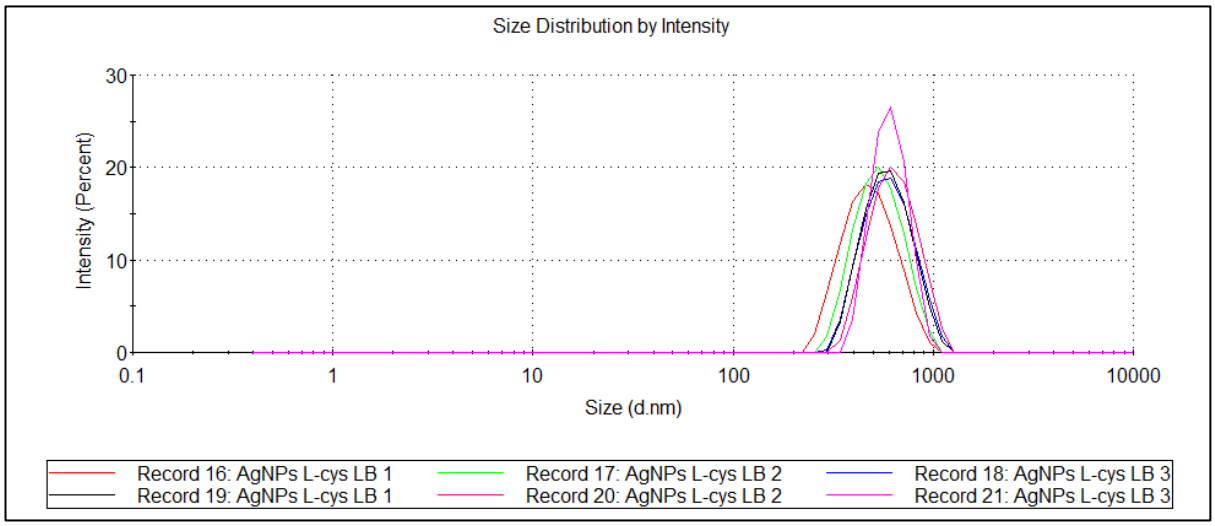

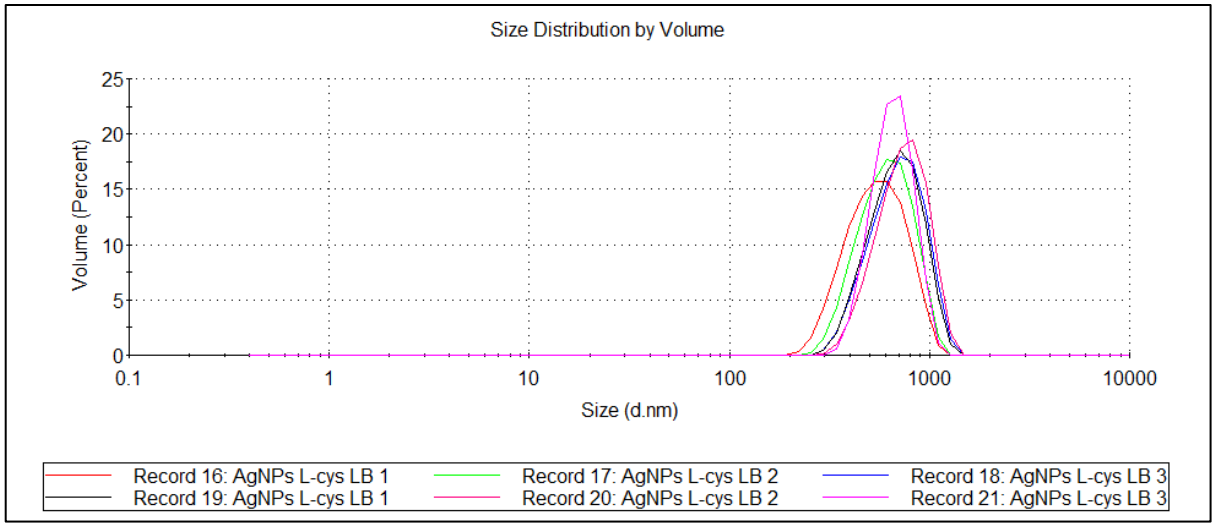


- AgNPcitLcys in F/2 medium:

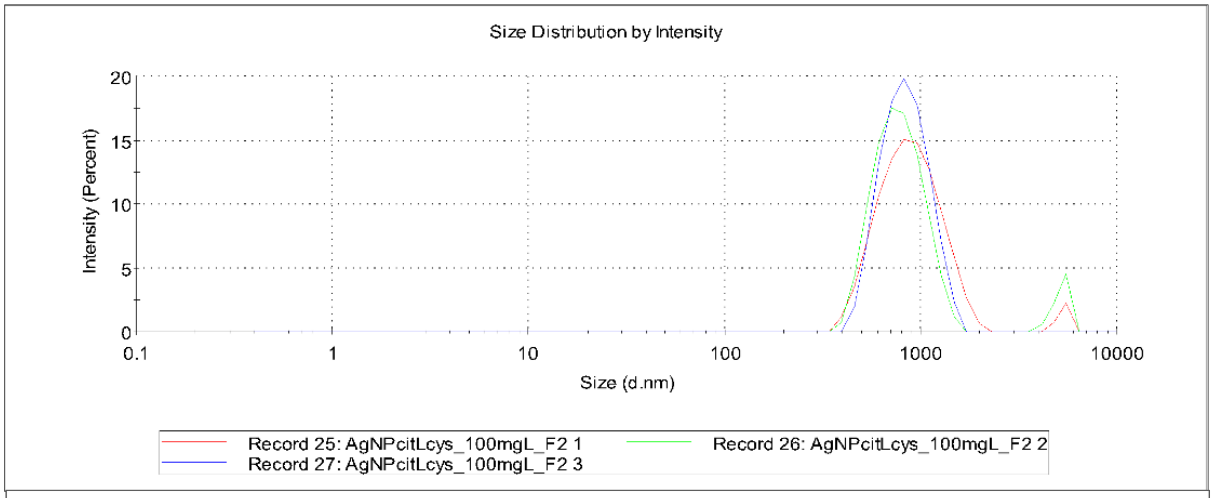


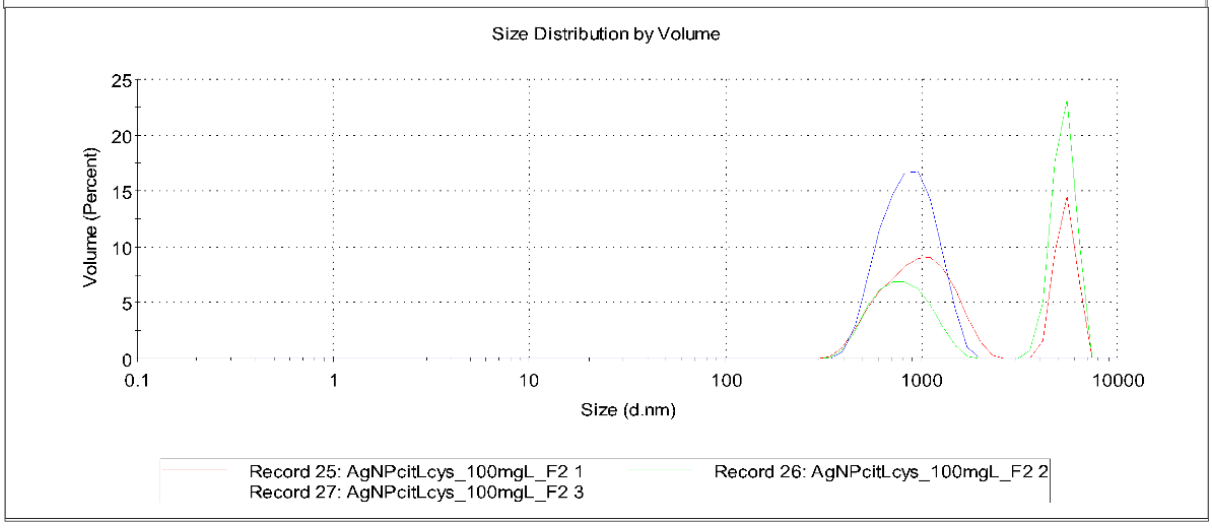

- AgNP3MPs in milliQ water:

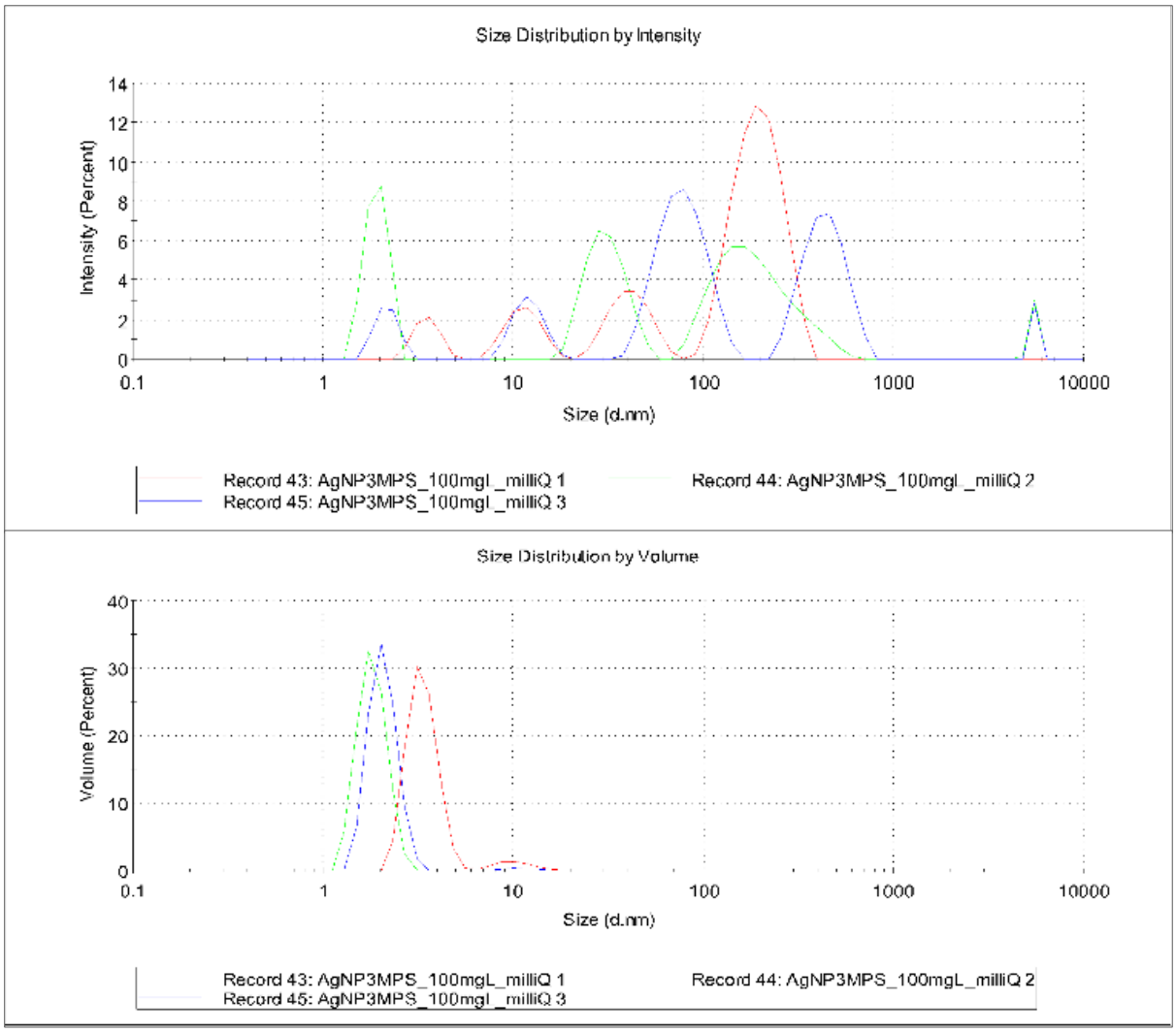


- AgNP3MPS in TG201 medium:

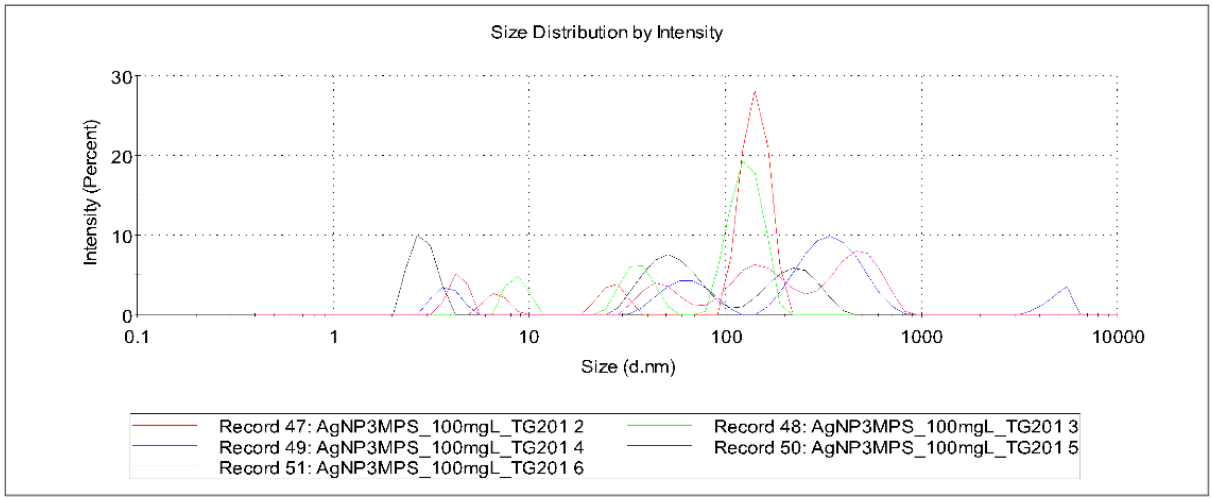

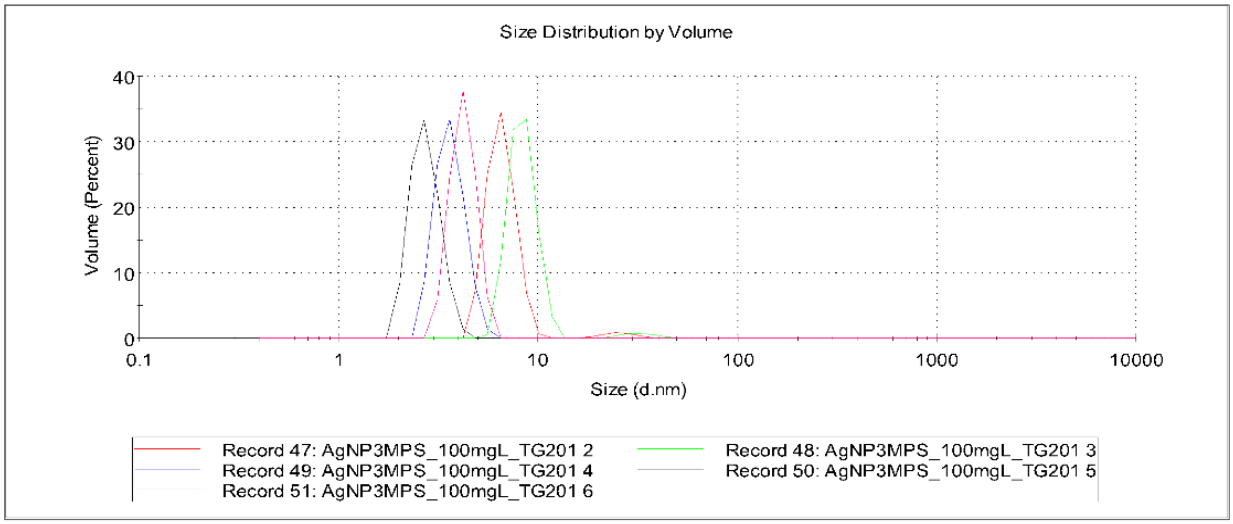


- AgNP3MPS in LB medium:

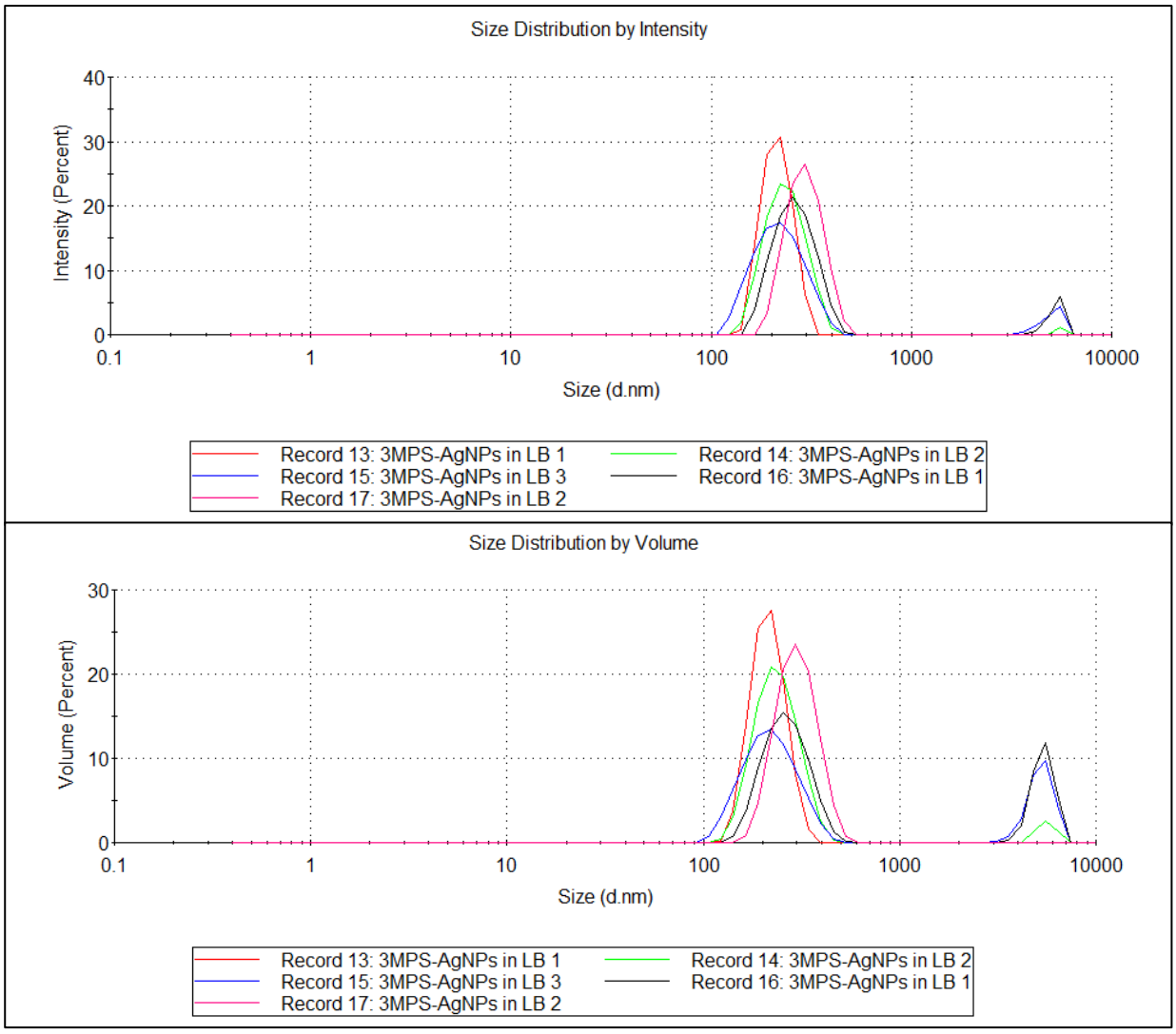

- AgNP3MPS in F/2 medium:

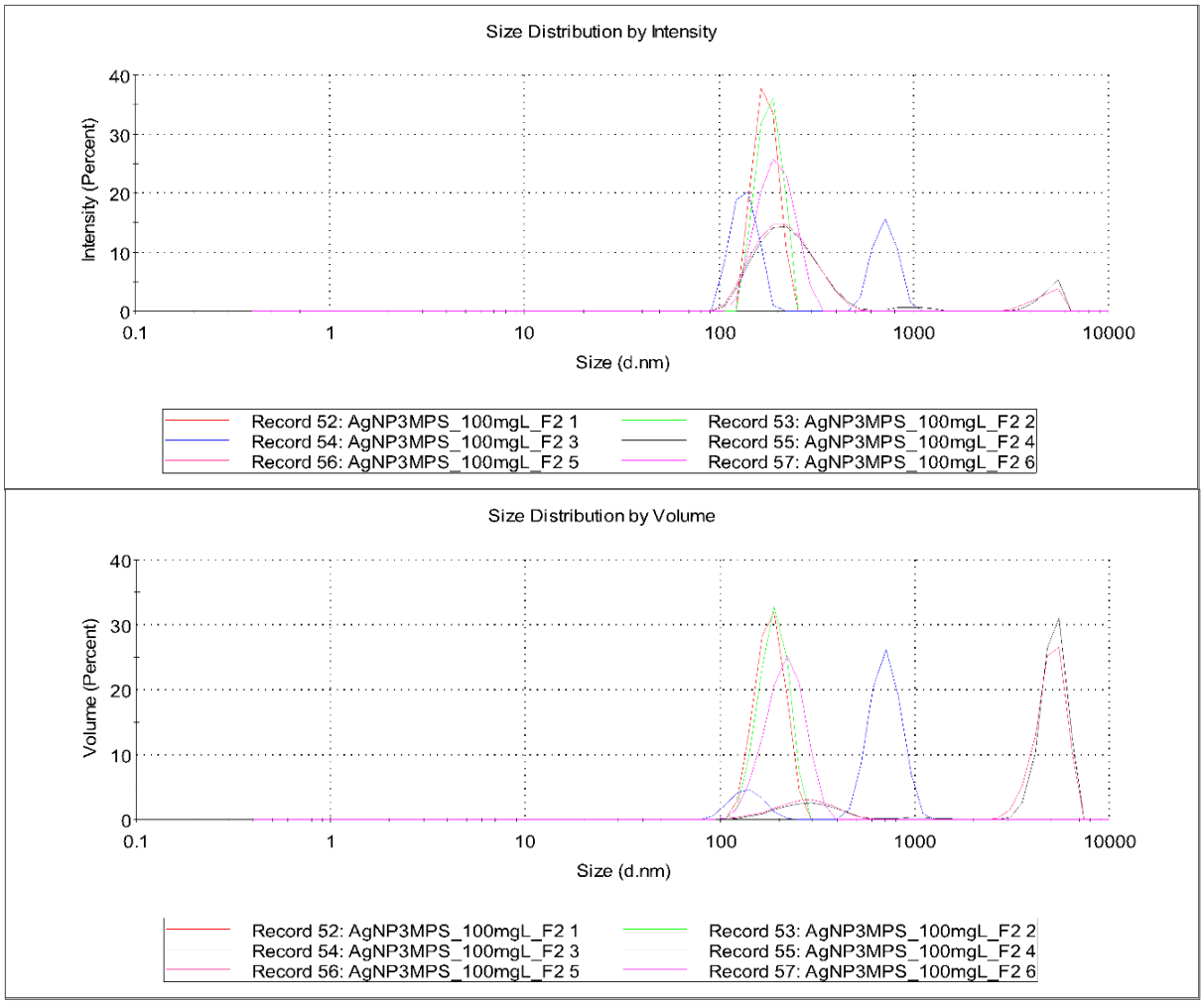

a)

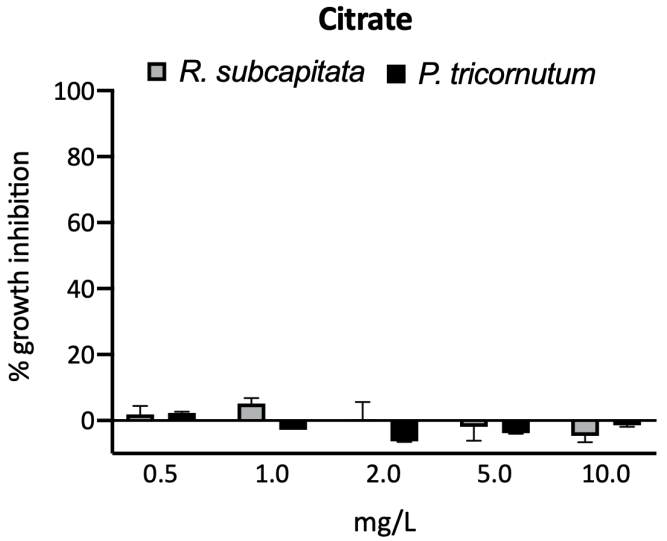


b)

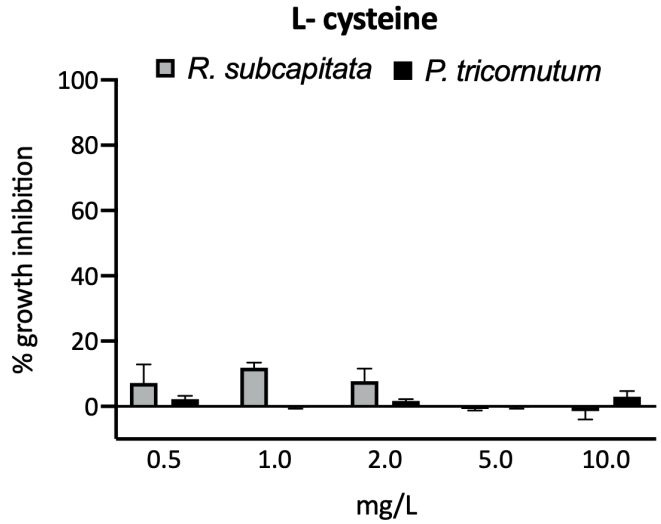


c)

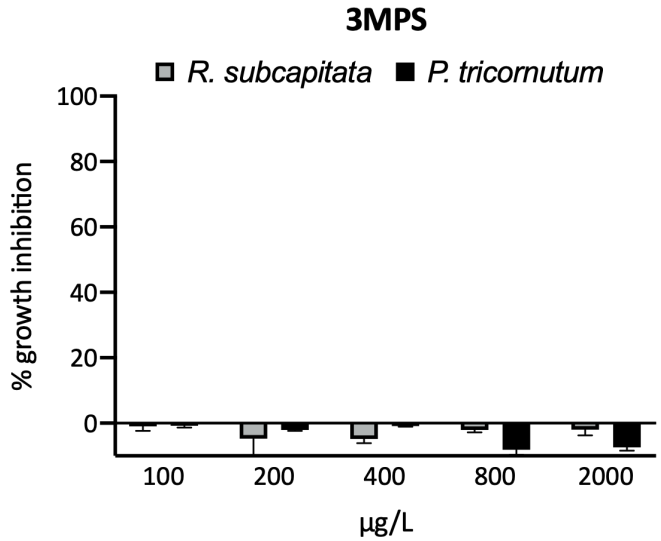


Figure S3. Percentage of growth rate inhibition compared to control of *R. subcapitata* and *P. tricornutum* exposed to a) citrate, b) L- cysteine at 0.5, 1, 2, 5, 10 mg/L and c) 3MPS at 100, 200, 400, 800, 2000 µg/L. Data shown as mean ± standard deviation.

REFERENCES


Baker C, Pradhan A, Pakstis L, Pochan DJ, Shah SI (2005): Synthesis and antibacterial properties of silver nanoparticles. Journal of Nanoscience and Nanotechnology 5, 244-249

Beddow J, Stolpe B, Cole PA, Lead JR, Sapp M, Lyons BP, Colbeck I, Whitby C (2017): Nanosilver inhibits nitrification and reduces ammonia-oxidising bacterial but not archaeal amoA gene abundance in estuarine sediments. Environmental Microbiology 19, 500-510

Bellingeri A, Casabianca S, Capellacci S, Faleri C, Paccagnini E, Lupetti P, Koelmans AA, Penna A, Corsi I (2020): Impact of polystyrene nanoparticles on marine diatom *Skeletonema marinoi* chain assemblages and consequences on their ecological role in marine ecosystems. Environmental Pollution 262, 114268

Bergami E, Bocci E, Vannuccini ML, Monopoli M, Salvati A, Dawson KA, Corsi I (2016): Nano-sized polystyrene affects feeding, behavior and physiology of brine shrimp *Artemia franciscana* larvae. Ecotoxicology and Environmental Safety 123, 18-25

Bergami E, Pugnalini S, Vannuccini M, Manfra L, Faleri C, Savorelli F, Dawson K, Corsi I (2017): Long-term toxicity of surface-charged polystyrene nanoplastics to marine planktonic species *Dunaliella tertiolecta* and *Artemia franciscana*. Aquatic Toxicology 189, 159-169

Bindhu M, Umadevi M (2015): Antibacterial and catalytic activities of green synthesized silver nanoparticles. Spectrochimica acta part A: Molecular and Biomolecular Spectroscopy 135, 373-378

Campbell J (2010): High-throughput assessment of bacterial growth inhibition by optical density measurements. Current Protocols in Chemical Biology 2, 195-208

Cervantes-Avilés P, Huang Y, Keller AA (2019): Multi-technique approach to study the stability of silver nanoparticles at predicted environmental concentrations in wastewater. Water Research 166, 115072

Domozych D, Ciancia M, Fangel JU, Mikkelsen MD, Ulvskov P, Willats WG (2012): The cell walls of green algae: a journey through evolution and diversity. Frontiers in Plant Science 3, 82

Faiz MB, Amal R, Marquis CP, Harry EJ, Sotiriou GA, Rice SA, Gunawan C (2018): Nanosilver and the microbiological activity of the particulate solids versus the leached soluble silver. Nanotoxicology 12, 263-273

Godoy-Gallardo M, Eckhard U, Delgado LM, de Roo Puente YJ, Hoyos-Nogués M, Gil FJ, Perez RA (2021): Antibacterial approaches in tissue engineering using metal ions and nanoparticles: From mechanisms to applications. Bioactive Materials 6, 4470-4490

Grassi G, Gabellieri E, Cioni P, Paccagnini E, Faleri C, Lupetti P, Corsi I, Morelli E (2020): Interplay between extracellular polymeric substances (EPS) from a marine diatom and model nanoplastic through eco-corona formation. Science of The Total Environment 725, 138457

Hayashi Y, Miclaus T, Scavenius C, Kwiatkowska K, Sobota A, Engelmann P, Scott-Fordsmand JJ, Enghild JJ, Sutherland DS (2013): Species differences take shape at nanoparticles: protein corona made of the native repertoire assists cellular interaction. Environmental Science & Technology 47, 14367-14375

Hou J, Zhou Y, Wang C, Li S, Wang X (2017): Toxic effects and molecular mechanism of different types of silver nanoparticles to the aquatic crustacean *Daphnia magna*. Environmental Science & Technology 51, 12868-12878

ISO/10253 (2006): Water quality — Marine algal growth inhibition test with *Skeletonema costatum* and *Phaeodactylum tricornutum* https://www.iso.org/standard/34811.html

Kalantzi I, Mylona K, Toncelli C, Bucheli TD, Knauer K, Pergantis SA, Pitta P, Tsiola A, Tsapakis M (2019): Ecotoxicity of silver nanoparticles on plankton organisms: a review. Journal of Nanoparticle Research 21, 65

Kari C, Nagy Z, Kovacs P, Hernadi F (1971): Mechanism of the growth inhibitory effect of cysteine on *Escherichia coli*. Microbiology 68, 349-356

Kleiven M, Macken A, Oughton DH (2019): Growth inhibition in *Raphidocelis subcapitata*– Evidence of nanospecific toxicity of silver nanoparticles. Chemosphere 221, 785-792

Kędziora A, Speruda M, Krzyżewska E, Rybka J, Łukowiak A, Bugla-Płoskońska G (2018): Similarities and differences between silver ions and silver in nanoforms as antibacterial agents. International Journal of Molecular Sciences 19, 444

Lankoff A, Sandberg WJ, Wegierek-Ciuk A, Lisowska H, Refsnes M, Sartowska B, Schwarze PE, Meczynska-Wielgosz S, Wojewodzka M, Kruszewski M (2012): The effect of agglomeration state of silver and titanium dioxide nanoparticles on cellular response of HepG2, A549 and THP-1 cells. Toxicology Letters 208, 197-213

Lazareva A, Keller AA (2014): Estimating potential life cycle releases of engineered nanomaterials from wastewater treatment plants. ACS Sustainable Chemistry & Engineering 2, 1656-1665

Le Costaouëc T, Unamunzaga C, Mantecon L, Helbert W (2017): New structural insights into the cell-wall polysaccharide of the diatom *Phaeodactylum tricornutum*. Algal Research 26, 172-179

Leal PP, Hurd CL, Sander SG, Armstrong E, Roleda MY (2016): Copper ecotoxicology of marine algae: a methodological appraisal. Chemistry and Ecology 32, 786-800

Lesniak A, Fenaroli F, Monopoli MP, Åberg C, Dawson KA, Salvati A (2012): Effects of the presence or absence of a protein corona on silica nanoparticle uptake and impact on cells. ACS nano 6, 5845-5857

Li L, Stoiber M, Wimmer A, Xu Z, Lindenblatt C, Helmreich B, Schuster M (2016): To what extent can full-scale wastewater treatment plant effluent influence the occurrence of silver-based nanoparticles in surface waters? Environmental Science & Technology 50, 6327-6333

Li P, Su M, Wang X, Zou X, Sun X, Shi J, Zhang H (2020): Environmental fate and behavior of silver nanoparticles in natural estuarine systems. Journal of Environmental Sciences 88, 248-259

Li W-R, Sun T-L, Zhou S-L, Ma Y-K, Shi Q-S, Xie X-B, Huang X-M (2017): A comparative analysis of antibacterial activity, dynamics, and effects of silver ions and silver nanoparticles against four bacterial strains. International Biodeterioration & Biodegradation 123, 304-310

Lish RAD, Johari SA, Sarkheil M, Yu IJ (2019): On how environmental and experimental conditions affect the results of aquatic nanotoxicology on brine shrimp (*Artemia salina*): A case of silver nanoparticles toxicity. Environmental Pollution 255, 113358

Ma Y, Metch JW, Yang Y, Pruden A, Zhang T (2016): Shift in antibiotic resistance gene profiles associated with nanosilver during wastewater treatment. FEMS Microbiology Ecology 92, 3

Malysheva A, Voelcker N, Holm PE, Lombi E (2016): Unraveling the complex behavior of AgNPs driving NP-cell interactions and toxicity to algal cells. Environmental Science & Technology 50, 12455-12463

Monopoli MP, Pitek AS, Lynch I, Dawson KA (2013): Formation and characterization of the nanoparticle–protein corona. In: Bergese P, Hamad-Schifferli K (eds) Nanomaterial

Interfaces in Biology. Methods in Molecular Biology (Methods and Protocols) 1025, 137-155

Morelli E, Gabellieri E, Bonomini A, Tognotti D, Grassi G, Corsi I (2018): TiO 2 nanoparticles in seawater: Aggregation and interactions with the green alga *Dunaliella tertiolecta*. Ecotoxicology and Environmental Safety 148, 184-193

Morones JR, Elechiguerra JL, Camacho A, Holt K, Kouri JB, Ramírez JT, Yacaman MJ (2005): The bactericidal effect of silver nanoparticles. Nanotechnology 16, 2346

OECD, 201 (2011) Test No. 201: Freshwater Alga and Cyanobacteria, Growth Inhibition Test , OECD Guidelines for the Testing of Chemicals, Section 2, OECD Publishing, Paris, https://doi.org/10.1787/9789264069923-en

Prosposito P, Mochi F, Ciotta E, Casalboni M, De Matteis F, Venditti I, Fontana L, Testa G, Fratoddi I (2016): Hydrophilic silver nanoparticles with tunable optical properties: Application for the detection of heavy metals in water. Beilstein Journal of Nanotechnology 7, 1654-1661

Prosposito P, Burratti L, Bellingeri A, Protano G, Faleri C, Corsi I, Battocchio C, Iucci G, Tortora L, Secchi V (2019): Bifunctionalized Silver Nanoparticles as Hg2+ Plasmonic Sensor in Water: Synthesis, Characterizations, and Ecosafety. Nanomaterials 9, 1353

Ramamoorthy S, Kushner D (1975): Binding of mercuric and other heavy metal ions by microbial growth media. Microbial Ecology 2, 162-176

Resgalla Jr C, Poleza F, Souza R, Máximo M, Radetski C (2012): Evaluation of effectiveness of EDTA and sodium thiosulfate in removing metal toxicity toward sea urchin embryo-larval applying the TIE. Chemosphere 89, 102-107

Rossetti A, Bono N, Candiani G, Meneghetti F, Roda G, Sacchetti A (2019): Synthesis and Antimicrobial Evaluation of Novel Chiral 2-Amino-4, 5, 6, 7-tetrahydrothieno [2, 3-c] pyridine Derivatives. Chemistry & Biodiversity 16, e1900097

Schiavo S, Duroudier N, Bilbao E, Mikolaczyk M, Schäfer J, Cajaraville M, Manzo S (2017): Effects of PVP/PEI coated and uncoated silver NPs and PVP/PEI coating agent on three species of marine microalgae. Science of the Total Environment 577, 45-53

Shimada T, Tanaka K, Ishihama A (2016): Transcription factor DecR (YbaO) controls detoxification of L-cysteine in *Escherichia coli*. Microbiology 162, 1698-1707

Siddiqui M, Mondal A, Sultan I, Ali A, Haq Q (2019): Co-occurrence of ESBLs and silver resistance determinants among bacterial isolates inhabiting polluted stretch of river Yamuna, India. International Journal of Environmental Science and Technology 16, 5611-5622

Sikder M, Lead JR, Chandler GT, Baalousha M (2018): A rapid approach for measuring silver nanoparticle concentration and dissolution in seawater by UV–Vis. Science of the Total Environment 618, 597-607

Silhavy TJ, Kahne D, Walker S (2010): The bacterial cell envelope. Cold Spring Harbor Perspectives in Biology 2, a000414

Sondi I, Salopek-Sondi B (2004): Silver nanoparticles as antimicrobial agent: a case study on *E. coli* as a model for Gram-negative bacteria. Journal of Colloid and Interface Science 275, 177-182

Sukhanova A, Bozrova S, Sokolov P, Berestovoy M, Karaulov A, Nabiev I (2018): Dependence of nanoparticle toxicity on their physical and chemical properties. Nanoscale Research letters 13, 1-21

Sütterlin S, Tano E, Bergsten A, Tallberg AB, Melhus Å (2012): Effects of silver-based wound dressings on the bacterial flora in chronic leg ulcers and its susceptibility in vitro to silver. Acta Dermato-Venereologica 92, 34-39

Theofilou SP, Antoniou C, Potamiti L, Hadjisavvas A, Panayiotidis M, Savva PG, Costa C, Fotopoulos V (2021): Immobilized Ag-nanoparticles (iNPs) for environmental applications: Elucidation of immobilized silver-induced inhibition mechanism of *Escherichia coli*. Journal of Environmental Chemical Engineering 9, 106001

Vaughn RH, Osborne JT, Wedding GT, Tabachnick J, Beisel CG, Braxton T (1950): The utilization of citrate by *Escherichia coli*. Journal of Bacteriology 60, 119-127

Wang H, Joseph JA (1999): Quantifying cellular oxidative stress by dichlorofluorescein assay using microplate reader. Free Radical Biology and Medicine 27, 612-616

Wu F, Harper BJ, Harper SL (2017): Differential dissolution and toxicity of surface functionalized silver nanoparticles in small-scale microcosms: impacts of community complexity. Environmental Science: Nano 4, 359-372

Zhang J, Shen L, Xiang Q, Ling J, Zhou C, Hu J, Chen L (2020): Proteomics reveals surface electrical property-dependent toxic mechanisms of silver nanoparticles in *Chlorella vulgaris*. Environmental Pollution, 114743

Zhang S, Gao H, Bao G (2015): Physical principles of nanoparticle cellular endocytosis. ACS nano 9, 8655-8671

# CONCLUSIONS

The purpose of this thesis was to extend the existing knowledge on ENP behaviour and toxicity towards aquatic organisms, with a particular focus on sub-lethal effects and chronic exposures. The investigation of ENP ecotoxicology is complicated by the numerous variables affecting the exposure outcome, posing difficulties to the extrapolation of generic guidelines for ENP risk assessment. Overall results highlighted the need to prolong exposure times in ecotoxicological studies and, more importantly, look beyond standard endpoints of toxicity, in order to provide more reliable data on the threat posed by ENP dispersion in the environment and their bio-interaction with aquatic organisms. Main findings can be summarized as follows:

- *Sub-lethal outcomes of nanoplastic exposure might affect population and its ecological role*

  The exposure of marine diatom *S. marinoi* to PS NPs demonstrated to reduce the length of algal chains instead of the rate of cell growth, upon 15 days of exposure. *S. marinoi* population, and similar chain-structured diatoms, may, hence, not suffer from acute PS NPs exposure but their ecological role (*e.g.,* bloom formation) could be influenced by impaired buoyancy of reduced chain length due to nanoplastic adhesion, facilitated by aggregation with their exudates. Such ecological implications are likely to be missed if only standard endpoints and acute toxicities are considered, therefore *ad hoc* ecotoxicity assays should be highly recommended, in agreement with guidelines only recently provided by the OECD (OECD 317, 2020).

- *Specific capping agents reduce AgNP acute effects, but chronic exposure reveals hidden toxicity*

  By coupling ENM design with ecotoxicity, the synthesis and use of AgNPs can be more environmentally safe. The double coating of citrate and L-cysteine on AgNPs revealed to be limiting Ag ion release and causing a low toxicity for both freshwater and marine microalgae. Long-term exposure, however, revealed severe effects on reproduction and survival of microcrustaceans, which were not anticipated by acute exposure. Chronic toxicity has proven

to be crucial for a correct and realistic assessment of AgNPcitLcys toxicity, as opposed to acute exposure, which underestimated ecological risk.

- *Surface coating determines the MoA of AgNPs*

  Effect comparison between AgNPcitLcys and AgNP3MPS revealed the role of the coating in driving AgNP MoA. AgNPcitLcys toxicity resulted always higher than expected based on dissolution values, leading to hypothesize the occurrence of a toxicity imputable to the nano-size, while the outcome of AgNP3MPS exposure appeared to be related to the amount of dissolved Ag, suggesting a dissolution-based toxicity.

Furthermore, obtained results stimulated further research on AgNPcitLcys for environmental applications. Even though AgNPcitLcys were not completely harmless to tested organisms, their toxicity was observed only at high concentrations and dissolution always showed to be low, allowing to plan the follow-up steps for their environmental application. These will involve the development of a hybrid nanostructured cellulose-based material functionalized with immobilized AgNPcitLcys, to be used as filter for heavy metal pollution, which, by preventing AgNPcitLcys to exert their nano-related toxicity, should satisfy the criteria of *ecosafety*.

## Future perspectives

The general picture drawn by the totality of obtained data underlines the need to further investigate the existing relations between ENPs and biota, in order to clarify the main driving forces behind ENP ecotoxicity. For instance, concerning AgNPs, the role of the coating in determining the predominance of a nano-related toxicity rather than a dissolution-related toxicity should be further studied, as well as which are the mechanisms determining the occurrence of nano-related toxicity and if these are consistent among different ENPs or are ENP-specific. If the origin of the detrimental effects borne by cells and organisms upon ENP/Ms exposure is understood, exposure outcome will be easier to predict and model. Knowledge on toxicity mechanisms could also help in the development of updated

ecotoxicity protocols in which not only test preparation and conduction is updated, as in OECD 317 guidelines (2020), but also the endpoints of toxicity, which should be built *ad hoc* for ENP/Ms. The occurrence of sub-lethal effects in acute exposure tests should be emphasized and long-term exposure follow-up should always be performed, in order not to underestimate the potential hazard of ENP/Ms. Also, gained information on toxicity mechanisms will allow a more ecologically-informed design process of ENP/Ms, not only for environmental purposes, allowing a lower impact for their use and disposal, especially in sight of future scenarios of increased pollution.

## Acknowledgments

Firstly, I should thank all the great scientists, who produced high quality scientific data and papers, deepening their knowledge and sharing it, giving me the possibility to further investigate, understand and be passionate about this subject. My contribution to the subject is minimal, but theirs, to me, is enormous. As it is that of my supervisor, Ilaria Corsi, who gave me the chance to discover and do something I didn't know I loved, scientific research.

Going back in time, I'll always be grateful to Albert Koelmans from the Wageningen University and Research who, for the first time, introduced me to scientific thinking, making me feel part of it. I am grateful to all the researchers who helped me, sharing their time and giving precious advice, to my former lab-partners who unfortunately, for the most part, have now taken different roads but provided me with an environment for confrontation, and to all the students I've taught something to, which was always more learning than teaching.

A big contribution to this work, among all, is that given me by my bearded, ruffled, funny-looking, lovely dog Mela, for reminding me about the real important things in life: the park, the woods, running and chasing chickens.